ISSN 1173-5996

POST-FLASHOVER DESIGN FIRES

BY

R Feasey

Supervised by

Dr Andy Buchanan

Fire Engineering Research Report 99/6
March 1999

This report was presented as a project report
as part of the M.E. (Fire) degree at the University of Canterbury

School of Engineering
University of Canterbury
Private Bag 4800
Christchurch, New Zealand

Phone 643 364-2250
Fax 643 364-2758

Post-flashover Design Fires

By

R. Feasey

Supervised by

Associate Professor A.H. Buchanan

A research project presented in partial fulfilment of the requirements for the degree of Master of Engineering in Fire Engineering

Department of Civil Engineering
University of Canterbury
Christchurch, New Zealand
February, 1999

ABSTRACT

This report reviews the modelling of post-flashover fires and compares the various methods of predicting temperature versus time in post-flashover compartment fires, including the historical development of theoretical approaches.

The report specifically addresses the use of the COMPF2 model as implemented in the COMPF2PC computer programme, as a prediction tool for post-flashover fire temperatures. Aspects of the computer code are compared with theory and experimental data. The results of many COMPF2PC simulations are compared with test fire data, in order to determine how best to characterise the input data to achieve the best simulation results with the computer programme.

It is found that with careful selection of input data, COMPF2PC can provide good prediction of post flashover fire temperatures for compartments with a fire load of greater than15 kg of wood per square metre of floor area, and for ventilation factors $A_V \sqrt{H} / A_T \geq 0.04$. Reliability of temperature prediction is poorer for ventilation factors ($A_V \sqrt{H} / A_T$) significantly less than 0.04.

Guidelines for use of the COMPF2PC programme are provided.

Based on the methodology developed during simulation of test fires, generalised fire temperature versus time curves are developed for a single compartment size and a range of compartment material properties. The generalised COMPF2PC temperature versus time curves are compared with those of alternative models in common use.

It is found that for a fire of fire load 1200 MJ m^{-2} of floor area, in a compartment of medium thermal inertia, depending on ventilation, the COMPF2PC model predicts fires which either have a significantly higher maximum temperature or longer duration (or both), than those predicted by the Eurocode Parametric fire, and the "Swedish" fire model of Magnusson and Thelandersson. This may have a significant impact on the calculation of time equivalent fires.

Recommendations for future development of the COMPF2PC programme are provided.

ACKNOWLEDGEMENTS

I have received assistance and support from many people and organisations, and wish to acknowledge :

- the assistance of Associate Professor Andy Buchanan who as supervisor, provided frequent advice, guidance and plenty of encouragement.

- the assistance of the Engineering School Library in obtaining reference material, much of it in the hard to find category.

- the support of my employer, Opus International Consultants Limited.

- the Opus technical library service TeLIS, which has provided excellent assistance, sometimes being able to source publications unobtainable through other avenues.

- Joël Kruppa of CTICM in France who provided fire test data and background publications on the experimental methodology used.

- the support of my dear wife Sally, who has had to put up with a part time husband especially over the last year, and my daughters Nicola and Claire, who have had far less of their father's time than ususal, and far less access to the family computer than they would have wished.

CONTENTS

Page

LIST OF TABLES

LIST OF FIGURES

NOMENCLATURE

A	area (m^2)
A_F	floor area (m^2)
A_T	total bounding surface area (m^2)
A_V	ventilation area (m^2)
b_p	combustion efficiency
C_d	discharge coefficient
C_p	heat capacity (J kg^{-1} K^{-1})
D	smallest fuel dimension (m)
g	gravitational acceleration (m s^{-1})
H	height of ventilation opening (m)
h	convective coefficients (W m^{-2} K^{-1})
h_c	combustion enthalpy (J)
Δh_c	calorific value (J kg^{-1})
Δh_p	total heat of pyrolysis (J kg^{-1})
k	thermal conductivity (W m^{-1} K^{-1})
m	mass (kg)
M_o	initial fuel mass (kg)
q	heat (J)
Q	heat flow (W)
R	rate of burning (kg s^{-1}, kg min^{-1},kg h^{-1})
r	stoichiometric air / fuel ratio
t	time (s, min, hr)
T	temperature (K)
v_p	regression velocity (m s^{-1})
w	molecular weight (kg mol^{-1})
W	fire load (kg m^{-2})
x	thickness dimension (m)
ϵ	emissivity
ρ	density (kg m^{-3})
σ	Stephan-Boltzmann constant (W m^{-2} K^{-4})

Subscripts

air	air
b	vaporisation
ep	excess pyrolysate
f	hot gases; pool
g	gas
o	ambient
p	pyrolysis
r	window radiation
v	ventilation, window
w	walls, including ceiling.

Superscripts

$\dot{}$	time rate
'''	per volume

1 INTRODUCTION

Fires within buildings are complex events. Fire effects within a compartment include heat release, increase in air temperatures, increase in radiation intensity, generation of toxic gases, reduction in visibility and increase in the temperature of structural and non-structural elements. Threats exist to the occupants, the structure, fire fighters and the environment.

The modelling of the effects of fires in their early stages of development is used to determine heat and smoke detector and sprinkler activation, to model smoke movement and the generation and transport of toxic gases, and provides a basis to estimate tenability for occupants within the building. Typically used for this type of evaluation is a zone model, which divides the fire compartment into a cool lower layer and hot upper layer, with the fire plume pumping heat and mass from the lower to upper layer. Zone models are applied up to flashover, at which time all the combustible materials within the fire compartment are burning. Flashover occurs typically when the gas temperature in the upper layer of the compartment under the ceiling reaches the order of 500 - 600 °C.

For post-flashover fires, threats to structural survival become paramount. A number of manual and computer based methods have been developed to predict post-flashover temperatures. With computer based prediction methods, a single zone model approach has been widely used. Some models cover both pre and post-flashover phases, but most remain singularly focussed on one phase.

This report presents a brief review of the historical development of the theory of post-flashover fires in Chapter 2, including parametric fires. It reviews the early development of mathematical models in the work of Kawagoe and Sekine, and Magnusson and Thelandersson. These were historically important attempts to predict compartment temperatures in post-flashover fires, and most subsequent models adopt methodologies derived from these earlier models. The range of post-flashover models developed subsequently is also briefly considered.

The assumptions and theory of the COMPF and COMPF2 computer model for post-flashover fires is examined in some detail in Chapter 3. The data on which the

COMPF2 programme is based is examined in Chapter 4 which also contains a critical review of the programme and elements there-in.

Real fire data used to evaluate the use of COMPF2 as a predictive tool is reviewed in Chapter 5. The use of the COMPF2 programme to predict the outcome of real fires, with comparison between observed data and predicted temperatures is detailed in Chapter 6. This also addresses methods of characterising different types of real fires in terms of the input parameters available for the COMPF2 programme.

Design fires for a range of fire loads, ventilation conditions and compartment materials, are then presented, on the basis of the COMPF2 simulations in Chapter 7, and a comparison made with Eurocode parametric and Swedish fire curves.

Conclusions including recommendations for modification to the COMPF2PC computer programme and input parameters are proposed in Chapter 8.

2 POST-FLASHOVER FIRES

2.1 Introduction

The temperature versus time curve for post-flashover fires has commonly been represented by one of a number of standard curves. Standard temperature versus time curves such as that from ISO (1975), take a form as indicated in Figure 2.1. The equation is of the form:

$$T_g = 20 + 345 \log_{10}(8t + 1)$$

where T_g = gas temperature in °C,
t = time in minutes.

Most fire ratings of structural components, partition systems and so on are carried out in a test facility where the temperature within the test chamber is varied as above, until either structural, integrity or insulation failures have occurred as relevant to the component being tested. The main feature of this and similar curves from various international standards, is that they are independent of various parameters known to affect fire intensity including fire load, ventilation areas, building thermal properties, etc., asymptote to infinity and never decline in temperature and are set by convention rather than by science.

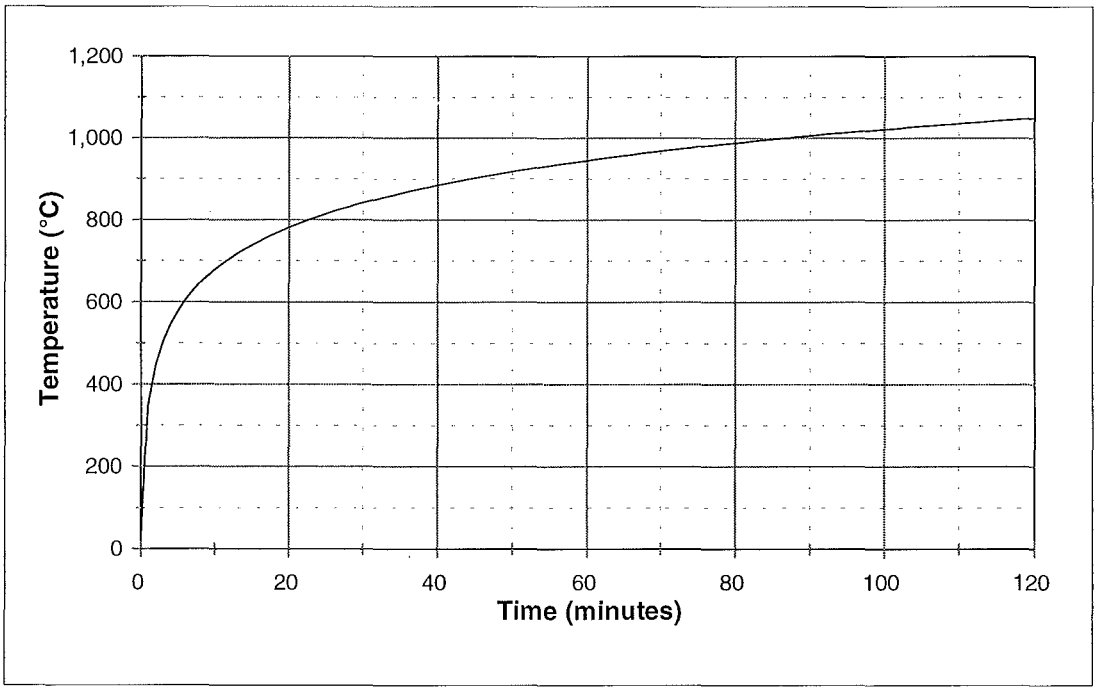

Figure 2.1 ISO 834 Temperature vs Time

Such standard curves may represent the short term effects of post-flashover fire reasonably well. In general they do not reliably represent the medium to long term exposure effects of real fires, which will always run out of fuel and ultimately decay in temperature as time increases. In particular, use of such curves to predict impact on structural capacity are usually but not always conservative.

In order to better represent real fires, parametric methods have been adopted particularly in Europe. These are largely based on the evaluation of experimental data.

Amongst the earliest theoretical methods for prediction of post-flashover fire temperatures were those of Kawagoe and Sekine (1963 & 1964), and Kawagoe (1967 & 1971). These were based on a simple heat balance in a room with a single window, and ventilation limited fires. This was further developed by Magnusson and Thelandersson (1970) who created a set of temperature versus time curves as an extension to this methodology, also restricted to ventilation limited fires.

2.2 **Parametric Fires**

Parametric fires take into account factors which are known to affect fire growth and intensity such as fire load density, compartment size, ventilation area, construction materials etc. Generically, they attempt to provide a more realistic prediction of actual temperature versus time than code or standard based approaches, which merely enshrine a particular curve by convention (such as the ISO 834 curve).

Parametric curves have been developed empirically, based on curve fitting to the observations of test fires; they are not based on actual calculations of pyrolysis, heat generation, heat transfer and gas flow rates.

The Eurocode (1996) defines a parametric fire temperature during the growth or increasing temperature phase of the form :

$$T_g = 1325 \, (1 - 0.324 \, e^{-0.2t^*} - 0.204 \, e^{-1.7t^*} - 0.472 \, e^{-19t^*})$$

where T_g = gas temperature (K)

t^* = $t \Gamma$ (h)

t = fire exposure time (h)

Γ	=	$(O / 0.04)^2 (1160 / b)^2$
b	=	the average value of $(k\rho c)^{1/2}$ of the compartment $1000 \leq b \leq 2000$ $(J\ m^{-2}\ s^{-0.5}\ K^{-1})$
O	=	opening factor $A_V \sqrt{H} / A_T$ $0.02 \leq O \leq 0.20$ $(m^{0.5})$
A_V	=	area of vertical opening (m^2)
H	=	height of vertical opening (m)
A_T	=	total area of enclosure of compartment incl. ceiling, walls, floor and opening (m^2)

This function allows real time (t) to be scaled by a parameter (Γ) to create a parametric time factor (t*). The scaling parameter (Γ) is a function of the relative opening factor and relative compartment thermal inertia, in comparison with standard values of ventilation factor O = 0.04 and thermal inertia parameter b = 1160 which combined, give a value of $\Gamma = 1$, in which case parametric time (t*) equals real time (t), and the temperature growth follows the ISO 834 curve. For compartments with $\Gamma > 1$, temperature growth rate is greater than that of the ISO 834 standard fire. For compartments with $\Gamma < 1$, the temperature growth rate is slower than that of the ISO 834 standard fire.

For the Eurocode parametric fire, the "scaled" time (t_d^*) at which the temperature begins decreasing is given by :

$$t_d^* = 0.00013\ q_{t,d}\ \Gamma / O$$

where $q_{t,d}$ = fire load density in MJ m^{-2} related to compartment total bounding surface area A_T

The "real" time (t_d) at which the Eurocode parametric fire temperature begins decreasing is given by :

$$t_d = 0.00013\ q_{t,d} / O$$

During the cooling phase, the temperature is assumed to decrease linearly at one of three rates between 625 and 250 °C h^{-1}, each of which is dependent on t_d^*, the scaled time as follows:

$$T_g = T_{(max)} - 625\,(t^* - t_d^*) \qquad t_d^* \leq 0.5 \text{ hours}$$

$$T_g = T_{(max)} - 250\,(3 - t_d^*)(t^* - t_d^*) \qquad 0.5 < t_d^* < 2 \text{ hours}$$

$$T_g = T_{(max)} - 250\,(t^* - t_d^*) \qquad t_d^* \geq 2 \text{ hours}$$

The temperature decay is within the range 250 - 625 °C per hour of "scaled" time. If the parametric fires are re-presented in terms of "real" time, it is apparent (Buchanan, 1998a) that well insulated compartments with good ventilation have very rapid decay rates, while poorly insulated compartments with limited ventilation openings have extremely slow decay rates. Buchanan notes that the rapid decay rates in the former case are at variance with measured experimental fires.

Along with the limits to thermal inertia and ventilation parameters discussed above, the parametric fire curve is valid for compartments of up to 100 m² floor area, without openings in the roof, with a maximum height of 4 metres. These constraints are presumably those of the physical tests on which the parametric fire equations are based.

The growth phase of the Eurocode parametric fire is based on those incorporated in the Swedish Building Regulations 1967, which are discussed in Magnusson and Thelandersson (1970). The general form of the current parametric fire and the linear decay characteristics of the Eurocode parametric fire were all entrenched in those Regulations.

An example Eurocode parametric temperature curve is presented in Figure 2.2 for a fire of moderately high fuel load (237 MJ m^{-2} of bounding surface area), but well ventilated with an opening factor O = 0.132)[1]. The compartment was of 3.1 x 3.6 plan dimensions with an internal height of 3.13 m, and a ventilation aperture of 3 m in width and 2 m height. The compartment boundaries were constructed from a mixture of brick and lightweight concrete. This combination of geometry and material properties leads to a scaling factor $\Gamma = 10.3$.

1

The compartment and fire properties are those of the test fire NFSC 69 which was one of many test fires used in COMPF2PC simulations. The results of those simulations are reported in Appendix B.

It can be seen that for this particular combination of fuel load, very high ventilation, compartment size and material properties, that the rate of temperature rise and peak temperature are well above those for the ISO curve at the same elapsed time. The decay rate is very fast, leading to a short fire duration.

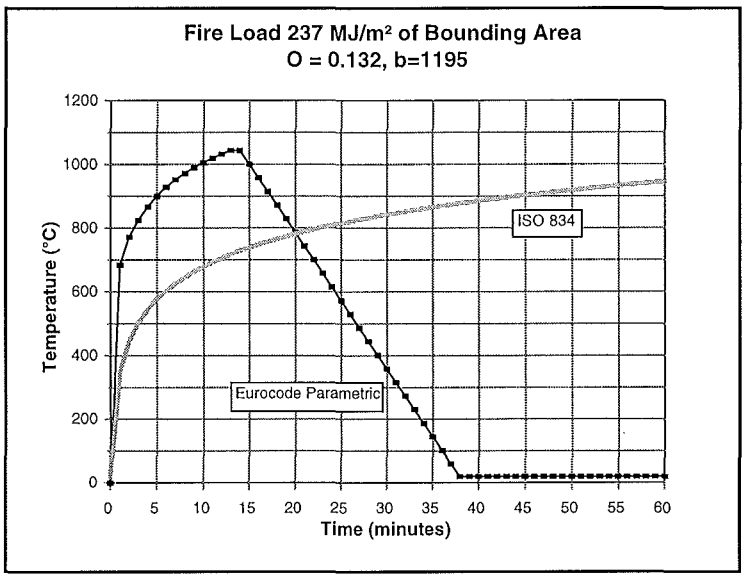

Figure 2.2 Eurocode Parametric and ISO 834 Fires

Because real fires invariably fail to follow an ISO-type characteristic temperature curve, many time-equivalent methods have been developed, to represent the real fire as an equivalent duration of "standard" fire curve, such as that contained in Annex E (Informative) of Eurocode (1996).

However the rapid predicted decay rate from the Eurocode parametric fire for a compartment with the properties of this example, may mis-represent the situation (Buchanan, 1998a), resulting in a time equivalent fire of too short a duration.

2.3 Kawagoe and Sekine

2.3.1 Background

Kawagoe (1958) carried out numerous test fires in the late 1940s and early 1950s in model scale and full scale rooms and houses of various construction. In conjunction with these tests, he developed the theoretical relationship of pyrolysis rate to ventilation now well established for ventilation limited fires. By analysing the fluid flows through an open ventilation aperture in a vertical wall of a fire compartment, he showed that pyrolysis rate was not only a function of ventilation area, but additionally of the height of the ventilation opening. Drysdale (1985) gives a summary of this derivation.

Subsequently Kawagoe and Sekine (1963, 1964) developed the first theoretical models for post-flashover fires which allowed the estimation of compartment temperatures from

the fire load, ventilation characteristics and the thermal characteristics of the enclosing surfaces of the compartment.

The underlying assumptions were :

(a) The emissivity and surface temperature inside the enclosure are completely uniform.

(b) The emissivity of the flame is 1.0, and the flame fills the compartment.

(c) The emissivity of the window is that of a black body.

(d) Parameters such as conductivity and specific heat remain constant with time.

Using the above assumptions they set up a heat balance solved by successive approximation to obtain the fire temperature, allowing fire temperature curves for various values of opening factors (ventilation) and enclosure conductivity to be developed.

2.3.2 Heat Balance

The heat balance (Kawagoe and Sekine, 1963) took the form :

$$Q_H = Q_W + Q_B + Q_L$$

where Q_H = quantity of heat released per unit time by combustion

Q_W = quantity of heat lost per unit time by heat transfer to walls

Q_B = quantity of heat lost per unit time by radiation through the window

Q_L = quantity of heat carried away per unit time by the combustion gases flowing through the ventilation opening.

Quantification of the above parameters was through a combination of empirically derived and theoretically derived relationships. For example the heat release rate (Q_H) was calculated from the formula :

$Q_H = R\,q$

where R is the rate of burning in kg min^{-1} or kg h^{-1} given by the formulae :

$R = 5.5\,A_V\sqrt{H}$ (kg min^{-1}), or,

$R = 330\,A_V\sqrt{H}$ (kg h^{-1})

where H = height of window (m)

A_V = area of window (m^2)

q = calorific value of wood (2575 kcal kg^{-1}, 10.78 MJ kg^{-1})

The formula for rate of burning (R) was originally empirically based, but had been justified on a theoretical basis (Kawagoe, 1958). The calorific value for wood used in the model is far lower than that normally expected. The lower value used was to account for incomplete combustion known to occur in ventilation limited fires, and was calculated from the equation :

$q = 3558\,(1 - m) + 1098\,m$ (kcal kg^{-1})

where m = the ratio of complete combustion

The value of m = 0.6 based on experimental measurement of fires, was used to calculate an "effective" nett calorific value of 2,575 kcal kg^{-1} (10.78 MJ kg^{-1}). This implies the actual nett calorific value for the fuel of 4,292 kcal kg^{-1} (18 MJ kg^{-1}).

Heat transfer through the walls (Q_W) was obtained from the equation :

$Q_W = q_R + q_C$

$= A_T\,k\,dt / dx$

where q_R = net heat flux radiated to walls

q_C = heat transferred by convection to walls

A_T = total area of inside wall surface exposed to the fire

k = thermal conductivity of the walls

dt / dx = temperature gradient across the walls

The temperature gradient term (dt / dx) was solved graphically.

Heat transfer (Q_B) through the ventilation opening in the wall was obtained from :

$Q_B = A_V\,(E_G - E_0)$

where A_V = area of window (m^2)

E_G = radiation intensity (kcal $m^{-2}\,h^{-1}$)

$= 4.88\,\{(273 + T_G)/100\}^4$ (kcal $m^{-2}\,h^{-1}$)

where T_G = flame temperature (°C)

E_0 = radiation intensity at ambient temperature

$= 4.88 \{(273 + T_0)/100\}^4$ (kcal m^{-2} h^{-1})

where T_0 = ambient temperature (°C)

Heat lost with the combustion gases (Q_L) was given as :

$Q_L = G\ c\ R\ (T_G - T_0)$

where G = volume of combustion gas (Nm^3 kg^{-1})

c = mean specific heat at constant pressure in (kcal Nm^{-3} K^{-1})

2.3.3 Results

Fire temperature versus time curves were calculated for various ventilation ratios within the range $0.014 \leq A_V \sqrt{H} / A_T \leq 0.30$, and the results compared with selected experimentally recorded temperature profiles. A range of profiles was prepared for variations in compartment materials, as reflected in the varied thermal conductivity values.

Fire loads values were chosen following surveys, and two nominal values were selected to cover a wide range of occupancies including apartments, hospitals, hotels, offices, schools, libraries, stores etc. A "normal" fire load of 50 kg m^{-2} of floor area and a "large" fire load of 100 kg m^{-2} of floor area were chosen. (Using a calorific value for wood of 16 MJ m^{-2} these correspond to fire loads of 800 and 1600 MJ m^{-2} respectively).

The "Fire Duration Time" was defined as the period from the beginning of temperature rise in the room, until the temperature begins to drop after most of the combustible material in the room has been burned. The fire duration time (t) was estimated from:

$t = W\ A_F / R$

where t = fire duration (min)

W = fire load (kg m^{-2})

A_F = floor area (m^2)

R = burning rate (kg min^{-1})

Which becomes after substituting for R:

$$t = W A_F / (5.5 A_V \sqrt{H}) \quad (min)$$

Application of this methodology implies a constant heat release rate from the time the fire initiates, until combustion of all available fuel.

Following expiry of the fire duration time (t), the decay was assumed to be linear, with the decay rate 10 °C min^{-1} for fires with t < 60 min, and 7 °C min^{-1} for fires with t > 60 min. The latter were established from observation of experimental fires.

For typical Japanese office buildings with a range of ventilation parameters from 0.034 to 0.23, with assumed fire loads of 100 and 50 kg m^{-2} the calculated fire durations were in the range 154 min ("large" fire load and low ventilation) to 18 min ("normal" fire load and high ventilation).

Compared with the Japanese Standard fire curve (i.e. the equivalent to the ISO 834 curve), the predicted fires were substantially hotter (by hundreds of °C) out to durations of over 120 min. An equal area method was proposed to allow the "time equivalent" Japanese Standard fire duration to be calculated.

2.3.4 Subsequent Development

In a subsequent paper (Kawagoe, 1967) the heat balance was refined to account for the heat required to warm up the air within the fire compartment (Q_R), although it was noted that this term was small compared with the others. Since the model used computer rather than manual and graphical prediction techniques, results were slightly different for the same nominal input data, but not sufficiently to alter the earlier conclusions.

Further consideration was given to the decay phase where linear decay rates had been assumed in the earlier publications (Kawagoe and Sekine 1963, 1964). The effect of different component parts of the compartment having different thermal properties due to their different materials of construction was also evaluated. Kawagoe found that although the predicted compartment temperature was only modestly affected by assuming "monolithic" area-weighted average properties for conductivity, density and specific heat, the predicted temperature profiles within the thickness of the bounding walls, was far more sensitive to variation between average and actual properties.

Kawagoe realised that the method had a number of theoretical "problems" due to the many arbitrary assumptions made (such as the effective calorific value of combustibles), but regarded it as a valuable engineering tool to provide a rational evaluation for structural survival in a fire, in comparison with the equally arbitrary standardised fire curves.

2.4 **Magnusson and Thelandersson**

2.4.1 Background

The objective of Magnusson and Thelandersson (1970) was to improve the methods available at the time by developing a model that was applicable to different ventilation factors, fire loads, and compartment material properties, which would reliably predict the growth, flaming combustion and decay phase temperatures of a fire burning wood-type fuel. They adopted a similar approach to that taken by Kawagoe and Sekine, using a combination of theory with calibration against experimental data.

At the time, the Swedish Building Regulations used a nominal fire growth curve similar in concept to the earlier referenced ISO (1975) curve. Those Regulations also contained a mechanism to crudely estimate the duration of fully flaming combustion, and an assumed 600 °C h^{-1} (10 °C min^{-1}) linear decay rate.

It was realised that the decay rate was critical in determining the actual temperatures reached especially by unprotected structural elements.

2.4.2 Heat Balance

Their approach is based on solving the equations for heat balance for a fire compartment, and heat flux through the bounding surfaces of the compartment, to obtain values for the heat released in the compartment and the temperature of the combustion gases . Their heat balance can be expressed as :

$$Q_C = Q_L + Q_W + Q_R + Q_B$$

where Q_C= heat energy released per unit time during combustion

Q_L= heat energy lost per unit time due to replacement of hot gases by cold air

Q_W = heat energy lost per unit time via walls, roof / ceiling and floor structures

Q_R = heat energy lost per unit time via radiation through openings

Q_B = heat energy stored per unit time in the gas within the fire compartment.

Of these terms, Q_B is negligible compared with the other factors, and was ignored.

2.4.3 Experimental Basis

Magnusson and Thelandersson found the quantity of real fire data of adequate standard was limited. Four data sets were analysed, each obtained from a different series of test burns by different researchers for varying purposes Sjölin (1969), Kawagoe (1958), Ödeen (1963) and the National Swedish Institute for Materials Testing.

Basic parameters for each test series are listed in Table 2.1. Complete data was not reported for all data sets.

Test Series	Plan Area (A_V) (m^2)	Total Surface Area (A_T) (m^2)	Ventilation Factor ($A_V\sqrt{H} / A_T$) ($m^{0.5}$)	Fire Load kg wood m^{-2} of bounding surface area	Approximate Fire Load kg wood m^{-2} of floor area	Comment
A	10.4 - 29.2	-	0.0237 - 0.068	3.5 - 8.1	-	Real furniture, 7 tests
B	≈ 8	48	0.0467	8.3 - 20.8	50 - 125	Wood Cribs
C	≈ 13	75	0.015 - 0.060	1.8 - 18.0	10.5 - 104	Forced ventilation
D	≈ 13	75	0.008 - 0.075	1.5 - 15.0	8.7 - 87	Multi level house

Table 2.1 Summary of Magnusson and Thelandersson's Test Data

Most noticeable is the modest size of the fire test compartments, and the narrow range of ventilation parameters for the test data used. The range of fire loads was considerable in comparison.

2.4.4 Methodology

Kawagoe and Sekine assumed a constant mass burning rate and hence a constant heat release rate within the compartment (a constant effective calorific value of the fuel was assumed) until all the fuel was consumed.

Magnusson and Thelandersson realised the problems with this approach and that the mass burning rate given by the relation $R= 5.5\ A_V\ \sqrt{H}$ (kg min^{-1}) expressed the maximum rate of mass burning under ventilation controlled conditions. They noted that the effective nett calorific value of 2,575 kcal kg^{-1} (10.78 MJ kg^{-1}) used by Kawagoe and Sekine, was only applicable during the fully flaming combustion phase, and that during the decay phase, the energy released per kg of fuel was higher (i.e. the . effective nett calorific value was higher than 2,575 kcal kg^{-1} (10.78 MJ kg^{-1}) used by Kawagoe and Sekine). Because there was little available basis to predict the variation in completeness of combustion with progress of the fire, they assumed that combustion was complete throughout the whole burning process, releasing in the range 3,500 - 4,500 kcal kg^{-1} (14.6 - 18.8 MJ kg^{-1}) during the complete course of the fire.

During the "flaming" phase of burning, they assumed the fire was ventilation limited with the mass rate of burning constant at $R= 5.5\ A_V\ \sqrt{H}$ (kg min^{-1}) and that the effective nett calorific value was 2,575 kcal kg^{-1} (10.78 MJ kg^{-1}) , giving a combustion rate (heat release rate) of 2,575 x R kcal min^{-1} (10.78 x R MJ min^{-1}).

For the problematic decay phase, they developed an iterative numerical solution using a computer based approach. For a given fire, the decay phase combustion rate (heat release rate) versus time curve was assumed to be a polygonal function of time, reducing to zero. Based on an assumed combustion rate decay curve, the compartment temperature versus time curve was calculated using the heat balance method. On a trial and error basis, the combustion rate versus time curve was varied, until the predicted temperature versus time curve best matched the experimental temperature profile.

Thus the variation of combustion rate with time was calculated to fit limited experimental data, rather than based on measured mass loss rates or known pyrolysis characteristics of real fuel.

The results were then systematized so that they could be applied to compartments with different geometries, ventilation conditions, and materials of construction, from those of the compartments in which the test data had been originally obtained.

Magnusson and Thelandersson also provided variations to the standard theory for multiple vertical openings with different heights, and also for the case where there is a horizontal opening in the ceiling. For the latter case a chart was developed to allow the "hybrid" ventilation factor was developed incorporating the area of the horizontal opening (A_H), the area of the vertical opening (A_V), the height of the horizontal opening above the horizontal centre of the vertical opening (h), and the height of the vertical opening (H).

Although there is slight variation of the hybrid ventilation factor with the ratio of horizontal and vertical aperture areas, and the compartment temperature, Buchanan (1998b) notes that the equivalent ventilation factor can be approximated by the equation :

$$(A\sqrt{H})_{combined} = 2.33\, A_H \sqrt{h} + A_V \sqrt{H} \qquad 0.3 < (A_H \sqrt{h} / A_V \sqrt{H}) < 1.5$$

Magnusson and Thelandersson defined the fire duration for the flaming phase, (t) in hours, as :

$$t = \frac{Q}{6280\, A_V \sqrt{H}}$$

where Q = Total heat release over the flaming period of the fire (MJ)
A_V = ventilation area (m^2)
H = height of ventilation opening (m)

The flaming fire duration is simply the fire load in MJ divided by the ventilation limited mass burning rate (330 $A_V \sqrt{H}$ kg hr^{-1}) multiplied by an assumed calorific value for the fuel of 19 MJ kg^{-1}. This equation implies that for ventilation limited fires, if the ratio of the fire load to the ventilation factor $A_V \sqrt{H}$ is constant, a constant fire duration will result. Thus a fire of fuel load 10 kg m^{-2} and ventilation factor $A_V \sqrt{H} / A_T$ =0.03 will have the same duration as a fire of 30 kg m^{-2} and ventilation factor $A_V \sqrt{H} / A_T$ =0.09.

2.4.5 Calculated Fires

Inherent in Magnusson and Thelandersson's methodology is that in order to calculate the variation in temperature with time for a wide range of compartment materials and geometries, fire and ventilation parameters, it was necessary to simplify and systematise the rate of combustion data derived from the limited range of fire tests analysed. They assumed (as for Kawagoe and Sekine 1963, 1964) that the maximum rate of combustion of wooden cribs was given by :

$$R_{max} = 330\ A_V \sqrt{H} \qquad (kg\ hr^{-1})$$

They similarly assumed the effective calorific value for wood was 2,575 kcal kg^{-1} (10.78 MJ kg^{-1}). They also assumed that the energy released per unit time during the growth phase of the fire was a polygonal function of time, up to the value which corresponds to that of the fully flaming combustion, assumed to be based on R_{max} . They found the best agreement between calculated temperature versus time curves and the test data, particularly in regards to the maximum compartment temperature and the duration of flaming combustion, by assuming a calorific value for wood of 2,500 - 2,800 kcal kg^{-1} (10.5 - 11.7 MJ kg^{-1}). The latter range is very low compared with both gross and nett values of most dry wood but consistent with the value used by Kawagoe and Sekine (1963, 1964).

The time temperature curves in the decay phase were obtained in this way, by changing the heat release rate to match the temperatures observed in the limited range of test fires.

The resulting trends were then extrapolated far beyond the test data to produce the graphs of the form shown in Figures 2.3 and 2.4. The degree of extrapolation can be estimated by considering that the highest fire load in any of the test data analysed was 375 MJ m^{-2} of total bounding surface area in Test Series B (Table 2.1 above, using a calorific value of 18 MJ kg^{-1} to convert from wood mass to energy). The Magnusson and Thelandersson graphs are produced for fire load densities of up to 360 Mcal m^{-2} (1,500 MJ m^{-2}). This is equivalent to fire load densities for wood of approximately 83 kg m^{-2} of bounding surface area, and assuming an approximately cubical compartment shape, a fire load density of 500 kg m^{-2} of floor area. In addition, none of the test data was obtained with a ventilation factor $A_V \sqrt{H} / A_T$ of greater than 0.075, but the simulation data is extrapolated to a ventilation factor of $A_V \sqrt{H} / A_T = 0.12$.

Magnusson and Thelandersson calculated temperature versus time curves for seven compartment configurations (A - G) for varying values ventilation factor ($A_V \sqrt{H} / A_T$) and fire duration (t). For all except enclosure type F, ventilation parameters $A_V \sqrt{H} / A_T$ of 0.01, 0.02, 0.04, 0.06, 0.08 and 0.12 $m^{0.5}$ were used. For each ventilation parameter, fires of 8 different durations were specified, resulting in 48 fire combinations for each enclosure type.

From the analysis of the test data, the time rate of combustion curves so deduced, were used together with the computer solved heat balance, to calculate complete temperature versus time graphs for a range of compartment geometries. Most of the compartment options have variations of forms of concrete or masonry. Refer to Appendix A for descriptions of the compartment geometries used.

2.4.6 Predicted Fire Curves (Swedish Curves)

Predicted temperature versus time curves based on the model of Magnusson and Thelandersson for Enclosure Type A and ventilation factor $A_V \sqrt{H} / A_T = 0.01$ and $A_V \sqrt{H} / A_T = 0.04$ are presented in Figures 2.3 and 2.4. These are now generically referred to as "Swedish Curves".

The Type A enclosure had surfaces of 200 mm thickness of concrete or brick construction with a thermal conductivity (k) of 0.81 W m^{-1} K^{-1}, and ρC_p of 1674 kJ m^{-3} K^{-1}. These are the same material properties as used for the Swedish Building Regulations 1967.

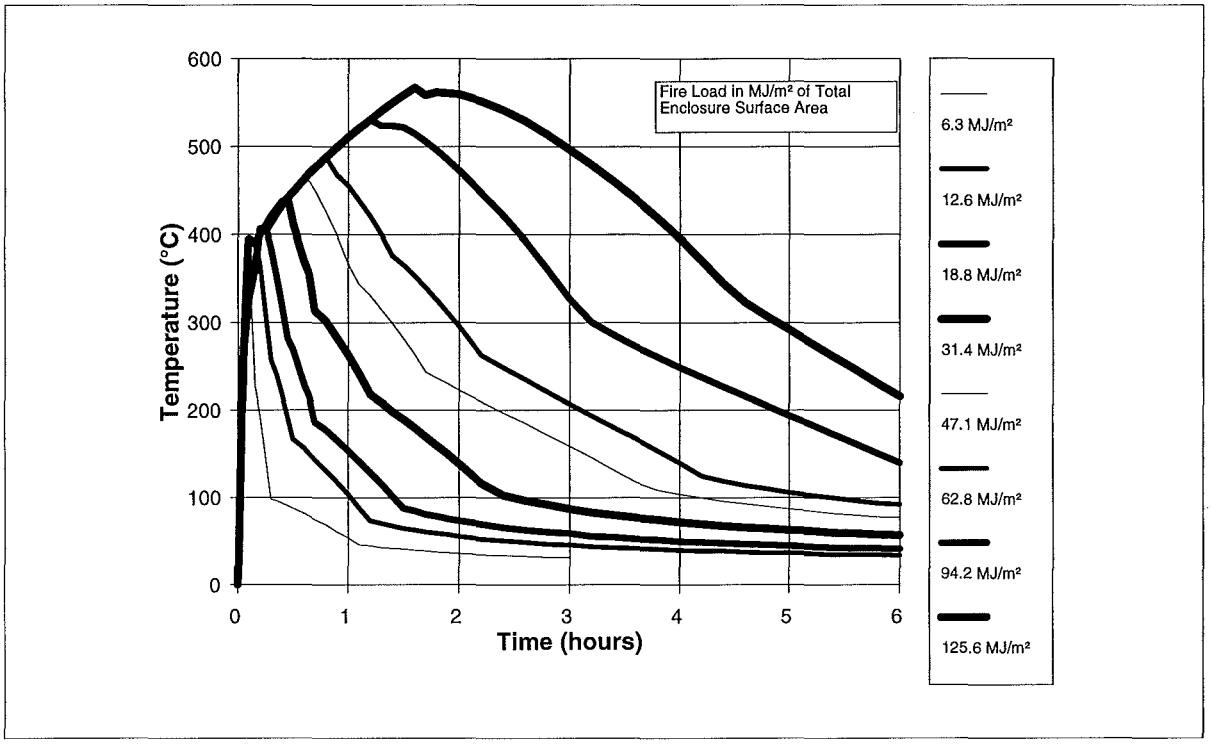

Figure 2.3 Magnusson and Thelandersson, Ventilation Factor = 0.01

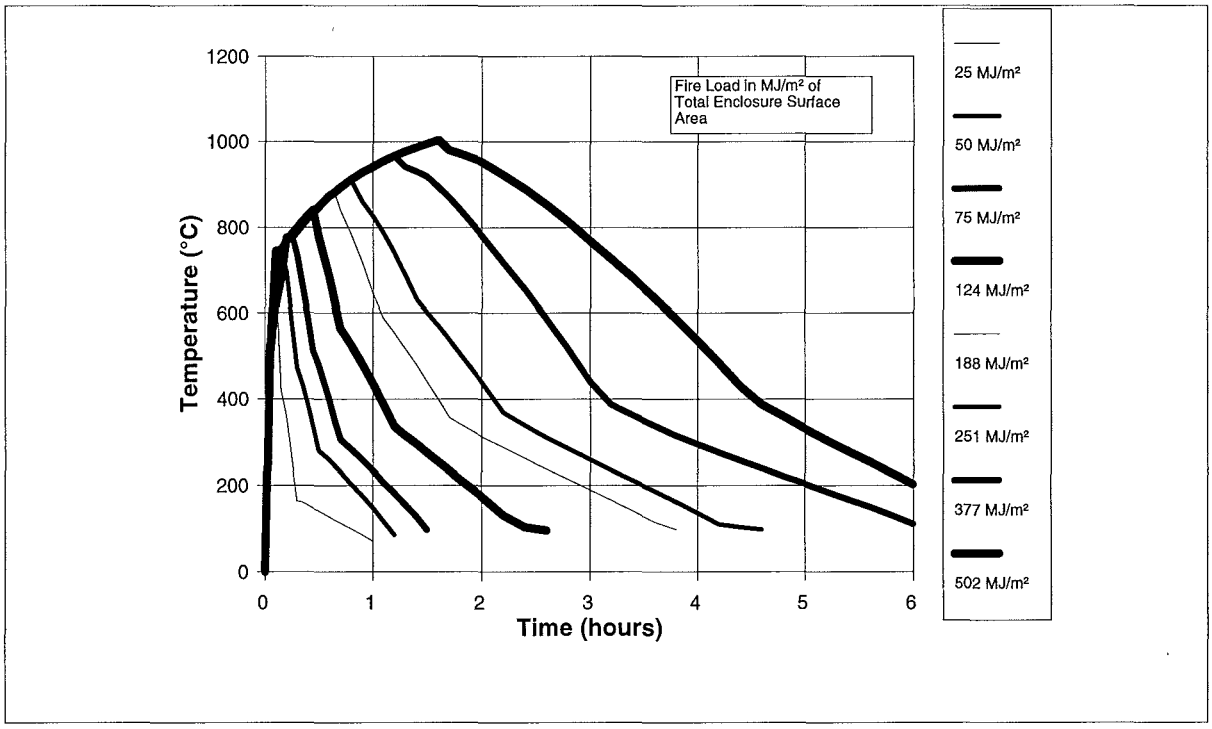

Figure 2.4 Magnusson and Thelandersson, Ventilation Factor =0.04

2.5 Other Mathematical Post-flashover Fire Models

2.5.1 Review by Harmathy and Mehaffey

Many other post-flashover fire models have subsequently been developed, for a variety of purposes. In their critical review of fourteen post-flashover compartment fire models, Harmathy and Mehaffey (1983) classified mathematical models according to a number of criteria believed to be of principal importance to structural behaviour in fires.

(a) Utility

Some models were created to assist the design of structures, while some were more focussed on investigation of a narrow range of aspects relating to the fire. Models were therefore classified as :

(1) Comprehensive

(2) Incomplete or qualitative.

(b) Interpretation of Fire Duration

Fires are often considered to have three main phases, namely, growth, fully developed and decay. Models variously consider only one phase or more, and make different assumptions as to the phase in which the energy of combustion is released. Harmathy and Mehaffey believe the distinction between the fully developed and decay periods are unimportant. More important is the period of time the gas temperatures are greater than those of the compartment boundaries during which heat is transferred into the structure.

The number of phases of fire development incorporated within models was therefore classified as :

(1) Three periods, full development plus simplified growth and decay

(2) Two periods, simplified development and decay

(3) One effective period, during which heat is transferred to the compartment boundaries.

(c) Process Variables

Harmathy and Mehaffey consider there are five significant dependant variables that describe a compartment fire during it's fully developed stage.

(1) Rate of air flow into the compartment

(2) Rate of pyrolysis of the fuel

(3) Heat generation within the compartment

(4) Temperature of the combustion gases

(5) Heat flux through the compartment boundaries

Equations developed to represent the above, can be time dependent, or may describe average conditions. Many models assume that the rate of air flow is constant (i.e. the fire is ventilation limited) and others assume that the rate of pyrolysis and rate of heat release are also constant.

Treatment of relevant variables allowed the models to be classified as either:

(1) Variables a function of time

(2) Variables averaged for the effective duration of the post-flashover period.

(d) Destructive Potential

The destructive potential of the fire can be considered to be related to the temperature of the gases as a function of time, the heat transfer rate to the boundaries as a function of time, and the fire duration. Harmathy (1980a, 1980b) developed the concept of a single "normalised" heat load (H) where:

$$H = \frac{1}{\sqrt{k \rho c}} \int_0^{t_{max}} q(t)\, dt$$

where $\sqrt{k \rho c}$ = thermal inertia of compartment boundaries

k = thermal conductivity (W m^{-1} K^{-1})

ρ = density (kg m^{-3})

c = specific heat (J kg^{-1} K^{-1})

$q(t)$ = heat transfer as a function of time (t)

Models were therefore classified as having the destructive potential of the fire represented by :

(1) Temperature history of fire gases

(2) Average heat transfer, average fire gas temperature and fire duration

(3) Normalised heat load (H)

(e) Compartment Characterisation

Post-flashover fire compartments are often assumed to be single zone "well stirred reactors" where temperature and other relevant parameters are equal in all parts of the space. Where boundaries have unequal thermal properties due

to differences in materials of construction, variable heat transmission will result. Use of area weighted values of $\sqrt{k \rho c}$ can overcome this objection.

The fire compartment is therefore regarded as :

(1) A single zone "well stirred reactor"

(2) Having several zones

(f) Rate of Burning

Models characterise the rate of burning from:

(1) Bona fide understanding of the mechanism of burning

(2) Assumed relationship

(3) Result of suitable tests

(4) A combination of bona fide knowledge and assumed relationships.

(g) Applicable Types of Fuel

Burning is an extremely complicated process, with substantial differences in the processes involved depending on whether fuels are char-forming (such as wood), or non-char forming such as plastics. The heat from oxidation of char-forming fuels provides the volatile products for flaming combustion. The burning of non-charring fuels has no in-built heat supply, and the pyrolysis process relies on radiation feedback to the fuel surface. The mass loss rate is therefore sensitive to compartment temperature, but insensitive to rate of air flow past the fuel. Models are therefore applicable to :

(1) Cellulosic (char-forming fuels)

(2) Non-charring fuels

(3) Any type of fuel

(h) Burning of Cellulosic Fuels

Although the burning rate of wooden fuels has been found to be a function of ventilation, the primary process of pyrolysis has little or nothing to do with gas phase reactions. The apparent coupling of pyrolysis rate with air supply is therefore difficult to explain. Harmathy suggests a zone within a compartment where the char on the fuel surface is strongly oxidised. This is the zone where most of the pyrolysis occurs. The size of the strong oxidising zone is approximately proportional to air flow, and moves across the compartment from the ventilation opening to the interior. If the air flow rate is sufficiently large, the zone of strong oxidising can extend to the whole compartment and the fire becomes fuel surface (or char surface) controlled.

Harmathy suggests the following semi-empirical equations for pyrolysis rate :

$R = 0.0236\ \Phi$ if $\Phi / \psi M_0 < 0.263$

$R = 0.0062\ \psi M_0$ if $\Phi / \psi M_0 \geq 0.0263$

where R = rate of pyrolysis (kg s^{-1})

Φ = ventilation factor ($\rho_a A_V \sqrt{(g H)}$)

where ρ_a = ambient air density (kg m^{-3})

g = acceleration due to gravity

ψ = specific surface of fuel (m^2 kg^{-1})

M_0 = initial mass of fuel (kg)

The pyrolysis rate of cellulosic fuels is considered to be controlled by:

(1) Ventilation or fuel surface area, depending on ventilation conditions

(2) Ventilation under any condition

(3) Ventilation, fuel surface area and porosity of fuel bed, depending on fuel geometry and ventilation conditions.

(i) Constancy of Burning Wood

Much experimental data indicates the pyrolysis rate is relatively constant for a long period of time, even though the fuel dimensions decrease as the fire progresses. This can be bypassed by making the pyrolysis rate (R) a function of the initial fuel state (e.g. initial mass or initial surface area) rather than the instantaneous values. Models that allow the fuel dimensions to change, also allow the pyrolysis rate to vary, leading eventually to a change from ventilation controlled to fuel surface controlled burning.

The rate of burning of cellulosic fuel is therefore :

(1) Constant and determined by pre-fire conditions

(2) Variable, and changing with progress of the fire.

(j) Stoichiometry of Combustion

Combustion of cellulosic fuels releases heat from both volatiles and char. Neither set of reactions is stoichiometric. Some models take account of the variation from stoichiometry, some do not.

Models therefore consider combustion to be :

(1) Imperfect (realistic)

(2) Stoichiometric

(k) Combustion Outside the Compartment

Various models consider the possibility of combustion of pyrolysis products outside the compartment is :

(1) Neglected (assumes all burning takes place in the compartment)

(2) Explicitly taken into account, empirically.

(l) Heat Transfer to Boundaries

Heat loss to the compartment boundaries is a significant factor in determining compartment temperatures. Heat is transferred by radiation and convection, although some models ignore the latter. The heat transfer to the boundary is therefore represented by :

(1) Radiation and convection terms

(2) Radiation only

(3) Infinite (surface temperature is same as fire temperature)

(m) Thickness of Compartment Boundaries

Models treat the compartment boundaries either as semi-infinite, or of fixed dimensions. Depending on the fire duration, the semi-infinite assumption may be a reasonable approximation.

Compartment boundaries are therefore treated as :

(1) Finite thickness slabs

(2) Semi-infinite solids

(n) Thermal Properties of Compartment Boundaries

Properties such as specific heat and conductivity can be wide functions of temperature for some materials. These parameters can be represented as averages over the period of fully developed fire (and therefore independent of changes in temperature) or as functions of temperature.

Dependence of thermal properties on temperature are classified as :

(1) Functions of temperature

(2) Constants representing average values over the "effective" fire duration.

Harmathy and Mehaffey reviewed the following fourteen post-flashover models according to the above criteria:

(A) Kawagoe, K. and Sekine, T. (1963)

(B) Ödeen, K. (1963)

(C) Magnusson, S.E. and Thelandersson, S. (1970)

(D) Tsuchiya, Y. and Sumi, K. (1971)

(E) Harmathy, T.Z. (1972)

(F) Nilsson, L. (1974)

(G) Babrauskas, V. and Williamson, R.B. (1975)

(H) Thomas, P.H. (1976)

(I) Tanaka, T. (1977)

(J) Bøhm, B. (1977)

(K) Bullen, M.L. and Thomas, P.H. (1978)

(L) Babrauskas, V. and Wickström, U.G. (1979)

(M) Harmathy, T.Z. (1980a and b)

(N) Wickström, U.G. (1981)

The characterisation of each of the above post-flashover fire models, according to the evaluation criteria of Harmathy and Mehaffey are summarised in several tables. In Table 2.2, each of the characterisation indicators for the various evaluation criteria (a) - (n) defined by Harmathy and Mehaffey are defined. In Tables 2.3a and 2.3b, those criteria are evaluated for each of the post flashover models.

	Characterisation Indicator			
Criterion	**1**	**2**	**3**	**4**
(a) Utility	Comprehensive	Incomplete / qualitative		
(b) Fire Duration	Three periods	Development and decay	One effective period	
(c) Variables	Time dependent	Averaged		
(d) Destructive Potential	Fire Temperature	Averaged heat transfer, average temperature and fire duration	Normalised heat load	
(e) Compartment	Single zone	Several zones		
(f) Rate of Burning	Bona fide understanding	Assumed relationship	Test results	Combination Bona fide and assumed
(g) Applicable Fuels	Cellulosic	Non-charring fuels	Any Type of fuel	
(h) Burning Cellulosic	Ventilation or Surface Controlled	Always ventilation controlled.\	Ventilation, fuel surface or porosity controlled	
(i) Constancy of wood Burning	Constant, depends on pre fire conditions	Variable, Changes with fire progress		
(j) Stoichiometry	Imperfect (realistic)	Stoichiometric		

	Characterisation Indicator			
Criterion	**1**	**2**	**3**	**4**
(k) Combustion Outside Compartment	Neglected	Accounted for		
(l) Heat Transfer to Boundaries	Radiation and Convection	Radiation Only	Surface Temp equals fire temperature.	
(m) Boundary Thickness	Finite slab	Semi-infinite Slab		
(n) Slab Thermal Properties	Fn (Temperature)	Averaged		

Table 2.2 Post-flashover Fire Model Review Criteria (after Harmathy and Mehaffey, 1983)

Criterion	Model						
	Kawagoe	Ödeen	Magnusson	Tsuchiya	Harmathy	Nilsson	Babrauskas
	Model A	Model B	Model C	Model D	Model E	Model F	Model G
a	1	2	1	1	1	1	1
b	2	2	1	2	3	1	2
c	1	1	1	1	2	1	1
d	1	1	1	1	2	1	1
e	1	2	2	1	2	2	1
f	1	2	3	4	1	3	4
g	1	3	3	3	1	3	3
h	2		2		1	3	
i	1	2		2	1		2
j	1	1	1	1	2	1	1
k	1	1	1	1	2	1	1
l	1	1	1	1	2	1	1
m	2	2	1	2	2	1	1

Table 2.3a Post-flashover Fire Model Evaluation (after Harmathy and Mehaffey, 1983)

Criterion	Model						
	Thomas	Tanaka	Bøhm	Bullen	Babrauskas	Harmathy	Wickström
	Model H	Model I	Model J	Model K	Model L	Model M	Model N
a	2	2	1	2	2	1	1
b		1	1			3	2
c		1	1			2	1
d		1	1			3	1
e	1	2	2	1	1	2	1
f		2	3	1	1	1	1
g		3	3	2	2	2	1
h			2			1	2
i		2		1	1	1	1
j	2		1	2	2	2	1
k			1	1	1	2	3
l			1	1	1	2	2
m			1	2	2	2	2

Table 2.3b Post-flashover Fire Model Evaluation (after Harmathy and Mehaffey, 1983)

In carrying out the above review of post-flashover fire models, Harmathy and Mehaffey were primarily attempting to review the completeness of various models and identify the applicability and suitability of the various models to specific post-flashover problem solving. No particular conclusions are drawn as to the merits of the various models. The referenced paper also examines fire spread between fire compartments by convection and destruction, and notes that fire spread by convection via openings, broken windows etc., is far more common than fire spread by destruction. In this respect they note the only model capable of yielding information on the potential for spread of fire is that of Harmathy (1980a).

2.5.2 Review by Janssens

A more recent review of mathematical pre-flashover and post-flashover fire models by Janssens (1992) identified the following post-flashover models in addition to those reviewed by Harmathy and Mehaffey (1983):

Thomas and Nilsson, L. (1973)
Schneider and Haksever (1980)
Nakaya and Akita (1983).

Janssens considers there are two fundamental types of mathematical fire model, probabilistic and deterministic. The former relies on detailed statistical data being available for all the crucial events relevant to the fire. Because of the lack of such data, the use of such models is severely restricted. Deterministic models predict the course of the fire using algorithms which define different aspects of the fire. They vary greatly in complexity and refinement. The simplest are zone models, which represent the fire compartment as one or two zones, with the most complex field models using finite element techniques which represent the space as many thousands of zones. It is noted that for most fire engineering problems, such detail is not required, and zone models will suffice. Janssens notes that while the use of field models will inevitably increase, they remain primarily a research tool rather than a cost effective engineering tool with widespread application, at present.

Most of the single compartment, post-flashover models are conceptually similar and calculate compartment gas temperatures from a heat balance which balances heat generation with cumulative heat losses. To obtain accurate estimates of the gas temperatures, an accurate assessment of the heat release rate is required. It is in the latter area that many of the fundamental differences between the mathematical models exist.

Ödeen (1963, 1970) split the heat release rate into two parts, one released inside the compartment and one outside, but then set the latter to zero. It was thus very similar to that of Kawagoe and Sekine (1963).

Tsuchiya and Sumi (1971) developed a hydrocarbon burning model where the fuel was characterised by a generalised formula $C_xH_yO_z$ with a pre-defined moisture content. Burning rate could be either ventilation limited (after Kawagoe & Sekine), or fuel surface

controlled where the burning rate is specified by the surface regression rate. The mass flow of combustion gases is calculated, and specific heat of those gases varied with temperature.

The model of Harmathy (1972) calculated a steady temperature averaged over the complete fire. The fraction of the heat release within the compartment varied as a function of the ratio of the compartment height to the flame height.

Thomas and Nilsson (1973) also developed a steady state model incorporating ventilation limited, crib porosity controlled, and crib fuel surface controlled fires. The heat release rate is calculated from the difference between the heat of combustion of the pyrolysed gases minus the heat required to pyrolyse the gases. Heat conduction through the wall was obtained by simple analytic expression rather than one of the more rigorous finite difference methods.

Bullen and Thomas (1979, 1980) developed a compartment model for liquid pool fires, with a radiation model to calculate radiation from the compartment to the liquid fuel, and thus estimate the mass loss rate of the fuel. Calculation of the heat loss through the walls was via a simplified method, rather than one of the more rigorous finite difference methods.

Bøhm and Hadvig (1982) developed a crib-based model with either wood or plastic combustible material.

Babrauskas (1975, 1979) developed the COMPF and subsequently the COMPF2 model. The latter has crib porosity, fuel surface, ventilation limited, and liquid pool capability. The model determines both convective and radiative heat transfer.

Nakaya and Akita (1983) developed a model for liquid fuel fires, with the conductivity of the wall being considered a linear function of temperature.

The COMPF2 model of Babrauskas (1979) is considered by Janssens to be "perhaps the most comprehensive" post-flashover fire model.

2.5.3 Fire Load Surveys

In examining the use of post-flashover fire models used for predicting structural resistance to fire, Harmathy and Mehaffey (1983) note that the two most important factors which affect the fire intensity, fire load and ventilation, are random variables. The mass of combustibles based on many surveys, (quoted in terms of wood equivalent fire load) varies widely with different occupancies, but equally widely within the same type of occupancy. Ventilation also has random characteristics depending on the number of windows and doors open, and the varying effects of stack effect due to temperature differences, and infiltration due to wind.

Typical mean and standard deviation of fire loads based on a survey of varying occupancies (after Harmathy and Mehaffey, 1983), and the 95th percentile (mean + 1.64 σ) are :

Occupancy	**Fire Load in kg of wood m $^{-2}$ floor area**		
	Mean	**Standard Deviation (σ)**	**95th Percentile**
Housing	30.1	4.4	37.3
Office	24.8	8.6	38.9
School	17.5	5.1	25.9
Hospital	25.1	7.8	37.9
Hotel	14.6	4.2	21.5

Table 2.4 Fire Load Survey (after Harmathy and Mehaffey, 1983)

Wider ranging surveys showing very wide variation in the above parameters is summarised (Babrauskas, 1976) in Table 2.5.

Fire Load in kg m^{-2} of Floor Area	**Cumulative Probability**			
	25%	**50%**	**80%**	**99%**
Offices USA	20	35	50	100
West Germany	25	43	60	130

Fire Load in kg m^{-2} of Floor Area		Cumulative Probability			
		25%	50%	80%	99%
	Sweden	24	28	38	70
	Holland	5	10	24	46
	England	5	20	32	110
Residences	Sweden	37	40	45	53
Schools	Sweden	17	22	26	43
Hotels	Sweden	15	18	22	34
Hospitals	Sweden	30	33	35	71

Table 2.5 Fire Load Survey (after Babrauskas, 1976)

2.6 Pre-Flashover Fire Models

2.6.1 Review by Janssens

Pre-flashover models are inherently more complex than post-flashover models. Many try to estimate movement of heat and gases between multiple compartments, in a growing fire scenario using a zone model approach. These normally approximate each compartment as having a hot upper zone and cooler lower zone, with energy and momentum being transferred between zones by the developing fire plume. The thermal properties within each zone are considered uniform. Some of the pre-flashover models have capabilities of modelling post-flashover conditions as well.

The range of pre-flashover models identified by Janssens (1992) was :

Authors	Model
Emmons, Mitler and Trefethen (1978)	HARVARD CFC III
Zukoski and Kubota (1980)	CALTECH
Quintiere and McCaffrey (1980)	NBS
Pape and Waterman (1981)	RFIRES
Emmons and Mitler (1982)	HARVARD CFC V

Authors	Model
MacArthur (1982)	DACFIR
Cooper, Stroup and Walton (1982)	ASET
Smith, Satija, Sauer and Green (1983)	OSU
Tanaka (1983)	BRI
Curtat (1983)	CSTB
Gahm, Rockett and Morita (1983)	HARVARD CFC VI
Hägglund (1983)	HYSLAV
Jones (1985)	FAST
Ho, Siu, Apostolakis and Flanagan (1986)	COMPBRN
Dietenberger (1987)	HEMFAST
Mitler and Rockett (1987)	FIRST
Davis and Cooper (1989)	LAVENT
Forney and Cooper (1990)	CCFM
Jones and Forney (1990)	CFAST
Wickström and Göransson (1990)	SP
Magnusson and Karlsson (1990)	LUND
Dietenberger (1991)	FFM
Birk (1991)	FIRM

Table 2.6 Pre-flashover Fire Models (after Janssens 1992)

The various HARVARD codes developed over a 10 year period by the Building and Fire Research Laboratory of the National Institute of Standards and Technology (NIST) were amongst the most comprehensive and widest used of the earliest developed pre-flashover models. These codes have been further developed to create the FIRST programme, which predicts fire growth in a single compartment with multiple passive vents, forced ventilation, and up to four combustible objects. The FAST programme was created by Jones in 1985, and has since been transformed into the most advanced of the zone model based smoke and fire transport models. Parts of the CCFM Programme were incorporated leading to CFAST (Peacock et al, 1997). A simplified version of the latter has subsequently been created, FASTLite (Portier et al, 1996). Both these programmes continue to be upgraded, with upgraded code available as beta

versions, often prior to the release of formal documentation describing the basis of the revised codes.

2.6.2 CFAST and FASTLite

Two of the currently very widely used pre-flashover fire models are CFAST and FASTLite. Both have capability of modelling post flashover fires.

CFAST is a two zone model mainly intended for pre-flashover fires. It has been developed continuously, and continues to be developed and verified by comparison with experiment (Jones et al, 1996). It allows up to three layers of differing materials for each of the compartment surfaces, and the ceiling, floor and walls can all be of different construction. Thermal properties are assumed constant for all materials, primarily because few real materials of construction have detailed temperature dependent thermo-physical properties well established. It is possible to run CFAST beyond flashover, but this is not common practice, because of the difficulty of specifying a heat release rate that is appropriate for pre-and post-flashover fires.

FASTLite is a "stripped down" version of CFAST, designed for easier use on smaller buildings. FASTLite has a special post-flashover module which is based in FIRE SIMULATOR from FPETOOL. This module allows the heat release rate to be controlled by fuel area or ventilation in a rational manner, with the combustion and temperature still calculated by the CFAST equations.

In a review of FASTLite's capability of predicting post-flashover fires, Buchanan (1998c) noted that flashover is assumed to occur at 600 °C, at which time the programme allows a number of user-selected options, to differentiate the pre and post-flashover behaviour, including fuel description and ventilation.

Both fuel surface and ventilation controlled burning regimes are allowed for post-flashover fires. For the fuel surface controlled regime, the burning rate (and the subsequent heat release rate) is based on the ambient heat radiation (which is fixed within the programme at a value of 70 kW m^{-2}), and the heat of gasification of the fuel (which is user-selectable). There is no dependence of burning rate with the fuel geometry. While appropriate to liquid pool fires, this approach is simplistic for bulky fuels such as wood, where the burning rate has various forms of fuel element size dependance. The fuel is effectively regarded as being spread across a varying fraction

of the internal surfaces of the fire compartment, depending on the user's selection of fuel properties.

Although a combustion efficiency term is allowed in the fuel surface controlled burning, this is not incorporated in the ventilation controlled burning equations.

The duration of burning for fuel controlled burning, is governed by the mass loss rate calculated as a function of the (fixed) radiation feed back to the fuel surface and the heat of gasification of the fuel.

Buchanan noted that especially for ventilation controlled fires, the calculated temperatures are higher than those predicted by other models, and although easy to use, FASTLite requires verification if it is to be used for the design of structures to resist post-flashover fires. Buchanan made no comparison with real fires. Amongst the suggestions for improvement were easier characterisation of fire load, better representation of wood burning via both crib burning and size dependent stick burning models, incorporation of a combustion efficiency factor for ventilation controlled fires, providing more detail on material properties within the database, allowing for heat loss through window radiation, and including the effect of ceiling openings.

3 COMPF2PC PROGRAMME

3.1 Introduction

The COMPF programme developed in 1975 (Babrauskas, 1975) to predict the time dependent temperature for a range of post-flashover fires, had a number of original features compared with the models in use at the time. These included the inclusion of fuel controlled fires (rather than only ventilation controlled fires), allowed for temperature dependent wall properties, and introduced the concept of "pessimisation". The latter is a technique developed to produce a maximum severity temperature versus time curve for a given fuel load, and compartment geometry. Pessimisation is discussed in some detail in Section 3.4.3.

COMPF was itself subsequently improved (Babrauskas, 1979) to produce the COMPF2 model and COMPF2PC programme. The latter added routines which dealt with pool fires, densely packed cribs, the option for steady state as well as transient solutions, the inclusion of SI units, and improved numerical techniques especially for equation solving. Both programmes were developed to provide a tool to address fire severity implications for specific structural design.

The COMPF2PC programme allows for the use of wood, plastic and liquid fuels. Programme output includes gas temperatures, heat flows and mass flow variables. The programme ignores the early stages of fire development, since the pre-flashover stages are not considered a threat to structural elements. The calculations start at a time immediately following flashover. The fire itself therefore effectively started some time in the past, and any fuel consumed before flashover is not included in the calculation. This displacement of time has been dealt with variously, with Thomas (1997) for example, adding six minutes to all calculated times for pre-flashover fire development.

3.2 Model Assumptions

The main assumptions included in the COMPF2 programme are :

(a) The fire compartment is very well stirred, and gas temperatures are equal at all locations within the compartment (that is, variations in temperature are ignored).

(b) The model is quasi-steady and while the variation in heat release rate and conduction losses is incorporated within the model, it ignores time rate of change terms in gas phase mass and energy balance.

(c) Ventilation is by a single aperture in a vertical wall only. The two way flow of hot gases exiting the window, and cold gases entering the window, is induced only by the fire. External wind effects, the effects of mechanical ventilation and air conditioning systems etc are ignored. The thermal discontinuity that must occur when cold outside air flows into the room in contra-flow to the hot products of combustion flowing out of the room, is assumed to be a layer close to the floor below the level of the window. The exact location below the window level is immaterial.

(d) Burning rate is controlled either by air supply or fuel availability. Specific gas phase kinetics are not modelled.

(e) Walls and ceiling are modelled as homogeneous solids of finite thickness. Materials of construction are allowed to have temperature dependent properties.

3.3 Model Theory

The detailed theory on which the COMPF programmes are based is described in detail (Babrauskas, 1976) and summarised in Babrauskas and Williamson (1978). A slightly altered version of the theory is summarised for the COMPF2 programme in Babrauskas (1979). The latter uses a heat balance equation of the form :

$$\dot{h}_c - \dot{m}_f (h_{T_f} - h_{298}) - Q_w - Q_r - Q_{ep} = 0 \qquad (3.1)$$

where $\dot{h}_c$ = combustion enthalpy of hot gases at T_g ($J\ s^{-1}$)

$\dot{m}_f$ = mass flow rate of hot gases ($kg\ s^{-1}$)

h_{T_g} = enthalpy of hot gases at T_g ($J\ kg^{-1}$)

h_{298} = enthalpy at ambient temperature ($J\ kg^{-1}$)

Q_w = heat flow through wall (W)

Q_r = heat flow through window by radiation (W)

Q_{ep} = heat loss via excess pyrolysates (W)

Window radiation loss (Q_r), with emissivity (ϵ) assumed equal to 1, is given by the simple radiative heat transfer expression of :

$$Q_r = A_v \sigma (T_g^4 - T_o^4) \qquad (3.2)$$

where A_v = ventilation area (m^2)

σ = Stephan Boltzmann constant (5.67×10^{-8} W m^{-2} K^{-4})

T_g = hot gas temperature (K)

T_o = ambient temperature (K)

Wall (and ceiling) losses are calculated using both convective and radiative components as follows :

$$Q_w = A_w [\sigma \frac{1}{1/\epsilon_g + 1/\epsilon_w - 1} (T_g^4 - T_w^4) + h (T_g - T_w)] \qquad (3.3)$$

where A_w = area of wall including ceiling (m^2)

σ = Stephan Boltzmann constant (5.67×10^{-8} W m^{-2} K^{-4})

ϵ_g = emissivity of hot combustion gases

ϵ_w = emissivity of wall including ceiling

T_g = hot gas temperature (K)

T_w = temperature of wall including ceiling (K)

h = convective heat transfer coefficient (W m^{-2} K^{-1})

The hot gas emissivity is a function of both band radiation from CO_2 and H_2O components of the combustion products, and radiation from the soot which is a product of incomplete combustion of the pyrolysates within the compartment. The emissivity of the soot component of the flame is expressed as a function of the absorption coefficient (which is a function of the material burning) and the flame thickness. For compartment sizes greater than 2 or 3 metres, the flame emissivity is close to 1 for most fuel types. A flame emissivity of $\epsilon_f = 0.9$ is assumed as the default.

Because of the assumption that the compartment is a well stirred reactor, the convective heat transfer coefficient for the wall (h) is difficult to characterise on the fire

side. Values used are based on correlations for turbulent flow over a flat plate. Several different versions are used, with Babrauskas (1976) and Babrauskas and Williamson (1978) giving the following expressions, which are based on McAdams (1954) :

$$h = K (T_g - T_w)^{1/3} \tag{3.4}$$

where h = heat transfer coefficient (W m^{-2} K^{-1})
T_g = hot gas temperature (K)
T_w = wall temperature (K)
K = 1.52 (horizontal surfaces, fire side,)
= 1.30 (vertical surfaces, fire side, Babrauskas and Williamson, 1978)

Babrauskas and Williamson (1978) note that under post-flashover conditions, the values of heat transfer coefficient (after McAdams, 1954) will be too low. Babrauskas (1979) provides the same form of expression for the fire side heat transfer coefficient but selects a value of K = 5.0 in Equation 3.4 to best fit the data. For the non-fire side, Babrauskas (1979) uses a coefficient of K=1.87 in Equation 3.4

Enthalpy of combustion, $\dot{h}_c$ is the lesser of the fuel controlled case of:

$$\dot{m}_p \Delta h_c b_p \tag{3.5}$$

where $\dot{m}_p$ = mass flow rate of pyrolysates (kg s^{-1})
Δh_c = calorific value (J kg^{-1})
b_p = combustion efficiency

or the ventilation controlled case of:

$$\frac{\dot{m}_{air}}{r} \Delta h_c b_p \tag{3.6}$$

where $\dot{m}_{air}$ = mass flow rate of air (kg s^{-1})
r = stoichiometric air / fuel ratio
Δh_c = calorific value (J kg^{-1})

b_p = combustion efficiency

In the equations above b_p is the combustion efficiency which is poorly known, with typical ranges used of $0.7 \leq b_p \leq 0.9$.

The air mass flow rate at the window is given by :

$$\dot{m}_{air} = \frac{2}{3} c_d \rho_o \left[2 g \frac{1 - W_g T_o / W_o T_g}{[1 + (W_o T_g / W_g T_o [1 + (\dot{m}_p / \dot{m}_{air})]^2)^{1/3}]^3} \right]^{1/2} A_v \sqrt{H} \qquad (3.7)$$

where c_d = loss coefficient for window

ρ_o = ambient air density (kg m^{-3})

W_g = molecular weight of hot gases (kg mol^{-1})

W_o = molecular weight of ambient air (kg mol^{-1})

A_v = ventilation area (m^2)

H = height of ventilation opening (m)

The discharge coefficient c_d is typically 0.68 for normal windows. However when the window occupies a very large fraction of the whole wall, the actual air inflows appear lower than predicted by use of the above value for the discharge coefficient, a value of closer to one half the normally used discharge coefficient value fits the data best (Babrauskas and Williamson, 1978). The molecular weight of the gaseous products of combustion W_f is again poorly known, and highly variable especially for unburnt fuel gases. The programme therefore assumes the molecular weight of fuel gas products is equal to that of nitrogen.

The programme does not allow explicitly for ventilation through multiple openings although elsewhere there are a number of methods with varying degrees of accuracy to represent multiple openings as a single equivalent opening (Magnusson and Thelandersson, 1970 and others).

The heat of combustion, Δh_c, is taken as the nett value, since the hot gas outflow is assumed to be above 100 °C, and the latent heat component is ignored. The stoichiometric ratio, r , is assumed constant for each material.

The outflow mass rate, $\dot{m}_f$ is calculated by mass conservation from the sum of $\dot{m}_{air}$ and the rate of pyrolysis, $\dot{m}_p$, which is poorly known. The fuel is assumed to be converted to CO_2 and H_2O, allowing the enthalpy of the outflow products to be calculated. Production of CO is ignored because it's mass fraction will be small, and because of the wish to ignore reaction kinetics. Only elemental carbon, hydrogen, oxygen and nitrogen have been considered for any particular fuel source.

The last term of Equation 3.1, Q_{ep} is the heat required to vaporise excess pyrolysates. This is already included in the heat of combustion Δh_c because of the definition used for the latter.

The second major equation to be solved is that for heat conduction through the wall.

$$\rho C_p \frac{\partial T_w}{\partial t} = \frac{\partial}{\partial x}\left(k \frac{\partial T_w}{\partial x}\right) + \dot{q}''' \qquad (3.8)$$

where ρ = density of walls and ceiling (kg m^{-3})
C_p = specific heat of wall (J $kg^{-1} K^{-1}$)
T_w = temperature of wall (K)
t = time (s)
x = distance through wall from fire side (m)
k = thermal conductivity of walls (W $m^{-1} K^{-1}$)
$\dot{q}'''$ = heat release per unit volume (J m^{-3})

The walls are assumed to be at an initial ambient temperature of T_o and subject to boundary conditions on the fire side of :

$$-k \frac{\partial T_w}{\partial x} = h\,[T_g - T_w(0)] + \epsilon\,\sigma\,[T_g^4 - T_w(0)^4] \qquad (3.9)$$

and on the unexposed side :

$$-k \frac{\partial T_w}{\partial x} = h\,[T_w(L) - T_0] + \epsilon\,\sigma\,[T_w(L)^4 - T_0^4] \qquad (3.10)$$

where T_g = temperature of hot gases (K)

h = convective heat transfer coefficient ($W\ m^{-2} K^{-1}$)
$T_w(0)$ = temperature of wall at x = 0 (K)
$T_w(L)$ = temperature of wall at x = L (K)
L = thickness of wall (m)
T_0 = ambient temperature (K)

The fire side heat transfer coefficient has been given in Equation 3.4. For the unexposed side the heat transfer coefficient is given by :

$$h = 1.87 [T_o - T_w(L)]^{1/3} \quad (3.11)$$

3.4 **Pyrolysis Rates**

3.4.1 Liquid or Thermoplastic Pools

Because thermoplastic fuels tend to melt and burn in a pool-like manner, pool fire theory is used to detail both. To use theory to predict the course of liquid pool fires, it is assumed that the fuel is pyrolysed solely by the radiant heat flux from the compartment, which the fuel sees with a view factor of one, and itself with a view factor of zero. In this case the pyrolysis rate is given by :

$$\dot{m}_p = A_f \frac{q}{\Delta h_p} \quad (3.12)$$

where $\dot{m}_p$ = mass flow rate of pyrolysates ($kg\ s^{-1}$)
A_f = area of fire (m^2)
q = $\epsilon\ \sigma\ (T_g^4 - T_b^4)$
T_g = hot gas fire temperature (K)
T_b = surface temperature at which pyrolysis occurs (K)
Δh_p = heat of pyrolysis ($J\ kg^{-1}$)

While (3.12) is adequate for a steady state solution, with a time varying fire, the initial radiation feedback from the hot compartment is much smaller than the feedback from the fire plume itself. A relatively crude empirically derived plume pyrolysis rate is used

(based on analysis of data from Burgess et al, 1961 and Modak and Croce, 1976) of the

$$\dot{m} = 0.0014\ A_f \left[\frac{\Delta h_c}{\Delta h_p}\right] \quad (kg\ s^{-1}) \tag{3.13}$$

form :

where A_f = area of fire (m^2)

Δh_c = calorific value $(J\ kg^{-1})$

Δh_p = heat of vaporisation $(J\ kg^{-1})$

Although crude, this term contributes little, therefore an approximate expression is considered justified. As the room temperature increases, the relative importance of this term reduces. For a room which acts as a black body in terms of its radiative heat transfer characteristics, and especially at high temperatures, the plume term should be negligible. The reducing interaction of the plume feedback to the pyrolysis rate as overall compartment temperatures increase, is modelled by multiplying the plume term with a factor before adding to the far-field term. The proportionality factor used, χ (≥ 0), is calculated from :

$$\chi = 1.0 - \frac{T_g^4 - T_b^4}{1700^4 - T_b^4} \tag{3.14}$$

where T_g = temperature of hot gases (K)

T_b = vaporisation temperature for fuel (K)

Thus for the plume, $\dot{m}_p = \dot{m}\ \chi$ (3.15)

The fact that plume effects are considered to affect pyrolysis rate when an inherent assumption for the programme is that gas temperatures are uniform throughout, is inconsistent. This inadequacy only effects the early stages of the modelling of fuels which require the use of the pool and thermoplastic code calculations.

3.4.2 Solid Fuels

For solid fuels, there is plentiful empirical data for mass loss rates from wood planks in post-flashover fires. The rates are very sensitive to the room radiation characteristics. For large isolated panels of wood, a range of burning regression rates of 0.007 - 0.015 mm/s was deduced as a function of temperature between 538 and 926 °C respectively by Schaffer (1966).

For large thin wood panel fuel, the regression velocity(v_p) from Tamanini (1974), can be applied when D < 0.05 m, and is given approximately by :

$$v_p = 1.7 \times 10^{-6} D^{-0.6} \quad (m\ s^{-1}) \tag{3.16}$$

This gives greater regression rates for panels with thinner sections.

For wooden items which are large in one dimension, and smaller but not thermally thin in the other dimensions, use of a constant regression rate on each surface would result in double counting at the corners. For various regularly shaped fuel elements, Babrauskas (1976) and Babrauskas and Williamson (1978) derived the following, based on a method developed by Ödeen (1963).

$$\frac{\dot{m}_p}{M_o} = \frac{F}{C}\left(\frac{m}{M_o}\right)^{1-1/F} \tag{3.17}$$

where M_o = total mass before fire (kg)

m = mass remaining at time (t) (kg)

F = 1 for an infinite plane

= 2 for cylinders and rectangular sticks

= 3 for spheres and cubes

and C, the time it takes for m to go to zero is given by ,

C = $D / 2 v_p$

where D = smallest original fuel dimension (m)

v_p = regression velocity ($m\ s^{-1}$)

Equation (3.17) can be integrated against time to show at any time (t):

$$\frac{m}{M_o} = \left(1 - \frac{t}{C}\right)^F, \quad \text{for the fuel amount (m)}$$

and, $\frac{\dot{m}_p}{M_o} = \frac{F}{C}\left(1 - \frac{t}{C}\right)^{F-1}$, for the mass loss rate ($\dot{m}_p$)

For varying shape factor (F) this leads to the following relationships for the mass loss rate as a function of initial fuel mass (M_0), nominal burning time ($C = D / 2\, v_p$) and actual time (t):

F=1 Infinite plane exposed on both sides, $\dot{m}_p = \frac{M_o}{C}$

F=2 Cylinder or rectangular stick, $\dot{m}_p = 2\frac{M_o}{C}\left(1 - \frac{t}{C}\right)$

F=3 Sphere or cube, $\dot{m}_p = 3\frac{M_o}{C}\left(1 - \frac{t}{C}\right)^2$

and for an infinite plane exposed on one side only, $\dot{m}_p = \frac{M_o}{2C}$

According to this model, the pyrolysis rate is constant for an infinite plane (F = 1), decreases linearly as a function of time for a long sticks (F = 2), and decreases as a parabolic function of time for spherical or cubical fuel elements (F = 3).

There are two regimes of crib burning, corresponding to well ventilated and under ventilated cribs. For sparsely packed wood cribs burned in the open air (corresponding to the well ventilated case), Yamashika and Kurimoto (1976) give a mass loss rate :

$$\frac{\dot{m}_p}{M_o} = \frac{0.027}{D^{1.6}}\left(\frac{m}{M_o}\right)^{1/2} \quad h^{-1} \qquad (3.18)$$

If the spacing of the crib sticks is sufficiently small, the pyrolysis rate will become limited by the rate at which gases can traverse the openings (the under ventilated case). For this, the pyrolysis rate can be approximated as being for a sparse crib, multiplied by ψ to allow for the effects of packing density, where ψ is given by :

$$\psi = 490\sqrt{hD}\left(\frac{S}{h}\right)^{3/2} \qquad (3.19)$$

where h = total height of crib (m)

S = clear spacing between sticks (m)

For wood cribs within compartments, the above correlations are not directly applicable, since the boundary conditions in a compartment fire are very different from those for an open air fire, with much higher ambient temperatures, and lower oxygen mass fractions within the compartment, particularly after flashover.

For wood crib fire data from Nilsson (1971) and Yamashika and Kurimoto (1976), Babrauskas (1979) developed a simplified set of relationships is used for three crib burning regimes. The pyrolysis rates used for the three regimes are as follows :

Fuel Surface Control

$$\dot{m}_p = \frac{4}{D} v_p \left(\frac{m}{M_o} \right)^{1/2} M_o \qquad (kg\,s^{-1}) \tag{3.20}$$

where v_p = regression rate ($m\,s^{-1}$)

D = dimension of stick (m)

m = mass of crib in kg at time(t) (s)

M_o = initial mass of crib (kg)

$v_p = 1.7 \times 10^{-6} D^{-0.6}$ ($m\,s^{-1}$)

and $m = M_o - \sum_{i=1}^{t} \dot{m}_i (t_i)\, \Delta t$

This implies that the pyrolysis rate varies with time as the mass of the crib reduces. The actual pyrolysis rate is proportional to the square root of the ratio of the fuel mass (m) at time (t) to the initial fuel mass (M_0). Once the combustible mass M_o is decided, the initial pyrolysis rate is solely a function of the fuel surface regression velocity and fuel element dimension.

Crib Porosity Control

$$\dot{m}_p = 4.4 \times 10^{-4} \left(\frac{S}{h_c} \right) \frac{M_o}{D} \qquad (kg\ s^{-1}) \tag{3.21}$$

S / h_c is the ratio of stick clear spacing to crib height, and other variables are as previously defined. This implies a nominally constant pyrolysis rate with time.

Room Ventilation Control

$$\dot{m}_p = 0.12\, A_v \sqrt{H} \qquad (kg\ s^{-1}) \tag{3.22}$$

where A_v = area of ventilation opening (m^2)
and H = height of ventilation opening (m)

This implies a constant pyrolysis rate independent of fuel characteristics. (The coefficient of Equation 3.22 is significantly at variance with the literature. This is discussed further in Section 4).

If crib burning is selected, the COMPF2PC programme calculates all three pyrolysis rates, and uses the lowest as the predictor of the pyrolysis rate at any particular time. This governing pyrolysis rate can be converted via the nett calorific value of the fuel, and a factor for the maximum fraction of pyrolysates burnt, to a governing heat release rate. The mechanism governing the heat release can change throughout the duration of a fire, especially from ventilation controlled to fuel surface control. For some fire loads and ventilation conditions, heat release rate will stay almost constant, being governed by the room ventilation control parameter for example. In other cases, the fire may be either crib porosity controlled (again with a nominally constant heat release rate) or fuel surface controlled, where the heat release rate varies with time.

Application of the model and it's sensitivity to various combination of parameters is discussed in Babrauskas and Williamson (1979).

(Note that the programme code differs from the theory detailed in Babrauskas and Williamson (1978) and Babrauskas (1979). Several "constants" in the theory are actually coded as functions of timber density within the computer code. In addition, the equation used to represent crib fuel surface controlled pyrolysis is different in the code, from that documented. Refer to Section 4.2 for a more detailed discussion).

3.4.3 Pessimisation

If all parameters affecting a fire are known, a deterministic model can be used to predict the temperature outcome. Usually not all parameters are known, particularly in the design phases of as yet unbuilt structures. The lack of complete knowledge leads to the desirability for alternative approaches. The simplest approach is a parametric

method which uses a design fire curve which is expected to be close to that which would occur. Thus relatively few design curves can provide a suitable design curve for a vast number of alternative fire engineering problems.

The main problem with a full deterministic approach is that the number of variables is large. Babrauskas (1976, 1979) developed the pessimisation approach as a tool to reduce the number of variables, by continually adjusting one or more of them to give the most conservative value (within limits). Pessimisation is therefore analogous to but the inverse of optimisation.

Pessimisation could result in a "worst case" approach, by putting all variables at the value required to create the most negative impact. For example simultaneous pessimisation of three variables such as fuel load, ventilation and boundary thermal properties, would provide a worst case fire with infinite duration and temperature at the adiabatic flame temperature (T_{ad}). This is of course, unrealistic, and therefore unhelpful for design purposes.

Babrauskas found that attempting to pessimise two significant variables simultaneously was little more useful than pessimising all variables simultaneously. The most useful approach resulted from specification of two variables and pessimising the remaining variable.

This approach is summarised in Table 3.1 which summarises the consequences of pessimisation of various combinations of the variables fuel load, ventilation and wall thermal properties:

Variable Specified (✓)			**Fire Duration**	**Fire Temperature**
Fuel Load	Ventilation	Wall Thermal		
P	P	P	Infinite	Adiabatic Flame Temp, T_{ad}
✓	P	P	Finite	T_{ad}
P	✓	P	Infinite	T_{ad}
P	P	✓	Infinite	Curve, close to T_{ad}
✓	✓	P	Finite	Usually less than T_{ad}
✓	P	✓	Finite	Curve, variable
P	✓	✓	Infinite	Curve, variable

Variable Specified (✓)			Fire Duration	Fire Temperature
Fuel Load	Ventilation	Wall Thermal		
✓	✓	✓	Finite	Curve, variable, deterministic

Table 3.1 Pessimisation Alternatives (after Babrauskas, 1976)

Pessimisation of only a single variable results in generally useful output, although pessimisation of wall thermal properties, can result in temperatures close to the adiabatic flame temperature if combustion conditions are close to stoichiometric. On this basis specification of wall properties and either ventilation or fuel load, and pessimisation of the non-specified variable, provides the most utility.

As incorporated into COMPF and COMPF2, fires can be specified as pessimised on pyrolysis, or pessimised on ventilation.

Pessimisation on Ventilation

If the actual ventilation conditions are specified absolutely, the pyrolysis rate can be varied to obtain the highest possible temperature at each time step. The latter occurs at close to stoichiometric conditions.

Conversely if the actual fuel load (and indirectly the pyrolysis rate by selection of either stick burning, crib burning or pool burning) is specified, the programme can vary the window width (and the ventilation factor) at each time step to obtain the maximum temperature. Since the window or ventilation geometry is specified as input to the programme, the pessimisation routine varies the window width to achieve higher compartment temperatures, using values only below or equal to those specified. This simulates the effect of only partial window opening and reduced ventilation, compared with the assumption that all windows would fully break during the earlier stages of the fire development.

The specified window height is used, and window widths are adjusted only to values which are less than the input value effectively specified (the input data is actually window area and window height).

The effects of the pessimisation routine are demonstrated in Figure 3.1 which shows a number of simulations using COMPF2PC for a fire compartment of heavy concrete construction, with wood fuel load of density 60 kg m^{-2} of floor area. All the fires are simulated as crib burns using Nilsson's formulae, with a fuel stick size of 0.075 m and a crib stick spacing to height ratio of 0.10.

The ventilation factor for the sample runs is varied from 0.01 - 0.10, and a single run pessimised on ventilation is shown (which has a nominal ventilation factor of 0.055).

For each of these fires, the predicted temperature, predicted pyrolysis rate, burning rate within the compartment, remaining fuel percentage, air mass flow rate into the compartment, and the heat release rate are tabulated for the initial (time = 0) condition, following 5 minutes of burning, and at the time of the predicted maximum temperature condition, for each of the ventilation ratios, including the pessimised ventilation condition, in Table 3.2.

Ventilation Factor ($m^{0.5}$)	Fire Phase	Temp. (°C)	Pyrolysis Rate (kg s^{-1})	Burning Rate (kg s^{-1})	Mass % Remaining	Air Flow In (kg s^{-1})	Heat Release (MW)
0.01	Initial	433	0.085	0.057	-	0.031	0.86
	5 minutes	479	0.085	0.057	95.9%	0.028	0.86
	At T_{max}	710**	0.085	0.057	58.2%**	0.028	0.86
0.03	Initial	717	0.247	0.165	-	0.90	2.49
	5 minutes	785	0.247	0.163	88.0%	0.89	2.46
	At T_{max}	1060	0.176	0.166	12.9%	0.90	2.41
0.05	Initial	867	0.417	0.274	-	1.49	4.14
	5 minutes	941	0.381	0.273	79.8%	1.48	4.12
	At T_{max}	1122	0.283	0.278	34.7%	1.52	4.05
0.10	Initial	924	0.436	0.428	-	3.15	6.44
	5 minutes	965	0.379	0.371	79.0%	3.18	5.59
	At T_{max}	967	0.370	0.362	82.4%	3.19	5.46
Pessimised	Initial	903	0.413	0.303	-	1.64	4.57
	5 minutes	990	0.344	0.304	80.9%	1.65	4.58
	At T_{max}	1128	0.260	0.255	35.5%	1.38	3.84

Table 3.2 Example Fires, Pessimised on Ventilation

** The peak temperature in this simulation had not been reached at the end of the simulation.

All fires show an initial state where the burning rate within the compartment is substantially less than the pyrolysis rate except for the very well ventilated fire (ventilation factor = 0.10). After 5 minutes, the poorly ventilated fires (ventilation factor =0.01 and 0.03) still have much the same burning and pyrolysis rates as their initial values. Conversely the relatively well ventilated fires (ventilation factor =0.05, 0.10 and pessimised) all show the pyrolysis rate reducing from the initial high value. The burning rate drops similarly, but not in proportion, indicating a reduction in unburnt pyrolysates.

Over or under ventilated fires have lower peak temperatures as evidenced by the fact that the fires with ventilation factors of 0.01 and 0.10 have lower peak temperatures than those with ventilation factors of 0.03 and 0.05.

The fire pessimised on ventilation has a similar temperature profile to that of the Ventilation Factor = 0.05 simulation initially, and similar to that of the Ventilation Factor = 0.03 simulation in its later stages. The fire pessimised on ventilation has an initial pyrolysis rate very close to that of the Ventilation Factor = 0.05 simulation, but the burning rate is significantly higher and the air inflow higher leading to a greater initial heat release rate and a greater initial compartment temperature. As the simulation progresses, after 5 minutes, the pyrolysis rate is slightly lower than that of the Ventilation Factor = 0.05 simulation, but the burning rate is still higher, compartment temperature higher by 49 °C, and the mass fraction remaining slightly higher. At the maximum temperature condition, the pessimised fire has a slightly greater remaining fuel mass fraction.

Pessimisation on Pyrolysis

A similar demonstration of pessimisation on pyrolysis is presented in Figure 3.2. The simulations are characterised for the same heavy weight compartment as used in the example above, with a fixed ventilation factor of 0.055. The fuel loads are varied from 15 to 120 kg m^{-2} of floor area, with the fuel packages being in the same form as for the ventilation pessimised fires discussed above. The pessimised fire presented is for the 60 kg m^{-2} fire load case. The predicted temperature, predicted pyrolysis rate, burning rate within the compartment, remaining fuel percentage, air mass flow rate into the

compartment, and the heat release rate are tabulated for the initial (time = 0) condition, following 5 minutes of burning, and at the time of the predicted maximum temperature condition, for each of the fire loads, including the pessimised pyrolysis condition, are presented in Table 3.3.

Fire Load ($kg\ m^{-2}$)	Fire Phase	Temp. (°C)	Pyrolysis Rate ($kg\ s^{-1}$)	Burning Rate ($kg\ s^{-1}$)	Fuel Mass % Remaining	Air Flow In ($kg\ s^{-1}$)	Heat Release (MW)
15	Initial	445	0.109	0.107	-	1.85	1.61
	5 minutes	460	0.095	0.093	79.0%	1.86	1.40
	T_{max}	462	0.108	0.106	82.4%	1.86	1.59
30	Initial	725	0.218	0.214	-	1.79	3.22
	5 minutes	764	0.189	0.185	79.0%	1.80	3.12
	T_{max}	764	0.211	0.207	79.0%	1.78	2.79
60	Initial	897	0.436	0.301	-	1.63	4.53
	5 minutes	976	0.379	0.301	79.0%	1.63	4.53
	At T_{max}	1127	0.308	0.302	41.2%	1.66	4.51
120	Initial	891	0.455	0.299	-	1.62	4.50
	5 minutes	966	0.455	0.293	89.0%	1.59	4.42
	At T_{max}	1224	0.320	0.300	10.5%	1.63	4.51
Pessimised	Initial	931	0.318	0.312	-	1.69	4.70
	5 minutes	1013	0.313	0.307	84.7%	1.67	4.62
	T_{max}	1223	0.307	0.301	0.0%	1.63	4.54

Table 3.3 Example Fire, Pessimised on Pyrolysis

The fires with lower fire loads (15 and 30 kg m^{-2}) maintain nominally constant pyrolysis and burning rates which are equal, indicating that close to complete combustion is achieved within the compartment. Those fires with higher fire loads (60 and 120 kg m^{-2}) reduce slowly in pyrolysis rate, and have relatively constant burning rates up to the time of maximum fire temperature, but those burning rates are substantially lower than the pyrolysis rate. This indicates ventilation limited fires are occurring with some combustion occurring outside the fire compartment. While maximum compartment temperatures increase with increasing fire load, the percentage of fuel remaining at the time of maximum compartment temperature decreases from 82.4% remaining at 15 kg m^{-2} fire load, to 10.4% remaining at the 120 kg m^{-2} fire load.

The fire pessimised on pyrolysis (at a 60 kg m^{-2} fire load) has a higher compartment temperature, a lower pyrolysis rate, a higher burning rate and a greater heat release rate than the 60 kg m^{-2} fire load simulation itself. The pyrolysis rate and burning rates reduce only slowly until all the fuel is expired, leading to the rather unconventional rapid decay characteristic. The pessimised fire achieves a maximum temperature 1 °C lower than that for the 120 kg m^{-2} fire load case after all the fuel has been burnt (remaining mass fraction = 0%).

It is apparent from Figure 3.2 that fires with higher fuel loads, reach higher maximum temperatures. The fire loads of 60 kg m^{-2} and above give growth curves that are closest to the pessimised curve. The pessimised on pyrolysis fire decays very rapidly because all fuel has been consumed at the time maximum compartment temperature is reached. This is different to the pessimised on ventilation example, where 35.5% of the fuel remains at the time maximum compartment temperature is reached.

Conclusions

It would appear that pessimisation on ventilation provides a more realistic temperature versus time profile than pessimisation on pyrolysis, because it still provides a reasonable decay curve. However not all fires pessimised on ventilation have the "well rounded" characteristic demonstrated in Figure 3.1. The pessimised temperature versus time prediction for a given fire load and ventilation factor, can still be highly variable as shown in Figures 3.3 and 3.4. These figures demonstrate that whether crib burning or stick burning is used, the pessimised fire prediction can still be highly variable both in terms of maximum temperature, and duration.

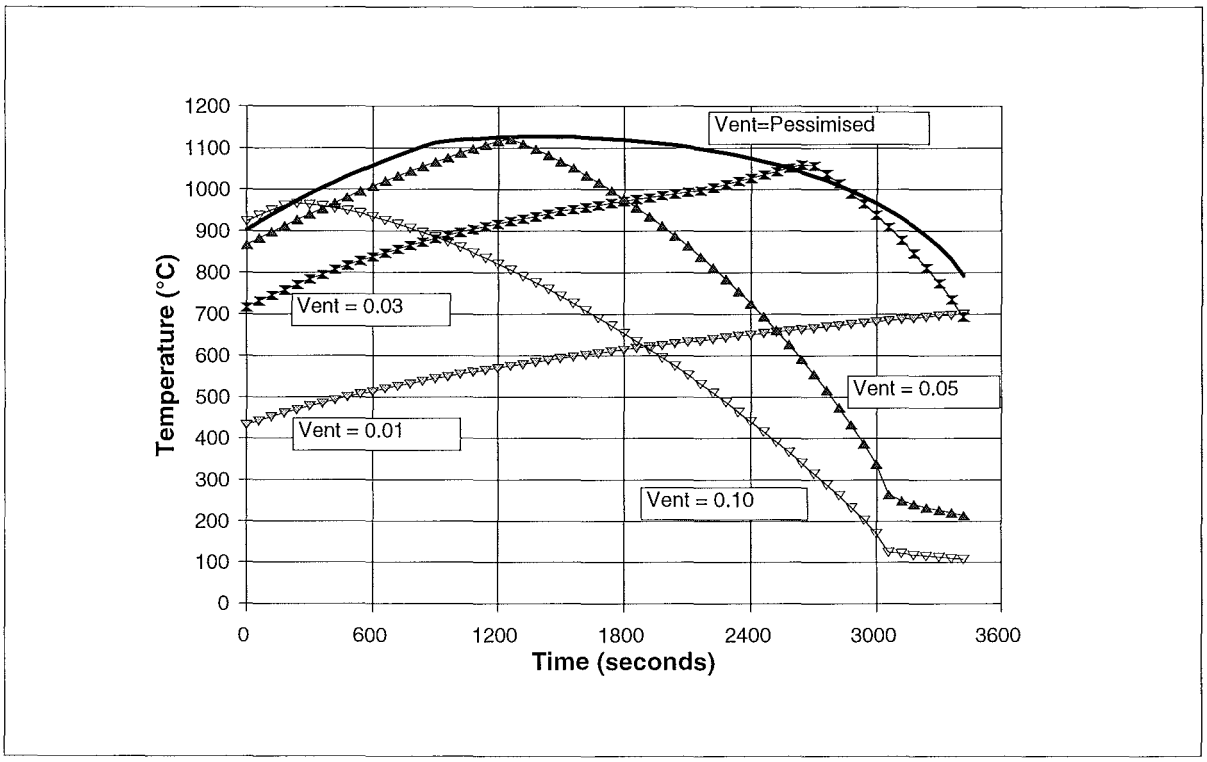

Figure 3.1 Fire Load 60 kg/m² Floor Area, Ventilation Factor 0.01 - 0.10, Pessimised on Ventilation

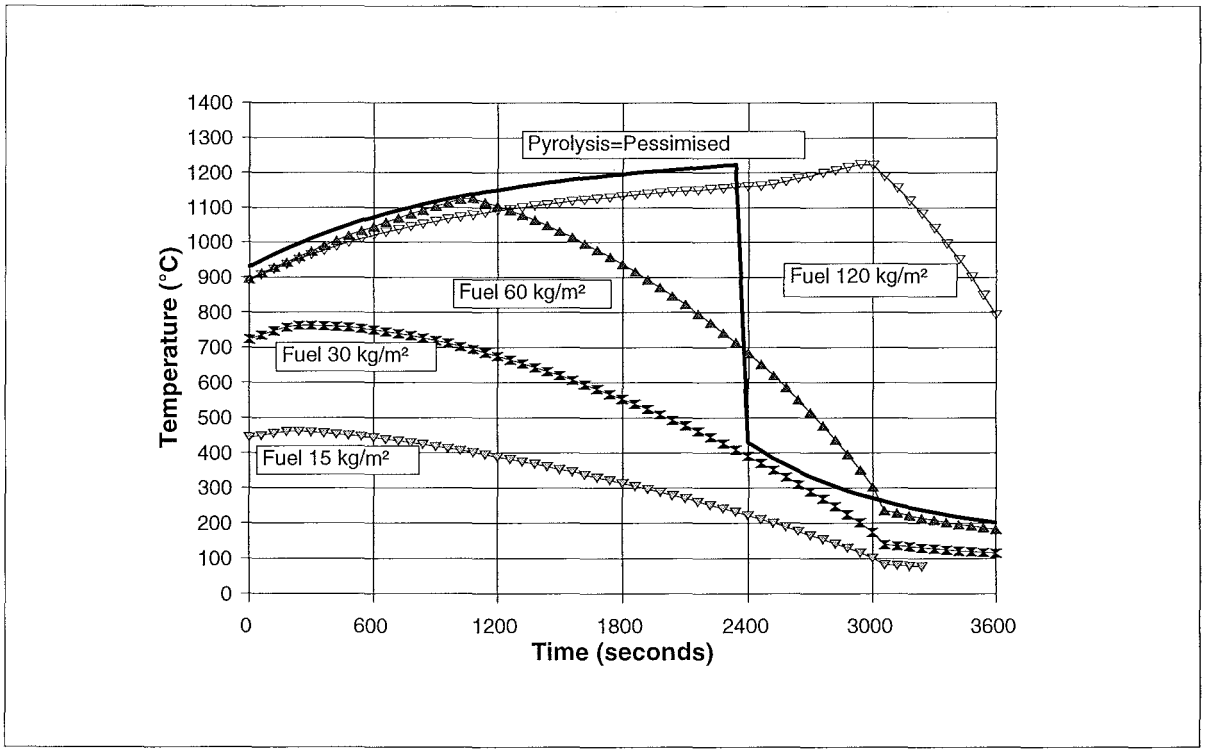

Figure 3.2 Fire Load 15 - 120 kg/m² Floor Area, Ventilation Factor 0.055, Pessimised on Pyrolysis

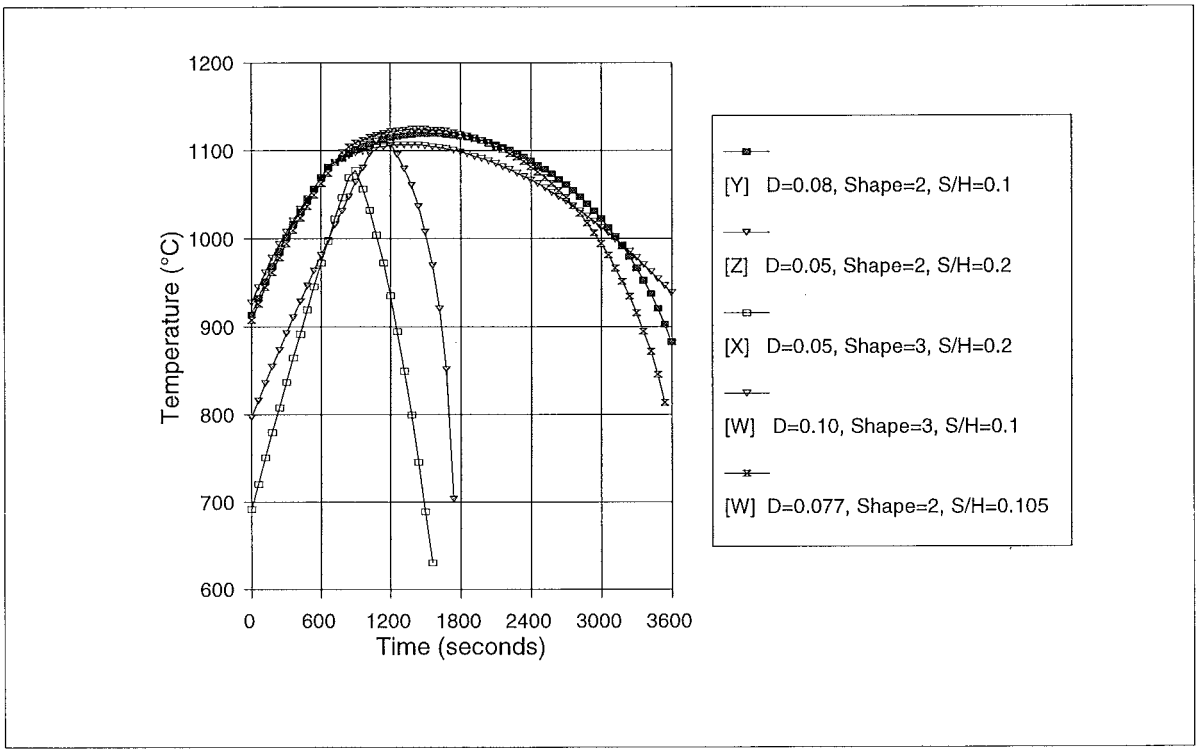

Fig. 3.3 Fire Load 60 kg/m², Ventilation Factor = 0.055, Various Crib Fires Pessimised on Ventilation

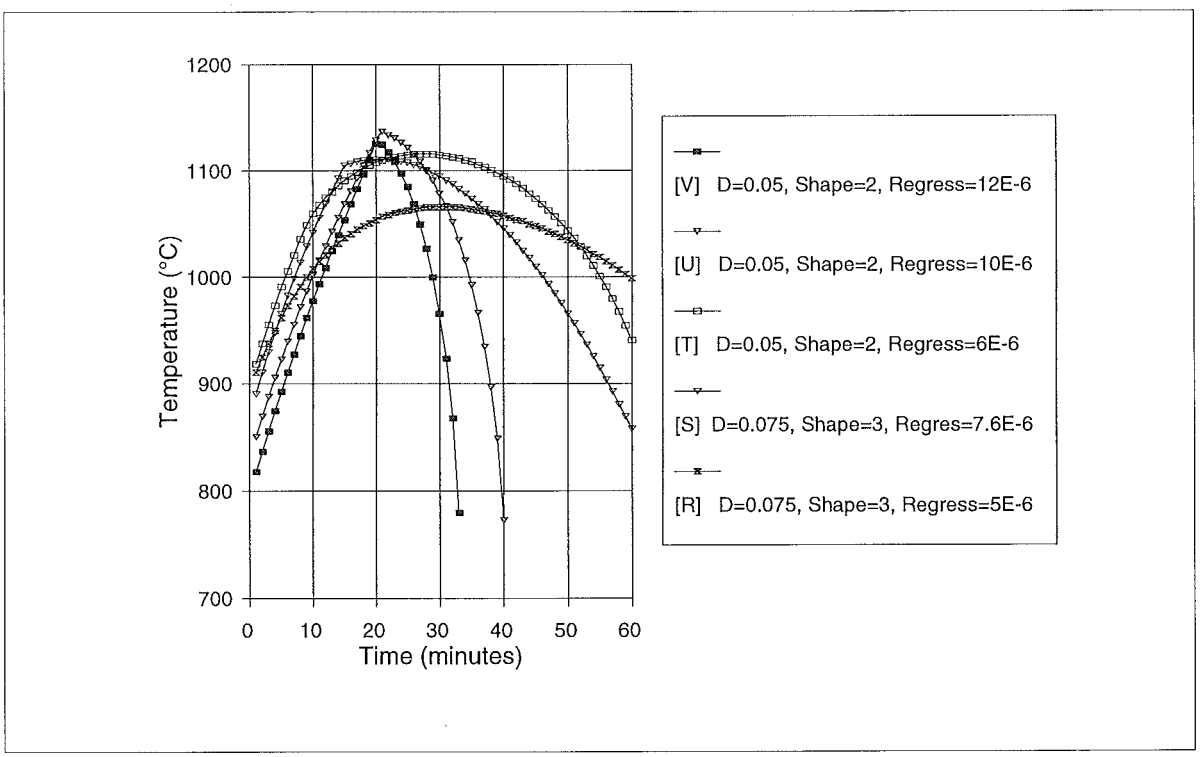

Fig. 3.4 Fire Load 60 kg/m², Ventilation Factor = 0.055, Various Stick Fires Pessimised on Ventilation

4 THE THEORETICAL AND EMPIRICAL BASIS OF COMPF2

4.1 Crib Burning in Compartments

COMPF2 contains equations based on correlations developed on crib burning experiments carried out by a number of experimenters. The original data and related data are examined.

4.1.1 CIB Crib Fires

Much of the experimental data in relation to crib combustion was obtained over a limited range of geometrical parameters. For example the wood stick thickness (b) and spacing (s) data for the CIB crib burning experiments was limited to the following ranges:

Fuel Thickness (b), (mm)	Spacing (s) (mm)	Spacing Ratio (s/b)	$(sb)^{0.5}$ (mm)	Probable controlling factor
10	30	3	17	Crib porosity, unless $A_V \sqrt{H} / A_T$ is small
20	6.6	⅓	11	Crib porosity, unless $A_V \sqrt{H} / A_T$ is small
20	20	1	20	Crib porosity, unless $A_V \sqrt{H} / A_T$ is small
20	60	3	34	Ventilation or surface control
40	40	1	40	Ventilation or surface control

Table 4.1 CIB Crib Burn Experiments, after Thomas (1974)

The CIB data showed (Thomas, 1974) that stick spacing ratio was a significant variable in comparison with the stick size itself.

4.1.2 Nilsson's Crib Fires

Nilsson (1971, 1974) reported tests at model scale in three cubical chambers with internal dimensions of 0.50, 0.75 and 1.0 metres. The front face of the cubical chamber was adjusted to give different ventilation conditions, with ventilation factors $A_V \sqrt{H} / A_T$ in the range 0.02 - 0.114 $m^{0.5}$. The test chamber construction was varied to create

different thermal properties from the base construction of 1.5 mm thick sheet steel, to sheet steel lined with asbestos sheet 10 mm thick of density 1020 kg m^{-3}, and sheet steel lined with 125 mm of light weight concrete of density 500 kg m^{-3}.

Most tests were carried out at a constant fire load, using wood sticks of constant cross sectional dimension of 25 x 25 mm. To determine the effects of crib porosity on the rate of pyrolysis, the number of sticks per layer, and the number of layers in each crib was varied. For these fires, the length of sticks was adjusted to give a constant length (fire load) of 35 MJ m^{-2} of total bounding surface area (approximately 2 kg m^{-2}) . At the same time the compartment properties were held constant (sheet steel and asbestos internal lining). The effects of crib porosity were evaluated for a range of ventilation factors.

The crib porosity factor ϕ, is given by :

$$\phi = N^{0.5} b^{1.1} A_v / A_s \qquad (4.1)$$

where N = number of layers in the crib

b = thickness of stick (assumed square cross section) (cm)

A_v = free horizontal area for vertical air flow through the crib (m^2)

$$A_v = (L - n b)^2 \qquad (4.2)$$

A_s = surface area of all sticks in the crib (m^2)

$$A_s = 2 n b \{2 N L + b [N - n(N - 1)]\} \qquad (4.3)$$

n = number of sticks per layer

L = length of each wooden stick (m)

Experiments were carried out using cribs with a range of porosity factors ϕ from 0.02 to 1.32 $cm^{1.1}$. These represent densely packed through to very porous cribs respectively.

With the stick size, fire load, and compartment geometry and materials held fixed, the mean rate of burning during the active part of the flaming phase which is assumed to occur between the burning of 80% and 30% of the initial mass (R_{80-30}), the maximum gas temperature (T_{max}) and mean gas temperature during the active flaming phase (T_{80-30}) were all investigated as a function of ϕ and the ventilation factor $A_V\sqrt{H} / A_T$.

The rate of burning R_{80-30} in kg min^{-1} is given approximately by :

$$R_{80-30} = \frac{1}{k}\left[(6.25\,\phi + 3.53)\,A\sqrt{H} - 0.165\,\phi + 0.153\right] \qquad (4.4)$$

The coefficient k was found experimentally to be 1.0 up to an opening factor ($A_V\sqrt{H} / A_T$) of 0.03, increasing linearly to a value of 1.5 as the opening factor increased to 0.07.

Nilsson also carried out test series to determine the effect of fire load in the range 17.5 - 87.5 MJ m^{-2} of total bounding surface area (approximately 1 - 5 kg m^{-2}). The tests were carried out with constant stick thickness (0.025 m), constant crib porosity (Φ = 0.5 cm $^{1.1}$), single ventilation factor ($A_V\sqrt{H} / A_T$ = 0.04) and single chamber construction (1.5 mm steel with 10 mm asbestos lining).

A similar series of tests to determine the effects of stick thickness in the range 0.01 - 0.05 m were carried out. For these two opening factors were used ($A_V\sqrt{H} / A_T$ = 0.04 and 0.114), the fire load was held nominally constant at 52.5 MJ m^{-2} of total bounding surface area (approximately 3 kg m^{-2}), and a single chamber construction was used (1.5 mm steel with 10 mm asbestos lining).

A final series of tests evaluated the effect of compartment construction with the fire load held constant at 35 MJ m^{-2} of total bounding surface area (approximately 2 kg m^{-2}), the crib porosity held constant (Φ = 0.5 cm $^{1.1}$), and the ventilation factor held constant ($A_V\sqrt{H} / A_T$ = 0.04).

4.2 COMPF2 and Wood Density Effects in Crib Fires

4.2.1 Background

The theory behind the operation of the COMPF2 programme as detailed in Babrauskas (1979) is summarised in Section 3. For the solid fuel / crib burning regime, the following programme code is contained within the subroutine "CRIB" which implements wood crib fires. There are a number of significant variations between the theory as described in Section 3, and the implementation within the programme code.

```
      SUBROUTINE CRIB
C
C        CRIB FIRE ROUTINE
C        EQUATIONS FOLLOW +NILSSON'S DATA FOR WOOD CRIBS.
C        OTHER FUEL CRIBS CAN BE TREATED IF PYROLYSIS CONSTANTS
C        ARE KNOWN.
C
```

4.2.2 Regression Rate Specified

If the regression rate is specified (i.e. the variable REGRES is non-zero), the rate of pyrolysis is calculated as follows :

```
      ......
   40 IF (REGRES.LE.0.0) GOTO 45
C        USE THIS FORMULA IF INPUT REGRES IS SPECIFIED
      RP= REGRES*2.*SHAPE/SIZE*FLREM**(1.-1./SHAPE)*WTFUEL**(1./SHAPE)
      GO TO 50
   45 CONTINUE
      ......
```

where

RP	= rate of pyrolysis (kg s^{-1})	
REGRES*2./SIZE	= 1/C	
SHAPE	= F	
FLREM	= m	(kg)
WTFUEL	= Mo	(kg)

The specified regression rate "REGRES" is substituted into Equation (3.17) based after Ödeen,(1963) , rearranged to calculate the pyrolysis rate (RP). With the regression rate specified, the fuel surface controlled and crib porosity controlled pyrolysis formulae which follow, are not calculated.

4.2.3 Fuel Surface Control

If the fuel surface regression parameter REGRES is not specified (i.e. it is set to zero), the fire is computed as a crib fire, which has governing equations for both crib porosity and crib fuel surface control.

For fuel surface controlled crib fires, the rate of pyrolysis (RP1) is calculated as follows:

```
C         FUEL SURFACE CONTROL
C         ASSUME CRIB STICK DENSITY RHOCR= 500 KG/M**3
      RHOCR= 500.
      REGREN= 1.24E-3/RHOCR*SIZE**(-0.6)
      RP1= REGREN*2.*SHAPE/SIZE*FLREM**(1.-1./SHAPE)*WTFUEL**(1./SHAPE)
      ......
```

This section of code first implements a modified form of Equation (3.16), the regression formula of Tamanini (1974), to calculate the regression rate (REGREN). The encoded form of the equation is different, in several respects from that detailed in Babrauskas (1976, 1979) and Babrauskas and Williamson (1978). The coefficient "1.7 x 10^{-6}" in Equation (3.16) after Tamanini, becomes a function of wood density (i.e. the coefficient is "1.24 x 10^{-3}/ ρ") in the programme code. The programme assumes that all wood fuel has density of 500 kg m^{-3}. If the value for wood density assumed in the programme of 500 kg m^{-3} is substituted into the equation in the computer code, the effective equation becomes :

```
REGREN= 2.48E-6*SIZE**(-0.6)
```

The coefficient of the regression rate equation is significantly at variance with the Equation (3.16) and will predict a regression rate (and pyrolysis rate) for fuel surface controlled crib fires approximately 46% higher than that based on the use of Tamanini's equation. To obtain the same effective coefficient "1.7 x 10^{-6}" as obtained by Tamanini, the wood density assumed in the programme would need to be 729 kg m^{-3}, which is far greater than the density of common (or uncommon) woods available in New Zealand and elsewhere. This value of the coefficient of the regression rate equation is also different from that listed in Babrauskas (1981), which recommends 2.2 x 10^{-6}, for slabs of dimension less than 0.05 m, and a constant rate of 8.5 - 10.0 x 10^{-6} for thick slabs of dimension greater than 0.05 m.

The calculated regression rate is then substituted, not into a coded form of Equation (3.20) as indicated in Babrauskas (1979), but into Equation (3.17) with a "calculated" surface regression rate rather than a "user specified" surface regression rate. The latter form of the equation implies that the pyrolysis rate of cribs can be a function of the shape factor (F), unlike Equation (3.20) which from Babrauskas, (1979), is based on the crib burning experiments of Nilsson (1971) and Yamashika and Kurimoto (1976), and effectively allows for no other than the expected stick geometry.

For the fuel surface controlled crib burning regime, the programme therefore "allows" a crib to be composed of spherical or cubic objects. As noted in Section 6 and Appendix B, this representation of the fuel package, actually provides one of the better means of reproducing test fire temperature versus time curves.

Thus the encoded form of the fuel surface controlled crib fire equation, is significantly at variance with the theory both within the programme documentation (Babrauskas, 1979) and elsewhere (Babrauskas, 1981).

It has subsequently been indicated (Babrauskas, 1998) that subsequent to the initial publication, improvements to the code were made by students at Berkeley and at the Worcester Polytechnic Institute (WPI). The incorporation of a density term was required (effectively to convert from volume pyrolysed to mass pyrolysed), and because of the inconsistency in charring rate literature, some judgement was used in modifying the code.

Given the sensitivity of pyrolysis rate to timber density, it should be noted that the actual density of wood can vary considerably from the programme's assumed value of 500 kg m^{-3}, with ranges from 340 - 650 kg m^{-3} (Table 5.12 of Drysdale, 1985).

Another problem is that there are several different definitions of wood density in common use, depending on the moisture content of the wood. The range of properties of woods typically used for furniture and construction purposes in New Zealand is highly variable. The specific density data for New Zealand timbers from Baines (1984) presented on the basis of nominal density (oven-dry mass / volume at 12% moisture content; oven dry basis) ranges for native timbers from 690 kg m^{-3} for hard beech to 410 kg m^{-3} for Kahikitaea (native white or yellow pine). The relatively common native timbers rimu, kauri, tawa and totara have densities of 520, 520, 650 and 430 kg m^{-3} respectively. Of the exotic timbers, pinus radiata is by far the most common, with an average density of 420 kg m^{-3}. Collins (1983) also provides useful background on the properties of New Zealand timbers.

Baines indicates that the typical net calorific value of oven dry wood in New Zealand is 19.2 MJ kg^{-1} ± 10%. As the moisture content of the wood increases, the net calorific value decreases. For example, at a moisture content of 10% (on wet wood basis) the calorific value has decreased to about 16.9 MJ kg^{-1} of wet wood, while at a 15% moisture content the net calorific value has decreased to 15.8 MJ kg^{-1}.

4.2.4 Crib Porosity Control

The calculated rate of pyrolysis (RP2) in crib fires controlled by the internal ventilation of the crib due to the stick array being closely packed, is implemented as follows :

```
      ......
C        CRIB POROSITY CONTROL
      RP2= 0.22*WTFUEL/(RHOCR*SIZE)*SH
      ......
```

This above code section calculates Equation (3.21). Again the constant coefficient "4.4 x 10^{-4}" as expressed in the theory, is a function of wood density in the computer programme, being expressed as 0.22/ρ. For ρ = 500 kg m^{-3}, the computer code and theory give the same answer.

It is of interest to compare the variation in calculated pyrolysis rate for the "standard" wood of 500 kg m^{-3} density, and a range of New Zealand native and exotic species for an initial fuel weight of WTFUEL = 1000 kg, actual fuel weight of FLREM = 1000 kg, stick dimension of D = 0.05 m, shape factor SHAPE = 2 for rectangular sticks, and spacing to height ratio for the crib of SH = 0.2.

Species	Density ($kg\ m^{-3}$)	Fuel Surface Control		Crib Porosity Control	
		Pyrolysis Rate ($kg\ s^{-1}$)	% Variation from Standard	Pyrolysis Rate ($kg\ s^{-1}$)	% Variation from Standard
Programme Standard	500	1.197	-	1.76	-
Pinus Radiata	420	1.425	19	2.095	19
Kauri	520	1.151	-3.8	1.692	-3.9
Rimu	520	1.151	-3.8	1.692	-3.9
Tawa	650	0.921	-23.1	1.354	-23.1
Totara	430	1.392	16.3	2.047	16.3

Table 4.2 Predicted Pyrolysis Rates For Varying Wood Density

It can be concluded that based on the correlations included within the programme, the

pyrolysis rates of real timbers can vary by at least ± 20% from the values predicted by the COMPF2PC programme because of variations of real timber density from the constant value assumed in the programme.

4.2.5 Ventilation Controlled Fires

The pyrolysis rate for ventilation controlled fires (RP3) is calculated as follows :

```
      ......
C        ROOM VENTILATION CONTROL
      RP3= 0.120*AWDOW*SQRT(HWDOW)
      ......
```

The above code section calculates Equation (3.22). The coefficient of 0.12 is greater than the value of 0.09 kg s^{-1} $m^{5/2}$ which has been found from both test data (Kawagoe, 1958), and theory (Drysdale, 1985).

Babrauskas appears to use the higher valued coefficient based on consideration of both the theory and actuality of ventilation controlled fires. The theory (Babrauskas (1976), Babrauskas and Williamson (1978), Drysdale (1985) and many others) shows that for a ventilation controlled post-flashover fire, with a single ventilation opening in a vertical plane, following some suitable substitutions for ambient air temperature, ambient air density and the loss coefficient of the ventilation aperture, that the mass flow rate of air into the fire is given by :

$$\dot{m}_{air} \approx 1880\ A_v\sqrt{H} \qquad (kg\ hr^{-1})$$

The stoichiometric combustion rate of wood is taken as 5.7 kg of air per kg of timber in deriving the above relationship. Therefore the mass rate of pyrolysis for wood in kg s^{-1}, for stoichiometric combustion is given by :

$$\dot{m}_p \approx \frac{1880}{3600\ 5.7} A_v\sqrt{H} \qquad (kg\ s^{-1})$$

or,

$$\dot{m}_p \approx 0.09\ A_v\sqrt{H} \qquad (kg\ s^{-1})$$

The form of the equation coded in COMPF2PC allows for the rate of pyrolysis to be enhanced by a factor of 1.3 to allow for compartment effects. If no change in air flow is assumed, then the enhancement factor can be described as an equivalence ratio ϕ, where ϕ is given by :

$$\phi = \frac{\dot{m}_{p\ ,\ actual}}{\dot{m}_{p\ ,\ stoichiometric}}$$

Babrauskas (1981) notes that the increase by a factor of approximately 1.3 of the equation coefficient, to a value of 0.12, "is presumed to account for the combined effects of heating and vitiating the crib intake air".

4.2.6 Actual Pyrolysis Rate

After calculating the three pyrolysis rates RP1, RP2 and RP3, the governing rate of pyrolysis (RP) as taken as the minimum of the set.

4.2.7 Calculation of Burning Rate

Within subroutine, the burning rate is calculated from the following code sequence :

```
RP= AMIN1 (RP1,RP2,RP3)
```

Calculates the governing pyrolysis rate.

```
50 RMF= RMA+RP
```

The mass flow of fire gases (RMF) is the sum of the mass flow of air (RMA) and the mass rate of pyrolysates (RP).

```
YCO2= 3.66667*CFLPC*RC/100./RMF
YH2O= (WFLPC*RP+9.0*HFLPC*RC)/100./RMF
YO2= (0.23*RMA-R0*RC)/RMF
YN2= 0.77*RMA/RMF +NFLPC*RP/100./RMF
YPYR= (RP-RC)/RMF
IF(YPYR.LT..0) YPYR= 0.
```

Calculates the mass fraction of carbon dioxide, water vapour, oxygen, nitrogen and unburnt pyrolysates. Note that the latter is calculated by difference between the mass rate of pyrolysis and the mass rate of combustion.

```
      MWOUT= 44.*YCO2+18.*YH2O+28.*YN2+32.*YO2+MWPYR*YPYR
```

Calculates the molecular weight of the exhaust gases from the calculated mass fractions of carbon dioxide, water vapour, nitrogen, oxygen and unburnt pyrolysates.

```
      HRATIO= 1./(1.+((TGAS/TAMB)*(MWIN/MWOUT)*(1.+RP/RMA)**2)
     1    **0.3333333333)
      IF(HRATIO.LT.0.2) HRATIO=0.2
C        NOTE HIN IS TAKEN AS POSITIVE
      HIN= HWDOW* HRATIO
```

Calculates the fractional height of the neutral plane above the bottom of the ventilation opening (HRATIO) and then converts to an absolute height in metres (HIN) by multiplying by the height of the ventilation opening (HWDOW). If the calculated fractional height is less than 0.2, it is set equal to 0.2. This code represents Equation 20 of Babrauskas and Williamson (1978).

```
      ZW=1.-MWOUT*TAMB/MWIN/TGAS
      IF(ZW)195,55,55
```

Calculates one minus the ratio of the fire gas density (MWOUT / TGAS) to ambient air density (MWIN / TAMB).

```
   55 VAVGIN= 0.666667*SQRT(2.*G*HIN*ZW)
```

Calculates the average inwards velocity (VAVGIN) through the ventilation aperture by multiplying ⅔ by the square root of 2 times "g" times the absolute height of the neutral plane above the bottom of the window (HIN) by the density factor (ZW) calculated earlier.

```
      RMA= CD*VAVGIN*HIN*BWDOW*DENSA
```

Calculates the mass flow rate of air (RMA), representing Equation 19 of Babrauskas and Williamson (1978), by multiplying the window loss coefficient (CD) by the average inwards air velocity (VAVGIN) by the height of the neutral plane above the bottom of the window (HIN) by the width of the window (BWDOW) by the density of ambient air (DENSA).

```
      RMF= RMA+RP
```

Mass flow rate of fire gases (RMF) equals the mass flow rate of air (RMA) plus the mass flow rate of fuel pyrolysis gases (RP).

```
      IF (RMA/R-RP) 60,60,65
   60 RC= BPF*RMA/R
```

Fuel surface or ventilation control is determined by determining whether the ratio of air mass flow (RMA) divided by the stoichiometric air /fuel ratio (R) is less than, equal to or greater than the calculated pyrolysis rate (RP).

For ventilation controlled combustion, (RMA/R - RP $\leq$ 0), the rate of combustion (RC) is calculated by multiplying the maximum fraction of pyrolysed fuel burnt (BPF) by the air mass flow rate (RMA) divided by the stoichiometric air/fuel mass ratio (R).

```
      GO TO 70
   65 RC= BPF*RP
      FC= .TRUE.
   70 CONTINUE
```

For fuel controlled fires, (RMA/R - RP > 0) the rate of combustion is calculated from the product of the maximum fraction of pyrolysed fuel burnt (BPF) and the calculated fuel mass flow rate of pyrolysis gases (RP). An indicator flag (FC) is set TRUE to indicate that fuel surface controlled combustion exists.

```
      QFIRE= RC*CVNET
```

The heat release rate (QFIRE) is calculated by multiplying the governing rate of combustion (RC) by the net calorific value of the fuel (CVNET).

The net calorific value of the fuel is calculated earlier in subroutine ICONDS from the expression :

```
      CVNET= CVGROS*(1.-WFLPC/100.)-(WFLPC+9.0*HFLPC)/100.*2440.E+3
C        LATENT HEAT OF H2O EVAPORATION= 2440E+3 J/KG AT 25 C
```

The net calorific value is calculated from the gross calorific value (CVGROS) corrected for the percentage of water by weight in the fuel (WFLPC) and the percentage of hydrogen by weight in the fuel (HFLPC).

4.3 **Evaluation of COMPF2 by Others**

4.3.1 Harmathy and Mehaffey

Using the review method Harmathy and Mehaffey (1982) as discussed in Section 2.5.1, the COMPF programme was found to be :

(a) Comprehensive (rather than incomplete or qualitative)

(b) Based on two periods or burning, full fire development and simplified decay

(c) Variables are treated as functions of time, and calculated from equations describing momentary conditions

(d) Destructive potential of fire is quantified by the temperature history of the fire gases

(e) The compartment is regarded as a well stirred reactor (single zone)

(f) Rate of burning is based on a combination of bona fide knowledge and assumed law

(g) Is applicable to any type of fuel

(h) Rate of burning of cellulosic fuel during the period of full fire development is variable, changing with the progress of the fire

(i) Combustion is considered to take place according to stoichiometric relations

(j) Combustion outside the compartment is ignored (rather than explicitly accounted for in an empirical manner)

(k) Heat transfer to the compartment boundaries consists of radiation and convection terms (rather than radiation only)

(l) Compartment boundaries are regarded as finite thickness slabs (rather than semi-infinite solids)

(m) Thermal properties of the compartment boundaries are a function of temperature (rather than averages)

4.3.2 Hettinger and Barnett

Hettinger and Barnett (1991) used COMPF2 to simulate the effects of fire in a vehicle tunnel in order to test the design methodology of tunnel smoke control ventilation systems. The design method for the smoke control system requires the heat release

rate of the design fire as an input parameter. The use of COMPF2 was considered appropriate because it was public domain, had been validated by comparison with experimental data, and had been shown to predict results comparable to other computer programmes. The pessimisation feature of COMPF2 was used to vary the burning rate during each simulation to produce the maximum temperature profiles.

Because ventilation due to both window and door openings were required to be modelled, the source code of COMPF2 was modified accordingly. Hettinger and Barnett noted that COMPF2 allows only one material and thickness of material in the external boundaries, requiring some compromises in the simulation of the rail car, as the partitions, doors, and ceiling were constructed of different materials and thicknesses. Similarly they noted that only one burning item could be modelled, requiring careful choice to simulate the effects for the different types of fuel actually present. Since the vehicle contained much fire resistant plastic (the fire resistant character is only evident during pre-flashover fires), the post-flashover fire behaviour was modelled as that of polycarbonate.

The programme code was modified to allow for the representation of multiple ventilation openings of different sizes.

They carried out sensitivity analyses, varying the maximum fraction of pyrolysates burned from 55 to 80%, and varying the net heat of combustion from 13.65 to 19.77 MJ kg^{-1}. In all cases, the mass of fuel was varied so that the total heat content of the rail car was constant.

They noted that results of COMPF2 simulations varied considerably with changes to the input data. The heat release rate varied approximately with the net calorific value and the fraction of pyrolysates burnt. The duration of sustained burning varied with the interior heat load because the fire is ventilation controlled.

4.3.3 Wade

Wade (1995) reviews the development of post-flashover fire models, including those of Kawagoe and Sekine (1963) , Ödeen (1963), Magnusson and Thelandersson (1970), Babrauskas(1975, 1979), Harmathy and Mehaffey (1983) and others. Determination of burning rate during the fuel controlled latter stages of a fire is noted to be the most difficult aspect of specifying fire conditions, with little data available on fuel controlled

burning rates under post-flashover conditions. Wade notes that Babrauskas (1981) contains the best overall summary of pyrolysis rate data, and that the COMPF2 model has been used successfully in engineering applications.

Wade notes the limited number of pre-flashover models that attempt to model post-flashover behaviour, and concludes that at a time when interest in post-flashover fire behaviour is increasing, little research appears to have been carried out for at least a decade.

4.3.4 Thomas

Thomas (1997) made extensive use of COMPF2PC to generate design fires to determine the validity of design methods for the structural resistance of light timber frame walls and floors. Thomas noted the considerable affect of fuel package geometry (stick size) on the predicted time temperature curve for fires of fixed fuel load, ventilation and compartment geometry and material properties.

Thomas used COMPF2PC to try and reproduce the "Swedish" fires of Magnusson and Thelandersson (1970). The COMPF2PC simulations were made using a compartment of 5 x 5 m plan dimensions, 3 m high, with a window height of 1.0 m. Materials of construction were as for the Magnusson and Thelandersson Type A compartment

The relatively low window height selected for the simulations, results in window widths of 2.2, 4.4, 8.8 and 13.2 m to achieve ventilation factors of 0.02, 0.04, 0.08 and 0.12. This implies that for the ventilation factor 0.04, the window width of 4.4 metres would be almost the full width of one of the 5 m walls. For ventilation factors of 0.08 and 0.12, the window width would be 1.76 wall lengths, and 2.64 wall lengths respectively. It should be noted that none of little if any of the test data which provides the background to the COMPF2 model has been obtained with wide continuous ventilation apertures on multiple sides of the fire compartment. Even ventilation apertures close to the full width of one face of the compartment, require special modelling treatment. This aspect is discussed further in Section 6.

Thomas explored a range of model fires, with crib burns with stick sizes of 23 and 100 mm, and stick burns at a range of fire load densities to match those used by Magnusson and Thelandersson. The percentage of pyrolysates burnt in the different simulations ranged from 70% to 85%.

Because of his interest in time equivalent fires, Thomas reports the duration of fully developed combustion calculated by COMPF2PC, reported by Magnusson and Thelandersson, and calculated manually for each fire. Because COMPF2PC simulations start in a post-flashover state, Thomas added 6 minutes to the duration of simulations to allow for the fact that the "Swedish" fires start at ambient temperature.

Thomas found that the range of calculated fully developed fire durations both between COMPF2PC simulations, and between the COMPF2PC, Swedish fire and manual calculation methods, was widely at variance, particularly at low fire loads. The consistency of all methods improved with increased fire load, although substantial variation on calculated duration still occurred.

For ventilation controlled fires, Thomas found the COMPF2PC simulations agreed well with the Swedish fires in the growth and fully developed phases (particularly at low and medium ventilation factors), except the COMPF2PC peak occurs later, and the decay is far more rapid. At high ventilation factor ($A_v \sqrt{H} / A_T = 0.12$) the COMPF2PC peak temperature prediction was several hundred degrees below that of the Swedish Fire equivalent.

For fuel surface controlled fires, similar characteristics are evident, except that the COMPF2PC decay phase is not quite as steep as for the ventilation controlled fires, and the discrepancy in maximum temperature at high ventilation factor compared with the Swedish fires, is not quite as great.

Thomas concludes that it is not possible to use COMPF2PC to produce a decay phase that is as long and as hot as the Swedish fires, because COMPF2PC does not make the incorrect assumption that all of the fuels energy is released within the fire compartment.

5 EXPERIMENTAL FIRE TEST DATA

5.1 Introduction

A simple test of the adequacy of a mathematical fire model is to predict the outcome of real fires. Many experimental fires have been burnt in controlled conditions in fire laboratories throughout the world. The vast majority have used dried timber sticks in the form of a crib as the fuel source. Some have used plastic or hydrocarbon liquid fuel, and a relatively modest number have burnt out compartments fitted out to represent either commercial or residential occupancies.

Some of the data available, and used for the purposes of this report, are discussed below.

5.2 NFSC Fires

A large number of fire tests using timber, paper, furniture and various mixtures, was carried out in instrumented compartments at the Centre Technique Industriel de la Construction Métallique in France. These are reported in Arnault, Ehm and Kruppa (1973, 1974) and Roy (1993a, 1993b, 1993c) in considerable detail, and made available electronically as a spreadsheet file.

The earlier tests of Arnault, Ehm and Kruppa (1973, 1974) were mainly wood fires, but some had a fuel load consisting of a mixture of wood, paper and furniture. Comprehensive information is provided for each test including internal compartment dimensions, window dimension and sill height, and the thickness and materials of construction for the four walls, floor and ceiling. The fire compartment walls were generally of brick construction, except the wall containing the ventilation aperture was of lightweight concrete, as was the ceiling, and the floor was of refractory concrete. For some tests an additional thin layer of insulation was placed on all internal surfaces except the floor. The fire load was indicated in terms of total kilograms of wood.

For the 1973 data, three temperature profiles are provided approximately at 5 minute intervals throughout each fire, for the mean temperature, maximum and minimum temperatures recorded in the compartment. Also recorded is the mass of wood burnt

and the rate of combustion in kg s^{-1}.

The 1974 data is similar, except that the density, specific heat and thermal conductivity of the construction materials is provided, and only the mean compartment temperature profile was presented. These fires contained mixtures of material such as wood slabs, paper and furniture. Although the total fire load was still presented in terms of mass of wood, the calorific input of non wooden materials such as paper, was expressed in terms of wood-equivalent mass.

The later tests of Roy (1993a, b, c) were carried out in similarly constructed chambers, using mainly wood fuel. Other test fire data from the same organisation included burning two motor cars within a larger chamber and bedroom furniture.

Kruppa (1998) indicates that for all the fires, ten thermocouple recordings were made, with five located 700 mm below ceiling level and five 1,050 mm above floor level. Given the typical compartment height, the vertical separation between the lower and upper thermocouple array was 1,380 mm. The maximum temperature profile presented in the data is actually the maximum temperature within the compartment at any thermocouple, for the particular time step. The minimum temperature is similarly the lowest thermocouple reading anywhere within the test compartment at each time step.

The range of NFSC test fire data is summarised in Table 5.1:

NFSC NO	INPUT NO	ROOM WIDTH (m)	ROOM LENGTH (m)	ROOM HEIGHT (m)	VENT WIDTH (m)	VENT HEIGHT (m)	FIRE LOAD (kg m^{-2})	$A_V\sqrt{H}/A_T$ ($m^{0.5}$)	FIRE LOAD
4	3	4.00	4.00	2.76	0.82	2.40		0.040	Multiple vents, 77kg Plastic, 785kg paper, 1140kg wood, 118kg wool fuel
4	4	12.00	12.00	2.76			53.9		Multiple vents, 320kg Plastic, 2795kg paper, 5830kg wood, 353kg wool fuel
4	5	4.00	4.00	2.76	0.82	2.40	64.3	0.040	Multiple vents, 538kg Plastic, 4360kg paper, 3335kg wood, 353kg wool fuel

NFSC NO	INPUT NO	ROOM WIDTH (m)	ROOM LENGTH (m)	ROOM HEIGHT (m)	VENT WIDTH (m)	VENT HEIGHT (m)	FIRE LOAD ($kg\ m^{-2}$)	$A_V\sqrt{H}/A_T$ ($m^{0.5}$)	FIRE LOAD
4	6	12.00	12.00	2.76			64.3		Multiple vents, 538kg Plastic, 4360kg paper, 3335kg wood, 353kg wool fuel
40	7	5.60	22.86	2.75	5.60	2.75	40.0	0.062	Wood 5115 kg
40	8	5.60	22.86	2.75	5.60	2.75	20.0	0.062	Wood 2557 kg
40	9	5.60	22.86	2.75	5.20	1.47	20.0	0.022	Wood 2557 kg
40	10	5.60	22.86	2.75	5.20	1.47	40.0	0.022	Wood 5115 kg
40	11	5.60	22.86	2.75	2.14	1.73	20.0	0.012	Wood 2557 kg
40	12	5.60	22.86	2.75	5.20	0.38	20.0	0.003	Wood 2557 kg
40	13	5.60	5.60	2.75	1.38	2.75	20.0	0.051	Wood 626 kg
40	14	5.47	22.78	2.68	5.06	2.68	20.0	0.055	Wood 2448 kg
40	15	5.60	22.86	2.75	10.12	2.75	20.0	0.112	Wood 2557 kg
70	16	3.38	3.68	3.13	1.18	0.90	30.0	0.015	Wood 372 kg
70	17	3.38	3.68	3.13	1.18	2.18	15.0	0.055	Wood 186 kg
70	18	3.38	3.68	3.13	1.18	2.18	30.0	0.055	Wood 372 kg
70	19	3.38	3.68	3.13	1.18	2.18	60.0	0.055	Wood 744 kg
70	20	3.38	3.68	3.13	1.95	2.18	15.0	0.091	Wood 186 kg
70	21	3.38	3.68	3.13	1.95	2.18	30.0	0.091	Wood 372 kg
70	22	3.38	3.68	3.13	1.95	2.18	60.0	0.091	Wood 745.3 kg
70	23	3.38	3.68	3.13	2.18	2.92	15.0	0.157	Wood 186 kg
70	24	3.38	3.68	3.13	2.18	2.92	30.0	0.157	Wood 372.6 kg
70	25	3.38	3.68	3.13	2.18	2.92	60.0	0.157	Wood 745.3 kg
70	26	3.38	3.68	3.13	1.18	2.18	15.0	0.055	Wood 186 kg
70	27	3.38	3.68	3.13	1.18	2.18	30.0	0.055	Wood 372 kg
70	28	3.38	3.68	3.13	1.95	2.18	30.0	0.091	Wood 372 kg
70	29	3.38	3.68	3.13	1.18	0.90	30.0	0.015	Wood 372.6 kg
70	30	3.38	3.68	3.13	1.18	2.18	15.0	0.055	Wood 186 kg
70	31	3.38	3.68	3.13	1.18	2.18	20.0	0.055	Wood 248 kg
70	32	3.38	3.68	3.13	1.18	2.18	30.0	0.055	Wood 372 kg
70	33	3.38	3.68	3.13	1.18	2.18	40.0	0.055	Wood 496 kg
70	34	3.38	3.68	3.13	1.18	2.18	60.0	0.055	Wood 745 kg
70	35	3.38	3.68	3.13	1.18	2.18	30.0	0.055	Wood 372 kg
70	36	3.38	3.68	3.13	1.18	2.18	30.0	0.055	Wood 372 kg
70	37	3.38	3.68	3.13	1.95	2.18	15.0	0.091	Wood 186.3 kg
70	38	3.38	3.68	3.13	1.95	2.18	20.0	0.091	Wood 248.4 kg
70	39	3.38	3.68	3.13	1.95	2.18	25.0	0.091	Wood 310.8 kg
70	40	3.38	3.68	3.13	1.95	2.18	30.0	0.091	Wood 372.6 kg
70	41	3.38	3.68	3.13	1.95	2.18	40.0	0.091	Wood 496.8 kg
70	42	3.38	3.68	3.13	1.95	2.18	60.0	0.091	Wood 745.3 kg
70	43	3.38	3.68	3.13	1.95	2.92	15.0	0.141	Wood 186.3 kg
70	44	3.38	3.68	3.13	1.95	2.92	20.0	0.141	Wood 248.4 kg
70	45	3.38	3.68	3.13	1.95	2.92	30.0	0.141	Wood 372.6 kg
70	46	3.38	3.68	3.13	1.95	2.92	60.0	0.141	Wood 745.3 kg
70	47	3.38	3.68	3.13	1.18	2.18	30.0	0.055	Wood 372 kg
70	48	3.38	3.68	3.13	1.18	2.18	30.0	0.055	Wood 372 kg (uniform 2 x L)

NFSC NO	INPUT NO	ROOM WIDTH (m)	ROOM LENGTH (m)	ROOM HEIGHT (m)	VENT WIDTH (m)	VENT HEIGHT (m)	FIRE LOAD ($kg\ m^{-2}$)	$A_V\sqrt{H}/A_T$ ($m^{0.5}$)	FIRE LOAD
70	49	3.38	3.68	3.13	1.18	2.18	30.0	0.055	Wood 372 kg (uniform 3 x L)
70	50	3.38	3.68	3.13	1.18	2.18	30.0	0.055	Wood 372 kg (uniform 3 x L)
70	51	3.38	3.68	3.13	1.18	2.18	30.0	0.055	Wood 372 kg (uniform 4 x L)
70	52	3.38	3.68	3.13	1.18	2.18	30.0	0.055	Wood 372 kg (uniform 5 x L)
71	53	3.38	3.68	3.13	1.18	2.18	30.0	0.055	Wood 372 kg (uniform (1/3)xL + (3/3)xL + (5/3)xL)
71	54	3.38	3.60	3.13	0.90	1.06	30.0	0.014	Furniture 190kg, Paper 162kg, Pine laths 20kg
71	55	3.38	3.60	3.13	1.18	2.18	15.0	0.056	Furniture 124kg, Paper 65kg
71	56	3.38	3.60	3.13	1.18	2.18	20.0	0.056	Furniture 170kg, Paper 58kg, Pine laths 20kg
71	57	3.38	3.60	3.13	1.18	2.18	22.0	0.056	Furniture 140kg, Paper 103kg, Pine laths 25kg
71	58	3.38	3.60	3.13	1.18	2.18	30.0	0.056	Furniture 151kg, Paper 184kg, Pine laths 37kg
71	59	3.38	3.60	3.13	1.18	2.18	30.0	0.056	Furniture 140kg, Paper 207kg, Pine laths 25kg
71	60	3.38	3.60	3.13	1.18	2.18	30.0	0.056	Furniture 170kg, Paper 182kg, Pine laths 20kg
71	61	3.38	3.60	3.13	1.18	2.18	45.0	0.056	Furniture 190kg, Paper 348kg, Pine laths 20kg
71	62	3.38	3.60	3.13	1.18	2.18	45.0	0.056	Furniture 140kg, Paper 361kg, Pine laths 37kg
71	63	3.38	3.60	3.13	1.18	2.18	30.0	0.056	Furniture 165kg, Paper 187kg, Pine laths 20kg
76	64	3.48	3.63	3.15	3.00	1.50	16.0	0.079	Wood 16 kg
76	65	3.48	3.63	3.15	3.00	1.50	30.0	0.079	Wood 30 kg
76	66	3.48	3.63	3.15	1.85	2.50	30.0	0.104	Wood
182	67	8.95	6.95	2.50	1.78	1.41	31.7	0.015	Wood
182	68	5.00	5.00	2.60	0.55	1.90	22.7	0.014	Cars - 2 off, Total Fire Load 8510 MJ, 15MJ/kg of Wood
182	69	5.76	5.51	2.60	1.40	1.90	14.2	0.030	Bedroom Furniture 451 kg (measured heat of combustion 16.6 MJ/kg)
	70	2.72	5.76	2.60	0.93	2.00	9.6	0.035	Bedroom Furniture 305 kg (measured heat of combustion 13MJ/kg)

NFSC NO	INPUT NO	ROOM WIDTH (m)	ROOM LENGTH (m)	ROOM HEIGHT (m)	VENT WIDTH (m)	VENT HEIGHT (m)	FIRE LOAD (kg m^{-2})	$A_V\sqrt{H}/A_T$ ($m^{0.5}$)	FIRE LOAD
	71	2.72	5.76	2.60	0.93	2.00	18.3	0.035	Bedroom Furniture 581 kg (measured heat of combustion 10 MJ/kg) Doubled ventilation after 31 min.
	79	3.10	3.60	3.13	3.00	2.00	90.9	0.132	Wood 1015 kg
	80	3.10	3.60	3.13	3.00	2.00	58.4	0.132	Wood 652 kg
	81	3.10	3.60	3.13	3.00	2.00	58.4	0.132	Wood 651 kg
	82	3.10	3.60	3.13	3.00	2.10	59.9	0.142	Wood 668 kg

Table 5.1 Summary of NFSC Test Fire Data

5.3 Fire Research Station, Cardington

Results from nine compartment test fires carried out at the Building Research Establishment Fire Research Station at Cardington, to simulate the behaviour of full scale fires, were reported in Kirby et al (1994). Most tests were carried out in a large compartment of nominal dimensions 23 m x 6 m x 3 m in height.

The test compartment roof was constructed of 200 mm aerated concrete slabs with walls of 215 mm lightweight concrete block. The floor consisted of 75 mm dense concrete, and was covered with 125 mm of sand. For all tests (except Test No. 8) the walls and ceiling were lined internally with 2 x 25 mm layers of ceramic fibre.

A range of tests was carried out with two fire load densities and variable ventilation. Although the permanent compartment structure was fully open at the 6 m wide entrance, the variable ventilation arrangements were made by constructing a temporary wall of lightweight concrete blocks across the open aperture. Tests were carried out with the exterior 6 m x 3 m aperture from fully open to one eighth open.

Fire loads of 20 or 40 kg m^{-2} were generated using wood cribs distributed evenly throughout the compartment. Generally each crib was 1 m square, and for the full size compartment tests, 33 were uniformly spread across the floor of the compartment in a 3 by 11 array, to create a fire load as uniform as possible. The sticks within each crib were 50 mm x 50 mm softwood, kiln dried to 10% moisture content, separated by a gap

of 50 mm. Typically each stick weighed 1 kg, equivalent to a mean density of 400 kg m^{-3}.

Temperatures were monitored above the second, sixth and tenth cribs (interior, middle and ventilated end of the compartment).

Most fires were ignited at the rear (interior) of the compartment at crib line 1. The highly dynamic fire spread behaviour was influenced by the high aspect ratio compartment shape. Following ignition, the fire would typically spread only slowly to adjacent cribs, would develop a hot gas layer, and then spread rapidly to the cribs near the ventilation opening at crib line 11. The time from ignition to complete involvement was between 9 and 30 minutes in most tests (taking longer with the plasterboard lined compartment test). After full development (flashover), the fire intensity at the cribs furthest from the ventilation opening would reduce due to lack of oxygen, with combustion eventually stopping. Burning would then progress from the "window" line back into the compartment.

In test 9, all cribs were ignited simultaneously, but following flashover, the same behaviour was noted. The data were obtained for the study of time equivalent fires as described by Wang et al (1996). Comparison was made of the observed temperature versus time with the predictions of Eurocode 1 Part 2.2, Pettersson et al (1976), and a formula of their own invention. The compartment and fire load data is presented in Table 5.2.

Parameter	Test No.								
	1	2	3	4	5	6	7	8	9
Fire load (kg)	5115	2558	2558	5115	2558	2558	2558	2558	2558
Fire load (kg m^{-2} of floor)	40	20	20	40	20	20	20	20	20
Fire load (MJ m^{-2} of floor)	760	380	380	760	380	380	380	402	380
Window width (m)	5.595	5.595	5.195	5.195	2.139	5.195	1.37	5.065	5.195
Window height (m)	2.75	2.75	1.47	1.47	1.73	0.375	2.75	2.68	2.75
Window area (m^2)	15.39	15.59	7.637	7.637	3.701	1.948	3.77	13.57	14.29
$A_v \sqrt{H} / A_T$ ($m^{0.5}$)	0.06	0.06	0.02	0.02	0.01	0.005	0.10	0.06	0.06

Table 5.2 BRE Compartment and Fire Data, after Kirby et al (1994)

Similarly the materials properties of the compartments are presented in Table 5.3.

Element	Material	Density ρ ($kg\ m^{-3}$)	Specific Heat Cp ($J\ kg^{-1}\ K^{-1}$)	Thermal Conductivity k ($W\ m^{-1}\ K^{-1}$)
Walls	Lightweight Concrete Blocks	1375	753	0.42
Roof	Aerated Concrete slabs	450	1050	0.16
Floor	Fluid Sand	1750	800	1.0
Lining (1)	Ceramic Fibre	128	1130	0.02
Lining (2)	Fireline Plasterboard	900	1250	0.24

Table 5.3 Compartment Material Properties, after Kirby et al (1994)

5.4 **BHP, Melbourne**

5.4.1 Fires in Offices

A series of fire tests has been carried out by BHP Australia in Melbourne. These have involved "real" furniture and office fit outs burnt within experimental compartments. While some tests were to evaluate sprinkler operation and therefore were therefore extinguished prior to flashover, some were allowed to burn out.

As reported by Thomas et al (1989) several tests were carried out to observe the nature of the fire generated by typical office fit outs, the fire effects on structural steelwork, and the fire spread characteristics to adjacent spaces. The test building structure was designed to represent a section of a larger building. The test segment had three levels, with the first level a car park, an atrium and three offices on the second level, and an open platform over the offices on the third level (with the atrium extending above). The offices were of 4 x 4 m plan dimensions. The structure was steel columns and beams supporting reinforced concrete floors on steel decking form work.

The fire load was the 45 kg m^{-2} wood equivalent. For this fire, the office was enclosed on three sides by a panel of one 12 mm layer of non fire rated board on the inside, and one layer of 16 mm fire rated board on the outside, on steel studs. The door had a one hour fire rating. The external wall had a "window" of plastic sheet, of dimensions 4,000

x 2,800 mm, "supported" on a partition of 900 mm high gypsum.

Following ignition by lighting a waste paper basket under a desk, the fire growth was slow, even given the presence of a window constructed of plastic sheet material. After combustion appeared to stop, the door to the exterior was opened for 8 minutes to allow the fire to re-establish. Flashover occurred after 26 minutes, and full room involvement lasted for 2 minutes, followed by burning of individual furniture items. Ceiling tiles began to fall after 27 minutes. Shortly after flashover, no ceiling tiles remained.

The air temperature history reflects the above sequence with temperatures reaching only 80 °C after 20 minutes, then increasing rapidly to over 1100 °C following the temporary increase of ventilation (via the office door), and the melting of the plastic "window". Temperatures then dropped rapidly to stabilise between 600 - 800 °C for about 30 minutes as the localised burning continued.

5.4.2 140 William Street

A series of four fire tests was carried out in Melbourne by Thomas et al (1992) prior to a refurbishment of the 140 William Street building. The tests were designed to investigate the effectiveness of the existing sprinkler installation, and the consequences of not respraying the steel structural elements to replace the asbestos fire protection which was being removed during the refurbishment. Replacement of the structural insulation would have been mandatory under the Building Code of Australia requirements. A test building was constructed to simulate the structural conditions at 140 William Street by additions to a test building previously used in fire tests. The combined area of 315 m^2 was still small compared with the floor area of the real building (1520 m^2 per level).

Two fire tests were used to test the effectiveness of the existing sprinkler system design, the third was to determine the effects of a non-sprinkler controlled fire on the unprotected composite floor slab, and the fourth tested whether unprotected steel beams could perform in a non-sprinkler controlled fire.

The fire load was normal office furnishings in a somewhat crowded arrangement, including workstations, book cases, books, magazines, plastic coated folders. The wood equivalent fire loads were 52 .1 - 53.9 kg m^{-2} in the third test and 64.3 - 67.5 kg m^{-2} for the fourth test. These are very high fire loads for an office, based on the survey

data of Harmathy (1983) and Babrauskas (1976). The peak temperature in the open plan area was 1254 °C, but temperatures dropped rapidly, and was below 600 °C in most locations 11 minutes following the peak temperature.

5.4.3 380 Collins Street

A fire test was carried out in December 1991 (Proe and Bennetts, 1994) in a building constructed to simulate a section of a multi-storey office building. The purpose was to collect fire data from a burn out of office furniture, in order to reach conclusions in regard to the protection of steel structures.

A typical office furniture layout was used, with an equivalent total fire load of 44 kg of wood per m^2 floor area. The fire compartment test area was 8.4 x 3.6 m, with two of the external boundaries similar to that of the proposed building, 10 mm plate glass windows supported in aluminium mullions. The other two exteriors were plain steel sheet (an attempt to simulate the effect of being part of a much larger compartment), A non-fire rated suspended ceiling was installed. The tiles were of plaster construction with a fibreglass backing blanket.

Fire growth was slow, and the door to the outside had to be opened several times over the first 12 minutes, until a window broke. Unassisted fire growth then lead to flashover after about 30 minutes. Only two ceiling tiles fell out, those around the perimeter were largely undamaged, and the remainder had lost part of their thickness, but still had an intact fibre glass backing.

It was concluded that the temperatures tended to be lower close to the windows during the fully developed phase. It was also concluded that the non-fire rated ceiling protected both the structural members above, and external columns close to windows.

Although it is not relevant to the immediate subject matter of this report, the writer notes that the conclusions in regard to the level of protection afforded by the non-rated ceiling may be far from universally applicable. Firstly the ceiling tiles of plaster plus fibreglass construction, are not universal in commercial ceilings. Most commercial tile systems do not have a fibre glass insulation layers, and are manufactured either from plaster, and common less expensive tile systems are manufactured from light weight compressed fibre. As such the thermal resistance of a normal commercial suspended ceiling would be lower than that of the test, and the thermal inertial characteristics would be much

worse for those ceiling systems based on compressed fibre tiles.

In addition, the ceiling in the test compartment as indicated in Figure 11(c) Photos Before Test (in the referenced report), had no penetrations for either recessed lighting or air conditioning or ventilation diffusers and grilles. Given that such penetrations will in most cases significantly compromise the thermal integrity of the ceiling grid (especially if a very common plenum return system is being used for the air conditioning or ventilation system), the conclusions from the test cannot be reliably be extrapolated.

6 SIMULATION OF FIRES USING COMPF2PC

6.1 Methodology

The COMPF2PC programme which implements the COMPF2 model, requires all input parameters for the programme to be specified. The programme input parameters fall into five basic categories :

(a) Type of simulation e.g. normal, adiabatic, steady state, pool fire, pessimised on ventilation, pessimised on pyrolysis etc, and other simulation control parameters such as the calculation and printing time increments, and the maximum time of the simulation run. Only a single fire type can be simulated in any one model execution.

(b) Compartment geometric details including ventilation arrangement and material specification including heat transfer properties.

(c) Type of fuel and it's characteristics, including the percentages of carbon, hydrogen, nitrogen, water and oxygen by weight, heat of gasification, the molecular weight and the specific heat of pyrolysis gases, and the maximum fraction of the fuel pyrolysates to be burnt.

(d) More detailed fuel parameters, e.g. stick size, stick shape, stick burning regression rate or crib parameters for wood fire simulation such as spacing to height ratio.

(e) Programme parameters which specify aspects of the simulation such as the number of layers to use for wall conduction calculations, whether time dependent values for conductivity and specific heat are used, and so on.

The 46 input parameters representing the above quantities are not arranged in logical groupings, but in alphabetical order. The input parameters and their typical values are presented in Table 6.1 for a wood burning simulation with a fire load of 40 kg m^{-2}, with the fuel represented as long wooden sticks, and the pyrolysis being fuel surface controlled with a surface regression rate of 10×10^{-6} m s^{-1}.

Parameter	Typical Value	Definition
ADIA	FALSE	If true, walls are adiabatic and only a steady-state solution is sought
AFLOOR	50	Area of floor (m^2)
AWALL	100	Gross area of walls and ceiling, including window (m^2)
AWDOW	6	Area of window (m^2) (Only a single opening is allowed).
BPF	0.9	Maximum fraction of pyrolysed fuel burned to be $\leq$ 1.0
CD	0.68	Discharge coefficient of ventilation opening
CFLPC	44.4	Percent of carbon in fuel by weight (%)
CPPYR1	0.1127	Coefficient for Heat capacity calculation of pyrolysis gases (J kg^{-1} K^{-1})
CPPYR2	1010	Coefficient for Heat capacity calculation of pyrolysis gases (J kg^{-1} K^{-1})
CVGROS	18800000	Upper calorific value for dry fuel (J kg^{-1})
DENSW	790	Wall density (kg m^{-3}) (Walls, floor and roof must be of the same material)
DHP	2400000	Total heat of gasification for fuel (J kg^{-1})
DTIME	60	Increment of time step for calculations (s)
EF	0.9	Gas emissivity, assumed grey
EISCAN	FALSE	If true, solve steady-state problem in POOL for a given EITA
EITA	1	Normalised air-fuel parameter for pool burning
FLOAD	40	Fuel load (kg of timber equivalent per m^2 floor area)
FLSPEC	FALSE	If true, pessimise ventilation for a specified pyrolysis rate
HFLPC	5.4	Percent of hydrogen by weight in fuel (%)
HWDOW	1.5	Window height (m)
IRUN	1	Run problem number
IX	10	Number of wall slices to be $\leq$ 10 for heat transfer calcs.
KTRACE	0	Print intermediate output if =1 (for debugging)
MTIME	3600	Maximum time for fire simulation (s)
MWPYR	28.97	Molecular weight of pyrolysis gases (g $g\text{-}mole^{-1}$)
NEWPLT	FALSE	If true, start new plot frame

Parameter	Typical Value	Definition
NEWPRP	TRUE	If true, new data arrays will be given
NFLPC	0	Percent of nitrogen by weight in fuel
OFLPC	0	Percent of oxygen by weight in fuel (%)
PLFUEL	FALSE	If true, fuel is a pool fire
PLOT	FALSE	If true, plot time-temperature curve
PNCH	FALSE	If true, punch time-temperature curve
PRNT	60	Interval at which results are to be printed (s)
REGRES	0	Rate of fuel regression (m s^{-1})
RPSPEC	FALSE	If true, use tabular input fuel pyrolysis
SH	0.15	Ratio of clear spacing between sticks to the crib height
SHAPE	2	Shape factor in pyrolysis equation for wood sticks (2 for sticks or cylinders, 3 for cubes or spheres)
SIZE	0.075	For cribs or stick burning, the smallest dimension of stick (m)
STEADY	FALSE	If true, only steady state solution is to be sought.
STOICH	FALSE	If true, EITA = 1 solution is sought in POOL
TBOILC	390	Fuel vaporisation temperature for pools (°C)
THICKW	0.2	Wall thickness (m)
TINPT	0	Optional input iteration gas temperature (K)
VTSPEC	FALSE	If true, pessimise pyrolysis rate for a specified ventilation
WFLPC	12	Percent of water by weight in fuel
	1 1 1 0 0	Number of pairs of data points in the following 5 lines
**	0.17, 0.17	Conductivity of wall, a function of temperature (W m^{-1} K^{-1})
**	840, 840	Specific heat of wall, a function of temperature (J kg^{-1} K^{-1})
**	0.5, 0.5	Emissivity of wall, a function of temperature
**	_ , _	Rate of pyrolysis as a function of time
**	_ , _	Rate of wall internal heat generation as a function of time

Table 6.1 Input Parameters to COMPF2PC Simulation

** Some parameters, such as the wall conductivity and specific heat are input by their location in the input data stream. By specifying the number

of pairs of data points for each, temperature dependent data or time dependent data can be entered. As shown in Table 6.1 the specific heat, conductivity and emissivity of the wall material are constant with temperature.

6.2 **Example Fire Simulation**

6.2.1 Getting Started

Following definition of the parameters relating to room geometry, room materials, and ventilation-related parameters, the fuel must be characterised. This is done for wood burning simulations, by entering the equivalent fire load in kg m^{-2} of floor area.

Then the type of fuel element is determined by specifying whether fuel is in the form of sticks/cylinders (Shape = 2) or cubes/spheres (Shape = 3) and whether crib burning (Crib Spacing to Height Ratio S/H specified) or stick burning (Regression rate > 0 specified) is to be used as the method of representation.

Random or arbitrary selection of these geometric parameters can create wildly different predictions of the output temperature versus time curve.

6.2.2 Compartment Properties

An example fire was analysed by simulating a series of fires in a compartment with the geometric and material properties, shown in Table 6.2.

Internal Width	3.38 m
Internal Length	3.68 m
Internal Height	3.13 m
Window Height (H)	2.18 m
Window Width	1.18 m
Window Sill Height	0.95 m
Wall material	Brick
Floor material	Refractory Concrete

Ceiling Material	Lightweight Concrete
Average compartment density	1,700 kg m^{-3}
Average compartment specific heat	840 J kg^{-1} K^{-1}
Average compartment conductivity	0.9 W m^{-1} K^{-1}
Fire Load	744 kg wood

Table 6.2 Example Fire, Compartment Material Properties

The relevant geometric and other parameters calculated for this compartment are shown in Table 6.3.

Total Area of Bounding Surfaces (A_T)	69.1 m^2
Window Area (A_V)	2.57 m^2
Floor Area (A_F)	12.4 m^2
Specific Fire Load	60.0 kg m^{-2} floor area
Ventilation Factor $A_V \sqrt{H}$	3.80 $m^{5/2}$
Ventilation Factor $A_V \sqrt{H} / A_T$	0.055 $m^{0.5}$

Table 6.3 Example Fire, Calculated Compartment Properties

6.2.3 Fuel Properties

A number of crib burning fires were simulated with the stick shape factor (SHAPE) = 2, and the maximum fraction of pyrolysates to be burnt within the compartment (BPF) set equal to 90%. The parameters altered from simulation to simulation were the stick diameter (D in metres) and the crib spacing to height ratio (SH) as shown in Table 6.4.

Simulation Identifier.	**Stick Diameter (D)**	**Crib Spacing to Height Ratio (SH)**
A	0.025	0.20
B	0.05	0.10
C	0.05	0.01
D	0.10	0.10

Simulation Identifier.	Stick Diameter (D)	Crib Spacing to Height Ratio (SH)
E	0.075	0.10

Table 6.4 Example Fire, Fuel Description Parameters

6.2.4 Simulation Results

The results of these crib fire simulations are presented in Figure 6.1 along with the experimental data for the test fire. The solid curves represent the maximum, mean and minimum temperature experimental data. It is evident from Figure 6.1 that the five COMPF2PC simulations produced an extremely wide variation in predicted temperature versus time curves.

These simulations raise the question as to why Simulation E for example, provides a relatively good representation of the real fire temperature curve when the other simulations are not only wildly adrift, some do not even look like the results of a real fire?

The temperature reached is affected primarily by the heat release rate prediction, which is itself dependent on the pyrolysis rate. Figure 6.2 shows the calculated pyrolysis rate curves for each of the simulations. It can be seen that Simulations A and B both have an extended period of high pyrolysis rate, followed by a very rapid drop in pyrolysis rate to zero. Simulation C has a very low constant pyrolysis rate for the complete period, and Simulation D has a moderate initial pyrolysis rate which decays slowly. Simulation E has a short period with a high constant pyrolysis rate, followed by a linear decay in the rate of pyrolysis somewhat faster than that of Simulation D, but much slower than the decay rates of Simulations A and B.

Of the fuel pyrolysed, not all is burnt within the compartment. This is demonstrated for each simulation in Figure 6.3, which plots the calculated burning rates. This graph provides a different perspective on the mechanisms at work. Fires A, B and E all actually have an initial burning rate well below their initial pyrolysis rate at approximately 0.27 kg s^{-1} burning rate compared with pyrolysis rates near 0.45 kg s^{-1}. Even though the maximum percentage combustion within the compartment is set at 90%, the programme

has calculated an initial rate of 60% due to the strong ventilation limited nature of the simulated fire. The burning rate curves for A, B and E are almost constant (in fact they initially decay slightly), but eventually begin to diverge. Simulations B and E have a slight increase in burning rate prior to the rate decaying, while Simulation A has only a steep and sudden decay in burning rate. Simulation D has a steady decay in burning rate throughout the simulation and Simulation C has a constant burning rate.

The burning rate curves are effectively reproduced in Figure 6.4 which plots the heat release rate inside the compartment for each simulation. The heat release rate is calculated from the predicted burning rate multiplied by the nett heat of combustion of the fuel (15.1 MJ kg^{-1}).

Figure 6.5 shows the percentage of fuel remaining as a function of time. Simulations A and B have almost identical curves until a few minutes before the fuel mass is expended, whereas Simulation E departs from the A and B curves after 10 minutes. The C and D curves decay more slowly (especially C), with Simulation C obviously indicating the potential to generate a low intensity fire of several hours duration.

Figure 6.6 plots the mass flow rate of air entering the fire compartment for each simulation. This demonstrates the dynamic nature of the air inflow. Simulations C and D have a relatively high starting air inflow, which increases slowly throughout the fire. Simulations A and B actually have a decreasing air inflow rate until late in the burning process, followed by a sharp increase in air flow immediately before the combustibles are exhausted. Simulation E is mid way between B and D, showing a steady increase in air inflow throughout the fire until the fuel is exhausted.

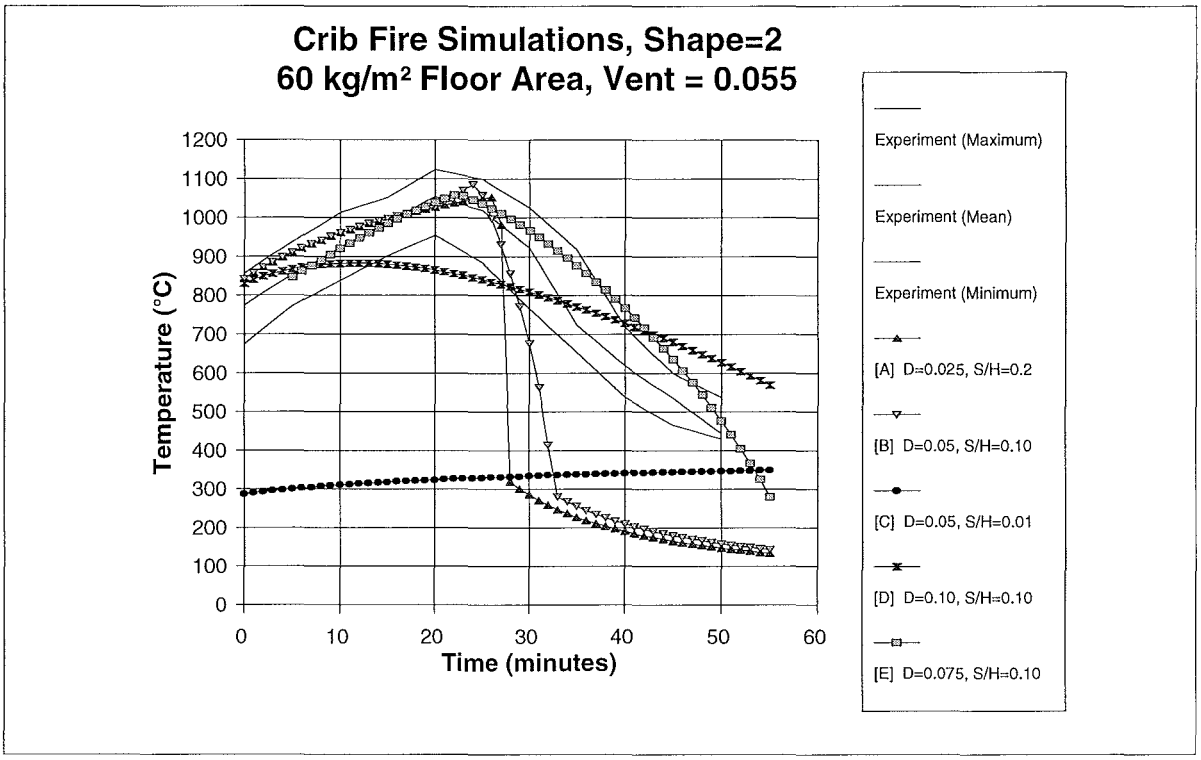

Fig. 6.1 Example Fire, Calculated Temperature vs Time Curves

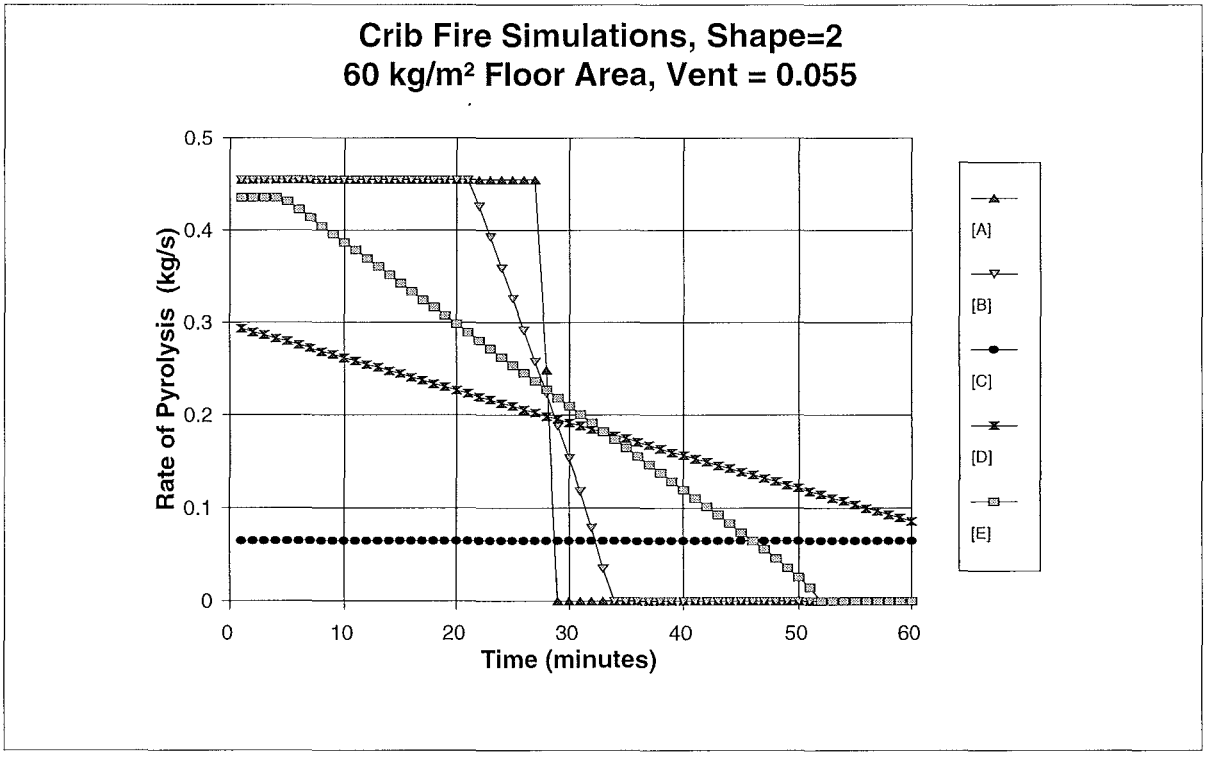

Fig 6.2 Example Fire, Calculated Pyrolysis Rates

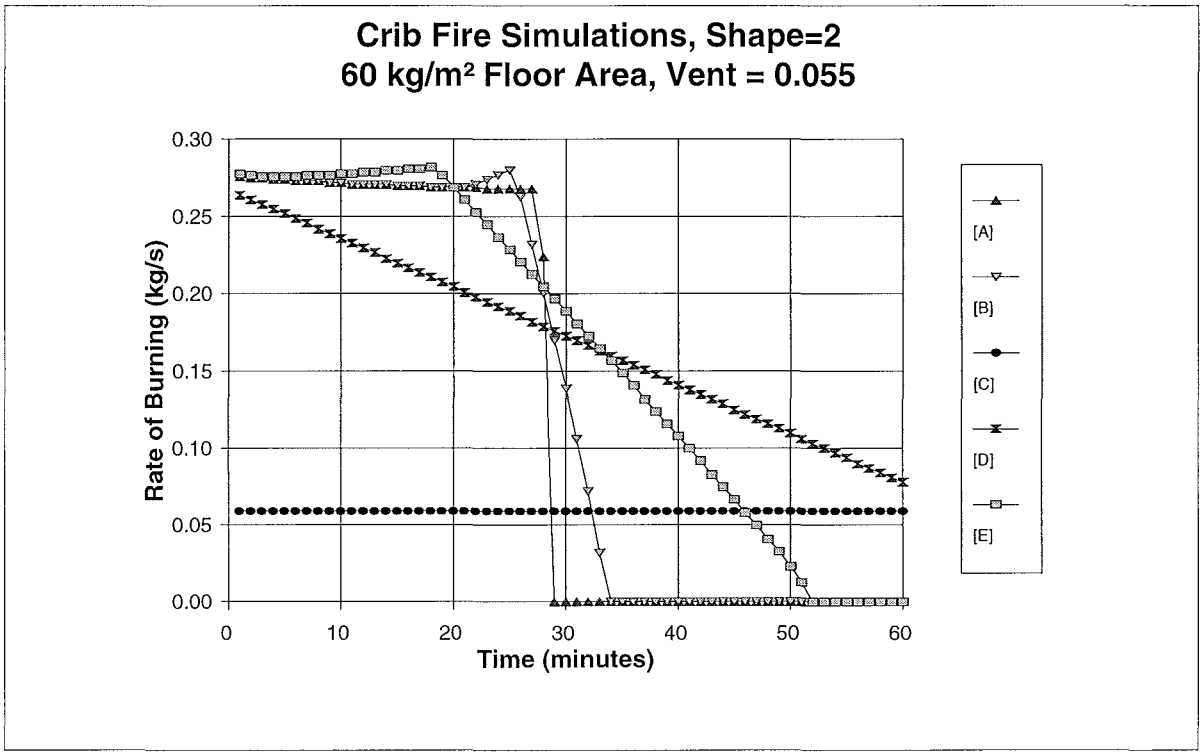

Fig. 6.3 Example Fire, Calculated Burning Rates

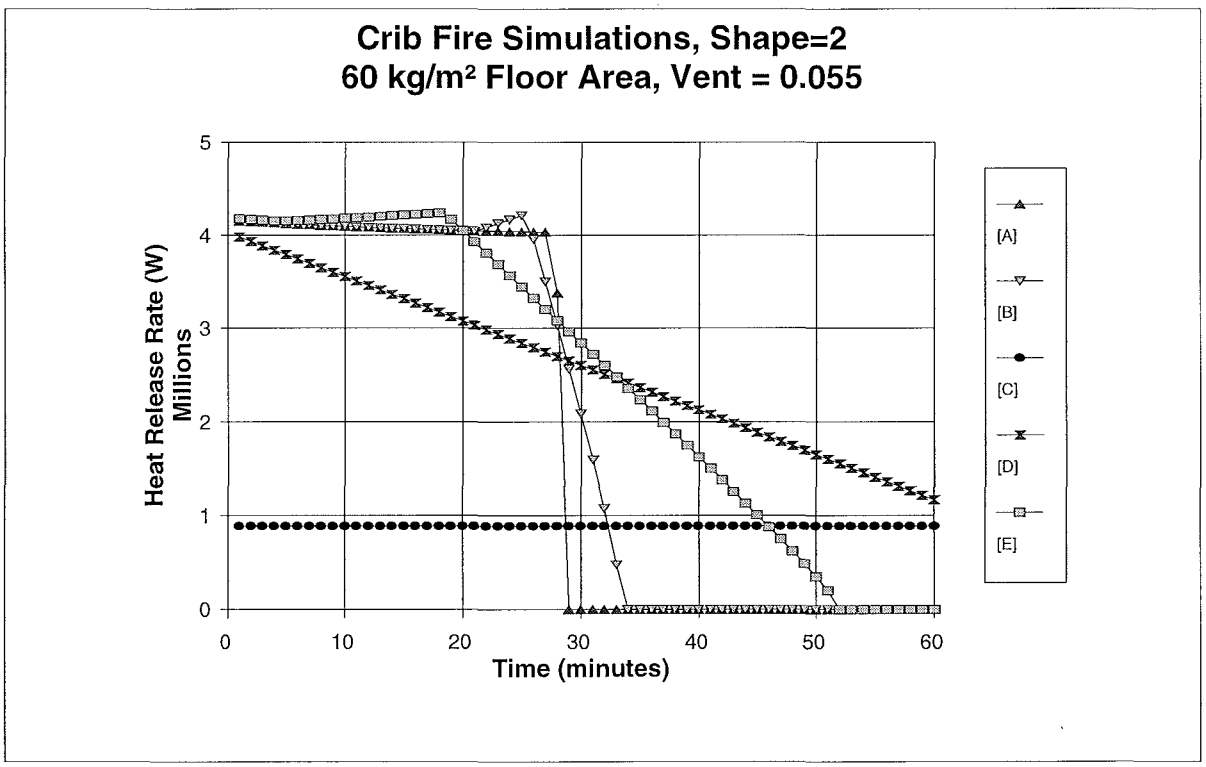

Fig. 6.4 Example Fire, Calculated Heat Release Rates

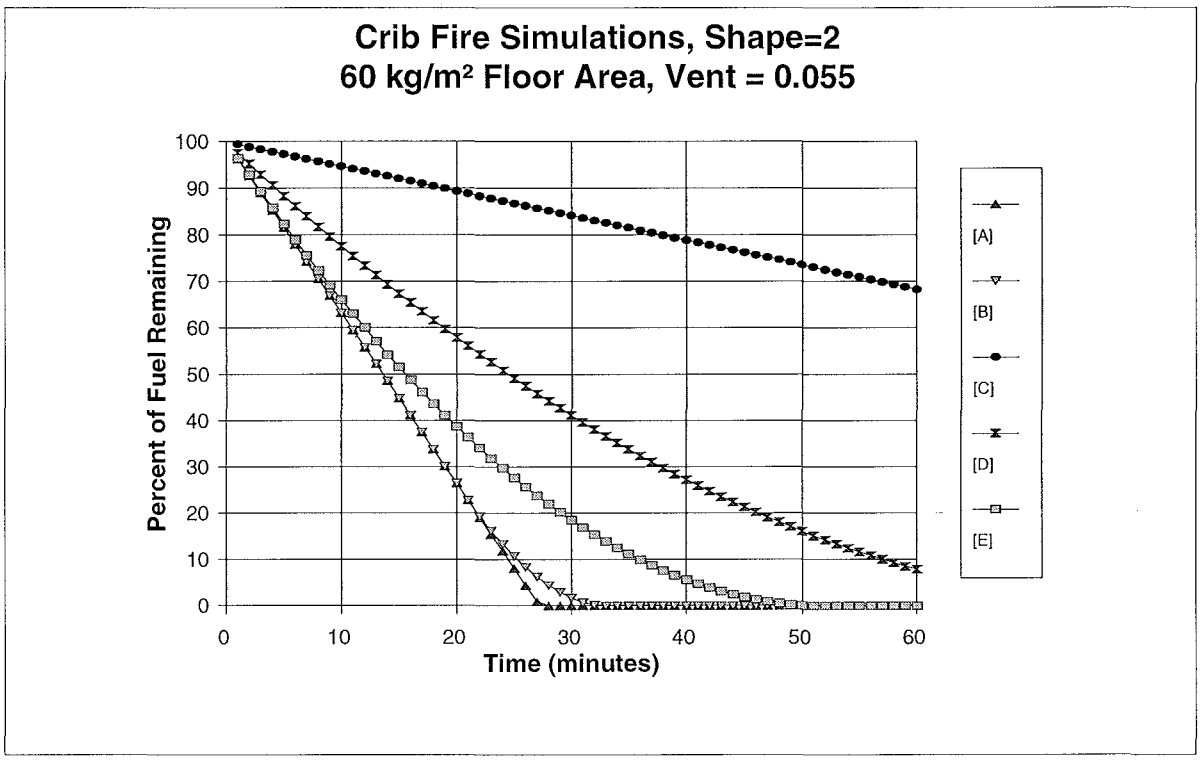

Fig. 6.5 Example Fire, Percent of Fuel Remaining

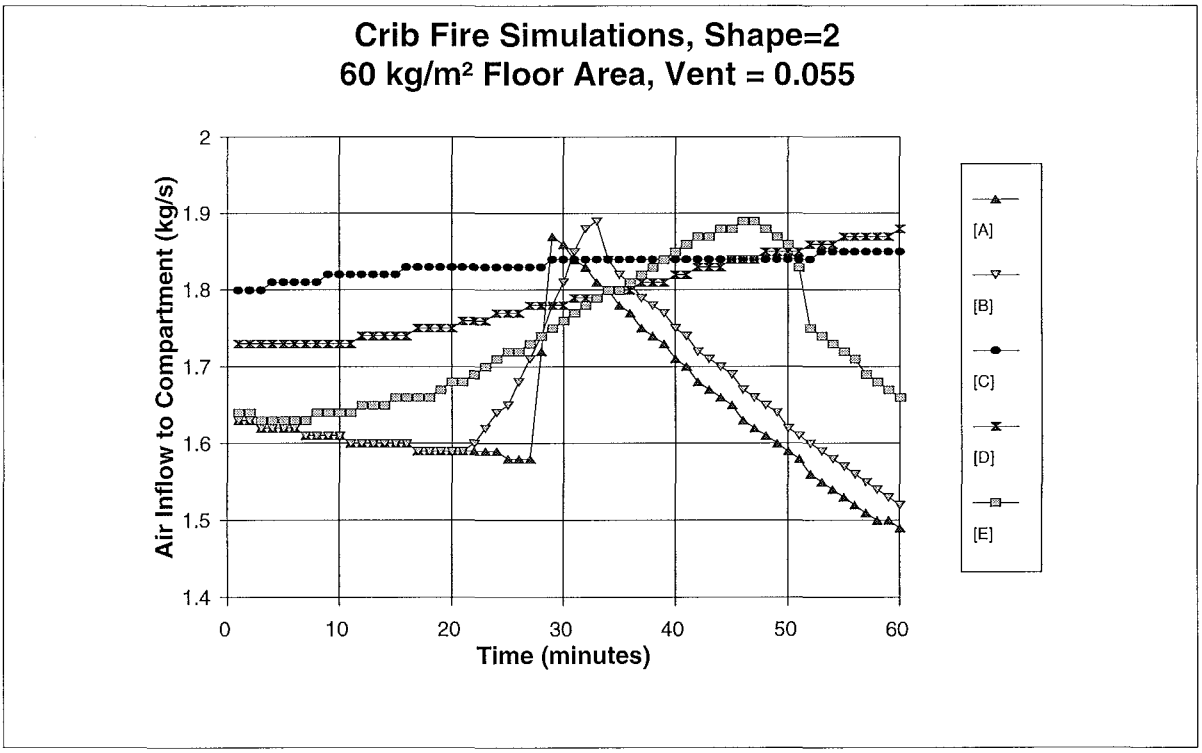

Fig. 6.6 Example Fire, Air Inflow Rate

6.2.5 Initial Pyrolysis Rates

As discussed in Section 3, the governing pyrolysis rate for the calculation of heat release rate is the minimum of those available for the burning mechanisms being considered, the latter being dependent on selected programme inputs.

The differences in pyrolysis rate and burning rate for the earlier Example Fire simulations, is caused by the change in governing equations for pyrolysis rate which are dependent on the characterisation of the fuel. For crib fires, there are three mechanisms which can set the initial pyrolysis rate :

(a) The fire is ventilation controlled.
(b) The crib fires are crib porosity controlled.
(c) The crib fires are fuel surface area controlled.

This can be seen for the Example Fire in Table 6.5.

Identifier	Diam. (D) (m)	Crib (Sc/Hc)	Pyrolysis rate (kg s^{-1})		
			Vent. Control	Crib Porosity Control	Crib Fuel Surface Control
A	0.025	0.200	0.456	2.619	2.700
B	0.050	0.100	0.456	0.655	0.891
C	0.050	0.010	0.456	0.065	0.891
D	0.100	0.100	0.456	0.327	0.294
E	0.075	0.100	0.456	0.436	0.466

Table 6.5 Example Fire, Initial Pyrolysis Rate by Possible Mechanism

Thus each of the Example Fire simulations can be reconsidered:

[A] Simulation [A] is strongly ventilation controlled (pyrolysis rate of 0.456 kg s^{-1}) with the crib porosity and crib fuel surface rates being far higher. This means that the pyrolysis rate remains constant at the ventilation limit, until nearly all the fuel has been consumed. This produces an almost constant heat release rate until all the fuel has been consumed, resulting in a very steep decay in temperature once the fuel runs out. The extremely rapid decay in temperature

following exhaustion of the fuel, gives the temperature profile an "unrealistic" appearance.

[B] Simulation [B] is moderately ventilation controlled, with the fuel surface control mechanism taking over in the latter stages of the fire, to give a rapid decay in the rate of burning (but less rapidly than that of [A]), producing a slightly fuller decay curve, which nevertheless, still looks "unrealistic".

[C] Simulation [C} is strongly crib porosity controlled. This mechanism produces a low governing pyrolysis rate, and low heat release rate. Coupled with diluting effect of relatively high air inflow rate, relatively low compartment temperatures result. The fire would burn for several hours if the simulation duration was extended.

[D] Simulation [D] is strongly crib fuel surface controlled from the beginning. Pyrolysis rate will vary as a function of the square root of the fractional mass remaining (refer Section 3). The steady decay in pyrolysis and burning rates, result in a steady reduction in heat release rate and a broad well-rounded temperature curve which under-estimates the peak temperatures by over 200 °C and over-estimates the fire duration.

[E] Simulation [E] is initially crib porosity controlled for a period of 5 minutes, with a pyrolysis rate close to that but just below that of the ventilation limit.. But because the initial fuel surface pyrolysis rate in only slightly above the crib porosity controlled pyrolysis rate, after a modest reduction in the fuel mass, the fuel surface controlled mechanism takes over. The combined effect is to produce a heat release rate curve which is nominally constant for 18 minutes, and then decays steadily, leading to a good prediction of the experimental temperature versus time curve.

6.2.6 Summary

The example fire discussed above, indicates some of the sensitivities in regard to the effects of fuel characterisation on predicted fire outcomes. Similar sensitivities occur whether fires are characterised as crib burning or stick burning, or whether the SHAPE parameter represents fuel in the form of sticks/cylinders (Shape=2) or cubes/spheres (Shape=3).

6.3 COMPF2PC Simulations of Test Fire Data

6.3.1 Introduction

The sensitivities discussed earlier in regards to the "example fire" have been explored in considerable detail, by simulating a significant number of experimental fires discussed in Section 5. A detailed discussion of each simulation including graphs of the original test data and all the simulations using different sets of COMPF2PC input parameters, is contained in Appendix B.

6.3.2 Fuel Package Definitions

Experimental fires (particularly the earlier sets) were each simulated using four different fuel package definitions to determine if any one fuel package characterisation consistently provided better simulations. The fuel packages were all considered to be wood arranged as following :

(a) crib burning with shape factor =2 (fuel elements shaped in the form of long sticks or cylinders)
(b) crib burning with shape factor =3 (fuel elements shaped in the form of cubes or spheres). Refer Section 4.2.3 for comment.
(c) stick burning with shape factor =2 (fuel elements shaped in the form of long sticks or cylinders)
(d) stick burning with shape factor =3 (fuel elements shaped in the form of cubes or spheres).

As noted in Section 3, each of these variants has (or should have) a different set of equations governing the predicted pyrolysis rate versus time, for a fire of the same nominal fire load and ventilation conditions.

6.3.3 Simulation Methodology

Up to 10 simulations were carried out for each fuel package definition for earlier simulations in order to get the best fit between simulation prediction and experiment. With experience this was able to be reduced to about 3 simulations for later test fires.

For each simulation, the fuel element dimension, regression rate, shape factor, crib spacing to height ratio were defined. From these the ventilation controlled pyrolysis rate, crib porosity controlled pyrolysis rate, crib fuel surface controlled pyrolysis rate and stick burning fuel surface controlled pyrolysis rate were calculated.

Random selection of input parameters associated with fuel geometry can easily produce simulated fires with temperature versus time curves which look nothing like either the experimental fire or any real fire.

6.3.4 General Simulation Characteristics as a Function of Fuel Package Definition

Even with the "best" selection of fuel characteristics, each of the above fuel package definitions consistently gave distinctly different results which was independent of both relative fire load and ventilation factor for the experimental fire.

(a) Crib burning with shape factor 2 could provide a reasonable fit over the peak temperature part of most simulations. The predicted temperature decay characteristic provided a rate of decay of temperature which increased with time until nearly all fuel was pyrolysed. This parabolic characteristic usually provided a poor fit later in the decay phase (below 600 °C) as the predicted rate of temperature decay became very steep, with the data generally having a decay that is exponential or quasi-linear, with a slower rate of decay than at earlier stages. The simulated fires would become non-conservative at temperatures as high as 700 °C.

(b) Crib burning with shape factor 3 provided a reasonable fit over the peak temperature part of most simulations. The predicted temperature decay characteristic had a decay of temperature which was almost linear with time until nearly all fuel was pyrolysed. This characteristic provided a better fit to the later stages of the simulation compared with poor fit later in the decay phase (below 600 °C) provide by the crib fire (shape factor =2) simulations.

(c) Stick burning with shape factor 2 provided a reasonable fit over the peak temperature part of most simulations. Characteristics during the decay phase were similar to those for crib burning with the same shape factor.

(d) Stick burning with shape factor 3 provided a reasonable fit over the peak

temperature part of most simulations. With appropriate characterisation of the fuel geometry, the predicted temperature decay characteristic had a decay of temperature which was approximately linear with time until nearly all fuel was pyrolysed. Although far from perfect, this fuel element characterisation consistently provided the best prediction of the decay phase, providing conservative estimates of temperature at any particular time to lower temperatures. Therefore later experimental fires, were simulated using only this fuel characterisation.

6.4 Analysis of Test Fires

The test fire data of Appendix B was analysed to determine which parameters (if any) could be used to systematise the generation of design fires.

Once the compartment and ventilation geometry and materials of construction are defined, the course of any fire simulation using COMPF2PC is totally dependent on the quantity of fuel, and the initial pyrolysis rate. Initial simulations were carried out on a trial and error basis generating wide range of initial pyrolysis rates, and an equally wide range of predicted temperature curves. As noted above, stick burning with a shape factor of 3 (cubes or spheres), consistently provided the best simulations. For each of the experimental NFSC fires simulated, the typical ratio of the initial pyrolysis rate of the best simulation, and the ventilation limited pyrolysis rate calculated from Equation 3.22, is listed in Table 6.6. Where good simulations can be achieved with a range of input data, a range of pyrolysis ratios is tabulated.

Reference No.	**Fire Load (kg wood m^{-2} of floor area)**	**Ventilation Factor $A_V \sqrt{H} / A_T$ ($m^{0.5}$)**	**"Best" Initial Pyrolysis Rate to Ventilation Controlled Pyrolysis Rate from Eq. 3.22**
NFSC -79	90.9	0.132	0.8 - 1.2
NFSC 70-46	60.0	0.157	0.45 - 0.55
NFSC 70-22	60.0	0.091	0.75
NFSC 70-19	60.0	0.055	0.91 - 0.98
NFSC 70-24	30.0	0.157	0.4

Reference No.	Fire Load (kg wood m^{-2} of floor area)	Ventilation Factor $A_V \sqrt{H} / A_T$ ($m^{0.5}$)	"Best" Initial Pyrolysis Rate to Ventilation Controlled Pyrolysis Rate from Eq. 3.22
NFSC 70-21	30.0	0.091	0.6
NFSC 71-58	30.0	0.056	0.8 - 0.9
NFSC 70-29	30.0	0.015	1.8
NFSC 70-16	29.9	0.015	1.0 - 1.7 *
NFSC 71-54	24.4	0.014	1.0 - 1.7 *
NFSC 70-44	20.0	0.157	0.2 - 0.25
NFSC -69	15.6	0.030	1.0 - 1.3
NFSC 70-23	15.0	0.157	0.16
NFSC 70-20	15.0	0.091	0.20 - 0.25
NFSC 70-17	15.0	0.055	0.42

Table 6.6 Pyrolysis Ratios for Best Simulations of Test Data

* Even the best simulations of these two fires were very poor.

The above data can be considered as a three dimensional "plain" of stick burning to ventilation limited pyrolysis ratio against fire load and ventilation factor. Based on the above data, and interpolating, the approximate best pyrolysis ratio (ratio of the initial pyrolysis rate of the best stick burning simulation, and the ventilation limited pyrolysis rate calculated from Equation 3.22) for a the range of fire loads and ventilation factors used to create design fires in the next section, is presented in Table 6.7.

Ventilation Factor $A_V \sqrt{H} / A_T$	Fire Load (MJ/m^2 of Floor Area)			
	200	400	800	1200
0.02	1.250	1.000	1.000	1.000
0.04	0.700	0.825	0.900	0.900
0.08	0.250	0.500	0.750	0.750
0.12	0.200	0.425	0.640	0.670

Table 6.7 Pyrolysis Ratios for Design Fire Parameters

It should be noted that few of the NFSC fire tests exceed a fire load of 60 kg m^{-2} (900 MJ m^{-2} based on the net calorific value of wood calculated by COMPF2PC of 15.1 MJ kg^{-1}). Unless test data existed for which a specific value of pyrolysis ratio could be determined, the pyrolysis ratio for the 1200 MJ m^2 fires used the next lowest fire load.

It should also be noted, that most of the NFSC fire test data was usually obtained at a ventilation factor $A_V \sqrt{H} / A_T$ of either 0.015, 0.055, 0.091 or 0.157 due to the four different configurations of the "end" wall of the test chamber used. Some of the results obtained for COMPF2 simulations at a ventilation factor of 0.015 were poor (refer Appendix B). Test 4 from Kirby et al (1994) was obtained at a slightly higher ventilation factor of 0.022, and a satisfactory simulation was achieved (although as discussed in Appendix B2, the data itself was unusual, with the temperature versus time curves being highly spatially variable). There is therefore greater uncertainty in Table 6.7 for the pyrolysis "ratios" at a ventilation factor of $A_V \sqrt{H} / A_T$ =0.02, and consequential lower reliability in the simulations at this ventilation factor.

Use of the pyrolysis ratios from Table 6.7 will be inherently conservative to the extent that the NFSC fire test data is conservative. The "maximum" temperature profile data were in fact the profile of the maximum temperature at any thermocouple in the test chamber at each time step. Since variation from location to location within the chamber was evident (and could be expected to be more substantial in larger fire compartments), the "maximum" temperature profile provides a conservative temperature history for any one point in the chamber.

6.5 Recommended Method for Use of COMPF2PC

The COMPF2PC programme gives best simulation results for fires of moderate to high fire load (fire load > 20 kg m^{-2} of floor area) and moderate to high ventilation factor ($A_V \sqrt{H} / A_T \geq 0.04$).

Results are more at variance with the test data at low fire load (<20 kg m^{-2}), and low ventilation factor ($A_V \sqrt{H} / A_T < 0.04$). Whether this is because of variance within the test data used, has not been resolved. In these cases, predicted compartment temperatures are often low, and the fuel parameter setup required to produce reasonable simulations of the test data are distinctly different from the fires with greater fire load and ventilation factor.

When the predicted compartment temperatures are less than required for flashover, the assumptions made in the COMPF2 model are less likely to be fulfilled, and the accuracy of the predictions could be expected to suffer.

Based on the simulations of test fire data discussed in Appendix B and the discussion above, the following method of using COMPF2PC can be proposed.

(a) Input data files are best prepared by editing one of the sample data files supplied with COMPF2PC. Be sure to preserve the syntax and case definitions (ie keep real numbers real, and integers integer)

- Characterise the fire load in wood equivalent kg m^{-2} of floor area by setting the input parameter FLOAD.

- Define the floor area (AFLOOR), wall area (AWALL) window area (AWDOW) and window height (HWDOW). Note that the wall area AWALL is in fact the gross area of the walls plus the ceiling, including the ventilation opening.

- Define the wall density (DENSW) and wall thickness (THICKW).

- Define the wall conductivity and specific heat. The latter are functions of temperature, and are input differently from other variables. (Refer to Babrauskas 1979 and the examples in Table 6.1).

- Characterise the fire as a stick burning fire by setting the value of the REGRES input value greater than zero. This selects stick burning as the pyrolysis mechanism.

- Calculate the ventilation controlled pyrolysis rate for the ventilation aperture using Equation 3.22.

- From Table 6.7, select the appropriate pyrolysis ratio, and multiply by the ventilation controlled pyrolysis rate, to determine the initial pyrolysis rate required for the simulation.

- Using Equation 3.17, with the shape factor F set to 3, select a fuel

element diameter (D) and surface regression rate (v_p) to achieve the required initial pyrolysis rate. (Either set the diameter and use a spreadsheet to solve for the regression rate, or vice versa)

- Set the ventilation aperture discharge coefficient (CD) to 0.68 for all fires except those where the ventilation aperture width is the full width (or nearly the full width) of the wall. In the latter case set the discharge coefficient CD to 0.34 - 0.40.

- Do not set the flags to pessimise the fire on ventilation or pyrolysis.

- Set the calculation time interval (DTIME) to 60 seconds.

- Set the printout time interval (PRNT) to 60, 120, 300 seconds as appropriate.

- Set the maximum execution time of the model (MTIME) to 3600, 7200 seconds or any other time as appropriate.

(b) Save the edited data input file with a new name.

(c) Execute COMPF2PC and when requested, input the new data file name, and the name of three output files. The programme will execute in less than a second on a Pentium class computer. The first two output files contain simulation predictions. The third output file contains error messages only and is normally empty. All output can be piped to the VDU if required, by specifying "CON" or console, as the output file name.

(d) Use a text editor to tidy up the output files (there are some spurious typographic characters), and remove redundant page headings where appropriate. Re-save the edited output files.

(e) Combine the output files using the "file combine" and "parsing" features of your preferred spreadsheet. Prepare graphs.

7 DESIGN FIRE PREDICTION

7.1 Background

Based on the simulation method discussed in Section 6.5 and documented in Section 6.4 and Appendix B, a range of generalised design fires are presented. The following fire load and compartment parameters are used :

- Fire loads of 200, 400, 800 and 1200 MJ m^{-2} of floor area
- Ventilation factors $A_V \sqrt{H} / A_T$ of 0.02, 0.04, 0.08 and 0.12 $m^{0.5}$
- Compartment construction - heavyweight (concrete) and lightweight (plasterboard)

The design fire predictions will be conservative to the extent that the NFSC fire data were conservative. (See Section 6.4). Note also the limitations to the reliability of the simulations for low ventilation ratio ($A_V \sqrt{H} / A_T$ <0.04) as discussed in Section 6.

7.2 Heavyweight Construction

The heavyweight compartment geometry and materials are defined in Table 7.1.

Specified Parameters	
Compartment Length	5.0 m
Compartment Width	5.0 m
Compartment Height	3.0 m
Ventilation Opening Height	2.0 m
Ventilation Opening Width	0.760, 1.556, 3.111, 4.667 m
Enclosing Boundary	Walls, ceiling and floor all of heavy concrete Density 2300 kg m^{-3} Specific Heat 1230 J kg^{-1} K^{-1} Thermal Conductivity 1.3 W m^{-1} K^{-1} Thickness 0.200 m
Calculated Parameters	
$\sqrt{(k\rho c_p)}$ for the compartment materials	1,918 J m^{-2} K^{-1} $s^{-0.5}$

Floor Area	25.0 m^2
Total Internal Surface Area	110.0 m^2
Ventilation Area	1.520, 3.111, 6.223, 9.334 m^2
Ventilation Parameter ($A_V \sqrt{H}$)	2.150, 4.400, 8.800, 13.200 $m^{5/2}$
Ventilation Parameter ($A_V \sqrt{H} / A_T$)	0.02, 0.04, 0.08, 0.12 $m^{0.5}$
Fire Load Density (wood equivalent)	13.25, 26.49, 52.98, 79.47 kg m^{-2} of floor area
Fire Load Density (wood equivalent)	3.01, 6.02, 12.04, 79.4718.06 kg m^{-2} of total bounding surface area

Table 7.1 Design Fires, Summary of Heavy Compartment Input Data

Most of the input parameters for each simulation were identical (except those relating to fire load or ventilation area). The following should be noted.

For ventilation factor $A_V \sqrt{H} / A_T = 0.12$, with the window height of 2 m, the window width is practically the full width of the compartment. In such circumstance a lower value of window discharge coefficient than the "standard" value of 0.68 is recommended; a value of $C_d = 0.40$ should be used. While providing the "best" solution for the compartment size and shape used, the results will be less accurate for compartments of significantly greater dimensions. The "design" fire presented is therefore the generic simulation with $C_d = 0.68$.

The generic fires presented in Figures 7.1 - 7.4 inclusive are for fire loads of 1200, 800, 400 and 200 MJ m^{-2} of floor area respectively. For each fire load, the graph contains a temperature versus time curve for ventilation factors ($A_V \sqrt{H} / A_T$) of 0.02, 0.04, 0.08 and 0.12.

It can be seen for example in Figures 7.3 and 7.4, that modest fire loads in well-ventilated compartments, produce lower maximum fire temperatures than the same fire load density in a compartment with a lower ventilation factor. The former fires are further from stoichiometric combustion.

The same data are presented in Figures 7.5 - 7.8 inclusive as a function of ventilation factors ($A_V \sqrt{H} / A_T$) of 0.02, 0.04, 0.08 and 0.12 respectively. Each graph contains a curve for fire loads 1200, 800, 400 and 200 MJ m^{-2} of floor area.

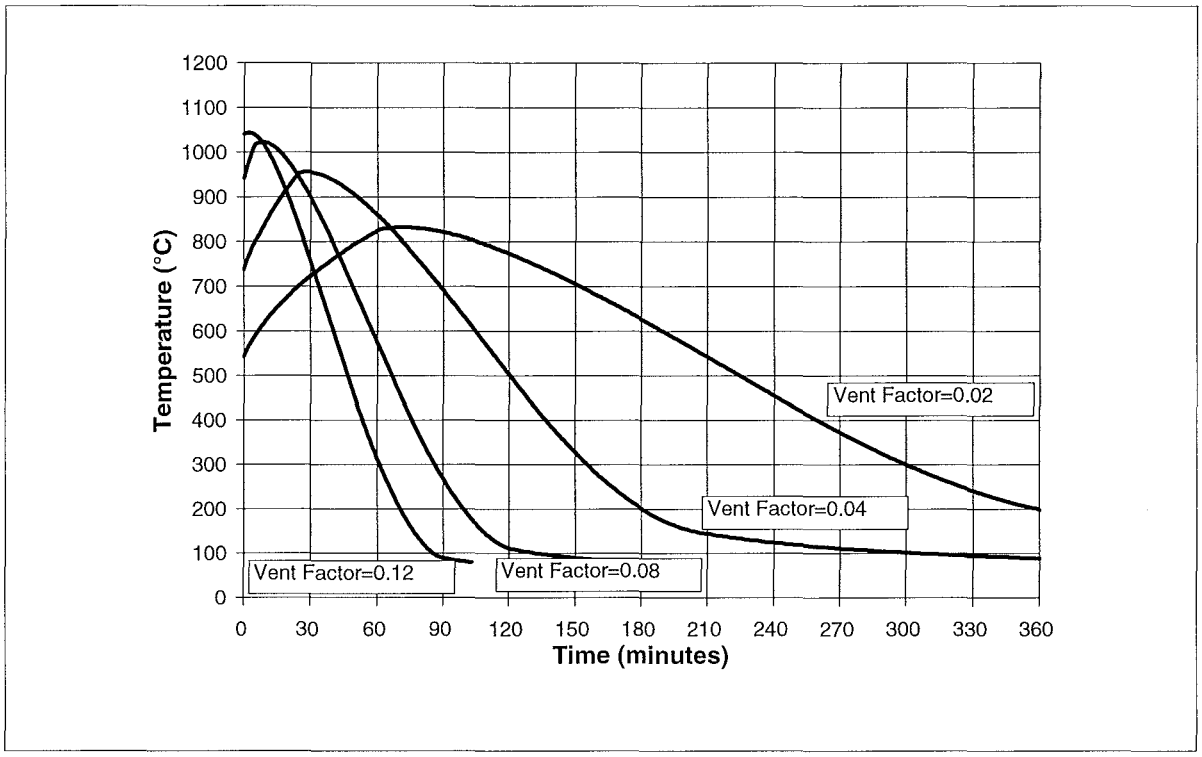

Fig 7.1 Design Fires, Heavy Compartment Construction, Fire Load 1200 MJ/m² of Floor Area

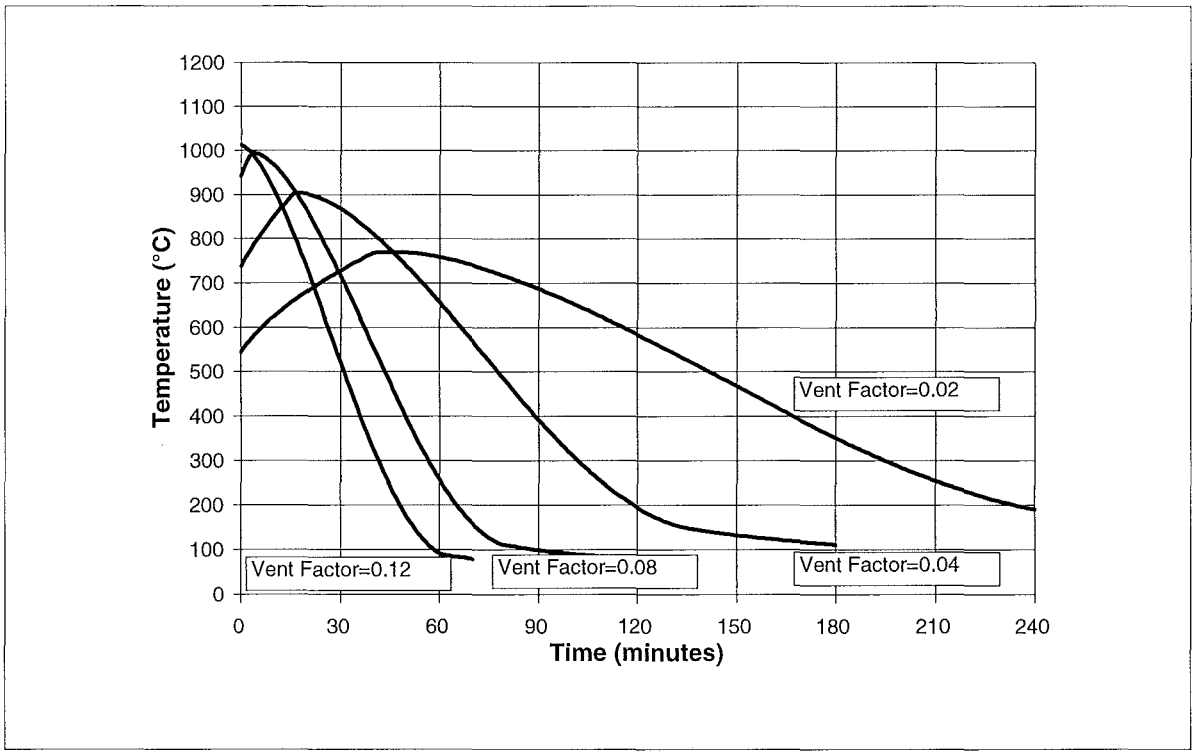

Fig 7.2 Design Fires, Heavy Compartment Construction, Fire Load 800 MJ/m² of Floor Area

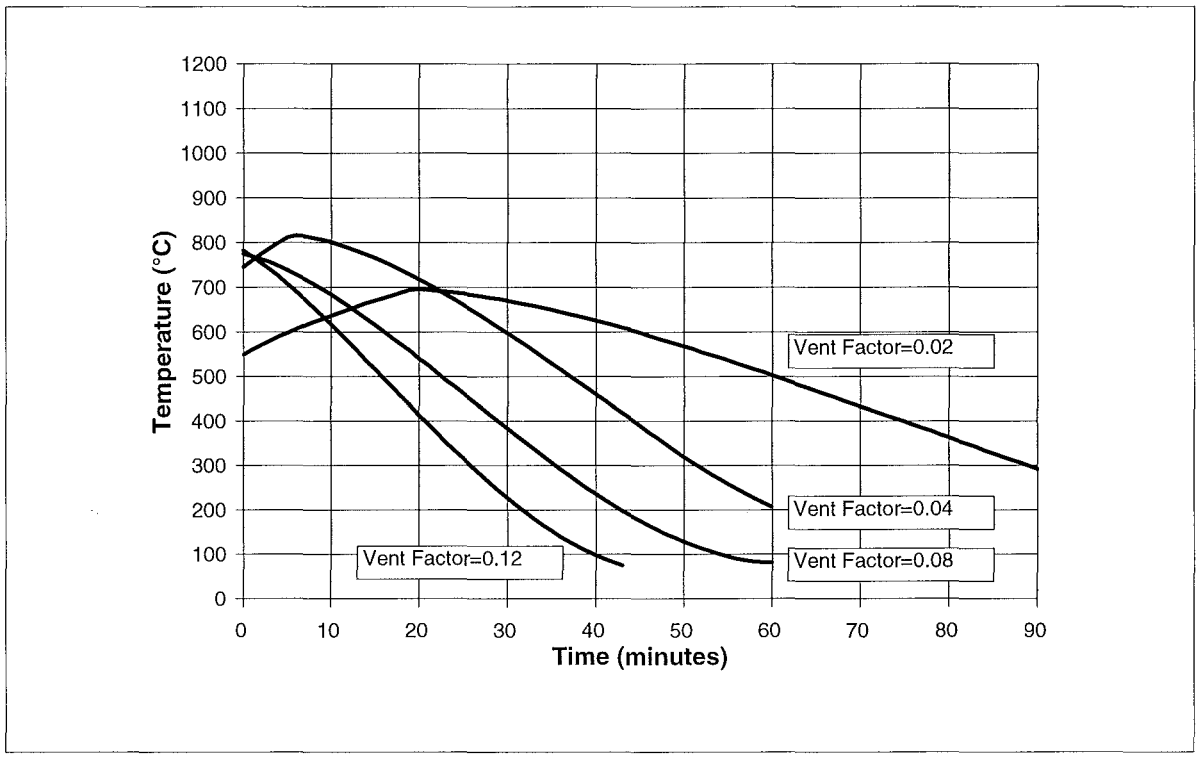

Fig 7.3 Design Fires, Heavy Compartment Construction, Fire Load 400 MJ/m² of Floor Area

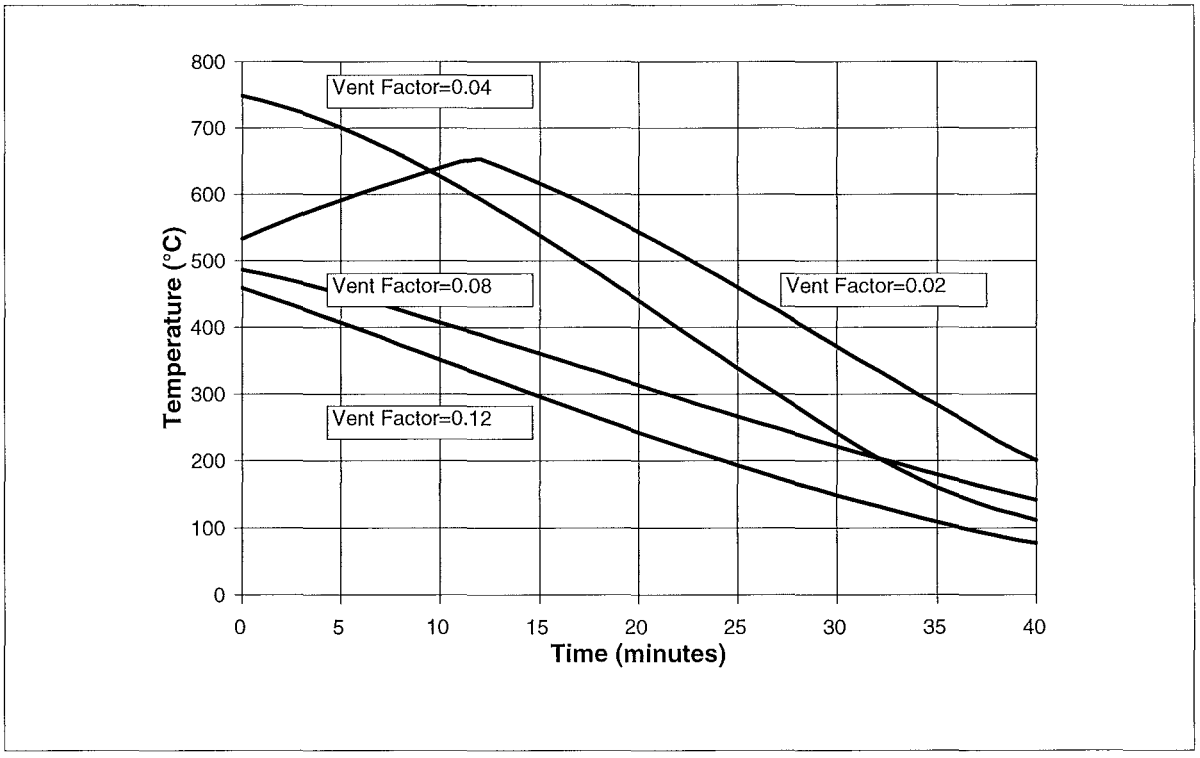

Fig 7.4 Design Fires, Heavy Compartment Construction, Fire Load 200 MJ/m² of Floor Area

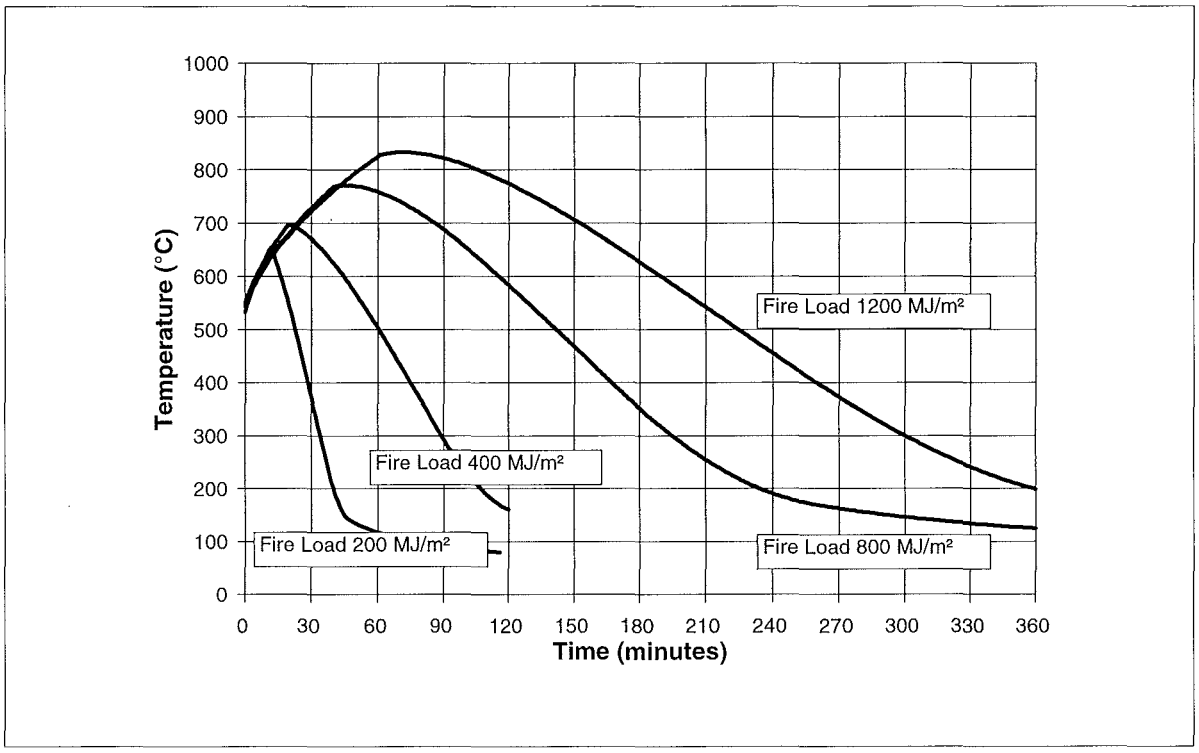

Fig 7.5 Design Fires, Heavy Compartment Construction, Ventilation Factor 0.02

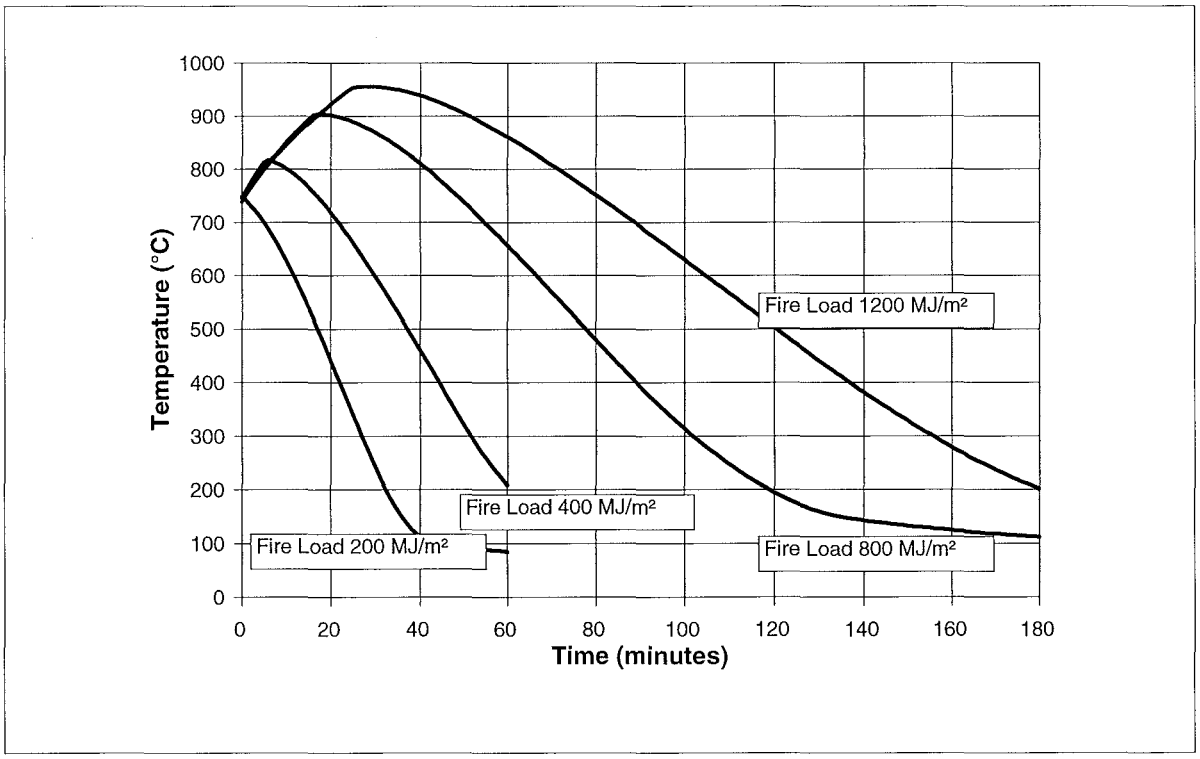

Fig 7.6 Design Fires, Heavy Compartment Construction, Ventilation Factor 0.04

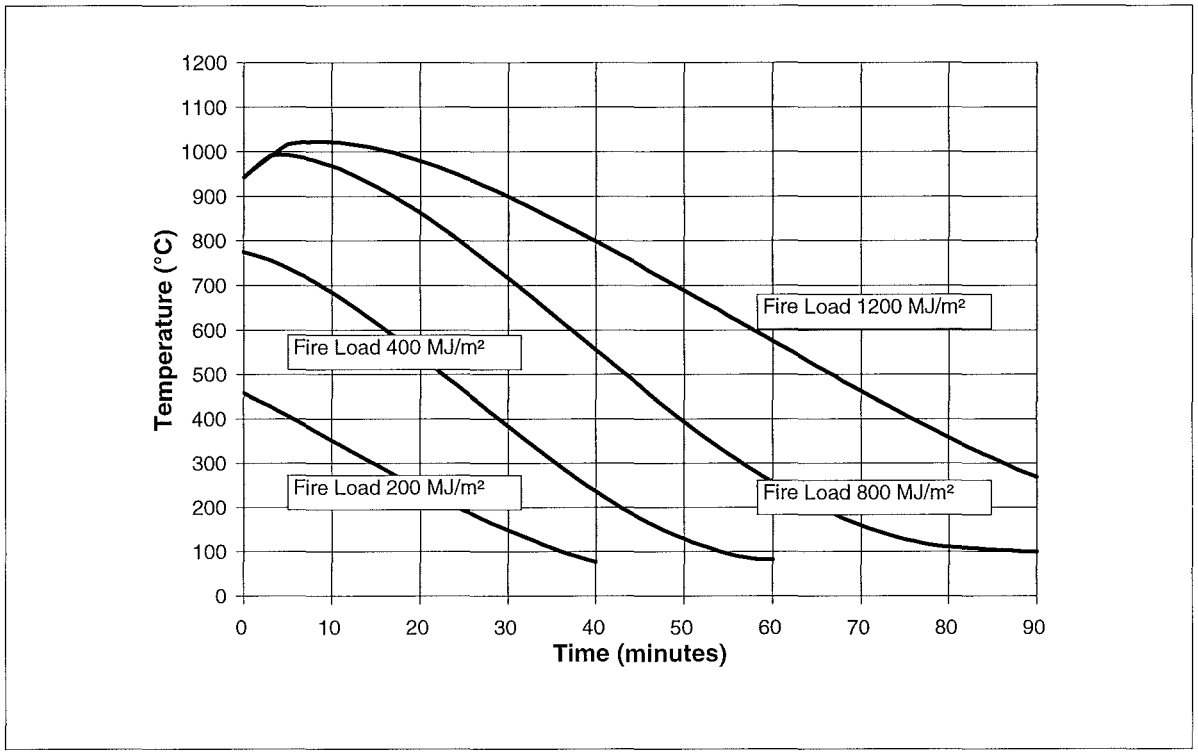

Fig 7.7 Design Fires, Heavy Compartment Construction, Ventilation Factor 0.08

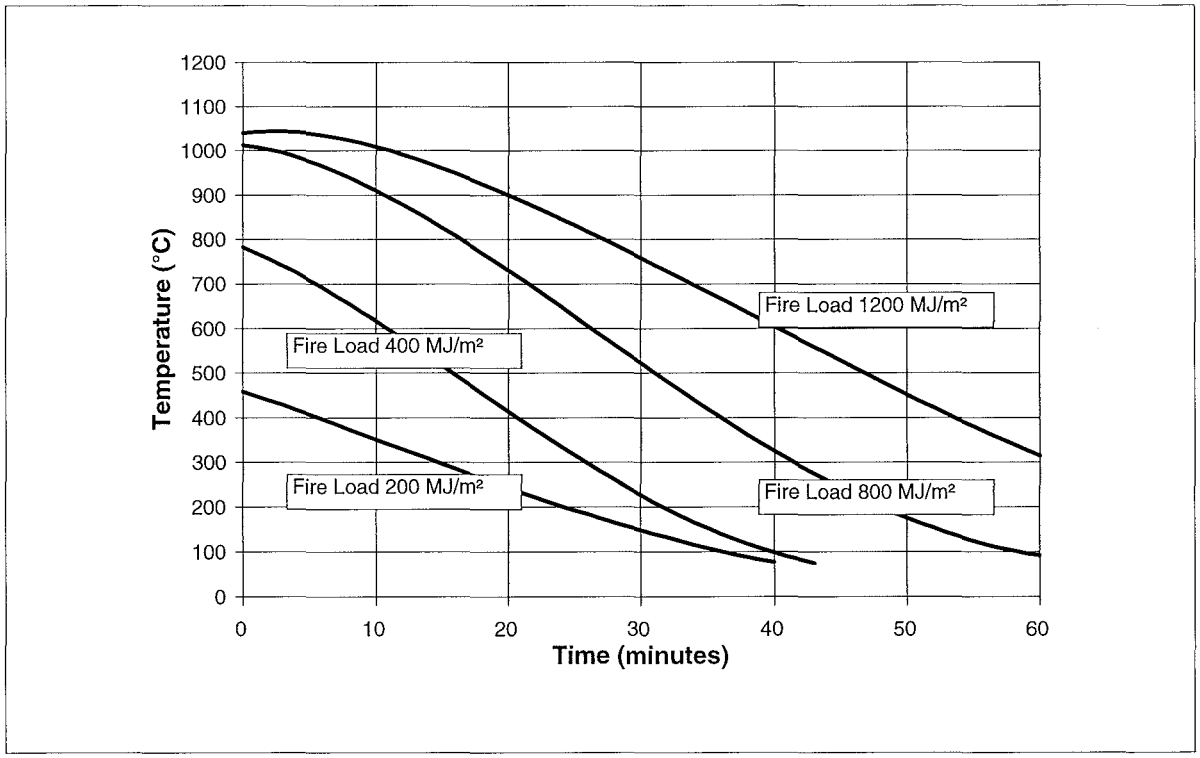

Fig 7.8 Design Fires, Heavy Compartment Construction, Ventilation Factor 0.12

7.3 Lightweight Construction

The lightweight compartment geometry and materials are defined in Table 7.2.

Specified Parameters	
Compartment Length	5.0 m
Compartment Width	5.0 m
Compartment Height	3.0 m
Ventilation Opening Height	2.0 m
Ventilation Opening Width	0.760, 1.556, 3.111, 4.667 m
Enclosing Boundary	Walls, ceiling and floor all of plaster board. Density 720 kg m^{-3} Specific Heat 1130 J kg^{-1} K^{-1} Thermal Conductivity 0.2 W m^{-1} K^{-1} Thickness 0.038 m
Calculated Parameters	
$\sqrt{(k\rho c_p)}$ for the compartment materials	403 J m^{-2} K^{-1} $s^{-0.5}$
Floor Area	25.0 m^2
Total Internal Surface Area	110.0 m^2
Ventilation Area	1.520, 3.111, 6.223, 9.334 m^2
Ventilation Parameter ($A_V \sqrt{H}$)	2.150, 4.400, 8.800, 13.200 $m^{5/2}$
Ventilation Parameter ($A_V \sqrt{H} / A_T$)	0.02, 0.04, 0.08, 0.12 $m^{0.5}$
Fire Load Density (wood equivalent)	13.25, 26.49, 52.98, 79.47 kg m^{-2} of floor area
Fire Load Density (wood equivalent)	3.01, 6.02, 12.04, 79.4718.06 kg m^{-2} of total bounding surface area

Table 7.2 Design Fires, Summary of Light Compartment Input Data

Most of the input parameters for each simulation were identical (except those relating to fire load or ventilation area). For $A_V \sqrt{H} / A_T = 0.12$, with the window height of 2 m, the window width is practically the full width of the compartment. In such circumstance a lower value of window discharge coefficient than the "standard" value of 0.68 is recommended; a value of $C_d = 0.40$ should be used. While providing the "best" solution

for the compartment size and shape used, the results will be less accurate for compartments of significantly different geometry. The "design" fire presented is therefore the generic simulation with $C_d = 0.68$.

The generic fires presented in Figures 7.9 - 7.12 inclusive are for fire loads of 1200, 800, 400 and 200 MJ m^{-2} of floor area respectively. Each graph contains a temperature versus time curve for ventilation factors ($A_V \sqrt{H} / A_T$) of 0.02, 0.04, 0.08 and 0.12.

The same simulations are presented in Figures 7.13 - 7.16 inclusive are for ventilation factors ($A_V \sqrt{H} / A_T$) of 0.02, 0.04, 0.08 and 0.12 respectively. Each graph contains a curve for fire load 1200,800, 400 and 200 MJ m^{-2} of floor area.

As with the heavy weight construction compartment graphs, it is evident that fires with modest fire loads in well ventilated compartments, produce relatively low maximum fire temperatures, due the diluting effect of excess air. At reduced ventilation factors, combustion conditions are closer to stoichiometry, and maximum temperatures are hotter.

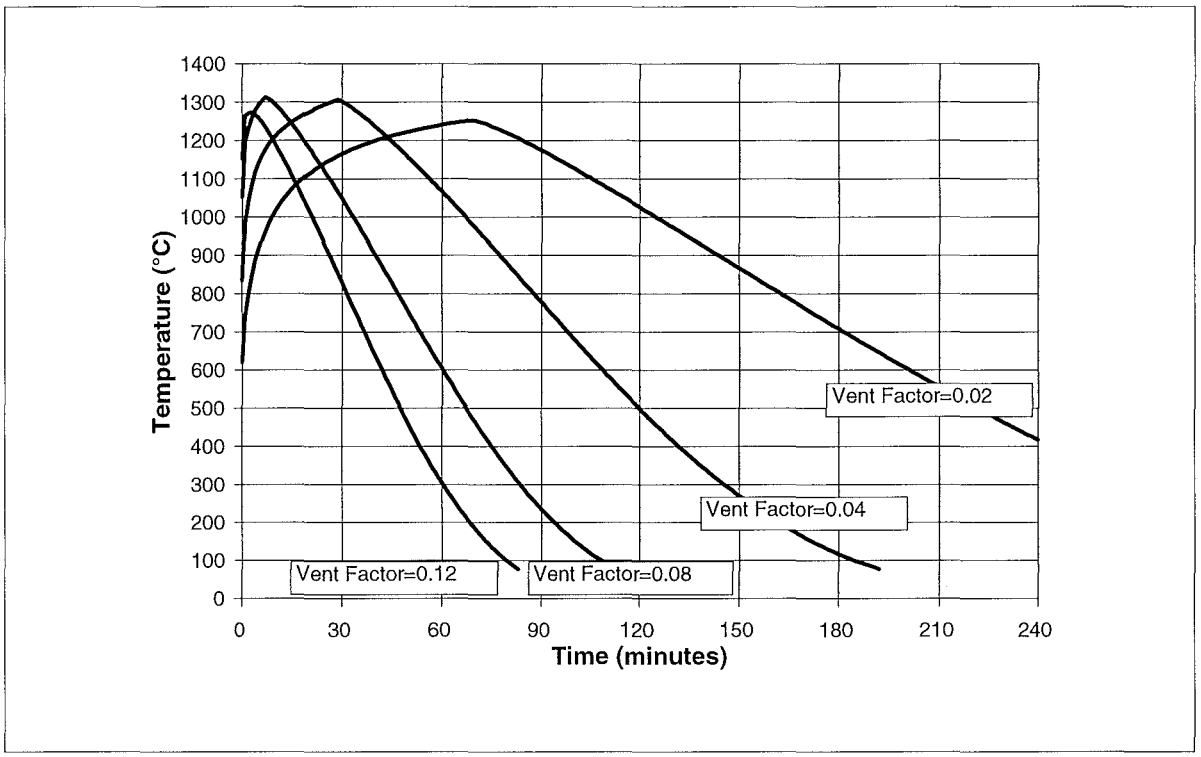

Fig 7.9 Design Fires, Lightweight Compartment Construction, Fire Load 1200 MJ/m² of Floor Area

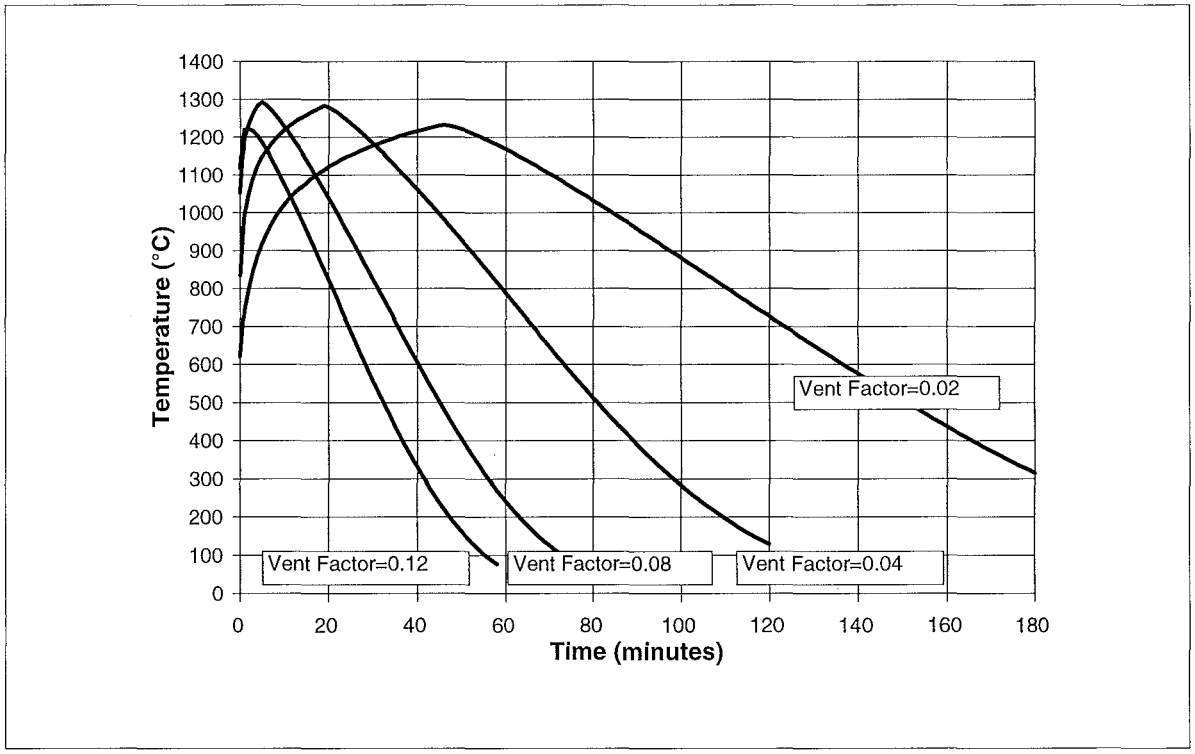

Fig 7.10 Design Fires, Lightweight Compartment Construction, Fire Load 800 MJ/m² of Floor Area

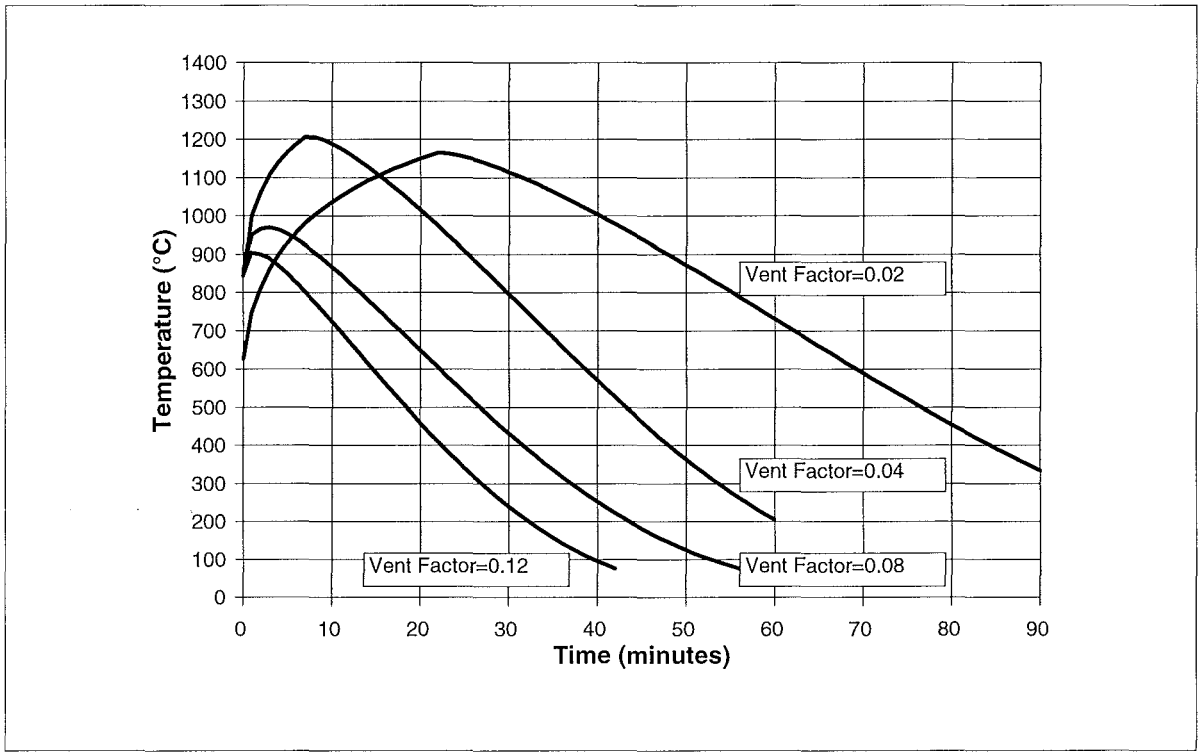

Fig 7.11 Design Fires, Lightweight Compartment Construction, Fire Load 400 MJ/m² of Floor Area

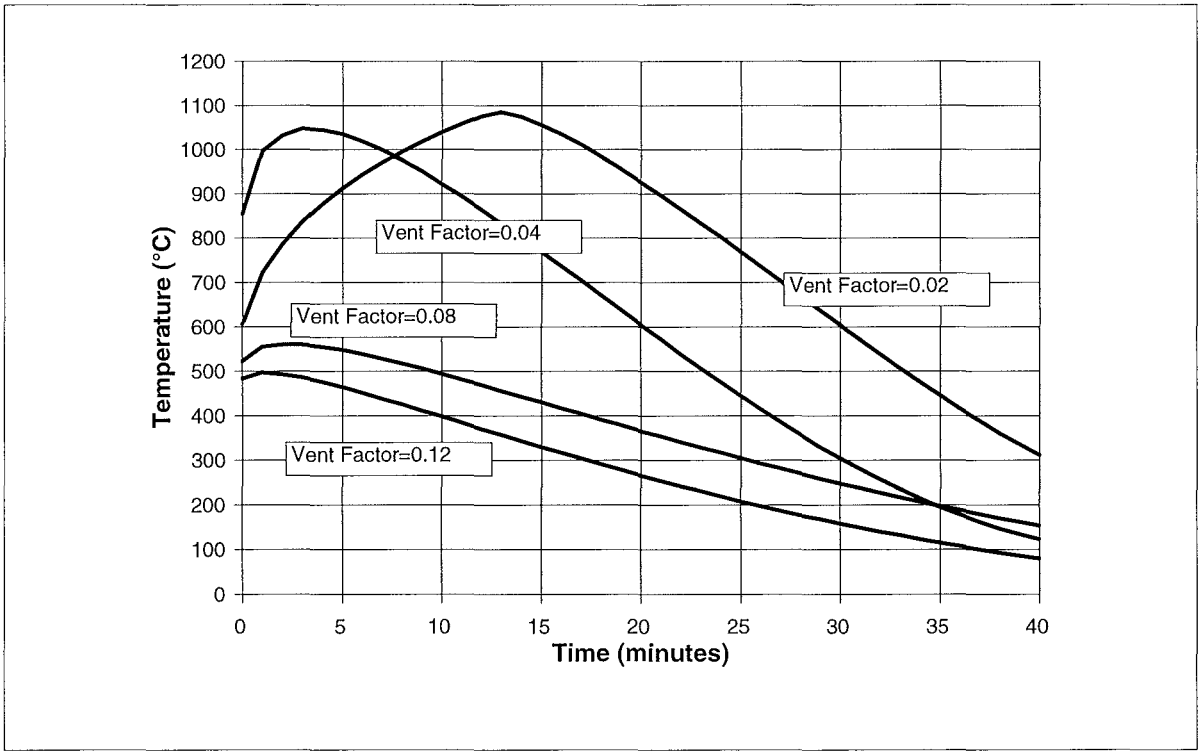

Fig 7.12 Design Fires, Lightweight Compartment Construction, Fire Load 200 MJ/m² of Floor Area

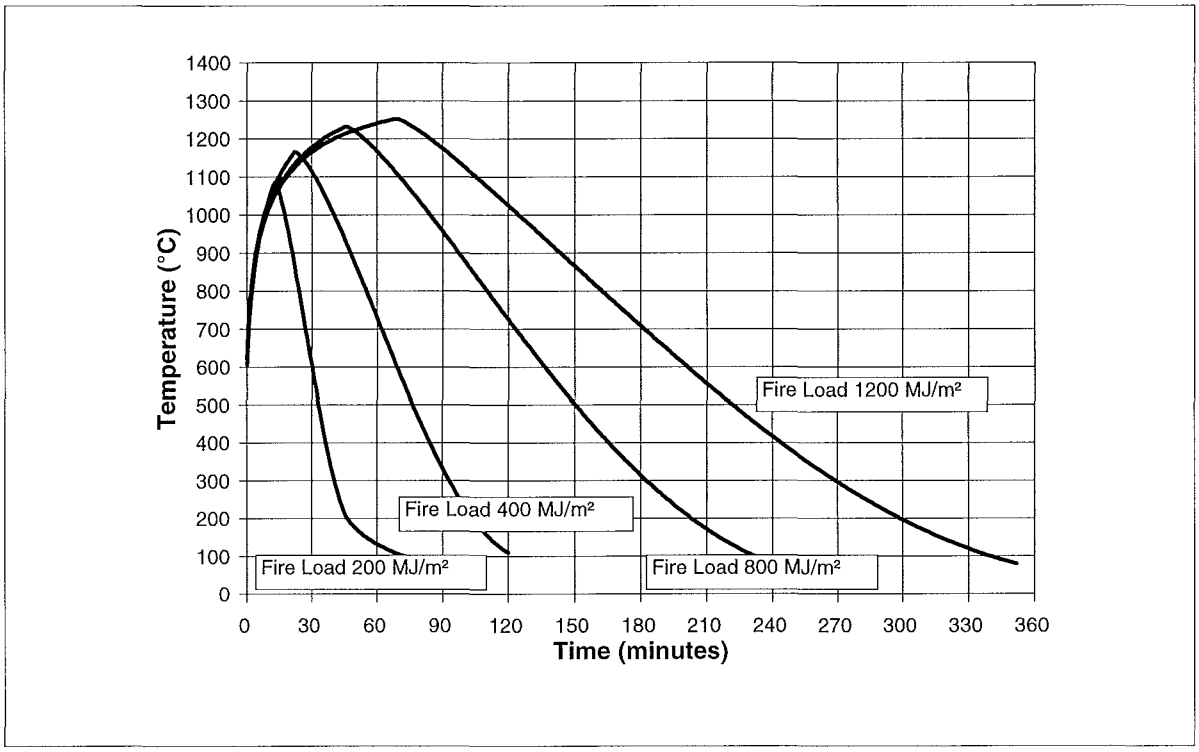

Fig 7.13 Design Fires, Lightweight Compartment Construction, Ventilation Factor 0.02

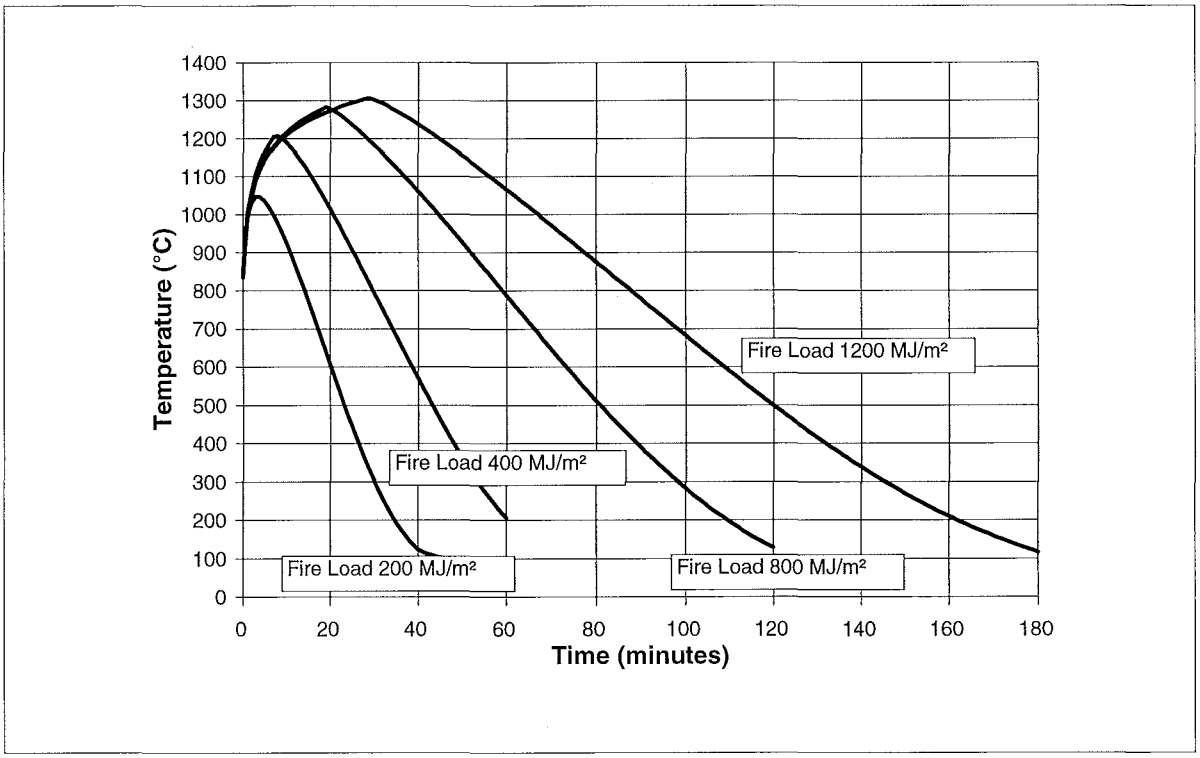

Fig 7.14 Design Fires, Lightweight Compartment Construction, Ventilation Factor 0.04

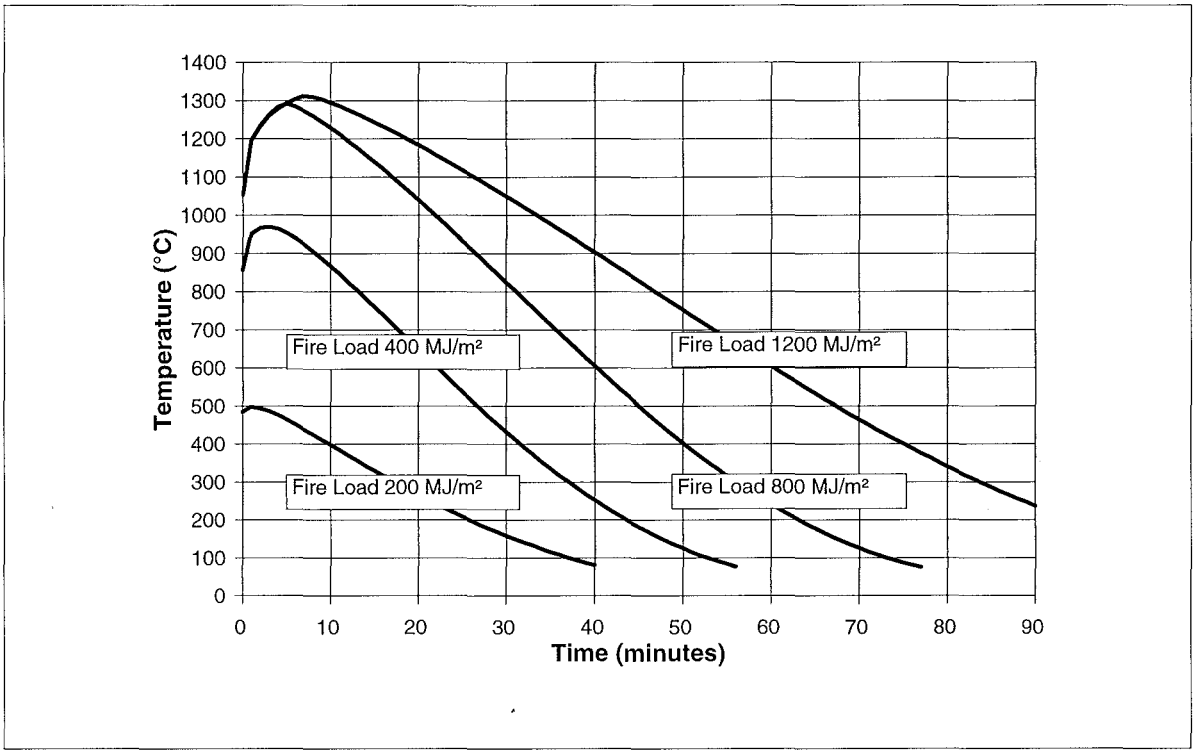

Fig 7.15 Design Fires, Lightweight Compartment Construction, Ventilation Factor 0.08

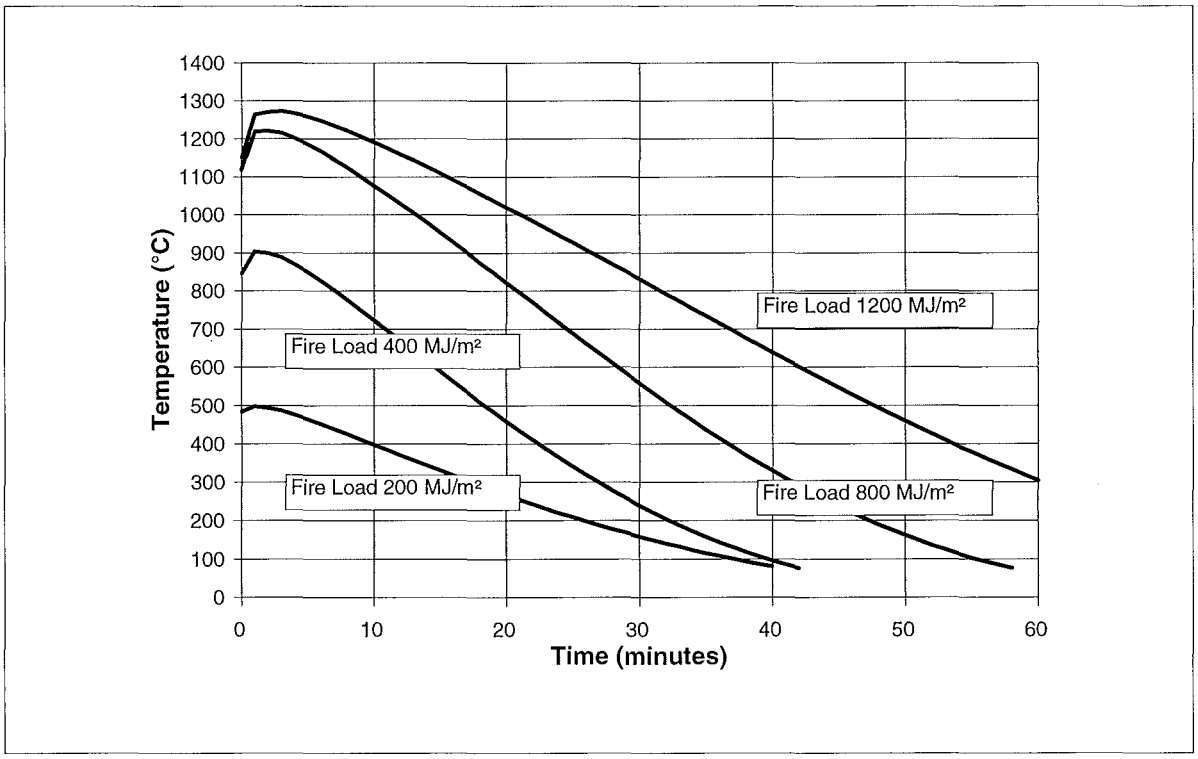

Fig 7.16 Design Fires, Lightweight Compartment Construction, Ventilation Factor 0.12

7.4 Comparison of COMPF2PC-Generated Design Fires

The COMPF2PC "Design" fires presented in Sections 7.2 and 7.3, are specific to the compartment material properties and compartment geometry selected. The "design" fires of Magnusson and Thelandersson were calculated for a series of compartment material properties, none of which were identical to those selected for the COMPF2PC "design" fires for either heavyweight or lightweight compartments. For the purposes of comparison, the COMPF2PC "Design" fire is recalculated for a compartment with material properties similar to that used for the "Type A" compartment used for the Swedish fires of Magnusson and Thelandersson. The "Type A" compartment has the following thermal properties :

conductivity (k)	= 0.7 kcal m^{-1} hr^{-1} K^{-1}	(0.81 W m^{-1} K^{-1})
density x specific heat (ρ C_p)	= 400 kcal m^{-3} K^{-1}	(1,674,000 J m^{-3} K^{-1})
giving a value of $\sqrt{(\rho\ C_p\ k)}$	=16.7 kcal m^{-2} $hr^{-0.5}$ K^{-1}	(1164.5 J m^{-2} K^{-1} $s^{-0.5}$)

The Type A compartment of Magnusson and Thelandersson therefore has a value of $\sqrt{(\rho\ C_p\ k)}$ approximately half way between that of the Heavyweight and Lightweight compartments for which COMPF2PC design fires are presented in Sections 7.2 and 7.3, and is representative of a compartment of mixed concrete, masonry and plasterboard construction. Comparison is made for fires of fire load 1200 MJ m^{-2} of floor area, or 273 MJ m^{-2} of total bounding surface area. The Swedish fires of Magnusson and Thelandersson are computed for a range of fire loads which varies with ventilation factor. The "Swedish" temperature profiles presented in the graphs are interpolated from the published data from fires of higher and lower fire density, except for ventilation factor $A_V \sqrt{H} / A_T = 0.02$, which has a maximum fire load density of 251 MJ m^{-2}.

Figures 7.17 and 7.18 for ventilation factors $A_V \sqrt{H} / A_T = 0.12$ and 0.08 show that the COMPF2PC design fires have a similar maximum temperature and longer duration than both the Eurocode Parametric fire and the Swedish fire. This is contrary to the findings of Thomas 1997, who found COMPF2PC simulations were several hundred degrees cooler than the Swedish fires at high ventilation factor (refer Section 4.3.4).

Figure 7.19 for ventilation factor $A_V \sqrt{H} / A_T = 0.04$ shows a hotter temperature and longer duration. In Figure 7.20, for ventilation factor $A_V \sqrt{H} / A_T = 0.02$, the COMPF2PC fire is hotter than the Eurocode and Swedish fires, but has a duration similar to that predicted by the Eurocode and Swedish fires.

Note the limitations to the reliability of the COMPF2PC simulations for low ventilation ratio ($A_V \sqrt{H} / A_T < 0.04$) discussed in Section 6.

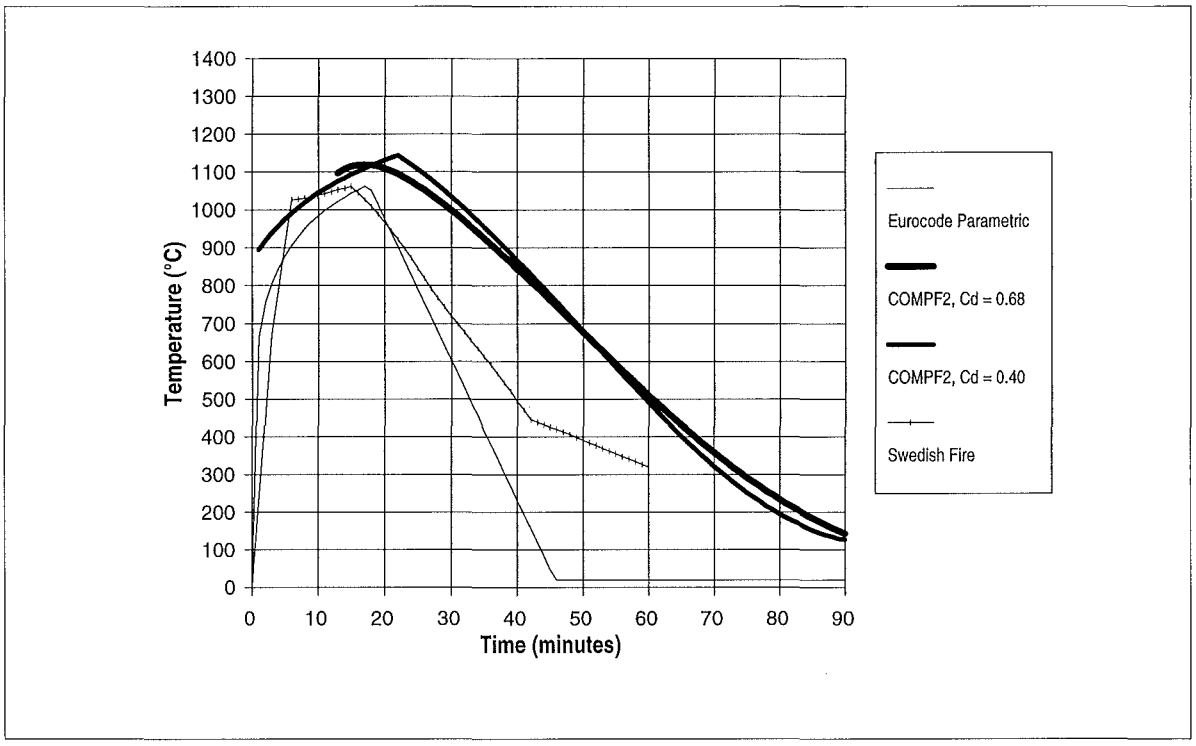

Fig. 7.17 Comparison of COMPF2, Eurocode Parametric and "Swedish" Fires
Fire Load 1200 MJ/m² Floor Area (273 MJ/m² Total Surface Area), Ventilation Factor = 0.12

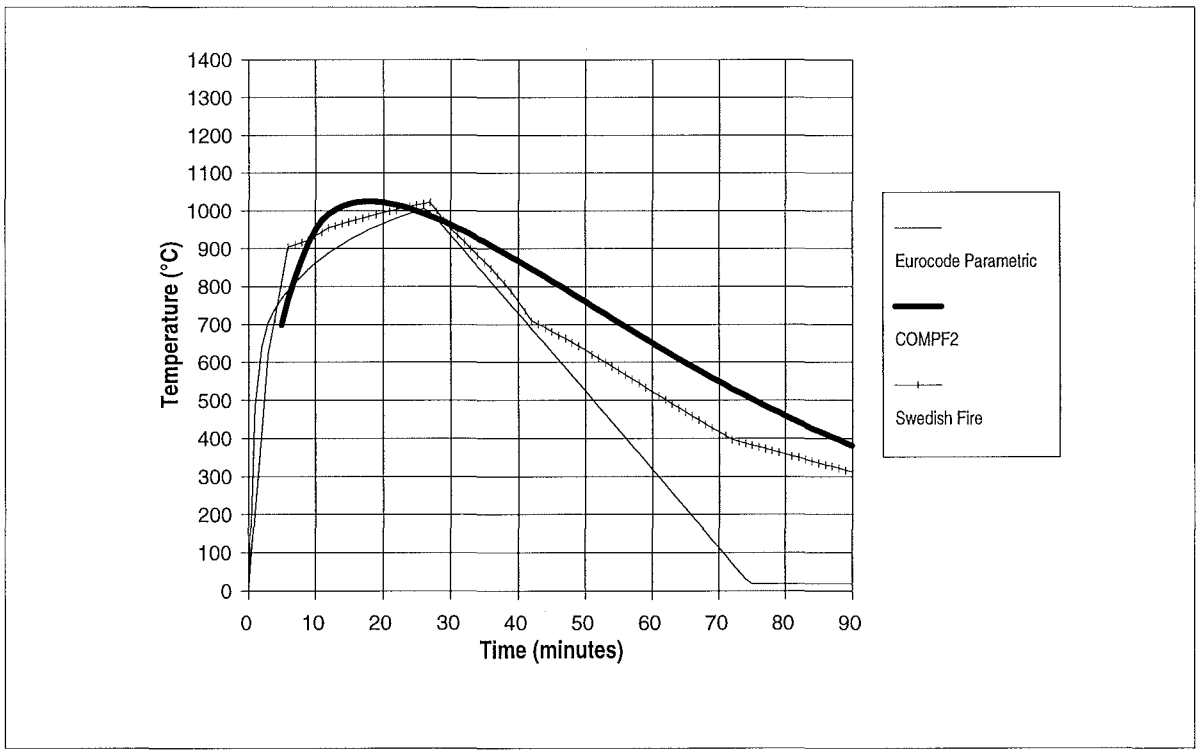

Fig 7.18 Comparison of COMPF2, Eurocode Parametric and "Swedish" Fires
Fire Load 1200 MJ/m² Floor Area (273 MJ/m² Total Surface Area), Ventilation Factor = 0.08

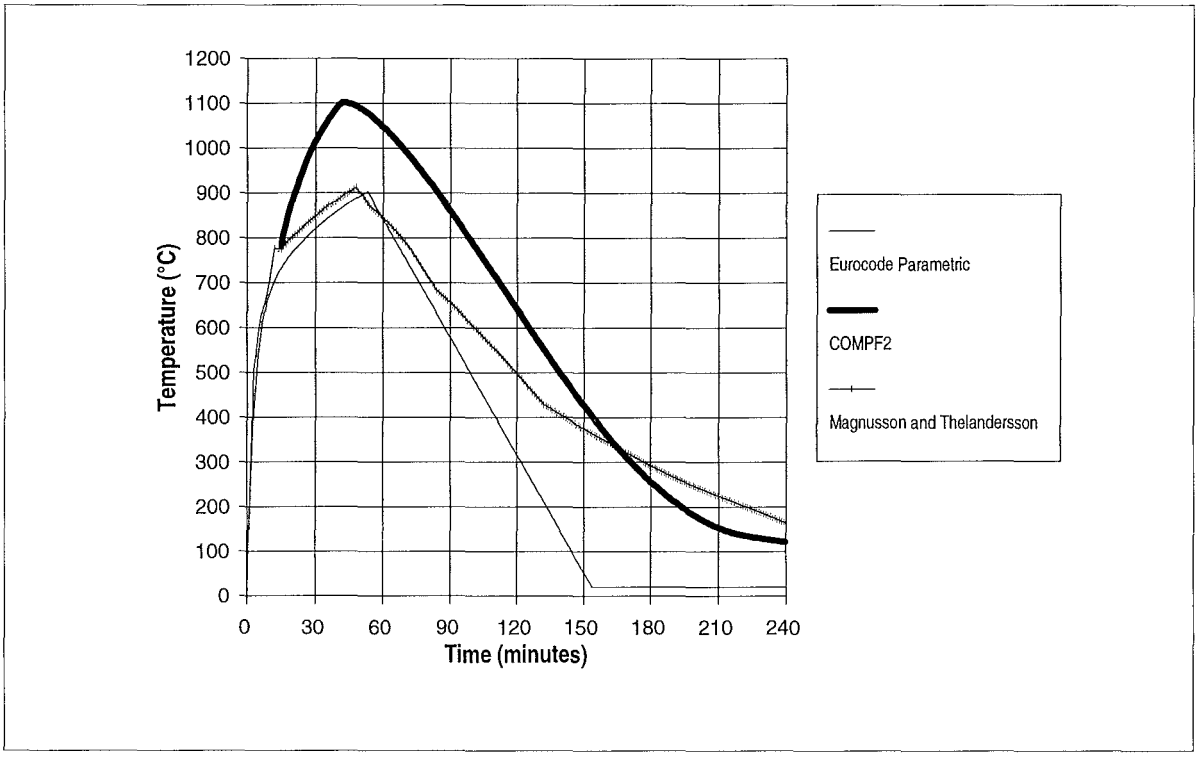

Fig 7.19 Comparison of COMPF2, Eurocode Parametric and "Swedish" Fires
Fire Load 1200 MJ/m² Floor Area (271 MJ/m² Total Surface Area), Ventilation Factor = 0.04

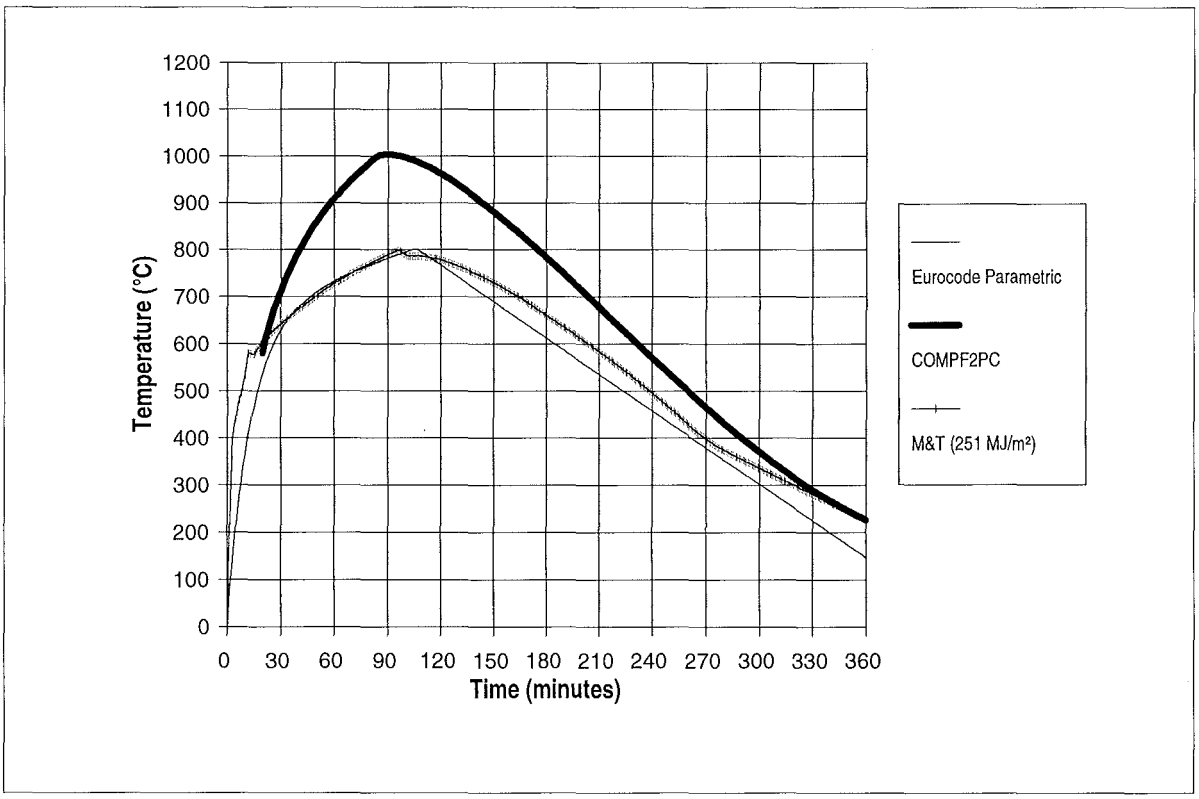

Fig 7.20 Comparison of COMPF2, Eurocode Parametric and "Swedish" Fires
Fire Load 1200 MJ/m² Floor Area (271 MJ/m² Total Surface Area), Ventilation Factor = 0.02

8 CONCLUSIONS AND RECOMMENDATIONS

8.1 Conclusions

It is concluded that :

(a) COMPF2PC can provide a reliable means of simulating the results of post flashover fires, especially for fires of moderate to high fire load (> 20 kg of wood equivalent per m^2 floor area) and moderate to high ventilation factor ($A_V \sqrt{H} / A_T \geq 0.04$).

(b) Careful characterisation of the fuel geometry is required to achieve adequate simulation results even within the above bounds.

(c) For fires characterised as the combustion of wood fuel, the best results are achieved by :

(i) characterising fuel elements as sticks with a shape factor (SHAPE) equal to 3.

(ii) using stick burning with a regression rate (REGRES) selected to utilise the stick fuel surface controlled pyrolysis rate model.

(iii) ensuring that the ratio of the stick fuel surface controlled pyrolysis rate to the ventilation limited pyrolysis rate is as per Table 6.7.

(d) For a fire load of 1200 MJ m^{-2} of floor area, and for ventilation factors $A_V \sqrt{H} / A_T \geq 0.04$, COMPF2 design fires have a significantly higher maximum temperature and longer duration than the Eurocode Parametric and Swedish fires for a compartment with the Swedish Fire Type A material properties. For ventilation factor $A_V \sqrt{H} / A_T = 0.02$, the maximum temperature is hotter, but duration similar to the Eurocode Parametric and Swedish fires.

This has significant implications for the calculation of time equivalent fires.

8.2 Recommendations

The following are recommended as worthwhile improvements to the COMPF2PC computer code :

(a) Update the user interface to allow :

(i) full screen editing of input data (rather than editing a text file),

(ii) better presentation of output data to suit electronic processing (the programme currently formats output to suit line-flow presentation, and requires extensive editing before it is suitable for importing into a spreadsheet for subsequent processing)

(iii) presentation of graphs

(b) Allow multiple layer construction for compartment boundaries to achieve more realistic modelling of the heat transfer to the structure and thereby a more realistic prediction of fire compartment gas temperature.

(c) Allow for different material selections for ceiling, walls and floor. Ideally, each wall element should be capable of having a different form of construction.

(d) Provide pre-flashover temperature prediction to allow the generation of complete temperature versus time profiles.

(e) Make wood density one of the input variables capable of being selected.

(f) Rationalise the crib burning formulae.

(g) Allow for horizontal vent openings in the roof.

(h) Allow for multiple windows of different sizes, including the case of ventilation apertures on multiple faces of the compartment, including cross-flow.

(i) Allow for time dependent ventilation area.

It is also recommended that :

(j) Further investigation be carried out into the methods of simulating fires especially those with low ventilation factor, to better characterise the methods developed within this report.

9 REFERENCES

Arnault, P., Ehm, H. and Kruppa, J. (1973) *Rapport Expérimental sur Les Essais Avec des Feux Naturels Exécutés Dans La Petite Installation de Maiziéres-lès-Metz*, Centre Technique Industriel de la Construction Métallique Report No. CECM 3/73611-F

Arnault, P., Ehm, H. and Kruppa, J. (1974) *Incendies Naturels avec des Meubleset du Papier Exécutés Dans La Petite Installation de Maiziéres-lès-Metz*, Centre Technique Industriel de la Construction Métallique Report No. 2.10.20-3

Babrauskas, V. (1975) *A Program for Calculating Post-Flashover Fire Temperatures*, Fire Research Group Report UCB FRG 75-2, University of California, Berkeley

Babrauskas, V. and Williamson, R.B. (1975) *Post-flashover Compartment Fires*, Fire Research Group Report No. UCB FRG 75-1, University of California, Berkeley

Babrauskas, V. (1976) *Fire Endurance in Buildings*, Dissertation submitted in Partial Satisfaction of the Requirements for the Degree of Doctor of Philosophy, University of California, Berkeley.

Babrauskas, V. and Williamson, R.B. (1978) 'Post-flashover Compartment Fires: Basis of a Theoretical Model', *Fire and Materials*, Vol. 2, No. 2, 39-53

Babrauskas, V. and Williamson, R.B. (1979) 'Post-flashover Compartment Fires': Application of a Theoretical Model, *Fire and Materials*, Vol. 3, No. 1, 1-7

Babrauskas, V. (1979) COMPF2 - *A Program for Calculating Post-flashover Fire Temperatures*, NBS Technical Note 991, Center for Fire Research, National Engineering Laboratory, National Bureau of Standards, U.S. Department of Commerce.

Babrauskas, V. and Wickström, U.G. (1979) 'Thermoplastic Pool Compartment Fires', *Combustion and Flame*, 34: 195-201 (1979)

Babrauskas, V. (1981) 'A Closed-form Approximation for Post-flashover Compartment

Fire Temperatures', *Fire Safety Journal*, 4, pp 63-73.

Babrauskas, V. (1998) Personal communication

Baines, J.T. (Ed) (1984) *Energy Data and Conversion Factors, A New Zealand Handbook*, First Edition, Report No. 100, New Zealand Energy Research & Development Committee, May 1984.

Birk, D. (1991) *An Introduction to Mathematical Fire Modeling*, Technomic Publishing Co., Lancaster, PA.

Bøhm, B. (1977) *Fully Developed Polyethylene and Wood Compartment Fires with Application to Structural Design*, Laboratory of Heating and Air Conditioning, Technical University of Denmark

Bøhm, B. and Hadvig, S. (1982) 'Nonconventional Fully Developed Polyethylene and Wood Compartment Fires', *Combustion and Flame*, Vol. 44, No. 1-3, pp 201 - 221.

Buchanan, A.H. (1998a) 'Performance Based Structural Design for Fire', *Proceeding International Conference International Conference on Performance Based Codes*, Maui, Hawaii, Society of Fire Protection Engineers, March 1998.

Buchanan, A.H. (1998b) Private Communication

Buchanan, A.H. ((1998c) 'Modelling Post-flashover Fires with FASTLite', *Journal of Fire Protection Engineering*, Vol 9, No 3

Bullen, M.L. and Thomas, P.H. (1978) 'Compartment fires with non-cellulosic fuels', *Seventeenth Symposium (International) on Combustion*, The Combustion Institute, p. 1139

Bullen, M.L. and Thomas, P.H. (1979) 'Compartment Fires with non-cellulosic fuels', *Colloquium of Fire and Explosion*, Fire Research Station, UK, 1979, 1139-1147

Bullen, M.L. and Thomas, P.H. (1980) 'Burning of Fuels in Fully-Developed Room Fires', *Fire Safety Journal*, 2 (1980), 275-281

Burgess, D.S., Strasser, A. and Grumer, J. (1961) *Fire Research Abstracts and Reviews*, Vol. 3, pp 177-192, 1961.

Collins, M.J. (1983) *Density Conversion for Radiata Pine*, FRI Bulletin No. 49, Forest Research Institute, Rotorua, New Zealand

Cooper, L. (1982) 'A Mathematical Model for Estimating Available Safe Egress Time in Fires', *J. of Fire & Materials*, **6**, 135-144

Cooper, L., Forney, G. and Moss, W. (1990), *The Consolidated Compartment Fire Model, (CCFM) Computer Code, Application CCFM.Vents Parts I-IV*, NISTIR 4342 - 4345, National Institute of Standards, Gaithersburg, MA.

Curtat, M. (1983) Modélisation de l'Essai de Coin, Centre Scientifique et Technique du Bâtiment, Rapport Final, Convention No. 79.61.02 avec le Ministère, de l'Urbanisme et du Logement, Paris.

Davis, W. and Cooper, L. (1989) *Estimating the Environment and the Response of Sprinkler Links in Compartment Fires with Draft Curtains and Fusible Link Actuated Ceiling Vents, Part II: User Guide for the Computer Code LAVENT*, NIST-IR-89-5122, National Institute of Standards, Gaithersburg, MA.

Dietenberger, M. (1987) *Improved Furniture Fire Model within FAST : HEMFAST-2*, Interim Technical Report UDR-TR-87-1135, University of Dayton Research Institute, Dayton, OH.

Dietenberger, M. (1991) *Technical Reference and User's Guide for FAST / FFM Version 3*, NIST-GCR-91-589, National Institute of Standards and Technology, Gaithersburg, MA.

Drysdale, D. (1985) *An Introduction to Fire Dynamics*, Wiley Interscience.

Emmons, H. Mitler, H. and Trefethen, L. (1978) *Computer Fire Code III*, Home Fire Project Technical Report No. 25, Harvard University, Cambridge, MA.

Eurocode (1996). *Eurocode 1: Basis of Design and Actions on Structures, Part 2.2 : Actions on Structures Exposed to Fires*, DD ENV 1991-2-2:1996

Garm, J. (1983) *Computer Fire Code VI - Vols 1 and 2*, NBSGCR 83-451, National Bureau of Standards, Gaithersburg, MA.

Hägglund, B. (1983) *A Room Fire Simulation Model*, Department of Defencse, FAO Report 620501-D6, Stockholm

Harmathy, T.Z. (1972) 'A new Look at Compartment Fires, Parts I and II', *Fire Technology*, **8**, 196, 326

Harmathy, T.Z. (1980a) 'Fire Severity: basis of fire safety design', *Presented at International Symposium on Fire Safety of Concrete Structures*, Fall Convention of the American Concrete Institute, San Juan, Puerto Rico, September 1980

Harmathy, T.Z. (1980b) ;The Possibility of Characterising the Severity of Fires by a Single Parameter', *Fire and Materials*, **4**, 71 (1980)

Harmathy, T.Z. and Mehaffey, J.R. (1983) 'Post-flashover Compartment Fires', *Fire and Materials*, Vol. 7, No. 2, pp 49 - 61.

Hettinger, J.C. and Barnett, J.R. (1991) 'Evolution of the Fire Development Scenario for Subway Vehicle Fires: Historical Observations, Vehicle Design Standards, and Application of the COMPF2 Post-Flashover Computer Model', *7th International Symposium on Aerodynamics and Ventilation of Vehicle Tunnels*, Brighton, 27-29 November, 1991

Ho, V., Siu, N., Apostolakis, G. and Flanagan, G. (1986) COMPBRN III - A Computer Code for Modeling Compartment Fires, NUREG / CR-4566, ORNL / TM-10005, Oak Ridge National Laboratory, Oak Ridge, TN.

ISO (1975) *Fire Resistance Tests.* Elements of Building Construction, ISO 834, International Organisation for Standardisation, Geneva

Janssens, M. (1992) 'Room Fire Models', Chapter 6, In: *Heat Release in Fires*, editors V. Babrauskas and S.L. Grayson, Elsevier.

Jones, W.W. (1985) 'A Multicompartment Model for Spread of Fire, Smoke and Toxic

Gases', *Fire Safety Journal*, **9**, 55-79

Jones, W.W., Forney, G.P. (1990) *A Programmer's Reference Manual for CFAST, the Unified Model of Fire Growth and Smoke Transport*, NIST Technical Note 1283, National Institute of Standards and Technology, Gaithersburg, MA.

Jones, W.W., Forney, G.P., Bailey, J.J. and Tatem, P.A. (1996) 'Comparison of CFAST Prediction to Real-Scale Fire Tests', *Proceedings of Fire Safety Conference on Performance Based Concepts*, October 15-17, 1996, Zurich, Switzerland.

Kawagoe, K. (1958) *Fire Behaviour in Rooms*, Report of the Building Research Institute, No. 27, September 1958

Kawagoe, K. (1967) *Estimation of Fire Temperature - Time Curve in Rooms*, Third Report, BRI Research Paper No. 29, Building Research Institute, Ministry of Construction, Japanese Government

Kawagoe, K. (1971) *Charts for Estimating the Equivalent Fire Duration on the Standard Temperature-Time Curve*, BRI Research Paper No. 45, Building Research Institute, Ministry of Construction, Japanese Government

Kawagoe, K. and Sekine, T. (1963) *Estimation of Fire Temperature-Time Curve in Rooms*, BRI Occasional Report No. 11, Building Research Institute, Ministry of Construction, Japanese Government

Kawagoe, K. and Sekine, T. (1964) *Estimation of Fire Temperature-Time Curve in Rooms*; Second Report, BRI Occasional Report No. 17, Building Research Institute, Ministry of Construction, Japanese Government

Kirby, B.R., Wainman, D.E., Tomlinson, L.N., Kay, T.R. and Peacock, B.N. (1994) *Natural Fires in Large Scale Compartments*, A British Steel Technical, Fire Research Station Collaborative Project, British Steel Technical, Swinden Laboratories, Moorgate, Rotherham.

Kruppa, J. (1998) Personal communication

MacArthur, C. (1982) *Dayton Aircraft Cabin Fire Model, Version 3, Volume 1: Physical Description*, DOT / FAA / CT-81 / 69-1, Federal Aviation Administration, Atlantic City, NJ.

Magnusson, S.E. and Thelandersson, S. (1970) *Temperature-Time Curves of Complete Process of Fire Development*, Civil Engineering and Building Construction Series No. 65, Acto Polytechnica Scandinavica.

Magnusson, S.E., Karlsson, B. and Andersson, B. (1990) 'Numerical Simulation of Room Fire Growth on Combustible Linings and a Rational Classification Model', In: *Proceedings of the Interflam '90 Conference*, University of Kent, Cambridge, UK.

McAdams, W.K. (1954) *Heat Transmission*, McGraw, New York

Mitler, H. and Emmons, H. (1981) *Documentation for CFC V, the Fifth Harvard Computer Fire Code*, NBSGCR 81-344, National Bureau of Standards, Gaithersburg, MA

Mitler, H. and Rockett, J. (1987) *User's Guide to FIRST,A Comprehensive Room Fire Model*, NBSIR 87-3595, National Bureau of Standards, Gaithersburg, MA.

Modak, A. and Croce, P.A. (1976) *Plastic Pool Fires*, Serial 22361-3, Factory Mutual Research Corporation, Norword, Mass.

Nakaya, I. and Akita, K. (1983) 'A Simulation Model for Compartment Fires', *Fire Safety Journal*, **5**, 157 - 165

Nilsson, L. (1971) *The Effect of Porosity and Air Flow on the Rate of Combustion of Fire in an Enclosed Space*, Report R22, Division of Structural Mechanics and Concrete Construction, Lund Institute of Technology, Lund (In Swedish with English summary).

Nilsson, L. (1974) *Time Curve of Heat Release for Compartment Fires with Fuel of Wooden Cribs*, Bulletin 36, Division of Structural Mechanics and Concrete Construction, Lund Institute of Technology, Lund, Sweden.

Ödeen, K. (1963) *Theoretical Study of Fire Characteristics in Enclosed Spaces (Bulletin 10)*, Division of Building Construction, Royal Institute of Technology, Stockholm.

Ödeen, K. (1970) *Standard Fire Endurance Tests - Discussion, Criticism and Alternatives*, American Society of Testing and Materials, Standard Technical Publication ASTM STP464, Philadelphia, 1970, pp 30-56

Pape, R., Waterman, T. and Eichler, (1981) *Development of a Fire in a Room from Ignition to Full Room Involvement - RFIRES*, NBSGCR 81-301, National Bureau of Standards, Gaithersburg, MA

Peacock, R.D., Reneke, P.A., Jones, W.W. and Bukowski, R.W. (1997) *A User's Guide for FAST 3.0 : Engineering Tools for Estimating Fire Growth and Smoke Transport*, Special Publication, Building and Fire Research Laboratory, National Institute of Standards and Technology, Gaithersburg, MD, February 1997

Pettersson, O., Magnusson, S.E. and Thor, J. (1976) *Fire Engineering Design of Steel Structures*, Publication 50, Swedish Institute of Steel Construction, Sweden

Portier, R.W., Peacock, R.D. and Reneke, P.A. (1996) *FASTLite: Engineering Tools for Estimating Fire Growth and Smoke Transport*, Special Publication 899, Building and Fire Research Laboratory, National Institute of Standards and Technology, Gaithersburg, MD.

Proe, D.J. and Bennetts, I.D. (1994) *Real Fire Test in 380 Collins Street Office Enclosure*, BHP Research Report No. BHPR/PPA/R/051/SG021A, September 1994.

Quintiere, J. and McCaffrey, B. (1980) *The Burning of Wood and Plastic Cribs in an Enclosure: Volume I.*, NBSIR 80-2054, National Bureau of Standards, Gaithersburg, MA.

Roy, F. (1993a) *Essais d'Incendies Naturels avec Profilés en Acier Nus et Protégés*, Centre Technique Industriel de la Construction Métallique Report No. 92-E-080

Roy, F. (1993b) *Essais d'Incendies Naturels avec Profilés en Acier Nus et Protégés*,

Centre Technique Industriel de la Construction Métallique Report No. 92-E-093

Roy, F. (1993c) *Essais d'Incendies Naturels avec Profilés en Acier Nus et Protégés*, Centre Technique Industriel de la Construction Métallique Report No. 92-E-094

Schaffer, E. L. (1966) *Review of Information Related to the Charring of Wood*, Research Note FPL-145, USDA Forest Prods. Lab., Madison

Schneider, V. and Haksever, A. (1980) *Wärmebilanz-berechnungen für Brandräume mit Unterschiedlichen Randbedingungen*, Technical University of Braunschweig, Germany FR.

Sjölin, W. (1969) *Fires in Residential Spaces Ignited by Heat Radiation from Nuclear Weapons*.

Smith, E. and Satija, S. (1983) 'Release Rate Model for Developing Fires', *ASME J. Heat Transfer*, **105**, 282-287.

Tamanini, F. (1974) *A Study of the Extinguishment of Wood Fires*, PhD Dissertation, Harvard University, Cambridge.

Tanaka, T. (1977) *A Mathematical Model of a Compartment Fire*, Building Research Institute, Research Paper No. 70, Tokyo.

Tanaka, T. (1983) *A Model of Multiroom Fire Spread*, NBSIR 83-2718, National Bureau of Standards, Gaithersburg, MA.

Tsuchiya, Y. and Sumi, K. (1971) 'Computation of the Behaviour of fire in an Enclosure', *Combustion and Flame*, **16**, 131

Thomas, G. C. (1997) *Fire Resistance of Light Timber Framed Walls and Floors*, Fire Engineering Research Report 97/7, University of Canterbury

Thomas, I.R., Bennetts, I.D., Proe, D.J., Lewins, R.R. and Almand, K.H. (1989) *Fire in Offices*, Structural Steel Development Group, BHP Steel, Melbourne, Australia.

Thomas, I.R., Bennetts, I.D., Dayawansa, P., Proe, D.J. and Lewins, R.R. (1992) *Fire Tests of the 140 William Street Office Building*, BHP Research - Melbourne Laboratories Rep. No. BHPR/ENG/R/92/043/SG2C, February, 1992

Thomas, P.H. and Nilsson, L. (1973) *Fully Developed Compartment Fires: New Correlations of Burning Rates*, Fire Research Note No 979, Fire Research Station.

Thomas, P.H. (1974) *The Effect of Crib Porosity in Recent Crib Experiments*, Fire Research Note No 999, Fire Research Station.

Thomas, P.H. (1976) *Some problem aspects of fully-developed room fires*, Fire Standards and Safety, ASTM Special Technical Publication 614, Philadelphia

Wade, C. (1995) *Post-Flashover Fire Models - A Review.* Centre for Firesafety Studies, Worcester Polytechnic Institute, FPE 520 Term Paper, 17 April 1995.

Wang, Y., Cooke, G and Moore, D. (1996) 'Large Compartment Fire Tests at Cardington and the Assessment of Eurocode 1', *IABSE Colloquium, Basis of Design and Actions on Structures, Background and Application of Eurocode 1*, Delft.

Wickström, U.G. (1981) *Temperature calculation of insulated steel columns exposed to natural fires*, Statens Provningsanstalt, National Testing Institute, *Technical Report SP-RAPP 1981:14*, Boras, Sweden

Wickström, U.G. and Göransson, U. (1990) 'Flame Spread Predictions in Room Corner Test Based on the Cone Calorimeter', In: *Proceedings of the Interflam '90 Conference*, University of Kent, Canterbury, UK.

Yamashika, S. and Kurimoto, H. (1976) *Burning Rate of Wood Crib*, Report of Fire Research Institute of Japan, No. 41, pp 8 - 15

Zukoski, E. and Kubota, T. (1980) 'Two-layer Modeling of Smoke Movement in Building Fires', *J. of Fire and Materials*, **4**, 17-27

APPENDICES

APPENDIX A - COMPARTMENT DEFINITIONS MAGNUSSON AND THELANDERSSON

1 Enclosure A

All surfaces 200 mm thick, of concrete, brick etc.

Thermal conductivity 0.7 kcal m^{-1} h^{-1} $°C^{-1}$ (0.81 W m^{-1} K^{-1})

ρC_p = 400 kcal m^{-3} $°C^{-1}$ (1674 kJ m^{-3} K^{-1})

These are the same material properties as used for the Swedish Building Regulations 1967.

The combined $\sqrt{(\rho C_p k)}$ value is 1164.5 J m^{-2} K^{-1} $s^{-0.5}$

2 Enclosure B

All bounding surfaces concrete 200 mm thick.

Thermal conductivity 1.4 e $^{-0.001\theta}$ kcal m^{-1} h^{-1} $°C^{-1}$, where θ is the temperature in °C.

Enthalpy (I) is a function of temperature (from Figure 17, Pg. 65, Magnusson and Thelandersson, 1970)

3 Enclosure C

All surfaces lightweight concrete of 200 mm thickness.

Density ρ = 500 kg m^{-3}

Thermal conductivity (k) a function of temperature (Refer Figure 16, Page 65, Magnusson and Thelandersson, 1970).

Enthalpy (I) a function of temperature (from Figure 17, Pg. 65, Magnusson and Thelandersson, 1970)

4 Enclosure D

Bounding surfaces of 50% concrete and 50% lightweight concrete.

Thermal properties and thicknesses as for B and C type enclosures.

5 Enclosure E

Lightweight concrete 50% of bounding surface area, with thickness, density and thermal properties as for Enclosure C.

Concrete 33% of bounding surface area with thickness and thermal properties as for Enclosure B.

The remaining 17% of the bounding surface area was a composite panel consisting of plasterboard (13 mm), insulating wool (100 mm), and brickwork (200 mm)

Plasterboard density = 790 kg m^{-3}

Insulation density = 50 kg m^{-3}

Brick density = 1800 kg m^{-3}

Remaining thermal properties from Figs. 16, 17 and 18 on pp 65 - 66, Magnusson and Thelandersson, 1970

6 Enclosure F

Sheet steel of 2 mm thickness for 80% of bounding surface area.

Thermal properties of steel from Figs. 17 and 19, Magnusson and Thelandersson, 1970

Concrete 200 mm thick for the remaining 20% of the bounding surface area.

Thermal properties of concrete as for the type B enclosure.

7 Enclosure G

Concrete for 20 % of the bounding surface area, with thickness and thermal properties for Enclosure B.

Remaining 80% of the bounding surface area, a composite panel consisting of 2 x 13 mm plaster boards, 100 mm cavity and 2 x 13 mm plaster boards supported in steel stud framing. The enthalpy of the plaster board as a function of temperature was also a function of the rate of temperature rise in the test compartment.

APPENDIX B - SIMULATION OF REAL FIRES USING COMPF2PC

Appendix B1 NFSC Fires

B1.1 Summary of Fires Simulated

The following NFSC fires were simulated. A wide range of fire loads is examined from over 90 down to 15 kg wood m^{-2} of floor area and an equally wide range of ventilation factors from 0.015 to 0.157 $m^{0.5}$. These are scheduled in Table B1.1.

Reference No.	Fire Load (kg wood m^{-2} of floor area)	Ventilation Factor $A_V \sqrt{H} / A_T$ ($m^{0.5}$)	Fuel Type
NFSC -79	90.9	0.132	Wood (1015 kg)
NFSC 70-46	60.0	0.157	Wood (745.3 kg)
NFSC 70-22	60.0	0.091	Wood (745.3 kg)
NFSC 70-19	60.0	0.055	Wood (744 kg)
NFSC 70-24	30.0	0.157	Wood (372.6 kg)
NFSC 70-21	30.0	0.091	Wood (372.6 kg)
NFSC 71-58	30.0	0.056	Furniture (151 kg), Paper (184 kg), Wood (37 kg)
NFSC 70-29	30.0	0.015	Wood (372.6 kg)
NFSC 70-16	29.9	0.015	Wood (372 kg)
NFSC 71-54	24.4	0.014	Furniture (190 kg), Paper (162 kg), Wood (20 kg)
NFSC 70-44	20.0	0.157	Wood (248.4 kg)
NFSC -69	15.6	0.030	Bedroom Furniture (451 kg)
NFSC 70-23	15.0	0.157	Wood (186 kg)
NFSC 70-20	15.0	0.091	Wood (186 kg)
NFSC 70-17	15.0	0.055	Wood (186 kg)

Table B1.1 NFSC Fires Simulated

In the following sections, different methods of modelling each of the experimental fires are discussed.

B1.2 NFSC -79

The compartment and ventilation opening geometry, materials of construction, fuel load, and relevant parameters calculated from the specified data, are as follows.

Specified Parameters	
Compartment Length	3.60 m
Compartment Width	3.10 m
Compartment Height	3.13 m
Ventilation Height	2.0 m
Ventilation Width	3.0 m
Sill Height	1.0 m
Wall Details	3 walls of 0.115 m normal brick + 0.160 m hard brick plus 1 wall of 0.175 m lightweight concrete
Ceiling Details	0.175 m lightweight concrete
Floor Details	refractory concrete
Fuel Load	1015 kg wood
Calculated Parameters	
Floor Area	11.16 m^2
Total Internal Surface Area	64.26 m^2
Ventilation Area	6.0 m^2
Ventilation Parameter ($A_V \sqrt{H}$)	8.485 $m^{5/2}$
Ventilation Parameter ($A_V \sqrt{H} / A_T$)	0.132 $m^{0.5}$
Fire Load Density	90.9 kg /m^2 of floor area
Fire Load Density	15.8 kg /m^2 of total bounding surface area

Table B1.2 NFSC -79 Input Data ; Fire Load 90.9 kg/m^2, Ventilation Factor 0.132

This fire has a high fire load and high ventilation factor.

From the initial data above, fires with the following stick size (D), regression rate (v_p), shape factor (F) and crib spacing to height ratio (S_c / H_c) were modelled, leading to the tabulated initial pyrolysis rates for stick burning, ventilation control, crib porosity control and crib fuel surface control mechanisms.

If the regression rate (v_p) is set to zero, the fire is calculated as a crib fire using the crib spacing to height ratio (S_c / H_c) which is specified. If the regression rate is specified, stick burning is assumed (and the crib burning equations are bypassed).

The lowest non-zero rate governs the initial fire development.

Note that the Shape = 2 defines a stick type fuel element (two dimensions smaller than the third), while Shape = 3 defines a cubic or spherical fuel element (approximately equal dimensions). Two initial pyrolysis rates for crib fuel surface controlled burning are calculated. The first is as per the theory presented by Babrauskas (1979) (as discussed in Section 3) and the second is as-programmed in the COMPF2PC computer programme (as discussed in Section 4). The latter is used in the various graphs which follow.

Identifier	Diam. (D) (m)	Stick Burn Regress Rate (v_p) (m/s)	Shape (F)	Crib (S_c/H_c)	Initial Pyrolysis Rate (kg/s)				
					Stick Burning	Vent. Control	Crib Porosity Control	Crib Fuel Surface (theory)	Crib Fuel Surface (progr)
A	0.050		2	0.150		1.018	1.340	0.833	1.215
B	0.045		2	0.150		1.018	1.489	0.986	1.438
C	0.065		2	0.150		1.018	1.031	0.547	0.799
D	0.075		2	0.175		1.018	1.042	0.435	0.635
E	0.065		3	0.100		1.018	0.687	0.547	1.198
F	0.075		3	0.100		1.018	0.595	0.435	0.953
G	0.100		3	0.200		1.018	0.893	0.275	0.601
H	0.050	1.2E-05	3		1.462	1.018			
I	0.050	1.0E-05	3		1.218	1.018			
J	0.075	1.2E-05	3		0.974	1.018			
K	0.075	1.0E-05	3		0.812	1.018			
L	0.075	1.0E-05	2		0.541	1.018			
M	0.050	1.0E-05	2		0.812	1.018			

Table B1.3 NFSC -79, Fire Simulation Parameters and Initial Pyrolysis Rates

NFSC -79, Crib Fire, Shape = 2 (Figure B1.1)

Identifier	Diam. (D) (m)	Shape (F)	Crib (S_c/H_c)	Initial Pyrolysis Rate (kg/s)			
				Vent. Control	Crib Porosity Control	Crib Fuel Surface (theory)	Crib Fuel Surface (progr)
A	0.050	2	0.150	1.018	1.340	0.833	1.215
B	0.045	2	0.150	1.018	1.489	0.986	1.438
C	0.065	2	0.150	1.018	1.031	0.547	0.799
D	0.075	2	0.175	1.018	1.042	0.435	0.635

The ventilation controlled pyrolysis rate is 1.018 kg s^{-1}. Stick size (D) and crib spacing to height ratio (S_c/H_c) are selected to provide pyrolysis rates slightly above the ventilation controlled pyrolysis rate for simulations A and B, and to provide pyrolysis rates slightly below the ventilation controlled pyrolysis rate for simulations C and D.

With simulations A and B, the fire will begin as ventilation controlled, but then become fuel surface controlled once part of the fuel has burnt away, due to the $(m / M_o)^{0.5}$ pyrolysis rate characteristic for surface controlled fires. Simulations C and D are fuel surface controlled from the beginning.

The peak fire temperature is well reproduced in Figure B1.1, with simulation C giving the closest to the test data. Simulation A is hotter by about 70 °C, and simulation D cooler by slightly over 100 °C.

The decay curves are convex, showing an increasing decay rate of temperature with time after the peak fire temperature has been reached. This is contradictory to the experimental data. It is nevertheless conservative, and over estimates temperatures during the decay phase above 400 - 650 °C. The predicted temperatures are non-conservative below this range. Sticks of smaller nominal dimensions (e.g. 0.05 m), produce higher maximum temperatures and steeper decay curves. More substantial sticks (0.10 m) produce lower maximum temperatures but a slower decay.

NFSC -79, Crib Fire, Shape = 3 (Figure B1.2)

Identifier	Diam. (D) (m)	Shape (F)	Crib (S_c /H_c)	Initial Pyrolysis Rate (kg/s)			
				Vent. Control	Crib Porosity Control	Crib Fuel Surface (theory)	Crib Fuel Surface (progr)
E	0.065	3	0.100	1.018	0.687	0.547	1.198
F	0.075	3	0.100	1.018	0.595	0.435	0.953
G	0.100	3	0.200	1.018	0.893	0.275	0.601

Crib porosity control initially governs for simulations E and F, with crib fuel surface control from the beginning in G.

The peak fire temperature is best predicted by Simulation F. The decay "curves" are almost linear following the peak temperature eventually developing a concave characteristic with decreasing rate of decay of temperature with time. This provides a slightly more realistic characteristic than the Shape = 2 Crib fires. These fires are generally conservative, and over estimate temperatures during the decay phase above 400 - 550 °C. The predicted temperatures are non-conservative below this range. More substantial fuel elements (e.g those of dimension 0.10 m) produce lower maximum temperatures but a slower decay.

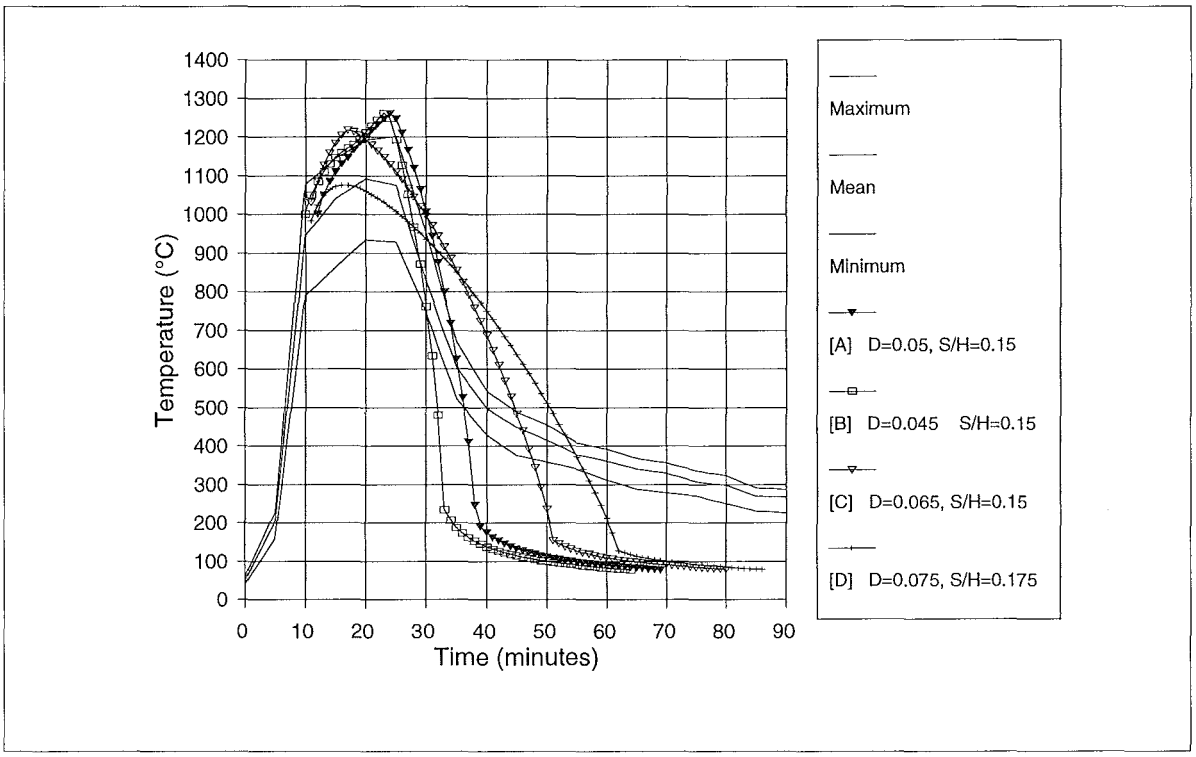

Figure B1.1 NFSC -79, 90.9 kg/m² Floor Area, Ventilation Factor = 0.132, Crib Fires, Shape = 2

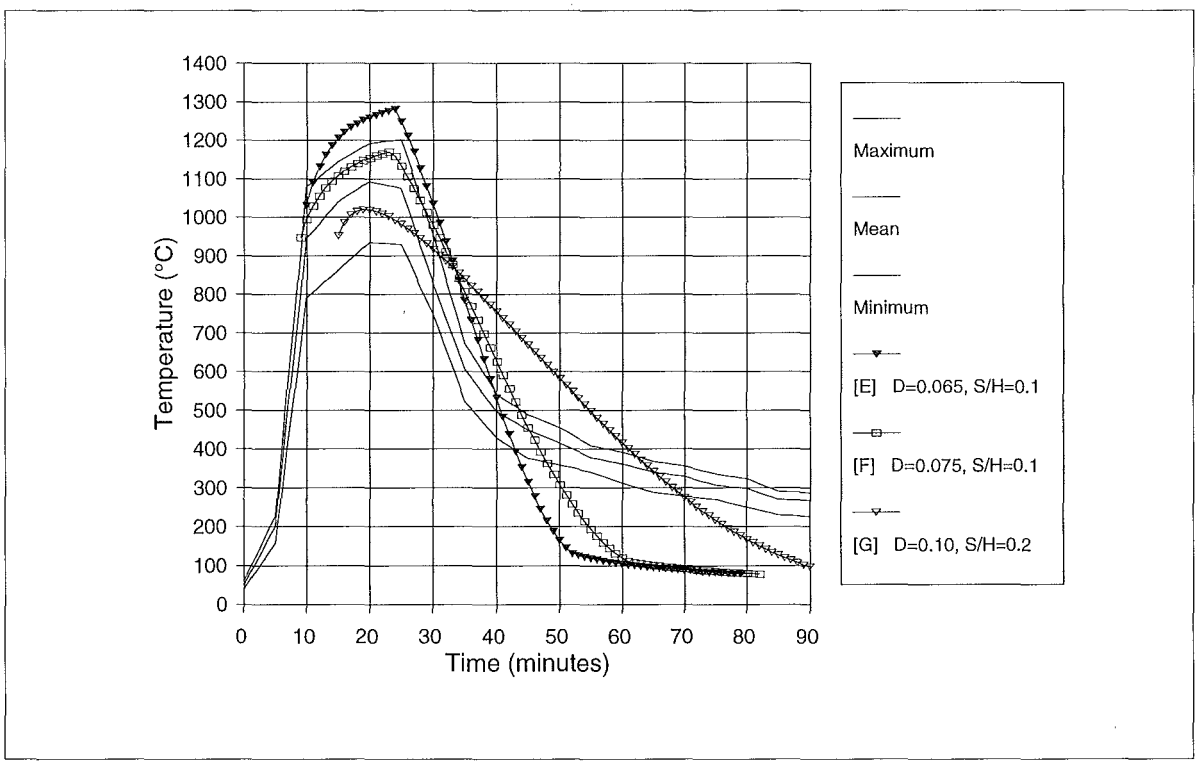

Figure B1.2 NFSC -79, 90.9 kg/m² Floor Area, Ventilation Factor = 0.132, Crib Fires, Shape = 3

NFSC -79, Stick Fire, Shape = 2 (Figure B1.3)

Identifier	Diam. (D) (m)	Stick Burn Regress Rate (v_p) (m/s)	Shape (F)	Initial Pyrolysis Rate (kg/s)	
				Stick Burning	Vent. Control
L	0.075	1.0E-05	2	0.541	1.018
M	0.050	1.0E-05	2	0.812	1.018

The two simulations are set up to give stick burning pyrolysis rates slightly and well below the ventilation controlled pyrolysis rate. Simulation M gives the closest prediction of the peak temperature, with Simulation L under-predicting the peak temperature by over 200 °C. As for the crib burning simulations with Shape = 2, the decay curves are convex and conservative down to about 400 °C.

NFSC -79, Stick Fire, Shape = 3 (Figure B1.4)

Identifier	Diam. (D) (m)	Stick Burn Regress Rate (v_p) (m/s)	Shape (F)	Initial Pyrolysis Rate (kg/s)	
				Stick Burning	Vent. Control
H	0.050	1.2E-05	3	1.462	1.018
I	0.050	1.0E-05	3	1.218	1.018
J	0.075	1.2E-05	3	0.974	1.018
K	0.075	1.0E-05	3	0.812	1.018

The four simulations are set up to have stick burning initial pyrolysis rates above and below the ventilation controlled pyrolysis rate. All four have almost the same maximum temperature, slightly above the actual peak fire temperature. Decay curves are almost linear, and conservative down to 450 - 550 °C.

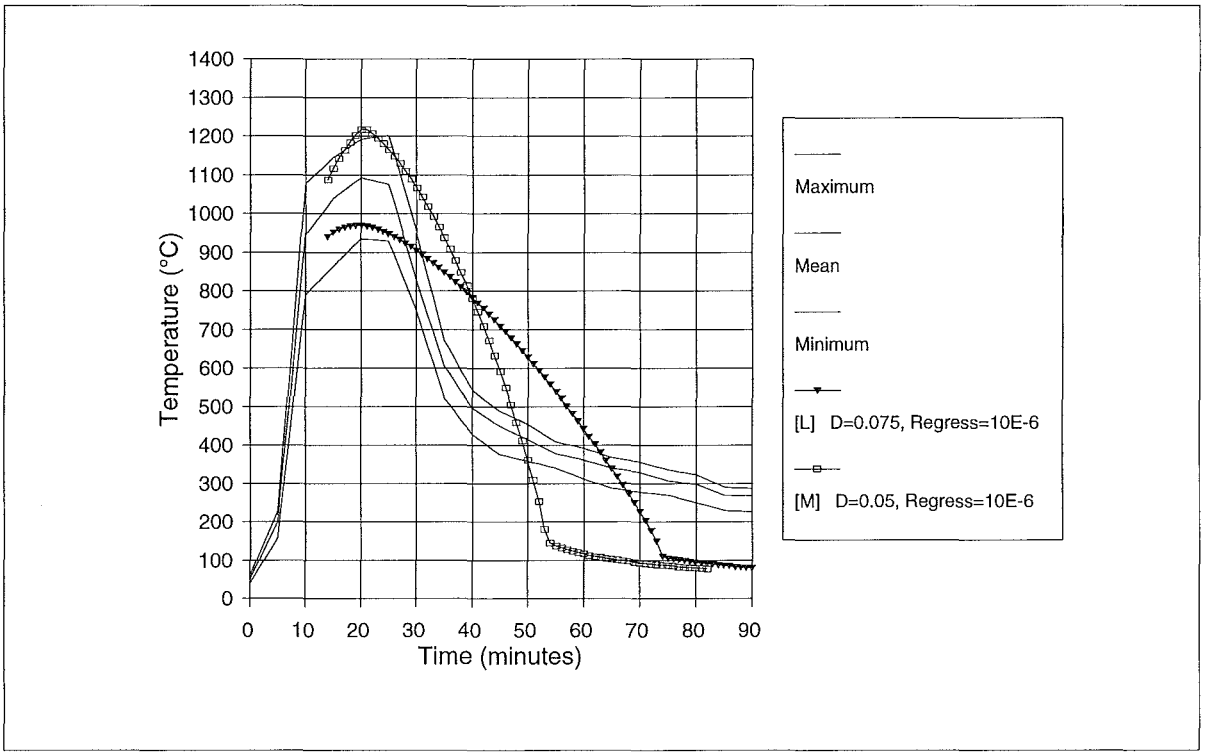

Figure B1.3 NFSC -79, 90.9 kg/m² Floor Area, Ventilation Factor = 0.132, Stick Fires, Shape = 2

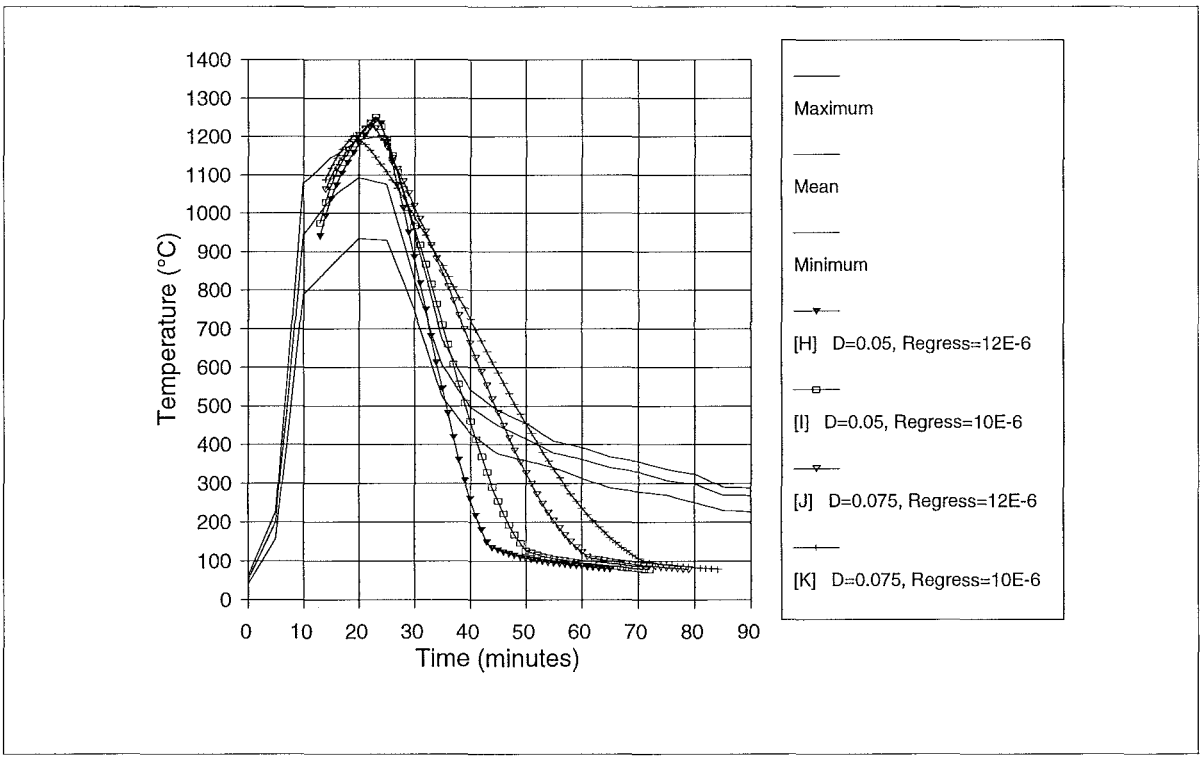

Figure B1.4 NFSC -79, 90.9 kg/m² Floor Area, Ventilation Factor = 0.132, Stick Fires, Shape = 3

B1.3 NFSC 70-19

The compartment and ventilation opening geometry, materials of construction, fuel load, and relevant parameters calculated from the specified data, are scheduled in Table B1.4.

Specified Parameters	
Compartment Length	3.68 m
Compartment Width	3.38 m
Compartment Height	3.13 m
Ventilation Height	2.18 m
Ventilation Width	1.18 m
Sill Height	0.95 m
Wall Details	3 walls of 0.115 m normal brick + 0.160 m hard brick plus 1 wall of 0.175 m lightweight concrete
Ceiling Details	0.175 m lightweight concrete
Floor Details	refractory concrete
Fuel Load	744 kg wood
Calculated Parameters	
Floor Area	12.44 m^2
Total Internal Surface Area	69.07 m^2
Ventilation Area	2.572 m^2
Ventilation Parameter ($A_V \sqrt{H}$)	3.798 $m^{5/2}$
Ventilation Parameter ($A_V \sqrt{H} / A_T$)	0.055 $m^{0.5}$
Fire Load Density	59.8 kg /m^2 of floor area
Fire Load Density	10.8 kg /m^2 of total bounding surface area

Table B1.4 NFSC 70-19 Input Data ; Fire Load 59.8 kg/m^2, Ventilation Factor 0.055

From the initial data above, fires with the following stick size (D), regression rate (v_p), shape factor (F) and crib spacing to height ratio (S_c / H_c)were modelled, leading to the tabulated initial pyrolysis rates for stick burning, ventilation control, crib porosity control and crib fuel surface control mechanisms. The lowest non-zero rate governs the initial fire development.

Identifier	Diam. (D) (m)	Stick Burn Regress Rate (v_p) (m/s)	Shape (F)	Crib (S_c /H_c)	Initial Pyrolysis Rate (kg/s)				
					Stick Burning	Vent. Control	Crib Porosity Control	Crib Fuel Surface (theory)	Crib Fuel Surface (progr)
A	0.075		2	0.100		0.456	0.436	0.319	0.466
B	0.050		2	0.050		0.456	0.327	0.611	0.891
C	0.075		2	0.110		0.456	0.480	0.319	0.466
D	0.100		3	0.125		0.456	0.409	0.201	0.441
E	0.075		3	0.100		0.456	0.436	0.319	0.698
F	0.050	7.0E-06	2		0.417	0.456			
G	0.075	1.2E-05	2		0.476	0.456			
H	0.100	1.3E-05	2		0.387	0.456			
I	0.050	5.0E-06	3		0.446	0.456			
J	0.075	7.0E-06	3		0.417	0.456			

Table B1.5 NFSC 70-19, Fire Simulation Parameters and Initial Pyrolysis Rates

NFSC 70-19, Crib Fire, Shape = 2 (Figure B1.5)

Identifier	Diam. (D) (m)	Shape (F)	Crib (S_c /H_c)	Initial Pyrolysis Rate (kg/s)			
				Vent. Control	Crib Porosity Control	Crib Fuel Surface (theory)	Crib Fuel Surface (progr)
A	0.075	2	0.100	0.456	0.436	0.319	0.466
B	0.050	2	0.050	0.456	0.327	0.611	0.891
C	0.075	2	0.110	0.456	0.480	0.319	0.466

Simulation A is crib porosity controlled at just below the ventilation limited pyrolysis rate. It will become fuel surface controlled relatively early. Simulation B is strongly crib porosity controlled. Simulation C is initially ventilation limited, but becomes fuel surface controlled relatively quickly.

The crib porosity-controlled fire [B] with crib spacing to height ratio (S/H) of 0.05, gives the most intense fire and over-predicts the maximum temperature by about 100 °C. It also decays extremely rapidly once the peak temperature is reached, and is non-conservative below 800 °C. The shape of the temperature versus time curve is relatively similar to that of the example fire pessimised on pyrolysis in Figure 3.2.

The other fire simulations become fuel surface-controlled relatively quickly, and have a convex decay curve which approximates the experimental data to about 500 °C reasonably well.

NFSC 70-19, Crib Fire, Shape = 3 (Figure B1.6)

Identifier	Diam. (D) (m)	Shape (F)	Crib (S_c/H_c)	Initial Pyrolysis Rate (kg/s)			
				Vent. Control	Crib Porosity Control	Crib Fuel Surface (theory)	Crib Fuel Surface (progr)
D	0.100	3	0.125	0.456	0.409	0.201	0.441
E	0.075	3	0.100	0.456	0.436	0.319	0.698

Both simulations are crib porosity controlled initially. Simulation D quickly becomes fuel surface controlled and predicts the maximum temperature to within 20 °C. The decay curve is only slightly conservative down to 500 °C. Simulation E remains crib porosity controlled for longer, and reaches a higher maximum temperature, prior to fuel surface control taking over and a substantially higher decay rate resulting, which is generally non-conservative for the maximum temperature profile, but reproduces the mean temperature profile moderately well.

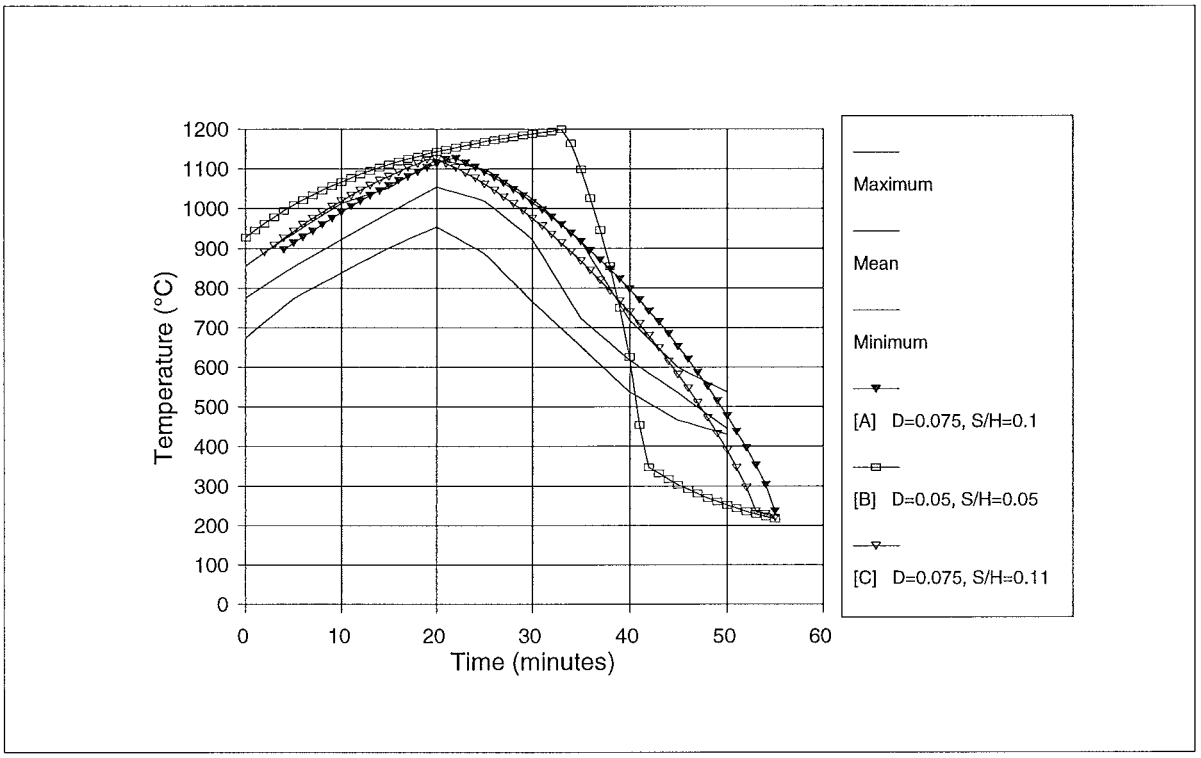

Fig B1.5 NFSC 70-19, 60 kg/m² Floor Area, Ventilation Factor = 0.055, Crib Fires, Shape = 2

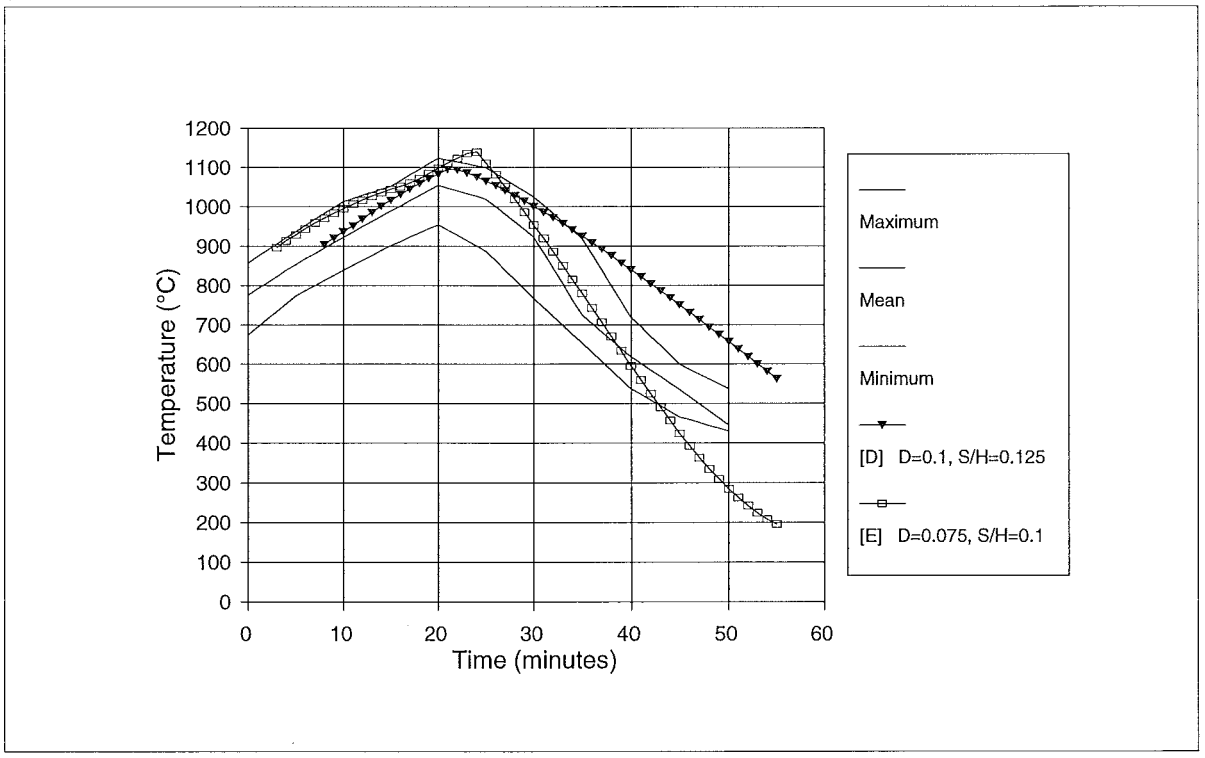

Fig B1.6 NFSC 70-19, 60 kg/m² Floor Area, Ventilation Factor = 0.055, Crib Fires, Shape = 3

NFSC 70-19, Stick Fire, Shape = 2 (Figure B1.7)

Identifier	Diam. (D) (m)	Stick Burn Regress Rate (v_p) (m/s)	Shape (F)	Initial Pyrolysis Rate (kg/s)	
				Stick Burning	Vent. Control
F	0.050	7.0E-06	2	0.417	0.456
G	0.075	1.2E-05	2	0.476	0.456
H	0.100	1.3E-05	2	0.387	0.456

The three simulations are structured with stick burning pyrolysis rates both above and below the ventilation limited pyrolysis rate.

All predict the maximum temperature well, with Simulation G, with the highest initial pyrolysis rate, having the greatest decay rate. It is non-conservative to a temperature of about 600 °C. Simulations F and H decay at a slower rate, providing a conservative estimate of fire temperatures down to 500 °C and below.

NFSC 70-19, Stick Fire, Shape = 3 (Figure B1.8)

Identifier	Diam. (D) (m)	Stick Burn Regress Rate (v_p) (m/s)	Shape (F)	Initial Pyrolysis Rate (kg/s)	
				Stick Burning	Vent. Control
I	0.050	5.0E-06	3	0.446	0.456
J	0.075	7.0E-06	3	0.417	0.456

The simulations were set up at or below the ventilation limited pyrolysis rate. Both predict the maximum compartment temperature to within 50 °C, and have an almost linear, non-conservative decay rate with is conservative to below 500 °C.

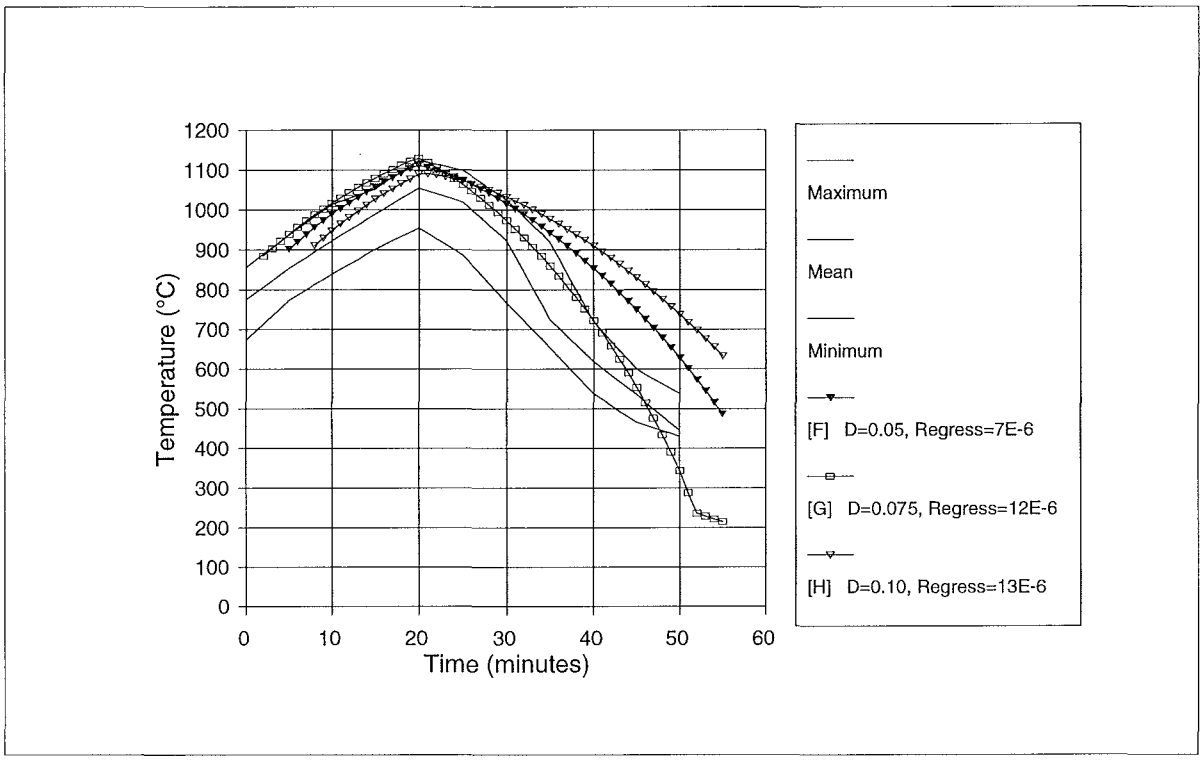

Fig B1.7 NFSC 70-19, 60 kg/m² Floor Area, Ventilation Factor = 0.055, Stick Fires, Shape = 2

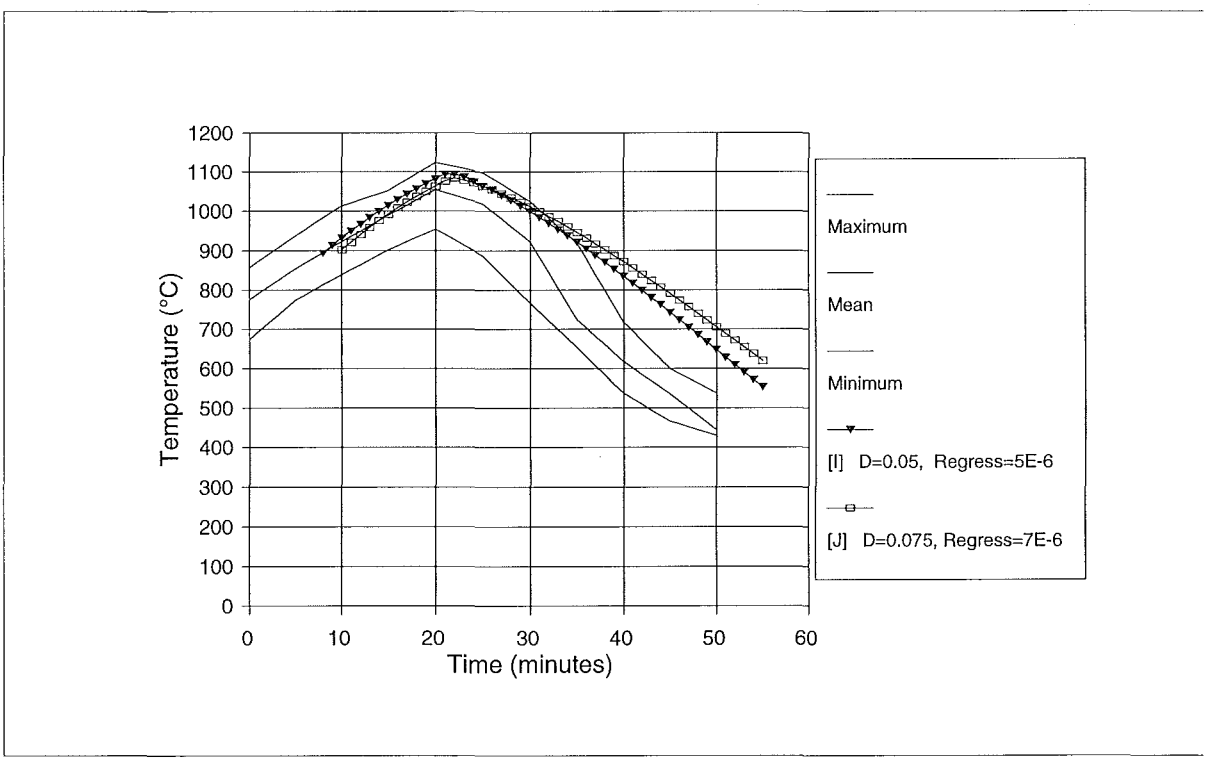

Fig B1.8 NFSC 70-19, 60 kg/m² Floor Area, Ventilation Factor = 0.055, Stick Fires, Shape = 3

B1.4 NFSC 70-46

The compartment and ventilation opening geometry, materials of construction, fuel load, and relevant parameters calculated from the specified data, are scheduled in Table B1.6.

Specified Parameters	
Compartment Length	3.68 m
Compartment Width	3.38 m
Compartment Height	3.13 m
Ventilation Height	2.92 m
Ventilation Width	2.18 m
Sill Height	0.95 m
Wall Details	3 walls of 0.115 m normal brick + 0.160 m hard brick plus 1 wall of 0.175 m lightweight concrete each with an 0.025 m layer of insulation
Ceiling Details	0.175 m lightweight concrete with an 0.025 m layer of insulation
Floor Details	refractory concrete
Fuel Load	745.3 kg wood
Calculated Parameters	
Floor Area	12.44 m^2
Total Internal Surface Area	69.07 m^2
Ventilation Area	6.366 m^2
Ventilation Parameter ($A_V \sqrt{H}$)	10.878 $m^{5/2}$
Ventilation Parameter ($A_V \sqrt{H} / A_T$)	0.157 $m^{0.5}$
Fire Load Density	59.9 kg /m^2 of floor area
Fire Load Density	10.8 kg /m^2 of total bounding surface area

Table B1.6 NFSC 70-46 Input Data ; Fire Load 59.9 kg/m^2, Ventilation Factor 0.157

From the initial data above, fires with the following stick size (D), regression rate (v_p), shape factor (F) and crib spacing to height ratio (S_c / H_c)were modelled, leading to the tabulated initial pyrolysis rates for stick burning, ventilation control, crib porosity control

and crib fuel surface control mechanisms. The lowest non-zero rate governs the initial fire development.

Identifier	Diam. (D) (m)	Stick Burn Regress Rate (v_p) (m/s)	Shape (F)	Crib (S_c /H_c)	Initial Pyrolysis Rate (kg/s)				
					Stick Burning	Vent. Control	Crib Porosity Control	Crib Fuel Surface (theory)	Crib Fuel Surface (progr)
A	0.050		2	0.120		1.305	0.787	0.612	0.892
B	0.050		2	0.100		1.305	0.656	0.612	0.892
C	0.050		2	0.075		1.305	0.492	0.612	0.892
D	0.060		2	0.110		1.305	0.601	0.457	0.667
E	0.05		3	0.100		1.305	0.656	0.612	1.338
F	0.075		3	0.125		1.305	0.547	0.320	0.700
G	0.065		3	0.125		1.305	0.631	0.402	0.880
H	0.050	1.0E-05	2		0.596	1.305			
I	0.060	1.2E-05	2		0.596	1.305			
J	0.045	1.0E-05	2		0.662	1.305			
K	0.050	8.0E-06	3		0.715	1.305			
L	0.075	1.0E-05	3		0.596	1.305			
M	0.075	1.1E-05	3		0.656	1.305			
N	0.100	1.5E-05	3		0.671	1.305			

Table B1.7 NFSC 70-46, Fire Simulation Parameters and Initial Pyrolysis Rates

This fire has a similar compartment geometry, thermal properties and fire load to that of NFSC 70-19 discussed in Appendix B1.3. It has a far greater ventilation area and ventilation factor.

NFSC 70-46, Crib Fire, Shape = 2 (Figure B1.9)

Identifier	Diam. (D) (m)	Shape (F)	Crib (S_c /H_c)	Initial Pyrolysis Rate (kg/s)			
				Vent. Control	Crib Porosity Control	Crib Fuel Surface (theory)	Crib Fuel Surface (progr)
A	0.050	2	0.120	1.305	0.787	0.612	0.892
B	0.050	2	0.100	1.305	0.656	0.612	0.892
C	0.050	2	0.075	1.305	0.492	0.612	0.892
D	0.060	2	0.110	1.305	0.601	0.457	0.667

Simulated fires (not shown on the graph) which were initially ventilation limited or crib

fuel surface controlled all produced very unacceptable results. Best results were obtained with fires initially crib porosity controlled at well below the ventilation limited pyrolysis rate and substantially below the fuel surface controlled pyrolysis rate. By using a modest stick size, and open crib, Simulation A developed peak temperatures about 200 °C above those actually recorded. The remaining simulations show flat plateaus at the calculated peak, varying from 1,000°C to 1,200 °C, with decay occurring following the transition to fuel surface control. Simulation D, with a slightly larger stick size (0.06 m compared with 0.05 m) develops an almost linear decay which is non-conservative down to below 500 °C.

NFSC 70-46, Crib Fire, Shape = 3 (Figure B1.10)

Identifier	Diam. (D) (m)	Shape (F)	Crib (S_c /H_c)	Initial Pyrolysis Rate (kg/s)			
				Vent. Control	Crib Porosity Control	Crib Fuel Surface (theory)	Crib Fuel Surface (progr)
E	0.050	3	0.100	1.305	0.656	0.612	1.338
F	0.075	3	0.125	1.305	0.547	0.320	0.700
G	0.065	3	0.125	1.305	0.631	0.402	0.880

Again ventilation limited fires and fuel surface controlled fires all produced unacceptable results, with fires initially crib porosity controlled giving the best simulations. The best results for Simulations F and G occur when the transition to fuel surface control is somewhat shorter than Simulation E, where the delayed transition produces a good estimate of peak temperature, but then decays too rapidly. This requires use of larger stick diameters to reduce the fuel surface controlled pyrolysis rate closer to the crib porosity controlled pyrolysis rate.

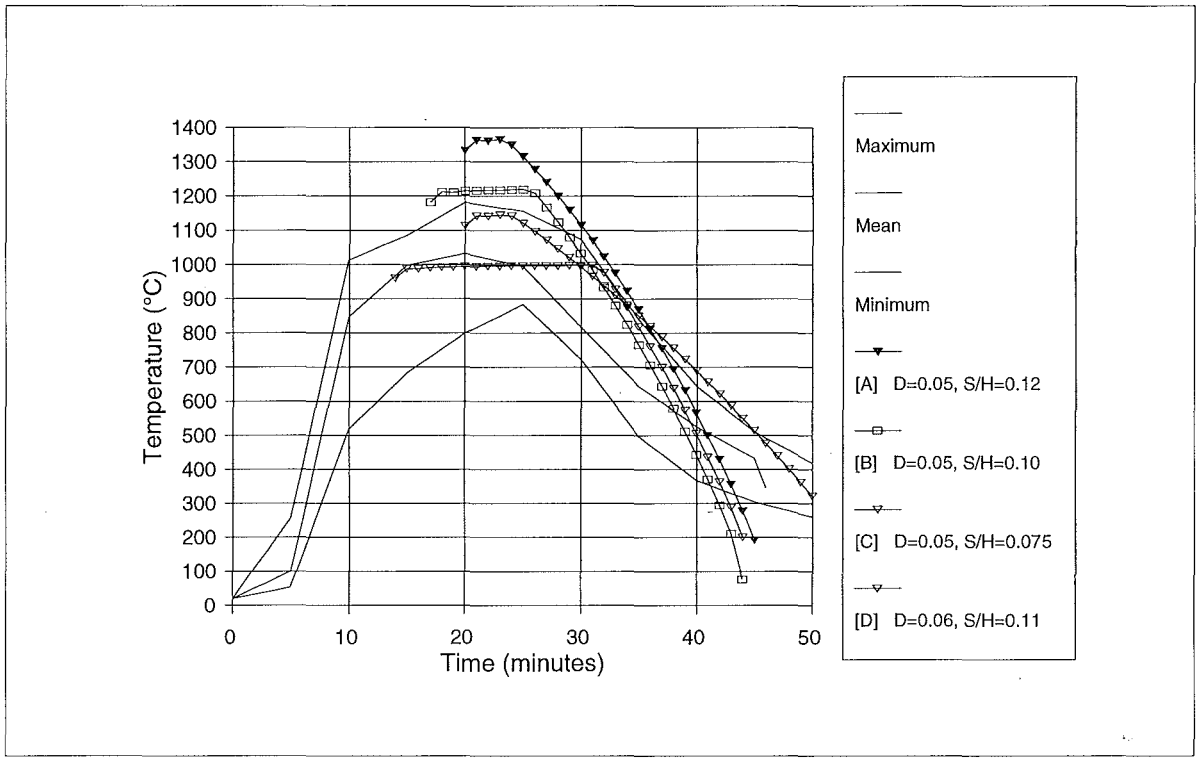

Fig B1.9 NFSC 70-46, 60 kg/m² Floor Area, Ventilation Factor = 0.157, Crib Fires, Shape = 2

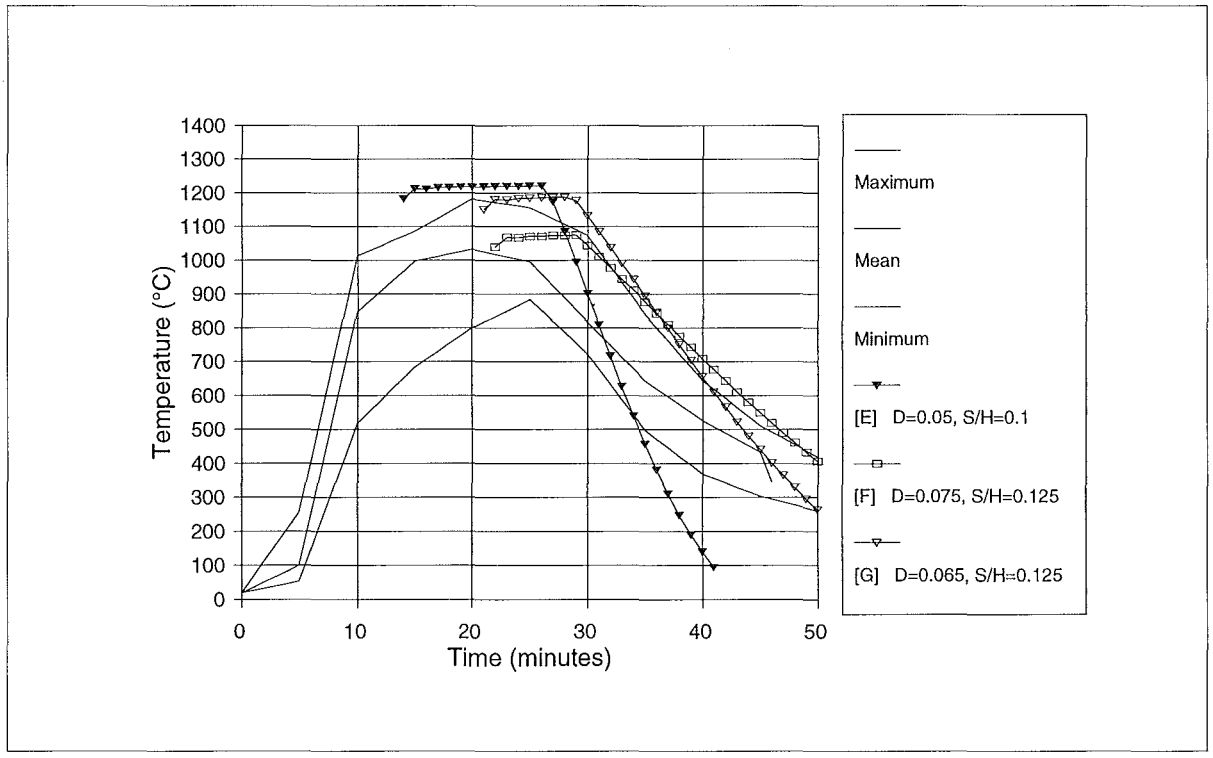

Fig B1.10 NFSC 70-46, 60 kg/m² Floor Area, Ventilation Factor = 0.157, Crib Fires, Shape = 3

NFSC 70-46, Stick Fire, Shape = 2 (Figure B1.11)

Identifier	Diam. (D) (m)	Stick Burn Regress Rate (v_p) (m/s)	Shape (F)	Initial Pyrolysis Rate (kg/s)	
				Stick Burning	Vent. Control
H	0.050	1.0E-05	2	0.596	1.305
I	0.060	1.2E-05	2	0.596	1.305
J	0.045	1.0E-05	2	0.662	1.305

Simulations H and I produce the same initial pyrolysis rate and same fire curve, because the ratio of stick size to fuel regression rate is identical. A similar pyrolysis rate and fire curve results in Simulation J by using a smaller stick Diameter and lower surface regression rate. Peak temperatures are well reproduced and the almost linear decay curves are conservative down to below 400 °C.

NFSC 70-46, Stick Fire, Shape = 3 (Figure B1.12)

Identifier	Diam. (D) (m)	Stick Burn Regress Rate (v_p) (m/s)	Shape (F)	Initial Pyrolysis Rate (kg/s)	
				Stick Burning	Vent. Control
K	0.050	8.0E-06	3	0.715	1.305
L	0.075	1.0E-05	3	0.596	1.305
M	0.075	1.1E-05	3	0.656	1.305
N	0.100	1.5E-05	3	0.671	1.305

Simulations K to N are set up with initial pyrolysis rates about half that of the ventilation limited pyrolysis rate. All produce reasonable estimates of the peak temperature with the best results from Simulations M and N. Decay curves are only slightly different slopes, with near linear drop in temperature conservatively predicted down to below 400 °C.

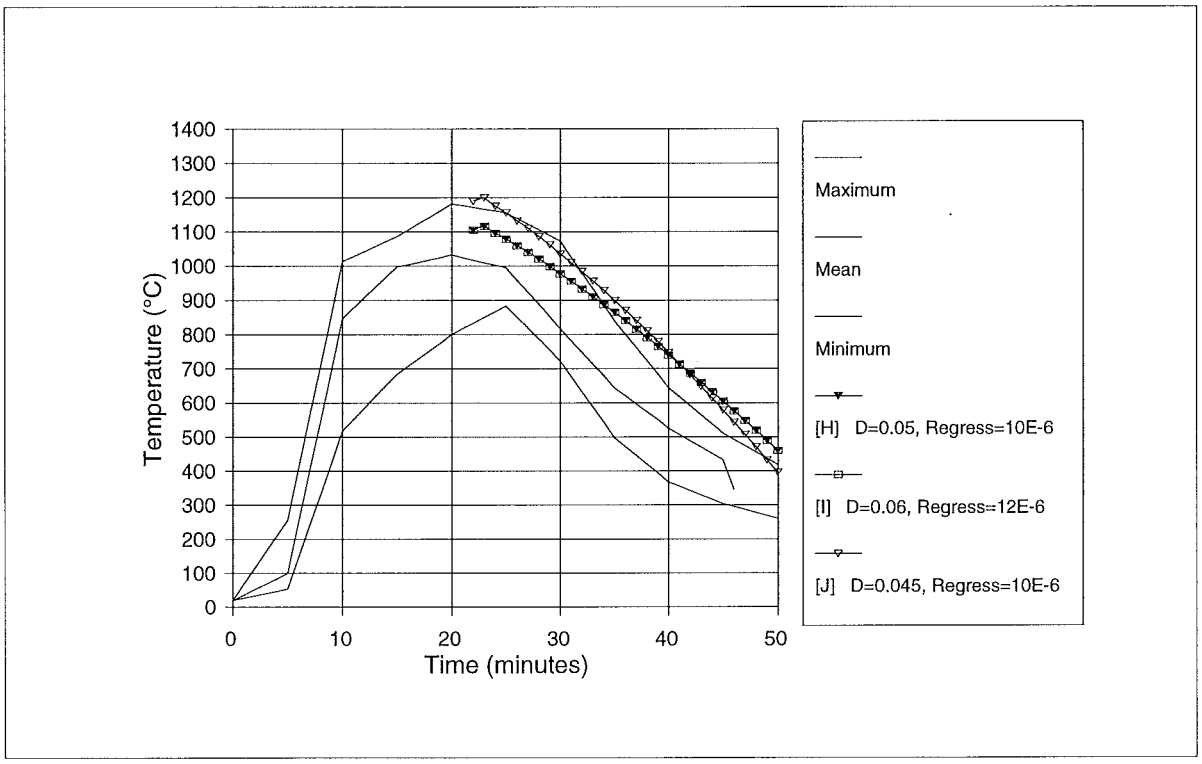

Fig. B1.11 NFSC 70-46, 60 kg/m² Floor Area, Ventilation Factor = 0.157, Stick Fires, Shape = 2

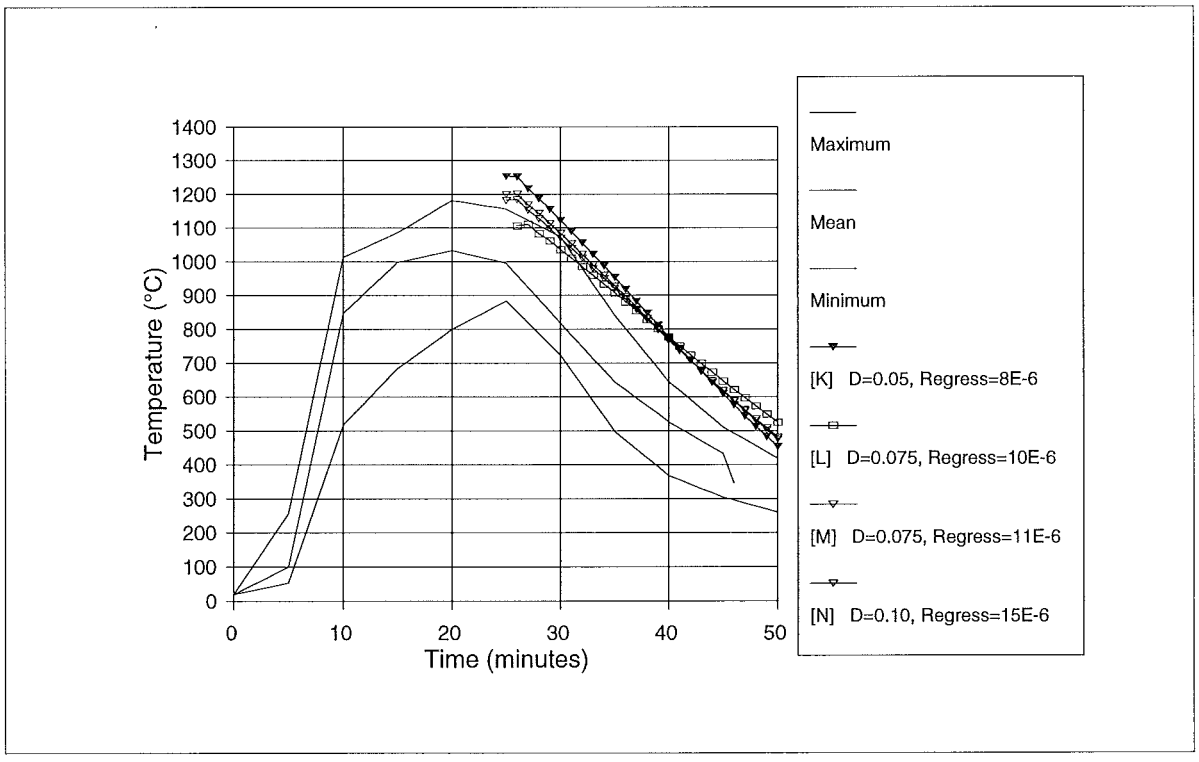

Fig. B1.12 NFSC 70-46, 60 kg/m² Floor Area, Ventilation Factor = 0.157, Stick Fires, Shape = 3

B1.5 NFSC 70-29

This fire has a moderate fire load, but very low ventilation area and ventilation factor. The compartment and ventilation opening geometry, materials of construction, fuel load, and relevant parameters calculated from the specified data, are scheduled in Table B1.8.

Specified Parameters	
Compartment Length	3.68 m
Compartment Width	3.38 m
Compartment Height	3.13 m
Ventilation Height	0.9 m
Ventilation Width	1.18 m
Sill Height	2.23 m
Wall Details	3 walls of 0.115 m normal brick + 0.160 m hard brick plus 1 wall of 0.175 m lightweight concrete each with 0.025 m of insulation
Ceiling Details	0.175 m lightweight concrete with 0.025 m of insulation
Floor Details	refractory concrete
Fuel Load	372.6 kg wood
Calculated Parameters	
Floor Area	12.44 m^2
Total Internal Surface Area	69.07 m^2
Ventilation Area	1.062 m^2
Ventilation Parameter ($A_V \sqrt{H}$)	1.008 $m^{5/2}$
Ventilation Parameter ($A_V \sqrt{H} / A_T$)	0.015 $m^{0.5}$
Fire Load Density	30.0 kg /m^2 of floor area
Fire Load Density	5.4 kg /m^2 of total bounding surface area

Table B1.8 NFSC 70-29 Input Data ; Fire Load 30 kg/m^2, Ventilation Factor 0.015

From the initial data above, fires with the following stick size (D), regression rate (v_p), shape factor (F) and crib spacing to height ratio (S_c / H_c)were modelled, leading to the

tabulated initial pyrolysis rates for stick burning, ventilation control, crib porosity control and crib fuel surface control mechanisms. The lowest non-zero rate governs the initial fire development.

Identifier	Diam. (D) (m)	Stick Burn Regress Rate (v_p) (m/s)	Shape (F)	Crib (S_c/H_c)	Initial Pyrolysis Rate (kg/s)				
					Stick Burning	Vent. Control	Crib Porosity Control	Crib Fuel Surface (theory)	Crib Fuel Surface (progr)
A	0.050		2	0.100		0.121	0.328	0.306	0.446
B	0.125		2	0.100		0.121	0.131	0.071	0.103
C	0.125		2	0.050		0.121	0.066	0.071	0.103
D	0.150		2	0.075		0.121	0.082	0.053	0.077
E	0.150		3	0.100		0.121	0.109	0.053	0.115
F	0.050		3	0.025		0.121	0.082	0.306	0.669
G	0.050		3	0.025		0.121	0.082	0.306	0.669
H	0.150	1.2E-05	2		0.119	0.121			
I	0.150	1.0E-05	2		0.099	0.121			
J	0.150	8.0E-06	2		0.079	0.121			
K	0.150	6.0E-06	2		0.060	0.121			
L	0.100	1.0E-05	2		0.149	0.121			
M	0.200	8.0E-06	2		0.060	0.121			
N	0.100	1.2E-05	3		1.930	0.121			
O	0.125	1.2E-05	3		1.544	0.121			

Table B1.9 NFSC 70-29, Fire Simulation Parameters and Initial Pyrolysis Rates

NFSC 70-29, Crib Fire, Shape = 2 (Figure B1.13)

Identifier	Diam. (D) (m)	Shape (F)	Crib (S_c/H_c)	Initial Pyrolysis Rate (kg/s)			
				Vent. Control	Crib Porosity Control	Crib Fuel Surface (theory)	Crib Fuel Surface (progr)
A	0.050	2	0.100	0.121	0.328	0.306	0.446
B	0.125	2	0.100	0.121	0.131	0.071	0.103
C	0.125	2	0.050	0.121	0.066	0.071	0.103
D	0.150	2	0.075	0.121	0.082	0.053	0.077

All simulations are excessively conservative generally over-predicting the peak temperatures, and particularly over-predicting the fire duration.

NFSC 70-29, Crib Fire, Shape = 3 (Figure B1.14)

Identifier	Diam. (D) (m)	Shape (F)	Crib (S_c/H_c)	Initial Pyrolysis Rate (kg/s)			
				Vent. Control	Crib Porosity Control	Crib Fuel Surface (theory)	Crib Fuel Surface (progr)
E	0.150	3	0.100	0.121	0.109	0.053	0.115
F	0.050	3	0.025	0.121	0.082	0.306	0.669
G	0.050	3	0.025	0.121	0.082	0.306	0.669

As with Crib Fires with Shape = 2, all fires are conservative both in temperature and duration. Fires F and G have identical fundamental parameters. Different wall configurations were explored, with the higher temperature trace being for a wall of thickness 0.025 m, density 128 kg m^{-3} and conductivity 0.02 W m^{-1} K^{-1}. The lower temperature trace is for a wall of thickness 0.250 m, density 500 kg m^{-3} and conductivity 0.2 W m^{-1} K^{-1}.

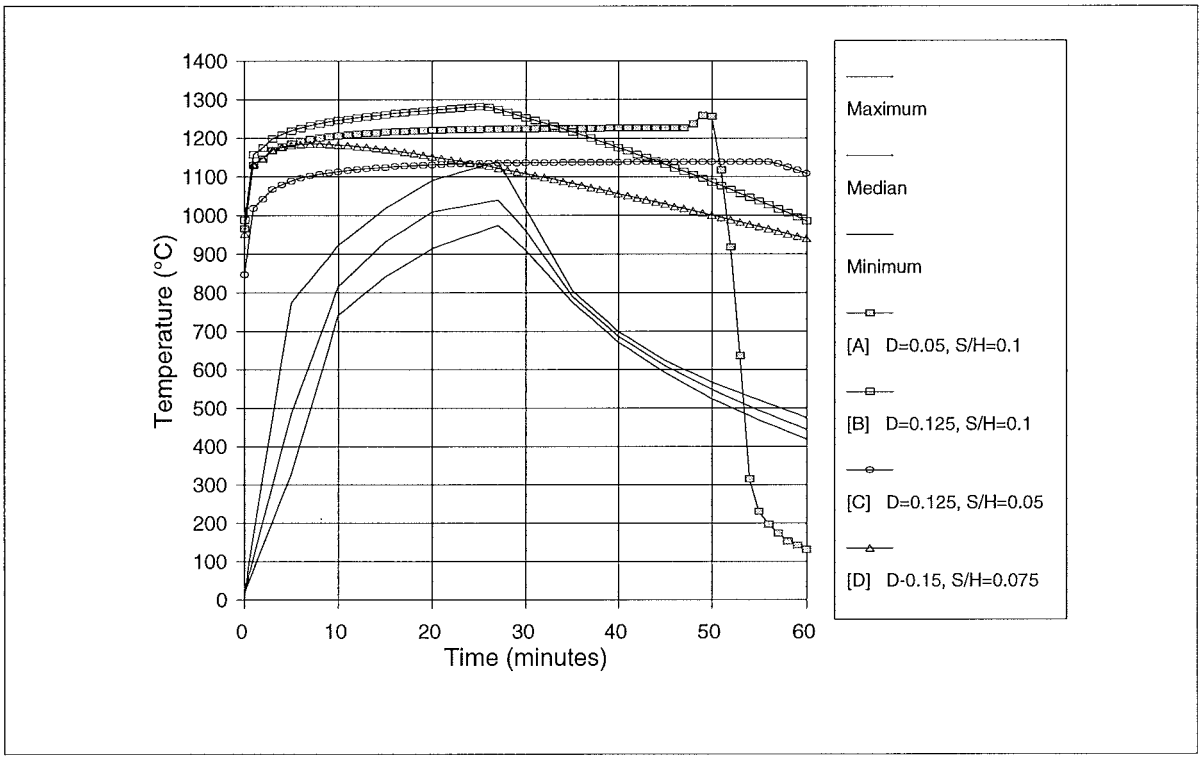

Fig. B1.13 NFSC 70-29, 30 kg/m² Floor Area, Ventilation Factor = 0.015, Crib Fires, Shape = 2

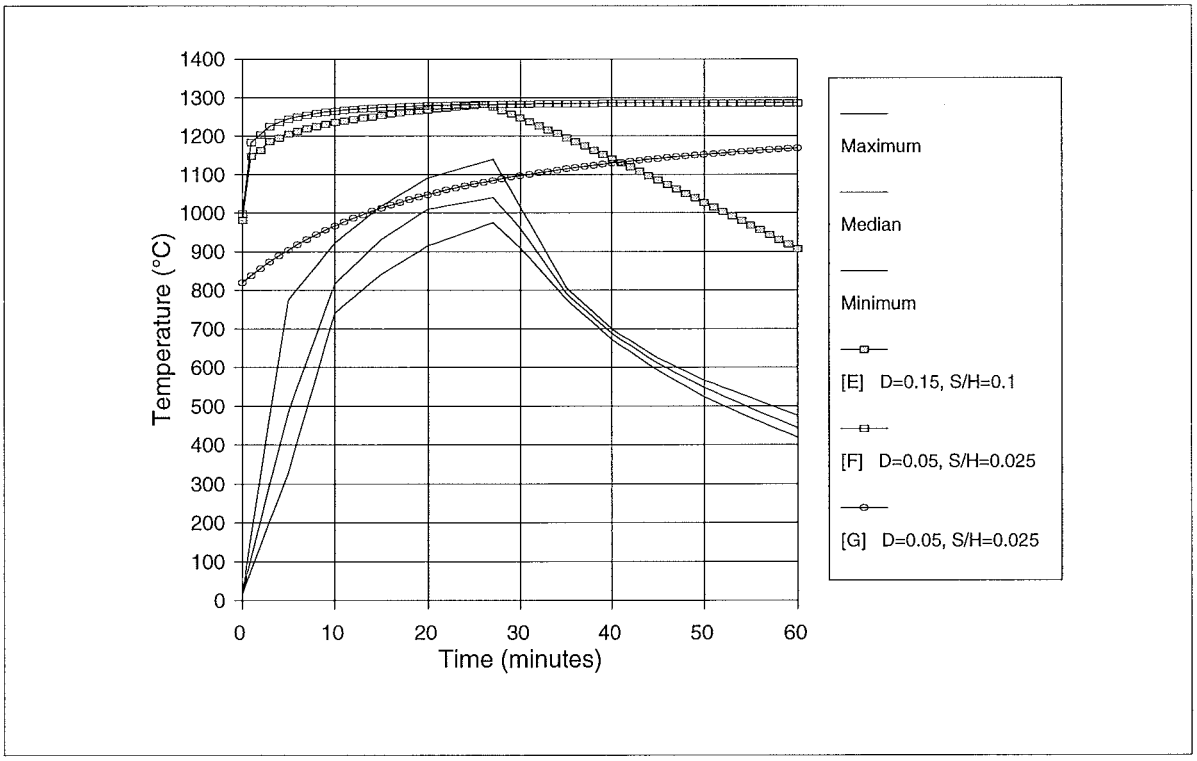

Fig. B1.14 NFSC 70-29, 30 kg/m² Floor Area, Ventilation Factor = 0.015, Crib Fires, Shape = 3

NFSC 70-29, Stick Fire, Shape = 2 (Figure B1.15)

Identifier	Diam. (D) (m)	Stick Burn Regress Rate (v_p) (m/s)	Shape (F)	Initial Pyrolysis Rate (kg/s)	
				Stick Burning	Vent. Control
H	0.150	1.2E-05	2	0.119	0.121
I	0.150	1.0E-05	2	0.099	0.121
J	0.150	8.0E-06	2	0.079	0.121
K	0.150	6.0E-06	2	0.060	0.121
L	0.100	1.0E-05	2	0.149	0.121
M	0.200	8.0E-06	2	0.060	0.121

As with crib fires, stick fires with Shape = 2 are very conservative both in temperature and duration.

NFSC 70-29, Stick Fire, Shape = 3 (Figure B1.16)

Identifier	Diam. (D) (m)	Stick Burn Regress Rate (v_p) (m/s)	Shape (F)	Initial Pyrolysis Rate (kg/s)	
				Stick Burning	Vent. Control
N	0.100	1.2E-05	3	1.930	0.121
O	0.125	1.2E-05	3	1.544	0.121

These simulations are the best at reproducing both the peak temperature and the general form of the measured fire curve. Simulation O has the BPF parameter (the maximum fraction of pyrolysates burnt within the compartment) reduced to 80% and reproduces the fire curve moderately well in terms of growth, maximum temperature Figure B1.13 Crib Fire, Shape =2 and conservative decay to about 500 °C.

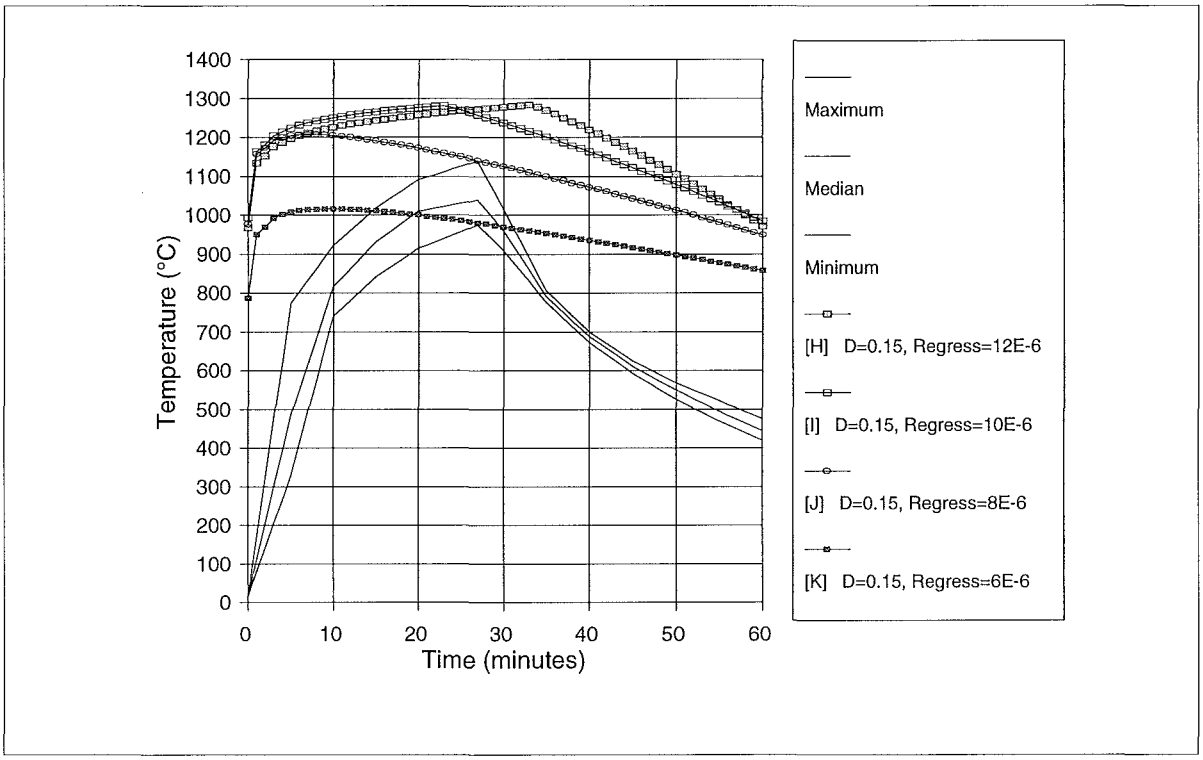

Fig. B1.15 NFSC 70-29, 30 kg/m² Floor Area, Ventilation Factor = 0.015, Stick Fires, Shape = 2

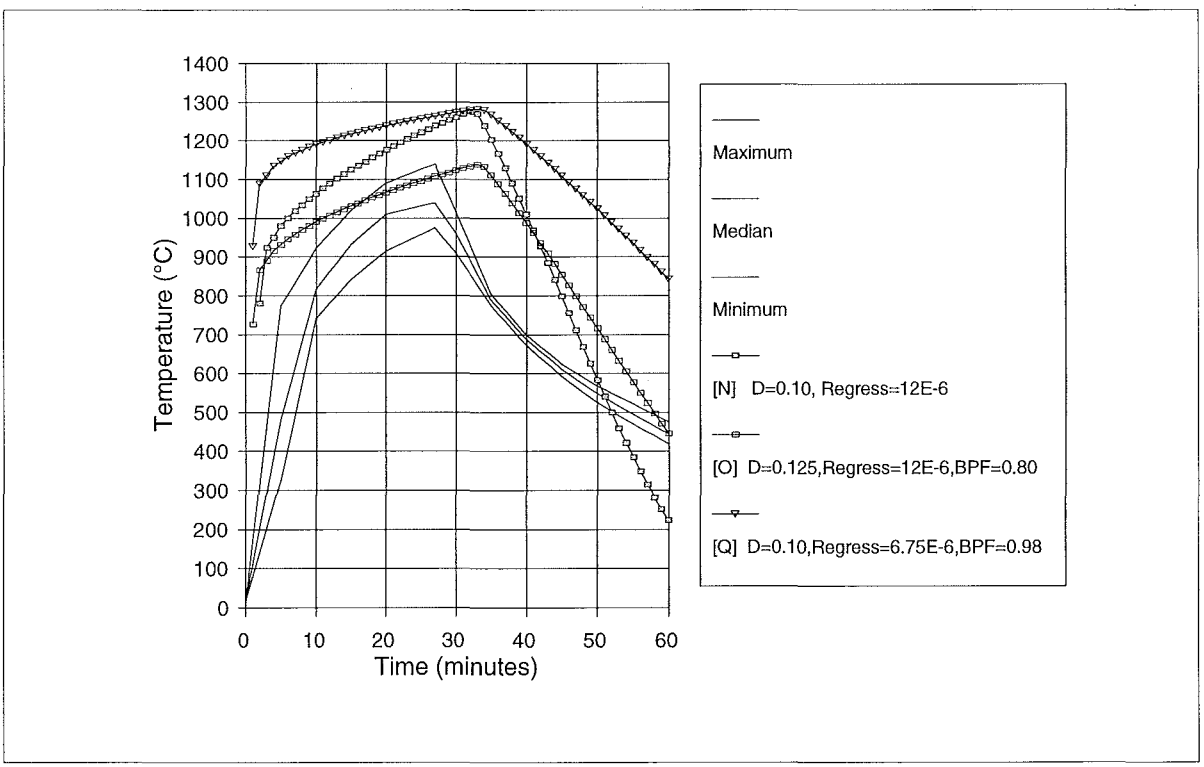

Fig. B1.16 NFSC 70-29, 30 kg/m² Floor Area, Ventilation Factor = 0.015, Stick Fires, Shape = 3

B1.6 NFSC 71-58

The compartment and ventilation opening geometry, materials of construction, fuel load, and relevant parameters calculated from the specified data, are scheduled in Table B1.10.

Specified Parameters	
Compartment Length	3.60 m
Compartment Width	3.36 m
Compartment Height	3.13 m
Ventilation Height	2.18 m
Ventilation Width	1.18 m
Sill Height	0.95 m
Wall Details	3 walls of 0.115 m normal brick + 0.160 m hard brick plus 1 wall of 0.175 m lightweight concrete
Ceiling Details	0.175 m lightweight concrete
Floor Details	refractory concrete
Fuel Load	151 kg furniture + 184 kg paper + 37 kg wood
Calculated Parameters	
Floor Area	12.10 m^2
Total Internal Surface Area	67.76 m^2
Ventilation Area	2.572 m^2
Ventilation Parameter ($A_V \sqrt{H}$)	3.798 $m^{5/2}$
Ventilation Parameter ($A_V \sqrt{H} / A_T$)	0.056 $m^{0.5}$
Fire Load Density	23.6 kg(equivalent) /m^2 of floor area
Fire Load Density	4.2 kg /m^2 of total bounding surface area

Table B1.10 NFSC 71-58 Input Data ; Fire Load 23.6 kg/m^2, Ventilation Factor 0.056

This fire has moderate to low fire load, and moderated ventilation. From the initial data above, fires with the following stick size (D), regression rate (v_p), shape factor (F) and crib spacing to height ratio (S_c / H_c)were modelled, leading to the tabulated initial pyrolysis rates for stick burning, ventilation control, crib porosity control and crib fuel surface control mechanisms. The lowest non-zero rate governs the initial fire

development.

Identifier	Diam. (D) (m)	Stick Burn Regress Rate (v_p) (m/s)	Shape (F)	Crib (S_c/H_c)	Initial Pyrolysis Rate (kg/s)				
					Stick Burning	Vent. Control	Crib Porosity Control	Crib Fuel Surface (theory)	Crib Fuel Surface (progr)
A	0.040		2	0.150		0.456	0.470	0.334	0.488
B	0.050		2	0.150		0.456	0.376	0.234	0.341
C	0.065		2	0.200		0.456	0.386	0.154	0.224
D	0.050		3	0.150		0.456	0.376	0.234	0.512
E	0.065		3	0.200		0.456	0.386	0.154	0.336
F	0.055		3	0.200		0.456	0.456	0.201	0.439
G	0.050	1.8E-05	2		0.410	0.456			
H	0.040	2.0E-05	2		0.570	0.456			
I	0.060	1.8E-05	2		0.333	0.456			
J	0.040	1.2E-05	3		0.513	0.456			
K	0.050	1.2E-05	3		0.410	0.456			
L	0.075	1.6E-05	3		0.365	0.456			

Table B1.11 NFSC 71-58, Fire Simulation Parameters and Initial Pyrolysis Rates

NFSC 71-58, Crib Fire, Shape = 2 (Figure B1.17)

Identifier	Diam. (D) (m)	Shape (F)	Crib (S_c/H_c)	Initial Pyrolysis Rate (kg/s)			
				Vent. Control	Crib Porosity Control	Crib Fuel Surface (theory)	Crib Fuel Surface (progr)
A	0.040	2	0.150	0.456	0.470	0.334	0.488
B	0.050	2	0.150	0.456	0.376	0.234	0.341
C	0.065	2	0.200	0.456	0.386	0.154	0.224

Simulations A and B have porosity controlled and fuel surface controlled initial pyrolysis rates close to the ventilation controlled initial pyrolysis rate. They reproduce the maximum temperature conservatively, and provide conservative estimates of the decay curve to 500 °C and 300°C respectively.. Simulation C is strongly fuel surface controlled at well below the ventilation controlled initial pyrolysis rate. It underestimates the peak temperature by about 200 °C, with a conservative estimate of decay temperatures down to 200 °C.

NFSC 71-58, Crib Fire, Shape = 3 (Figure B1.18)

Identifier	Diam. (D) (m)	Shape (F)	Crib (S_c/H_c)	Initial Pyrolysis Rate (kg/s)			
				Vent. Control	Crib Porosity Control	Crib Fuel Surface (theory)	Crib Fuel Surface (progr)
D	0.050	3	0.150	0.456	0.376	0.234	0.512
E	0.065	3	0.200	0.456	0.386	0.154	0.336
F	0.055	3	0.200	0.456	0.456	0.201	0.439

Simulations D, E and F are set up to be initially crib porosity, fuel surface and fuel surface controlled respectively. Reproduction of peak temperatures is conservative by up to 100 °C, and decay curves are approximately linear, and conservative to 450, 400 and 250 °C respectively. Simulation F provides the best overall simulation

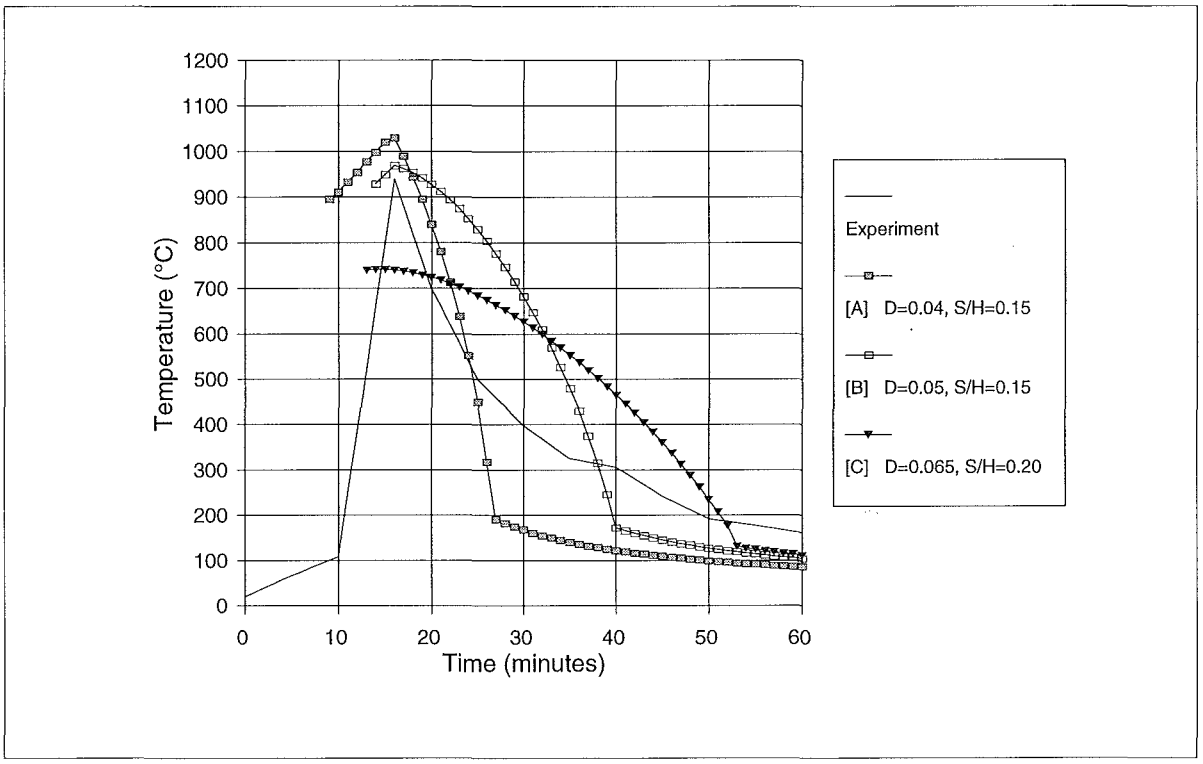

Fig. B1.17 NFSC 71-58, 23.6 kg/m² Floor Area, Ventilation Factor = 0.056, Crib Fires, Shape = 2

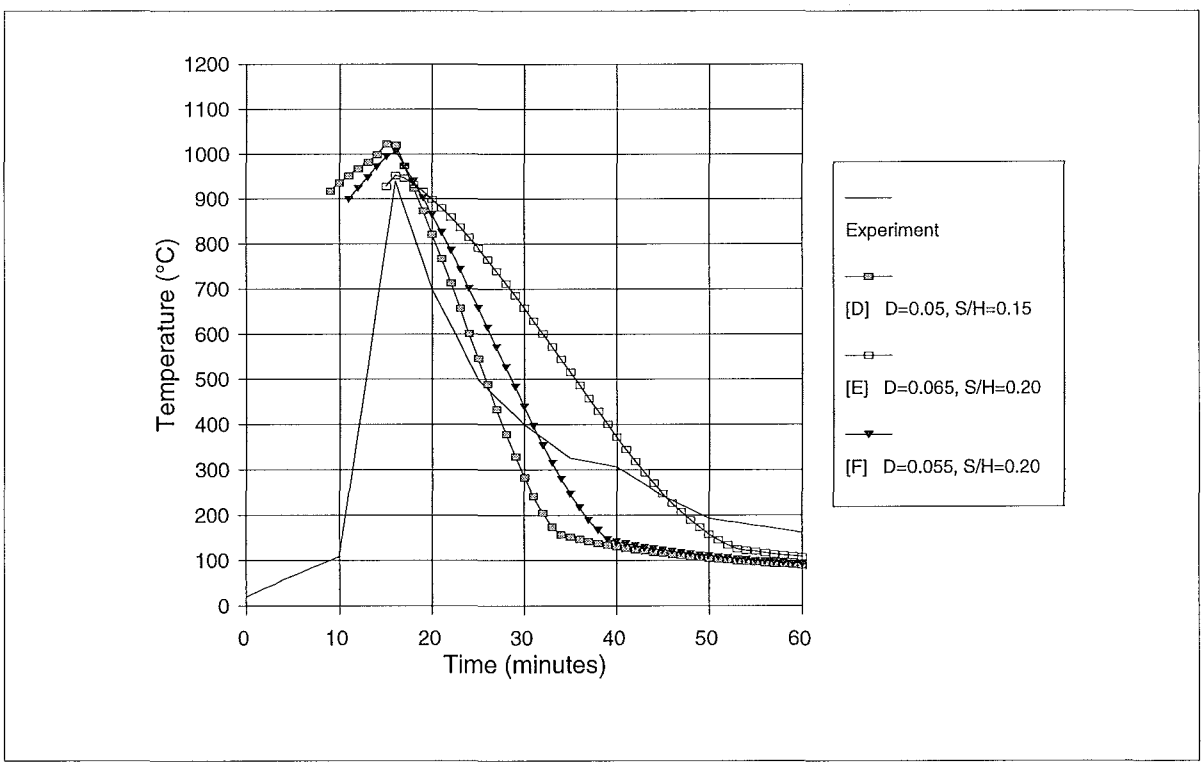

Fig. B1.18 NFSC 71-58, 23.6 kg/m² Floor Area, Ventilation Factor = 0.056, Crib Fires, Shape = 3

NFSC 71-58, Stick Fire, Shape = 2 (Figure B1.19)

Identifier	Diam. (D) (m)	Stick Burn Regress Rate (v_p) (m/s)	Shape (F)	Initial Pyrolysis Rate (kg/s)	
				Stick Burning	Vent. Control
G	0.050	1.8E-05	2	0.410	0.456
H	0.040	2.0E-05	2	0.570	0.456
I	0.060	1.8E-05	2	0.333	0.456

Simulations G, H and I are respectively, set up to have initial pyrolysis rates slightly below, well above and well below the ventilation limited pyrolysis rate. Peak temperatures are slightly conservatively estimated, with concave decay curves which are conservative to 600, 400 and 300 °C respectively. Simulation I provides the closest estimate of peak temperature and provides the most conservative estimate of the decay profile.

NFSC 71-58, Stick Fire, Shape = 3 (Figure B1.20)

Identifier	Diam. (D) (m)	Stick Burn Regress Rate (v_p) (m/s)	Shape (F)	Initial Pyrolysis Rate (kg/s)	
				Stick Burning	Vent. Control
J	0.040	1.2E-05	3	0.513	0.456
K	0.050	1.2E-05	3	0.410	0.456
L	0.075	1.6E-05	3	0.365	0.456

Simulations J, K and L are respectively set up to have initial pyrolysis rates slightly above, slightly below and well below the ventilation limited pyrolysis rate. Peak temperatures are slightly conservatively estimated, with almost linear decay curves which are conservative to 500, 300 and 300 °C respectively. Simulation L provides the closest estimate of peak temperature and provides the most conservative estimate of the decay profile down to about 300 °C..

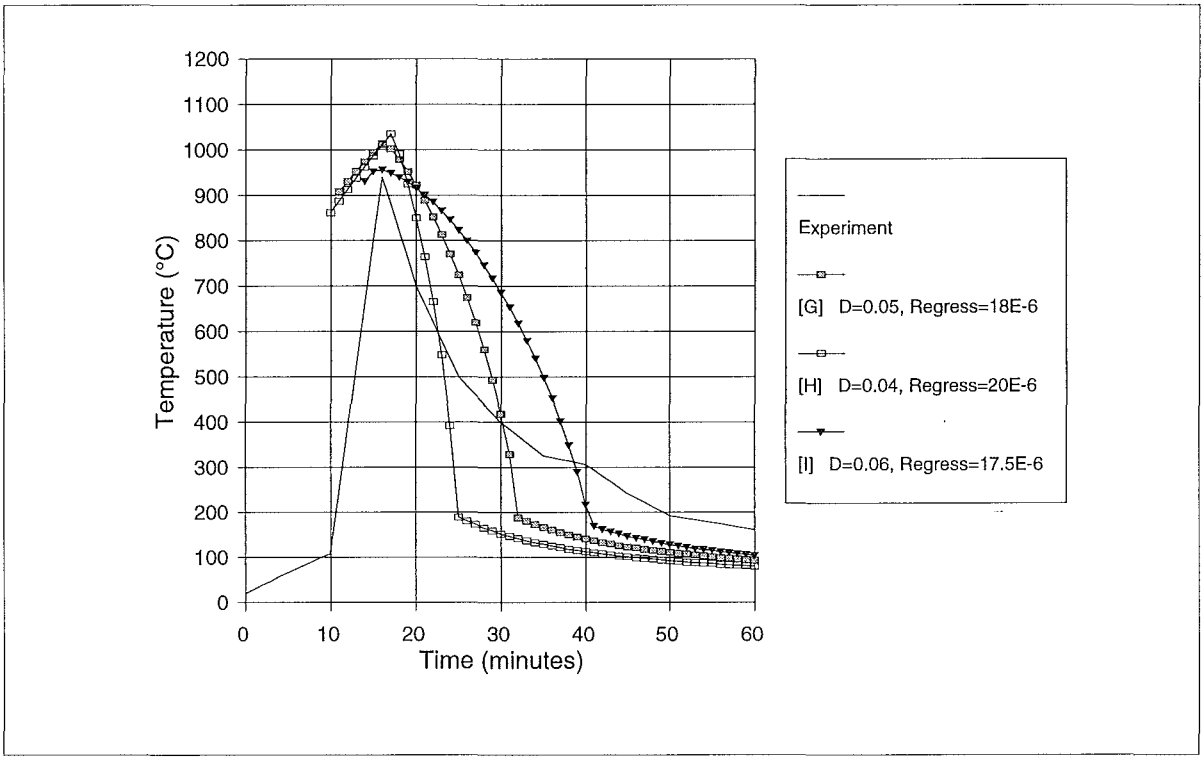

Fig. B1.19 NFSC 71-58, 23.6 kg/m² Floor Area, Ventilation Factor = 0.056, Stick Fires, Shape = 2

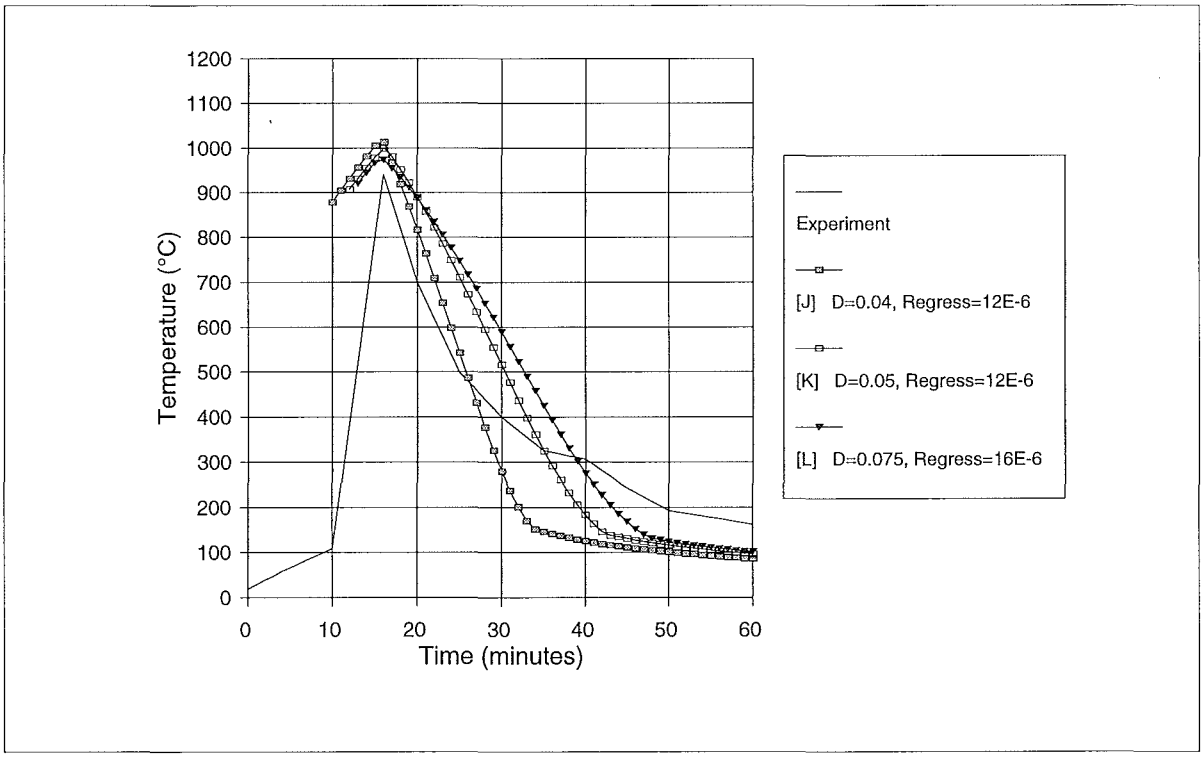

Fig. B1.20 NFSC 71-58, 23.6 kg/m² Floor Area, Ventilation Factor = 0.056, Stick Fires, Shape = 3

B1.7 NFSC 70-44

The compartment and ventilation opening geometry, materials of construction, fuel load, and relevant parameters calculated from the specified data, are scheduled in Table B1.12.

Specified Parameters	
Compartment Length	3.68 m
Compartment Width	3.38 m
Compartment Height	3.13 m
Ventilation Height	2.92 m
Ventilation Width	2.18 m
Sill Height	0.95 m
Wall Details	3 walls of 0.115 m normal brick + 0.160 m hard brick plus 1 wall of 0.175 m lightweight concrete each with 0.025 m of insulation
Ceiling Details	0.175 m lightweight concrete with 0.025 m of insulation
Floor Details	refractory concrete
Fuel Load	248.4 kg wood
Calculated Parameters	
Floor Area	12.44 m^2
Total Internal Surface Area	69.07 m^2
Ventilation Area	6.366 m^2
Ventilation Parameter ($A_V \sqrt{H}$)	10.878 $m^{5/2}$
Ventilation Parameter ($A_V \sqrt{H} / A_T$)	0.157 $m^{0.5}$
Fire Load Density	20.0 kg /m^2 of floor area
Fire Load Density	3.6 kg /m^2 of total bounding surface area

Table B1.12 NFSC 70-44 Input Data ; Fire Load 20 kg/m^2, Ventilation Factor 0.157

This fire has a low fire load and is well ventilated. From the initial data above, fires with the following stick size (D), regression rate (v_p), shape factor (F) and crib spacing to height ratio (S_c / H_c)were modelled, leading to the tabulated initial pyrolysis rates for

stick burning, ventilation control, crib porosity control and crib fuel surface control mechanisms. The lowest non-zero rate governs the initial fire development.

Identifier	Diam. (D) (m)	Stick Burn Regress Rate (v_p) (m/s)	Shape (F)	Crib (S_c /H_c)	Pyrolysis Rate (kg/s)				
					Stick Burning	Vent. Control	Crib Porosity Control	Crib Fuel Surface (theory)	Crib Fuel Surface (progr)
A	0.050		2	0.100		1.305	0.219	0.204	0.297
B	0.050		2	0.125		1.305	0.273	0.204	0.297
C	0.075		2	0.200		1.305	0.291	0.107	0.155
D	0.075		2	0.100		1.305	0.146	0.107	0.155
E	0.050		2	0.113		1.305	0.246	0.204	0.297
F	0.075		3	0.100		1.305	0.146	0.107	0.233
G	0.075		3	0.150		1.305	0.219	0.107	0.233
H	0.050		3	0.150		1.305	0.328	0.204	0.446
I	0.050		3	0.100		1.305	0.219	0.204	0.446
J	0.065		3	0.125		1.305	0.210	0.134	0.293
K	0.065		3	0.150		1.305	0.252	0.134	0.293
L	0.050	1.2E-05	2		0.238	1.305			
M	0.035	1.1E-05	2		0.312	1.305			
N	0.035	1.0E-05	2		0.284	1.305			
O	0.065	1.5E-05	2		0.229	1.305			
P	0.050	1.0E-05	3		0.298	1.305			
Q	0.050	9.0E-06	3		0.268	1.305			
R	0.065	1.2E-05	3		0.275	1.305			

Table B1.13 NFSC 70-44, Fire Simulation Parameters and Initial Pyrolysis Rates

NFSC 70-44, Crib Fire, Shape = 2 (Figure B1.21)

Identifier	Diam. (D) (m)	Shape (F)	Crib (S_c /H_c)	Initial Pyrolysis Rate (kg/s)			
				Vent. Control	Crib Porosity Control	Crib Fuel Surface (theory)	Crib Fuel Surface (progr)
A	0.050	2	0.100	1.305	0.219	0.204	0.297
B	0.050	2	0.125	1.305	0.273	0.204	0.297
C	0.075	2	0.200	1.305	0.291	0.107	0.155
D	0.075	2	0.100	1.305	0.146	0.107	0.155
E	0.050	2	0.1125	1.305	0.246	0.204	0.297

Simulations A, B, D and E are all set up to be initially slightly crib porosity controlled reverting to crib fuel surface control. Both initial pyrolysis rates are set to be well below the initial ventilation limited pyrolysis rate. Distinctly different peak temperatures are estimated, Simulations C and D with a larger stick size 0.075 m, produce low peak temperatures and a very slow decay rate.

NFSC 70-44, Crib Fire, Shape = 3 (Figure B1.22)

Identifier	Diam. (D) (m)	Shape (F)	Crib (S_c /H_c)	Initial Pyrolysis Rate (kg/s)			
				Vent. Control	Crib Porosity Control	Crib Fuel Surface (theory)	Crib Fuel Surface (progr)
F	0.075	3	0.100	1.305	0.146	0.107	0.233
G	0.075	3	0.150	1.305	0.219	0.107	0.233
H	0.050	3	0.150	1.305	0.328	0.204	0.446
I	0.050	3	0.100	1.305	0.219	0.204	0.446
J	0.065	3	0.125	1.305	0.210	0.134	0.293
K	0.070	3	0.150	1.305	0.252	0.134	0.293

Simulations F to K are all slightly crib porosity controlled reverting to crib fuel surface controlled in later stages of combustion. This creates a constant pyrolysis rate period providing the approximately constant temperature portion of the calculated curves. There is a very wide range of calculated peak temperature. Simulation K overestimates the peak temperature by 100 °C and decays too fast.

Simulations I and K provide reasonable approximations to the experimental data, with [I] being more conservative on the decay, but underestimating the peak temperature.

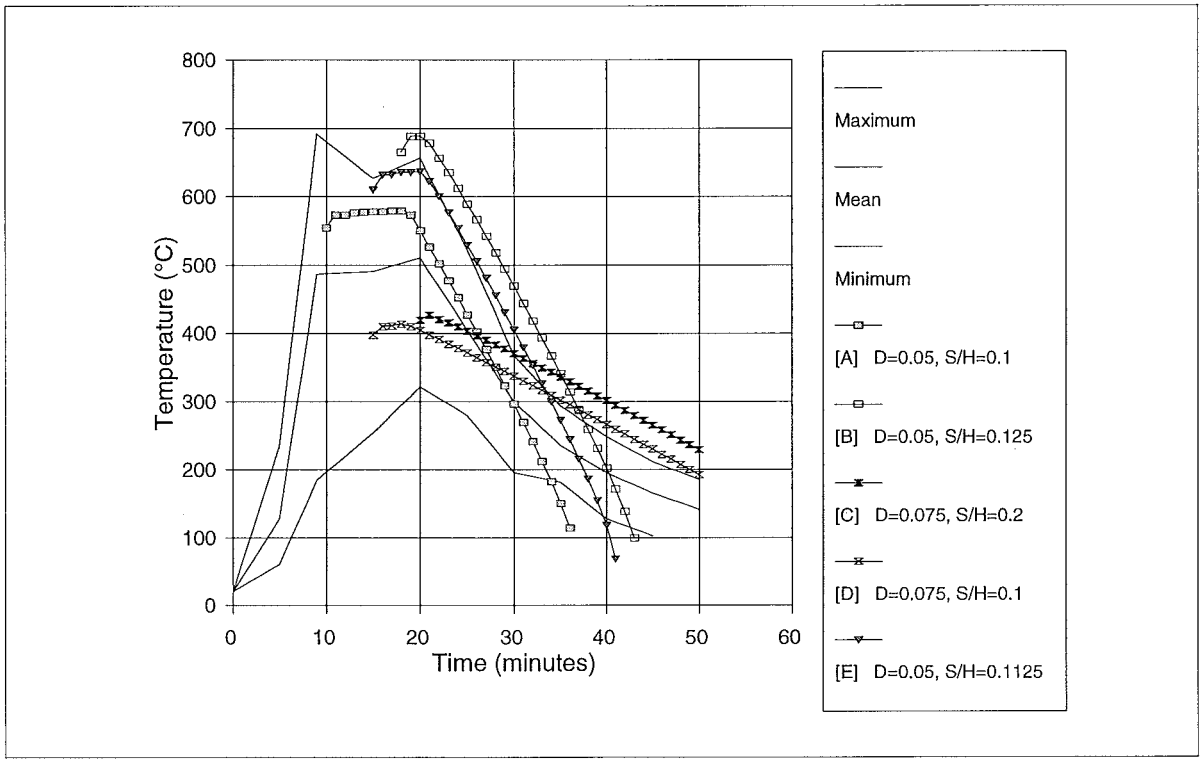

Fig. B1.21 NFSC 70-44, 20 kg/m² Floor Area, Ventilation Factor 0.157, Crib Fires, Shape = 2

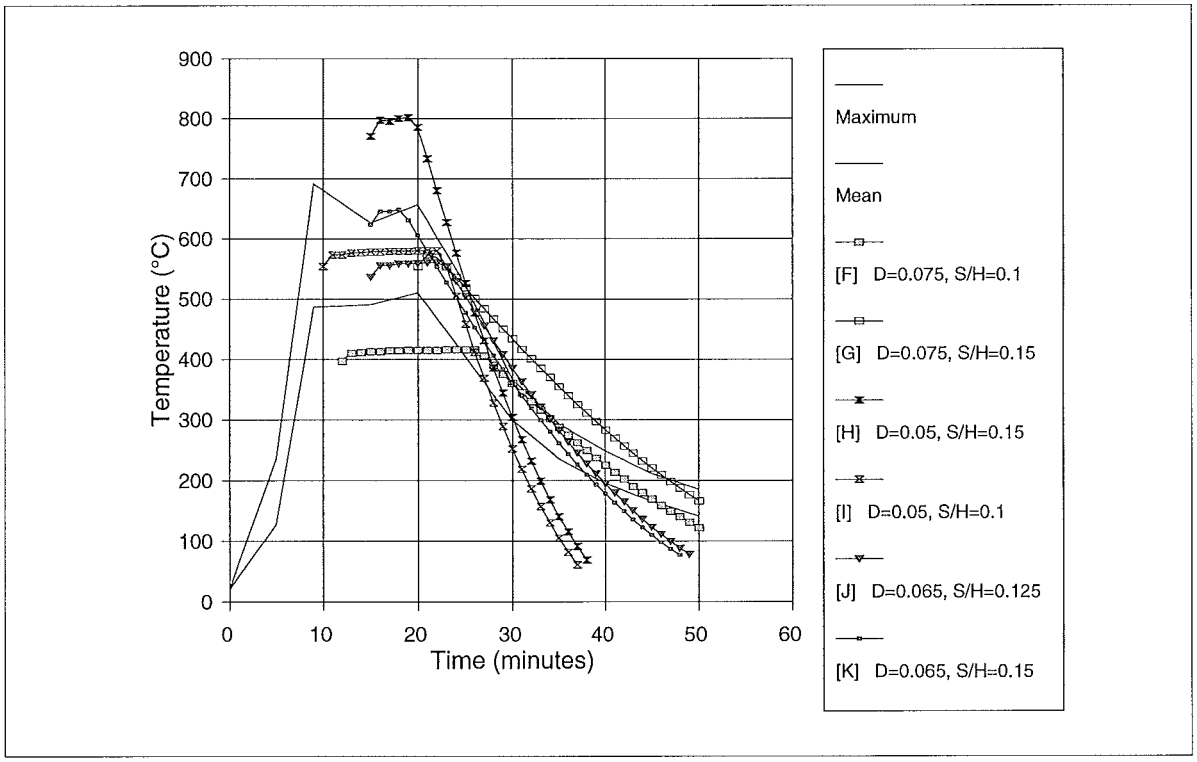

Fig. B1.22 NFSC 70-44, 20 kg/m² Floor Area, Ventilation Factor 0.157, Crib Fires, Shape = 3

NFSC 70-44, Stick Fire, Shape = 2 (Figure B1.23)

Identifier	Diam. (D) (m)	Stick Burn Regress Rate (v_p) (m/s)	Shape (F)	Initial Pyrolysis Rate (kg/s)	
				Stick Burning	Vent. Control
L	0.050	1.2E-05	2	0.238	1.305
M	0.035	1.1E-05	2	0.312	1.305
N	0.035	1.0E-05	2	0.284	1.305
O	0.065	1.5E-05	2	0.229	1.305

All simulations give reasonable peak temperature estimates, and close to linear decay curves which are conservative above 300 °C.

NFSC 70-44, Stick Fire, Shape = 3 (Figure B1.24)

Identifier	Diam. (D) (m)	Stick Burn Regress Rate (v_p) (m/s)	Shape (F)	Initial Pyrolysis Rate (kg/s)	
				Stick Burning	Vent. Control
P	0.050	1.0E-05	3	0.298	1.305
Q	0.050	9.0E-06	3	0.268	1.305
R	0.065	1.2E-05	3	0.275	1.305

All simulations give reasonable peak temperature estimates, and close to linear decay curves which are only slightly conservative above 250 °C.

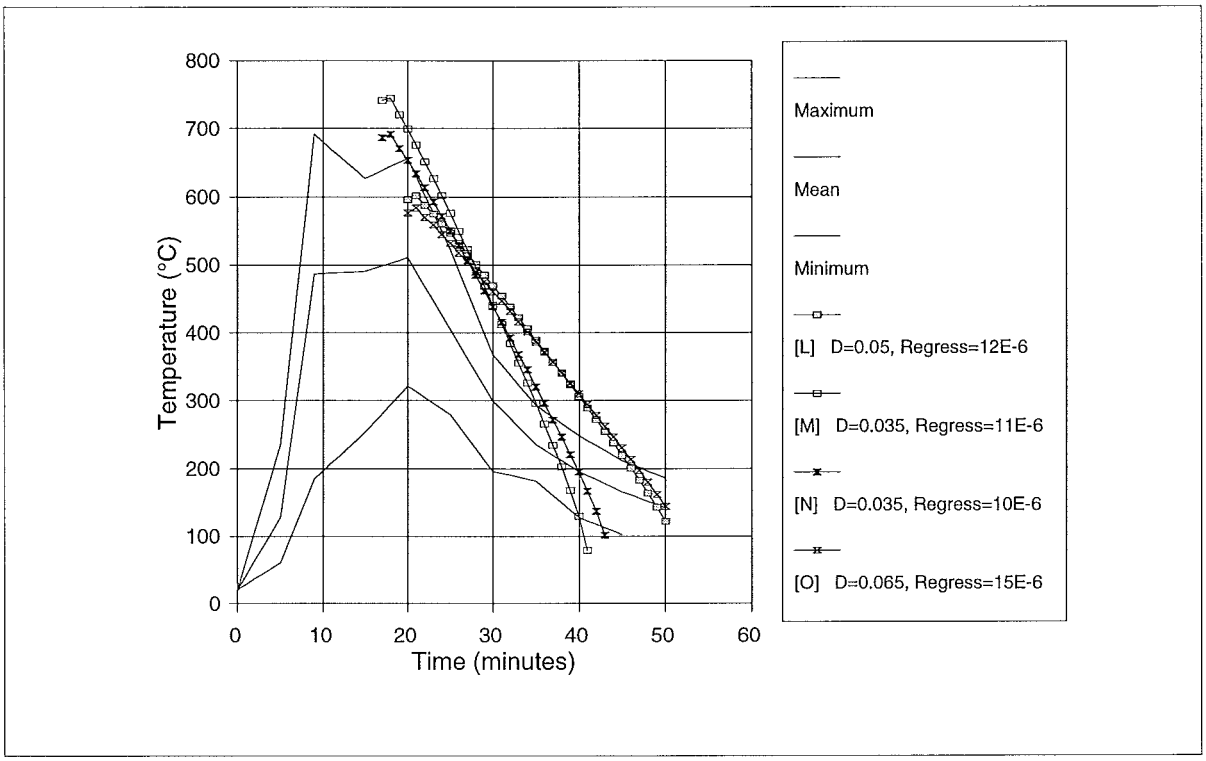

Fig. B1.23 NFSC 70-44, 20 kg/m² Floor Area, Ventilation Factor 0.157, Stick Fires, Shape = 2

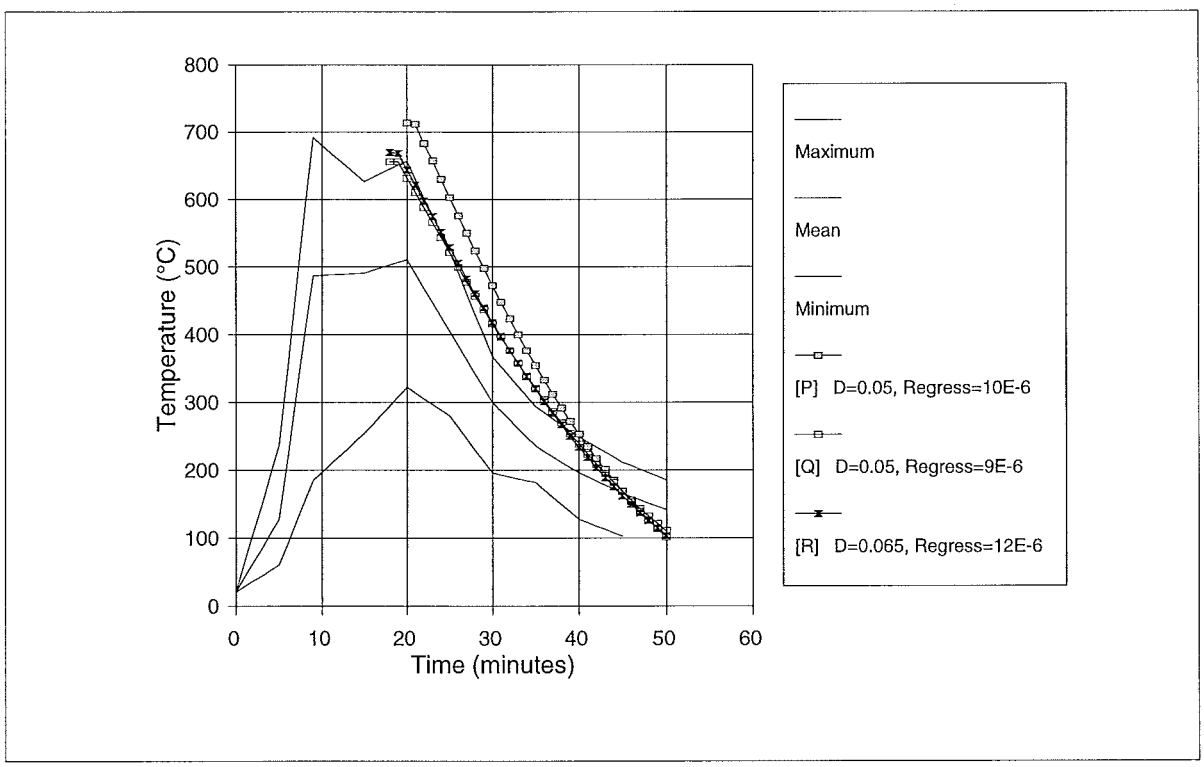

Fig. B1.24 NFSC 70-44, 20 kg/m² Floor Area, Ventilation Factor 0.157, Stick Fires, Shape = 3

B1.8 NFSC -69

The compartment and ventilation opening geometry, materials of construction, fuel load, and relevant parameters calculated from the specified data, are scheduled in Table B1.14.

Specified Parameters	
Compartment Length	5.51 m
Compartment Width	5.76 m
Compartment Height	2.60 m
Ventilation Height	1.9 m
Ventilation Width	1.4 m
Sill Height	0.4 m
Wall Details	4 walls of 0.20 m cellular concrete
Ceiling Details	0.035 m calcium silicate insulation
Floor Details	0.026 m plaster board
Fuel Load	451 kg bedroom furniture
Calculated Parameters	
Floor Area	31.74 m^2
Total Internal Surface Area	122.08 m^2
Ventilation Area	2.66 m^2
Ventilation Parameter ($A_V \sqrt{H}$)	3.667 $m^{5/2}$
Ventilation Parameter ($A_V \sqrt{H} / A_T$)	0.030 $m^{0.5}$
Fire Load Density	15.6 kg /m^2 of floor area
Fire Load Density	4.1 kg /m^2 of total bounding surface area

Table B1.14 NFSC -69 Input Data ; Fire Load 15.6 kg/m^2, Ventilation Factor 0.030

This fire has a low fire load and low ventilation factor. From the initial data above, fires with the following stick size (D), regression rate (v_p), shape factor (F) and crib spacing to height ratio (S_c / H_c)were modelled, leading to the tabulated initial pyrolysis rates for stick burning, ventilation control, crib porosity control and crib fuel surface control mechanisms. The lowest non-zero rate governs the initial fire development.

Identifier	Diam. (D) (m)	Stick Burn Regress Rate (v_p) (m/s)	Shape (F)	Crib (S_c /H_c)	Pyrolysis Rate (kg/s)				
					Stick Burning	Vent. Control	Crib Porosity Control	Crib Fuel Surface (theory)	Crib Fuel Surface (progr)
A	0.050		2	0.100		0.440	0.436	0.407	0.594
B	0.050		2	0.075		0.440	0.327	0.407	0.594
C	0.075		2	0.100		0.440	0.291	0.213	0.310
D	0.085		2	0.125		0.440	0.321	0.174	0.254
E	0.075		2	0.125		0.440	0.364	0.213	0.310
F	0.050		3	0.125		0.440	0.545	0.407	0.890
G	0.075		3	0.200		0.440	0.582	0.213	0.465
H	0.080		3	0.200		0.440	0.545	0.192	0.420
I	0.080		3	0.200		0.440	0.545	0.192	0.420
J	0.080		3	0.200		0.440	0.545	0.192	0.420
K	0.050	1.1E-05	2		0.436	0.440			
L	0.075	1.6E-05	2		0.423	0.440			
M	0.075	1.2E-05	3		0.476	0.440			
N	0.050	1.0E-05	3		0.595	0.440			
O	0.100	1.8E-05	3		0.535	0.440			

Table B1.15 NFSC -69, Fire Simulation Parameters and Initial Pyrolysis Rates

NFSC -69, Crib Fire, Shape = 2 (Figure B1.25)

Identifier	Diam. (D) (m)	Shape (F)	Crib (S_c /H_c)	Initial Pyrolysis Rate (kg/s)			
				Vent. Control	Crib Porosity Control	Crib Fuel Surface (theory)	Crib Fuel Surface (progr)
A	0.050	2	0.100	0.440	0.436	0.407	0.594
B	0.050	2	0.075	0.440	0.327	0.407	0.594
C	0.075	2	0.100	0.440	0.291	0.213	0.31
D	0.085	2	0.125	0.440	0.321	0.174	0.254
E	0.080	2	0.125	0.440	0.364	0.213	0.31

Simulations A and B with stick size of 0.05 m, are initially crib porosity controlled, at just below the initial ventilation controlled pyrolysis rate. They overestimate peak

temperatures (only [B] is plotted). Simulations C and E with a stick size of 0.075 m are initially crib porosity and fuel surface controlled respectively. The fuel surface controlled pyrolysis rate is below the initial ventilation limited pyrolysis rate. Both reproduce peak temperatures reliably; and provides a conservative estimate of decay temperature down to about 300 °C.

Simulation D is strongly fuel surface controlled, and while having a conservative decay curve to 300 °C, underestimates the peak temperature by over 100 °C.

NFSC -69, Crib Fire, Shape = 3 (Figure B1.26)

Identifier	Diam. (D) (m)	Shape (F)	Crib (S_c/H_c)	Initial Pyrolysis Rate (kg/s)			
				Vent. Control	Crib Porosity Control	Crib Fuel Surface (theory)	Crib Fuel Surface (progr)
F	0.050	3	0.125	0.440	0.545	0.407	0.890
G	0.075	3	0.200	0.440	0.582	0.213	0.465
H	0.080	3	0.200	0.440	0.545	0.192	0.420
I	0.080	3	0.200	0.440	0.545	0.192	0.420
J	0.080	3	0.200	0.440	0.545	0.192	0.420

Simulations F and G are ventilation limited and over-predict the peak temperature, with an over-rapid decay. Simulations H, I and J are slightly crib fuel surface controlled and are set up with BPF parameter of 98%, 70% and 85% respectively. Simulation J provides the best estimate of peak compartment temperature. All three decay curves are similar, and slightly conservative down to 350 °C.

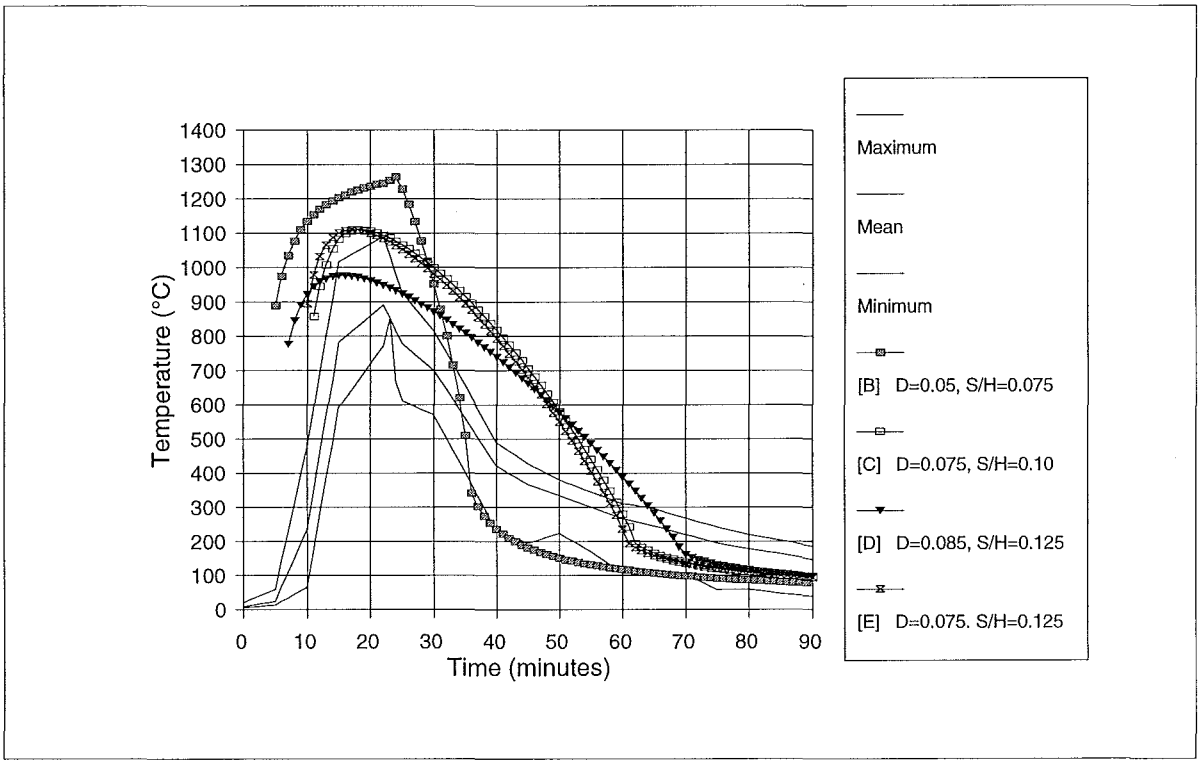

Fig. B1.25 NFSC -69, 15.6 kg/m² Floor Area, Ventilation Factor 0.03, Crib Fires, Shape = 2

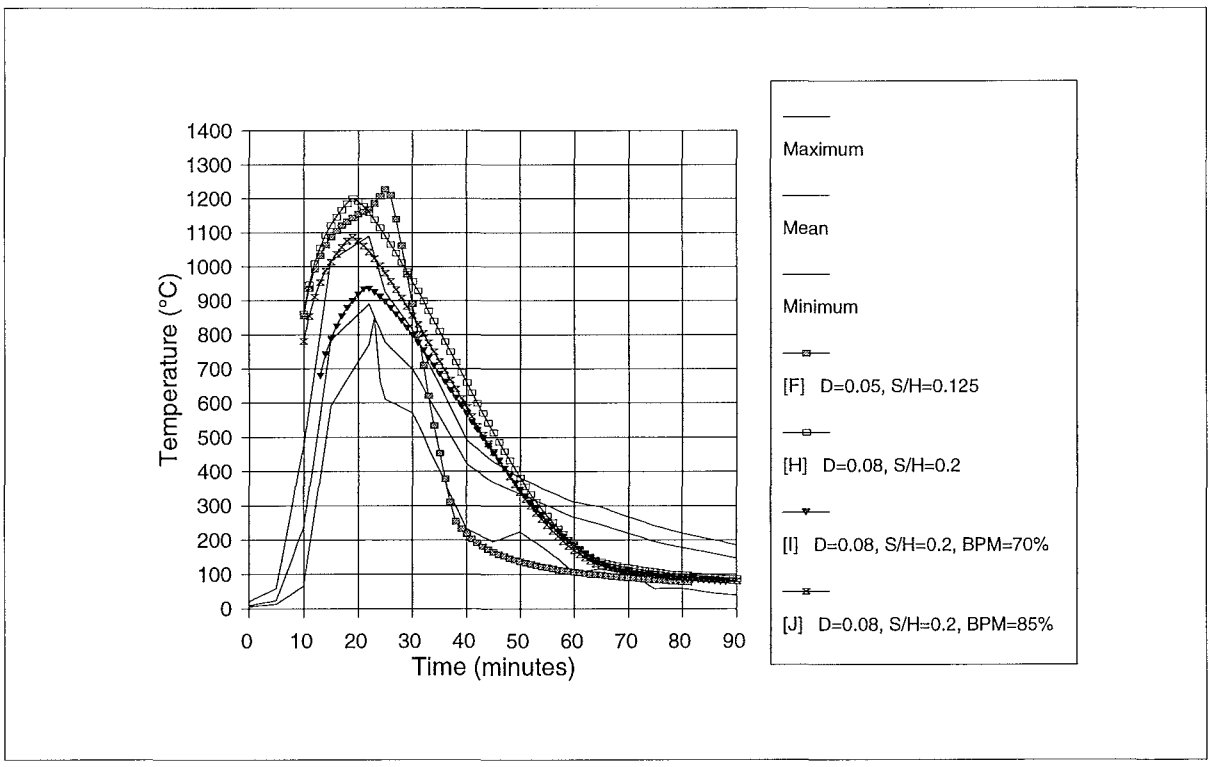

Fig. B1.26 NFSC -69, 15.6 kg/m² Floor Area, Ventilation Factor 0.03, Crib Fires, Shape = 3

NFSC -69, Stick Fire, Shape = 2 (Figure B1.27)

Identifier	Diam. (D) (m)	Stick Burn Regress Rate (v_p) (m/s)	Shape (F)	Initial Pyrolysis Rate (kg/s)	
				Stick Burning	Vent. Control
K	0.050	1.1E-05	2	0.436	0.440
L	0.075	1.6E-05	2	0.423	0.440

Simulations K and L have initial pyrolysis rates slightly below that of the ventilation limited pyrolysis rate. They predict peak temperature well, and provide a slightly conservative decay curve down to 400°C.

NFSC -69, Stick Fire, Shape = 3 (Figure B1.28)

Identifier	Diam. (D) (m)	Stick Burn Regress Rate (v_p) (m/s)	Shape (F)	Initial Pyrolysis Rate (kg/s)	
				Stick Burning	Vent. Control
M	0.075	1.2E-05	3	0.476	0.440
N	0.050	1.0E-05	3	0.595	0.440
O	0.100	1.8E-05	3	0.535	0.440

Simulations M, N and O have initial pyrolysis rates slightly above the ventilation limited pyrolysis rate. They all have a BPF parameter of 85%. Peak temperatures are well predicted, with the decay conservative to about 450 °C in the case of Simulation [M].

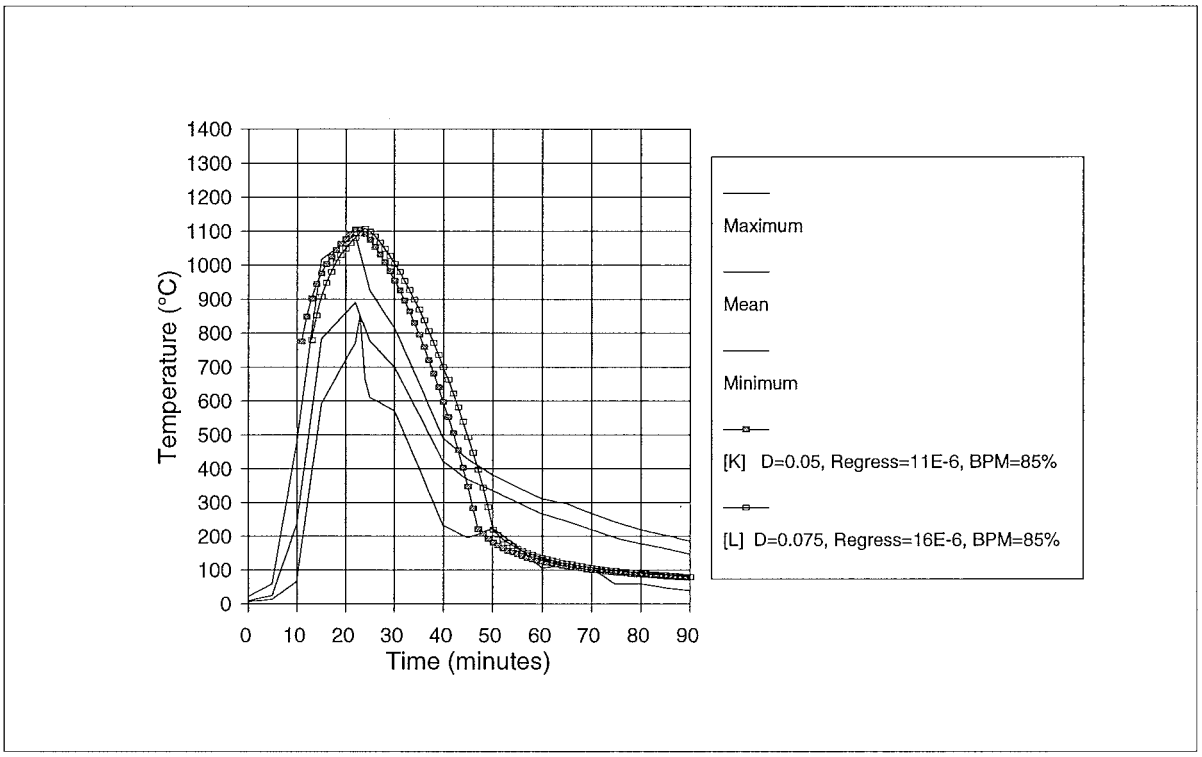

Fig. B1.27 NFSC -69, 15.6 kg/m² Floor Area, Ventilation Factor 0.03, Stick Fires, Shape = 2

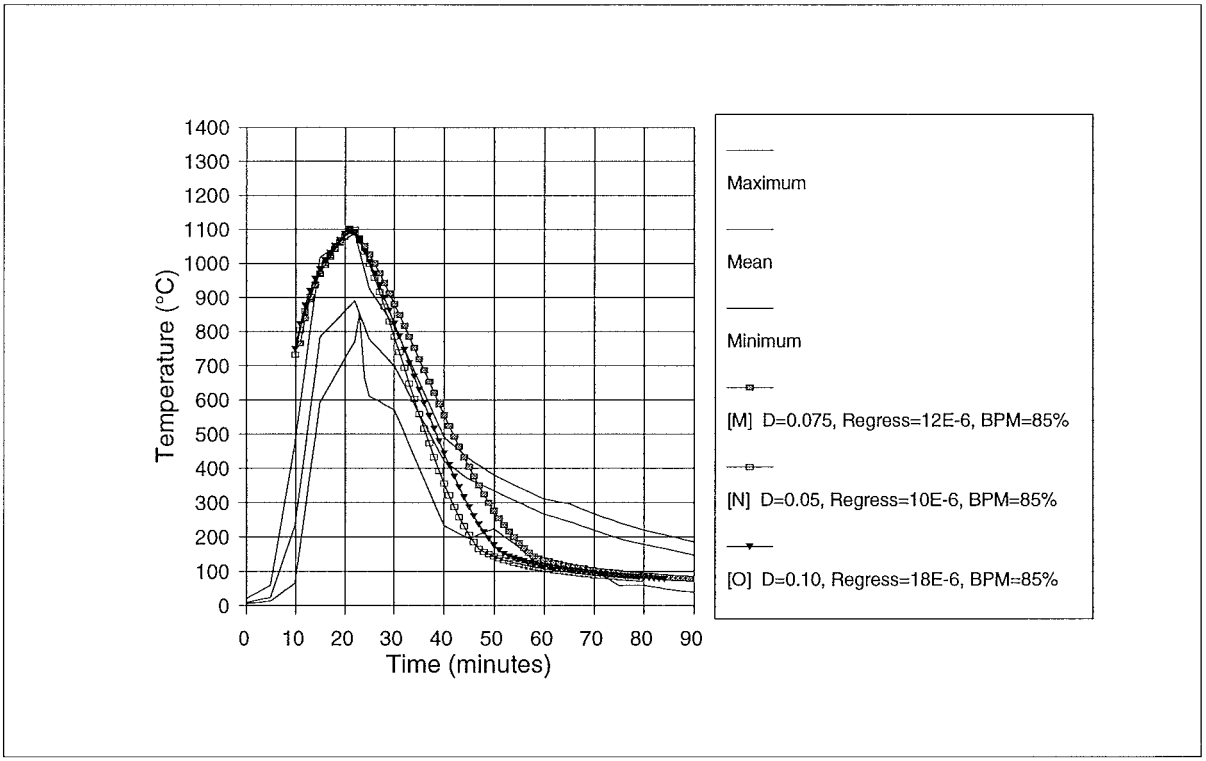

Fig. B1.28 NFSC -69, 15.6 kg/m² Floor Area, Ventilation Factor 0.03, Stick Fires, Shape = 3

B1.9 NFSC 70-20

The compartment and ventilation opening geometry, materials of construction, fuel load, and relevant parameters calculated from the specified data, are scheduled in Table B1.16.

Specified Parameters	
Compartment Length	3.68 m
Compartment Width	3.38 m
Compartment Height	3.13 m
Ventilation Height	2.18 m
Ventilation Width	1.95 m
Sill Height	0.95 m
Wall Details	3 walls of 0.115 m normal brick + 0.160 m hard brick plus 1 wall of 0.175 m lightweight concrete
Ceiling Details	0.175 m lightweight concrete
Floor Details	refractory concrete
Fuel Load	186 kg wood
Calculated Parameters	
Floor Area	12.44 m^2
Total Internal Surface Area	69.07 m^2
Ventilation Area	4.251 m^2
Ventilation Parameter ($A_V \sqrt{H}$)	6.277 $m^{5/2}$
Ventilation Parameter ($A_V \sqrt{H} / A_T$)	0.091 $m^{0.5}$
Fire Load Density	15.0 kg /m^2 of floor area
Fire Load Density	2.7 kg /m^2 of total bounding surface area

Table B1.16 NFSC 70-20 Input Data ; Fire Load 15 kg/m^2, Ventilation Factor 0.091

This fire has a very low fire load and moderately high ventilation factor. From the initial data above, fires with the following stick size (D), regression rate (v_p), shape factor (F) and crib spacing to height ratio (S_c / H_c)were modelled, leading to the tabulated initial pyrolysis rates for stick burning, ventilation control, crib porosity control and crib fuel surface control mechanisms. The lowest non-zero rate governs the initial fire

development.

Identifier	Diam. (D) (m)	Stick Burn Regress Rate (v_p) (m/s)	Shape (F)	Crib (S_c/H_c)	Pyrolysis Rate (kg/s)				
					Stick Burning	Vent. Control	Crib Porosity Control	Crib Fuel Surface (theory)	Crib Fuel Surface (progr)
A	0.050		2	0.15		0.753	0.246	0.153	0.223
B	0.050		2	0.05		0.753	0.082	0.153	0.223
C	0.050		2	0.10		0.753	0.164	0.153	0.223
D	0.050		2	0.08		0.753	0.123	0.153	0.223
E	0.050		3	0.20		0.753	0.327	0.153	0.334
F	0.075		3	0.20		0.753	0.218	0.080	0.175
G	0.075		3	0.10		0.753	0.109	0.080	0.175
H	0.065		3	0.10		0.753	0.126	0.100	0.220
I	0.050	1.2E-05	2		0.179	0.753			
J	0.075	1.2E-05	2		0.119	0.753			
K	0.063	1.2E-05	2		0.143	0.753			
L	0.075		3	0.15		0.753	0.164	0.080	0.175
M	0.050	1.2E-05	3		1.529	0.753			
N	0.075	1.2E-050	3		1.019	0.753			
O	0.075	1.0E-05	3		0.849	0.753			

Table B1.17 NFSC 70-20, Fire Simulation Parameters and Initial Pyrolysis Rates

NFSC 70-20, Crib Fire, Shape = 2 (Figure B1.29)

Identifier	Diam. (D) (m)	Shape (F)	Crib (S_c/H_c)	Initial Pyrolysis Rate (kg/s)			
				Vent. Control	Crib Porosity Control	Crib Fuel Surface (theory)	Crib Fuel Surface (progr)
A	0.050	2	0.15	0.753	0.246	0.153	0.223
B	0.050	2	0.05	0.753	0.082	0.153	0.223
C	0.050	2	0.10	0.753	0.164	0.153	0.223
D	0.050	2	0.08	0.753	0.123	0.153	0.223

All simulations have initial pyrolysis rates well below the ventilation limited pyrolysis rate.

Simulation A is fuel surface controlled, but greatly over-estimates peak fire temperatures. Simulations B, C and D are all crib porosity controlled, reverting to fuel surface controlled. The peak fire temperature is best estimated by Simulation B , but the decay curve is too steep. None represents the experimental really well, tending to overestimate the overall duration.

NFSC 70-20, Crib Fire, Shape = 3 (Figure B1.30)

Identifier	Diam. (D) (m)	Shape (F)	Crib (S_c/H_c)	Initial Pyrolysis Rate (kg/s)			
				Vent. Control	Crib Porosity Control	Crib Fuel Surface (theory)	Crib Fuel Surface (progr)
E	0.050	3	0.20	0.753	0.327	0.153	0.334
F	0.075	3	0.20	0.753	0.218	0.080	0.175
G	0.075	3	0.10	0.753	0.109	0.080	0.175
H	0.065	3	0.10	0.753	0.126	0.100	0.220
L	0.075	3	0.15	0.753	0.164	0.080	0.175

Simulation E which is initially fuel surface controlled, massively over-predicts the peak compartment temperature. The other simulations have significantly lower initial pyrolysis rates, with the most reliable, Simulation L being slightly crib porosity controlled initially before reverting to crib fuel surface control. The peak temperature is well estimated, and the decay curve reliably predicted down to 170 °C.

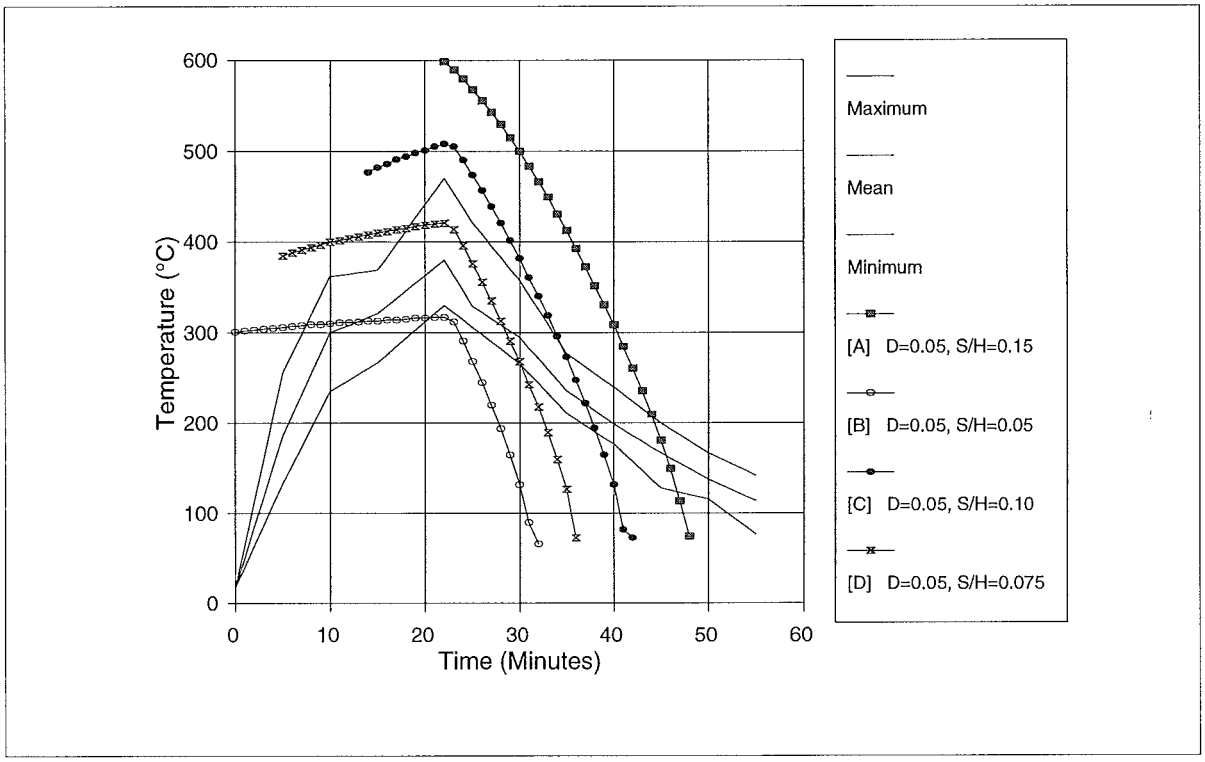

Fig. B1.29 NFSC 70-20, 15 kg/m² Floor Area, Ventilation Factor = 0.091, Crib Fires, Shape = 2

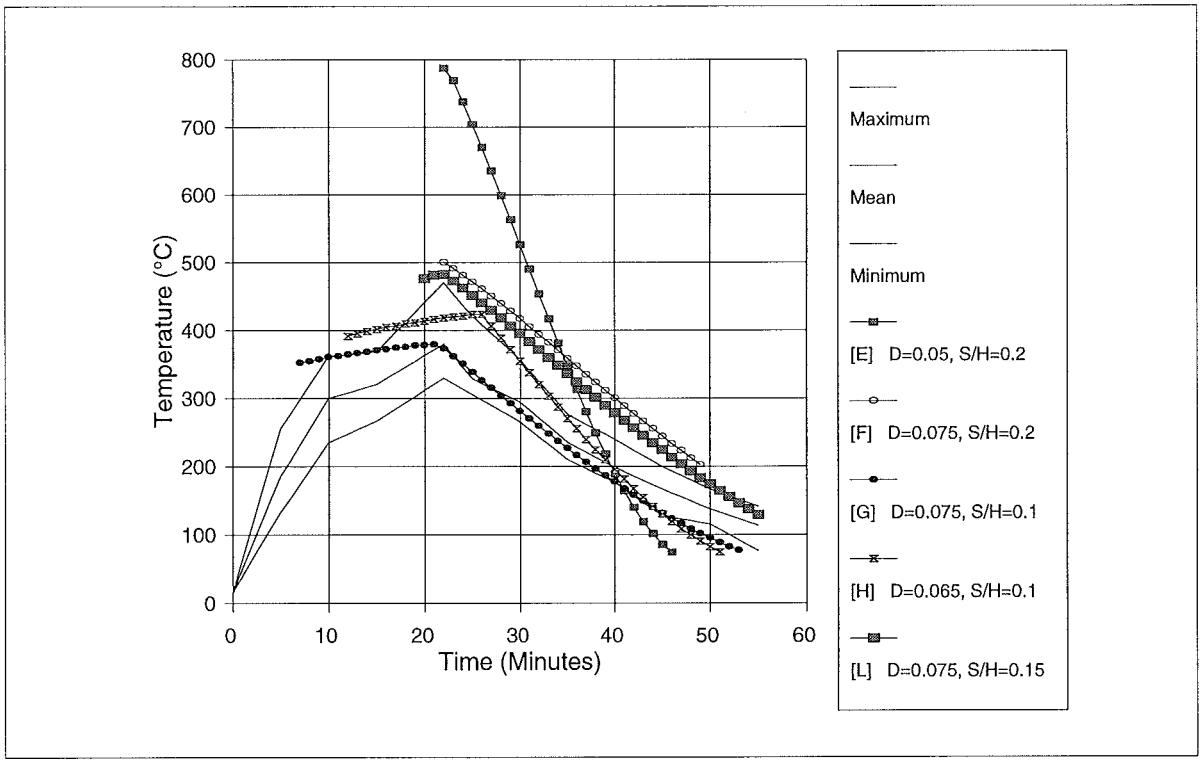

Fig. B1.30 NFSC 70-20, 15 kg/m² Floor Area, Ventilation Factor = 0.091, Crib Fires, Shape = 3

NFSC 70-20, Stick Fire, Shape = 2 (Figure B1.31)

Identifier	Diam. (D) (m)	Stick Burn Regress Rate (v_p) (m/s)	Shape (F)	Initial Pyrolysis Rate (kg/s)	
				Stick Burning	Vent. Control
I	0.050	1.2E-05	2	0.179	0.753
J	0.075	1.2E-05	2	0.119	0.753
K	0.063	1.2E-05	2	0.143	0.753

Simulations I, J and K have initial pyrolysis rates well below the ventilation controlled pyrolysis rate. Simulation K provides the best estimate of peak temperature, and a conservative decay profile estimate down to less than 200 °C.

NFSC 70-20, Stick Fire, Shape = 3 (Figure B1.32)

Identifier	Diam. (D) (m)	Stick Burn Regress Rate (v_p) (m/s)	Shape (F)	Initial Pyrolysis Rate (kg/s)	
				Stick Burning	Vent. Control
M	0.050	1.2E-05	3	1.529	0.753
N	0.075	1.2E-05	3	1.019	0.753
O	0.075	1.0E-05	3	0.849	0.753

Simulations have initial stick burning pyrolysis rate greater than the ventilation controlled pyrolysis rate, with the latter governing. Simulations O and N provide a good estimate of peak temperature, and a slightly conservative decay to below 200 °C.

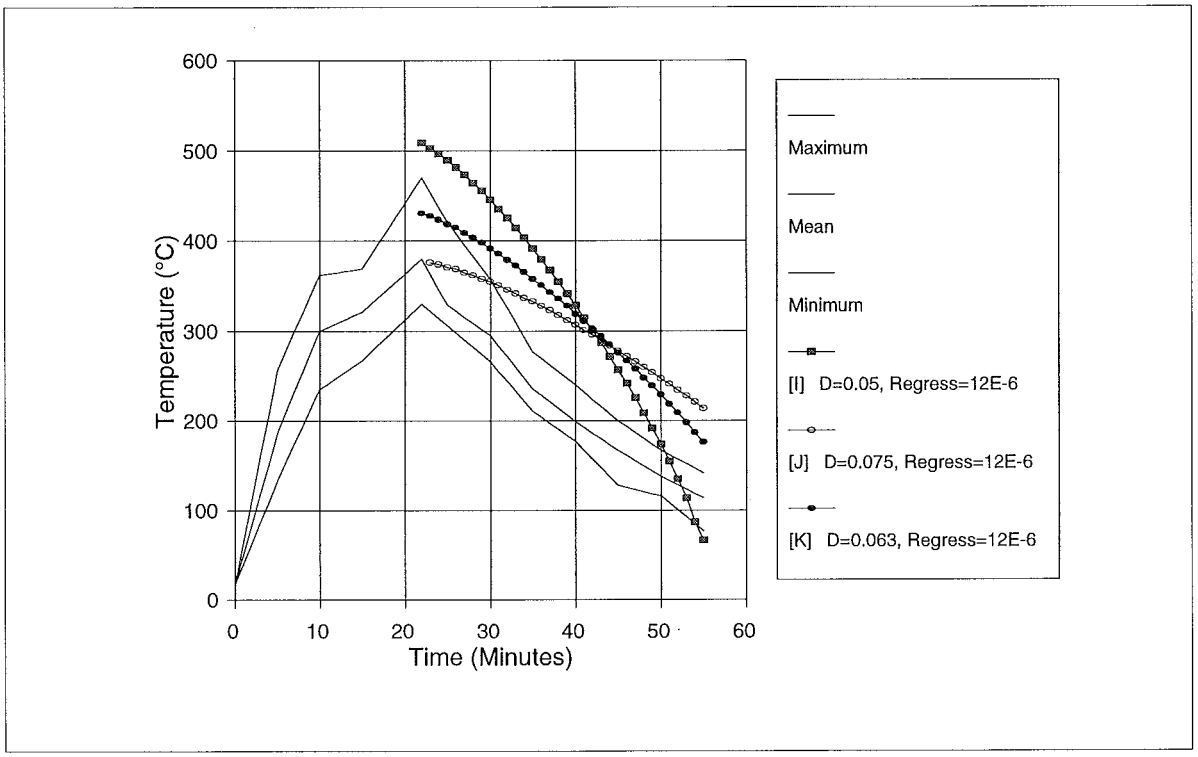

Fig. B1.31 NFSC 70-20, 15 kg/m² Floor Area, Ventilation Factor = 0.091, Stick Fires, Shape = 2

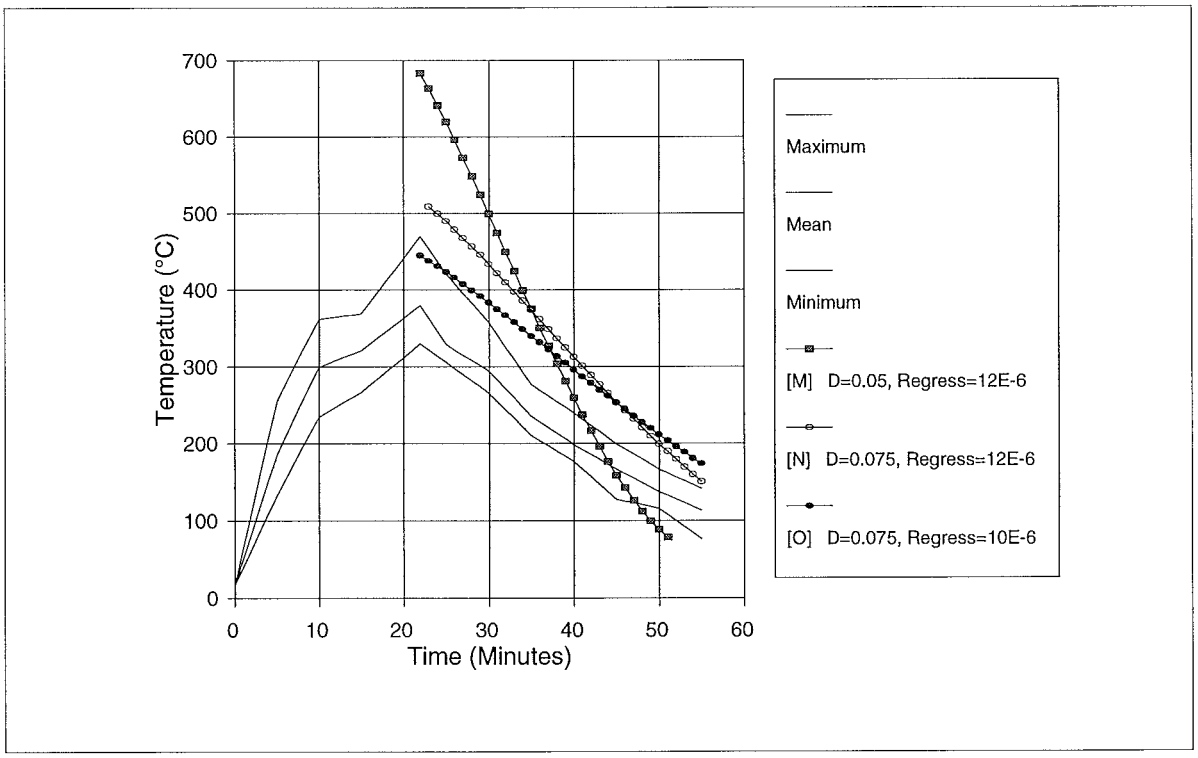

Fig. B1.32 NFSC 70-20, 15 kg/m² Floor Area, Ventilation Factor = 0.091, Stick Fires, Shape = 3

B1.10 NFSC 70-16

The compartment and ventilation opening geometry, materials of construction, fuel load, and relevant parameters calculated from the specified data, are scheduled in Table B1.18.

Specified Parameters	
Compartment Length	3.68 m
Compartment Width	3.38 m
Compartment Height	3.13 m
Ventilation Height	0.90 m
Ventilation Width	1.18 m
Sill Height	2.23 m
Wall Details	3 walls of 0.115 m normal brick + 0.160 m hard brick plus 1 wall of 0.175 m lightweight concrete
Ceiling Details	0.175 m lightweight concrete
Floor Details	refractory concrete
Fuel Load	372 kg wood
Calculated Parameters	
Floor Area	12.44 m^2
Total Internal Surface Area	69.07 m^2
Ventilation Area	1.06 m^2
Ventilation Parameter ($A_V \sqrt{H}$)	1.006 $m^{5/2}$
Ventilation Parameter ($A_V \sqrt{H} / A_T$)	0.015 $m^{0.5}$
Fire Load Density	29.9 kg /m^2 of floor area
Fire Load Density	5.4 kg /m^2 of total bounding surface area

Table B1.18 NFSC 70-16 Input Data ; Fire Load 29.9 kg/m^2, Ventilation Factor 0.015

This fire has a moderate fire load and very low ventilation factor. From the initial data above, fires with the following stick size (D), regression rate (v_p), and shape factor (F) were modelled, leading to the tabulated initial pyrolysis rates for stick burning, ventilation control mechanisms. The lowest non-zero rate governs the initial fire development.

Identifier	Diam. (D) (m)	Stick Burn Regress Rate (vp) (m/s)	Shape (F)		Pyrolysis Rate (kg/s)	
					Stick Burning	Vent. Control
A	0.100	1.0E-06	3	BPF=0.8	0.022	0.121
B	0.100	4.3E-06	3	BPF=0.98	0.097	0.121
C	0.100	5.4E-06	3	BPF=0.98	0.121	0.121
D	0.100	6.5E-06	3	BPF=0.98	0.145	0.121
E	0.100	9.5E-06	3	BPF=0.98	0.212	0.121

Table B1.19 NFSC 70-16, Fire Simulation Parameters and Initial Pyrolysis Rates

NFSC 70-16, Stick Fire, Shape = 3 (Figure B1.33)

Simulations have initial stick burning pyrolysis rate both less than and greater than the ventilation controlled pyrolysis rate. None of the simulations reliably reproduced the experimental data. Because of the very low ventilation limited pyrolysis rate, none of the crib burning or stick burning simulations could produce anywhere enough heat release to reach the maximum experimental compartment temperature. The minimum temperature compartment profile could be approximated, with the best simulations [D] and [E] having initial pyrolysis rates 1.75 times and 1.2 times the ventilation limited pyrolysis rate respectively.

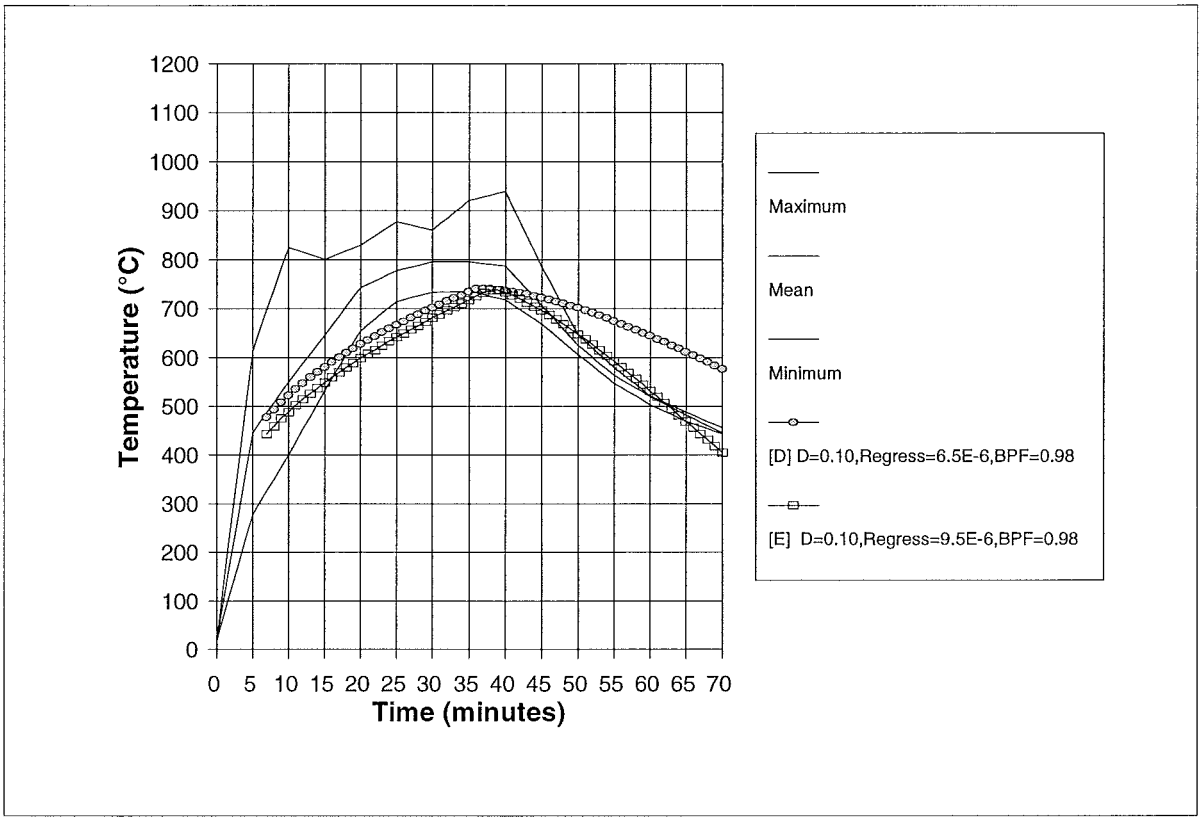

Fig.B1.33 NFSC 70-16, Fire Load 29,9 kg/m² Floor Area, Ventilation Factor = 0.015, Stick Fires, Shape = 1

B1.11 NFSC 71-54

The compartment and ventilation opening geometry, materials of construction, fuel load, and relevant parameters calculated from the specified data, are scheduled in Table B1.20.

Specified Parameters	
Compartment Length	3.60 m
Compartment Width	3.36 m
Compartment Height	3.13 m
Ventilation Height	1.06 m
Ventilation Width	0.90 m
Sill Height	2.07 m
Wall Details	3 walls of 0.115 m normal brick + 0.160 m hard brick plus 1 wall of 0.175 m lightweight concrete
Ceiling Details	0.175 m lightweight concrete
Floor Details	refractory concrete
Fuel Load	190 kg furniture, 162 kg paper and 20 kg pine, or 295.3 kg wood equivalent
Calculated Parameters	
Floor Area	12.1 m^2
Total Internal Surface Area	67.76 m^2
Ventilation Area	0.954 m^2
Ventilation Parameter ($A_V \sqrt{H}$)	0.982 $m^{5/2}$
Ventilation Parameter ($A_V \sqrt{H} / A_T$)	0.014 $m^{0.5}$
Fire Load Density	24.4 kg /m^2 of floor area
Fire Load Density	4.4 kg /m^2 of total bounding surface area

Table B1.20 NFSC 71-54 Input Data ; Fire Load 24.4 kg/m^2, Ventilation Factor 0.014

This fire has a moderate fire load and very low ventilation factor. From the initial data above, fires with the following stick size (D), regression rate (v_p), and shape factor (F) were modelled, leading to the tabulated initial pyrolysis rates for stick burning, ventilation control mechanisms. The lowest non-zero rate governs the initial fire

development.

Identifier	Diam. (D) (m)	Stick Burn Regress Rate (vp) (m/s)	Shape (F)	Crib (Sc/Hc)	Pyrolysis Rate (kg/s)		
					Stick Burning	Vent. Control	Crib Porosity Control
A	0.100	1.2E-05	3	BPF=0.98	0.207	0.118	
B	0.100	8.4E-06	3	BPF=0.98	0.148	0.118	
C	0.100		3	0.091		0.118	0.118

Table B1.21 NFSC 71-54, Fire Simulation Parameters and Initial Pyrolysis Rates

NFSC 71-54, (Figure B1.34)

Stick burning simulations have initial stick burning pyrolysis rate greater than the ventilation controlled pyrolysis rate. Because of the very low ventilation limited pyrolysis rate, none of the crib burning or stick burning simulations could produce anywhere enough heat release to reach the maximum experimental compartment temperature. The best simulations [A] and [B] were those selected with initial pyrolysis rates 1.75 times and 1.25 times the ventilation limited pyrolysis rate respectively. These both produced peak temperatures more than 200 °C lower than the experimental data. At higher and lower relative pyrolysis rates other stick burning simulations were even more inferior.

A crib porosity controlled fire [C], with the initial crib pyrolysis rate set equal to the ventilation limited pyrolysis rate was tried. The latter type of fire has the advantage that the pyrolysis and burning rates can be held nominally constant for a period, allowing a steadier heat release rate to be simulated. Little improvement in the simulation of the experimental data resulted. None of the simulations reliably reproduced the experimental data.

It is evident that for this fire (NFSC 71-54) and the previous fire (NFSC 70-16), both tests had the small ventilation aperture created by raising the sill level of the "window" to 2.07 and 2.23 m respectively. The high location of the ventilation aperture in relation to the fuel load, may have enhanced burning rates to create more intense fires than would normally be expected for this compartment size, material properties, fire load and ventilation. Further investigation is warranted.

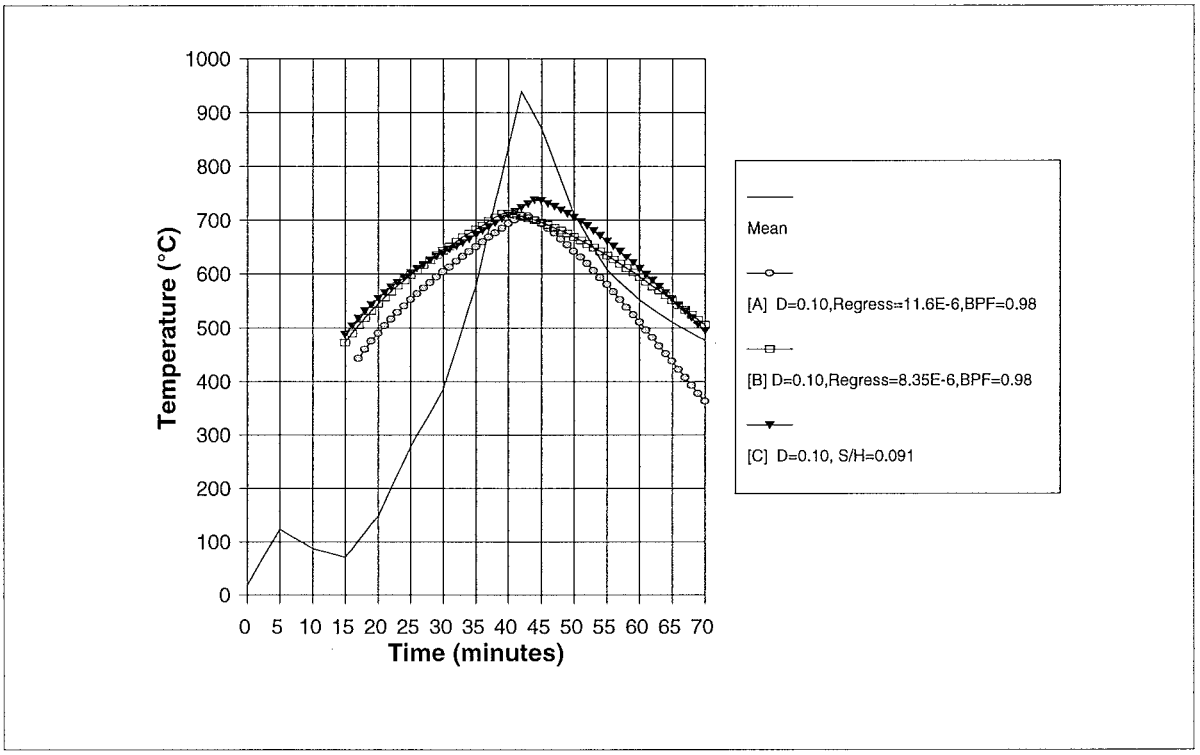

Fig. B1-34 NFSC 71-54, FIre Load 24.4 kg/m² Floor Area, Ventilation Factor =0.014, Stick and Crib Fires

B1.12 NFSC 70-24

The compartment and ventilation opening geometry, materials of construction, fuel load, and relevant parameters calculated from the specified data, are scheduled in Table B1.22.

Specified Parameters	
Compartment Length	3.68 m
Compartment Width	3.38 m
Compartment Height	3.13 m
Ventilation Height	2.92 m
Ventilation Width	2.18 m
Sill Height	0.95 m
Wall Details	3 walls of 0.115 m normal brick + 0.160 m hard brick plus 1 wall of 0.175 m lightweight concrete
Ceiling Details	0.175 m lightweight concrete
Floor Details	refractory concrete
Fuel Load	327.6 kg wood
Calculated Parameters	
Floor Area	12.44 m^2
Total Internal Surface Area	69.07 m^2
Ventilation Area	6.366 m^2
Ventilation Parameter ($A_V \sqrt{H}$)	10.878 $m^{5/2}$
Ventilation Parameter ($A_V \sqrt{H} / A_T$)	0.157 $m^{0.5}$
Fire Load Density	30 kg /m^2 of floor area
Fire Load Density	5.4 kg /m^2 of total bounding surface area

Table B1.22 NFSC 70-24 Input Data ; Fire Load 30 kg/m^2, Ventilation Factor 0.157

This fire has a moderate fire load and high ventilation factor. From the initial data above, fires with the following stick size (D), regression rate (v_p), shape factor (F) and crib spacing to height ratio (S_c / H_c) were modelled, leading to the tabulated initial pyrolysis rates for stick burning, ventilation control, crib porosity control and crib fuel surface control mechanisms. The lowest non-zero rate governs the initial fire

development.

Identifier	Diam. (D) (m)	Stick Burn Regress Rate (vp) (m/s)	Shape (F)	Crib (Sc/Hc)	Pyrolysis Rate (kg/s)				
					Stick Burning	Vent. Control	Crib Porosity Control	Crib Fuel Surface (theory)	Crib Fuel Surface (progr)
A	0.029		2	0.100		1.305	0.558	0.716	1.044
B	0.025		2	0.070		1.305	0.457	0.927	1.352
C	0.050		2	0.200		1.305	0.656	0.306	0.446
D	0.039		2	0.200		1.305	0.841	0.455	0.664
E	0.045		2	0.200		1.305	0.723	0.358	0.522
F	0.058		3	0.250		1.305	0.702	0.239	0.522
G	0.029	1.0E-05	2		0.522	1.305			1.094
H	0.043	1.0E-05	3		0.522	1.305			0.856

Table B1.23 NFSC 70-24, Fire Simulation Parameters and Initial Pyrolysis Rates

NFSC 70-24, Crib Fire, Shape = 2 (Figure B1.35)

Identifier	Diam. (D) (m)	Shape (F)	Crib (Sc/Hc)	Initial Pyrolysis rate (kg/s)			
				Vent. Control	Crib Porosity Control	Crib Fuel Surface (theory)	Crib Fuel Surface (progr)
A	0.029	2	0.100	1.305	0.558	0.716	1.044
B	0.025	2	0.070	1.305	0.457	0.927	1.352
C	0.050	2	0.200	1.305	0.656	0.306	0.446
D	0.039	2	0.200	1.305	0.841	0.455	0.664
E	0.045	2	0.200	1.305	0.723	0.358	0.522

Simulations [A] and [B] are crib porosity controlled, resulting in fires of almost constant pyrolysis rate, burning rate, and heat release rate, until nearly all the fuel load is combusted. This causes the rapid decay in temperature. Simulations [C], [D] and [E] are all crib fuel surface controlled, with [C] and [D] overestimating and underestimating the peak temperature respectively. Simulation [E] provides the best simulation of peak temperature, and has a conservative concave decay curve to about 300 °C.

NFSC 70-24, Crib Fire, Shape = 3 (Figure B1.36)

Identifier	Diam. (D) (m)	Shape (F)	Crib (Sc/Hc)	Initial Pyrolysis Rate (kg/s)			
				Vent. Control	Crib Porosity Control	Crib Fuel Surface (theory)	Crib Fuel Surface (progr)
F	0.058	3	0.250	1.305	0.702	0.239	0.522

Simulation [F] provides a good estimate of the peak temperature, and a conservative approximately linear decay down to 300 °C.

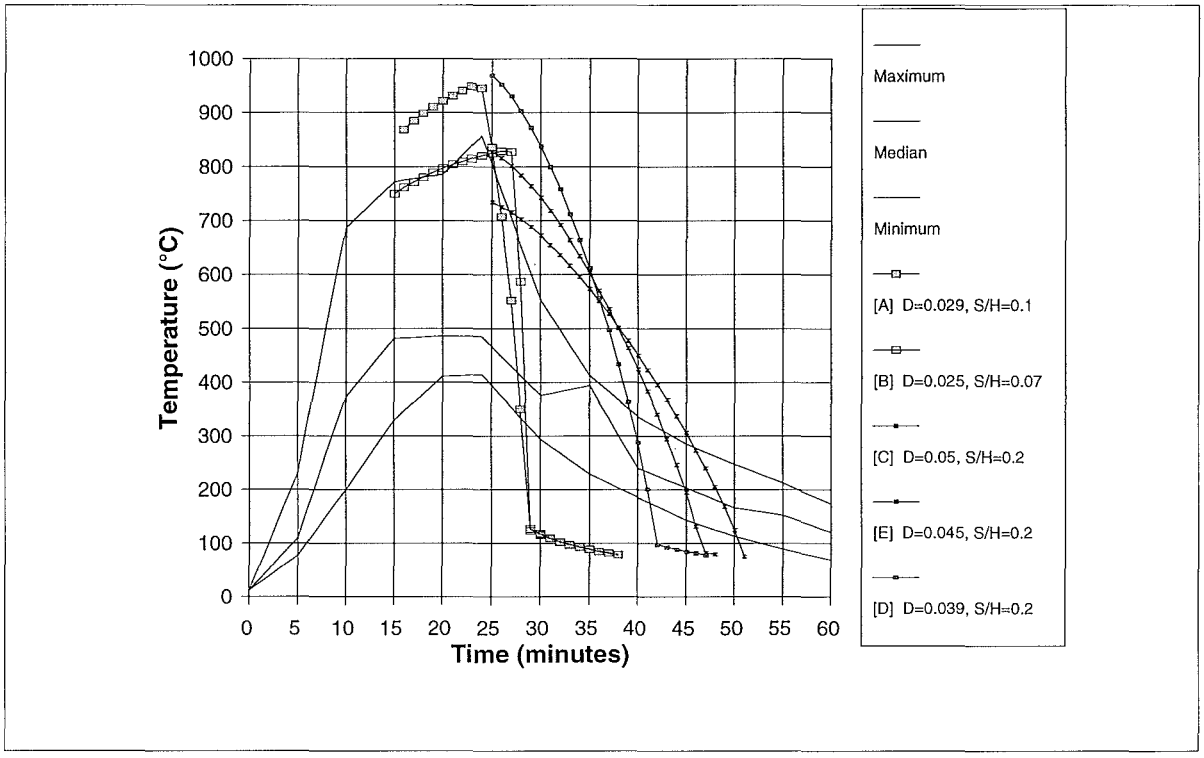

Fig B1.35 NFSC 70-24, Fire Load 30 kg/m² Floor Area, Ventilation Factor 0.157, Crib Fires, Shape = 2

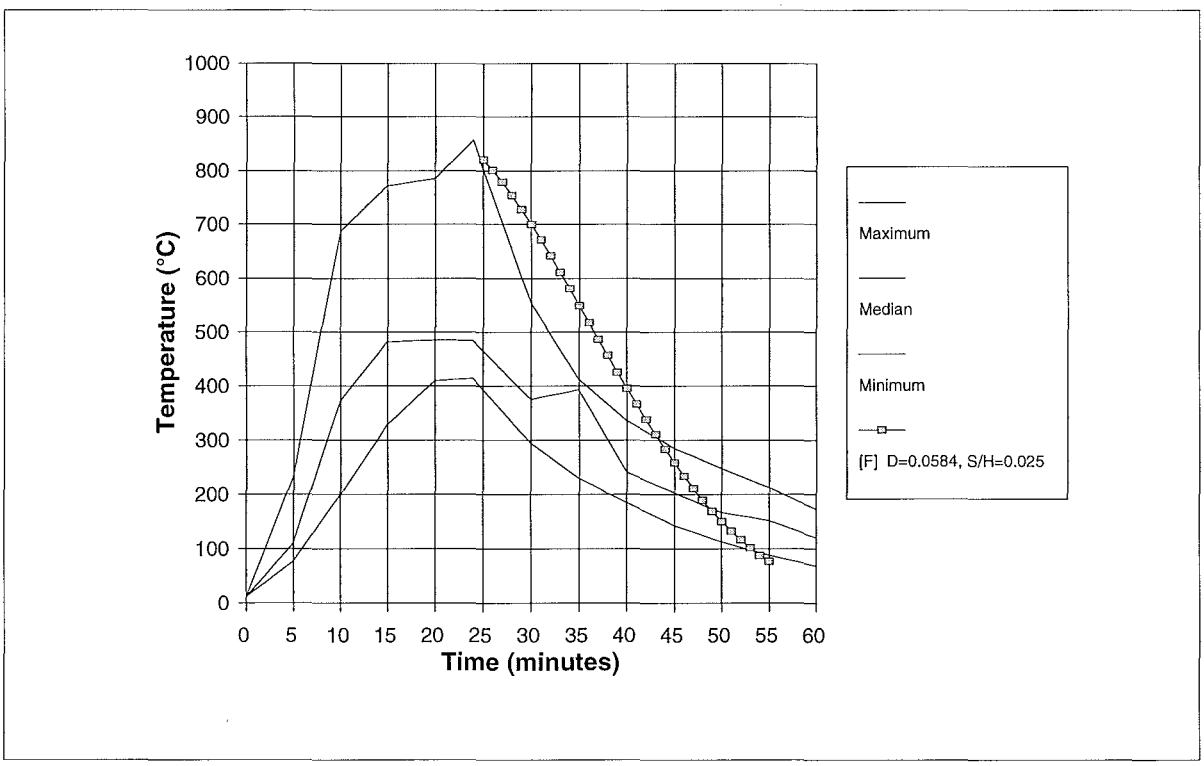

Fig B1.36 NFSC 70-24, Fire Load 30 kg/m² Floor Area, Ventilation Factor 0.157, Crib Fires, Shape = 3

NFSC 70-24, Stick Fire, Shape = 2 (Figure B1.37)

Identifier	Diam. (D) (m)	Stick Burn Regress Rate (vp) (m/s)	Shape (F)	Pyrolysis Rate (kg/s)	
				Stick Burning	Vent. Control
G	0.029	1.0E-05	2	0.522	1.305

Simulation [G] provides a good estimate of the peak temperature, and a conservative concave representation of the decay down to a temperature of about 300 °C.

NFSC 70-24, Stick Fire, Shape = 3 (Figure B1.38)

Identifier	Diam. (D) (m)	Stick Burn Regress Rate (vp) (m/s)	Shape (F)	Pyrolysis Rate (kg/s)	
				Stick Burning	Vent. Control
H	0.043	1.0E-05	3	0.522	1.305

Simulation [H] provides a good estimate of the peak temperature, and a conservative approximately linear representation of the decay down to a temperature of about 300 °C.

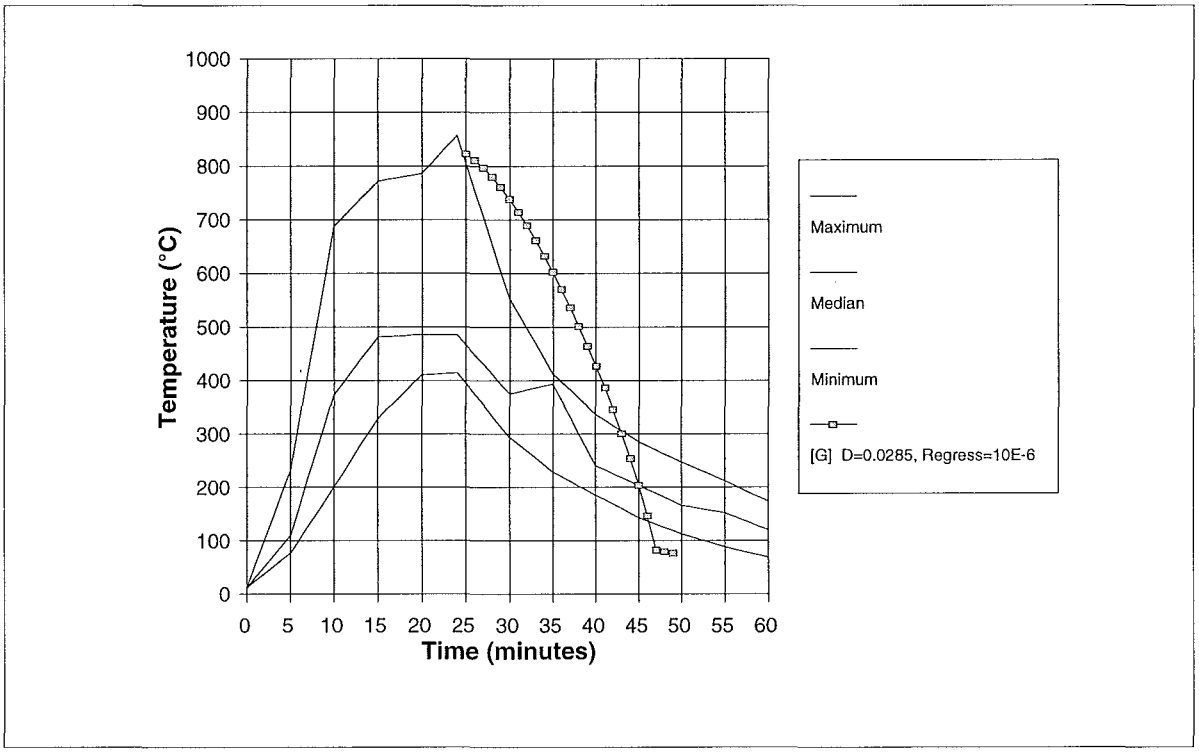

Fig B1.37 NFSC 70-24, Fire Load 30 kg/m² Floor Area, Ventilation Factor 0.157, Stick Fires, Shape = 2

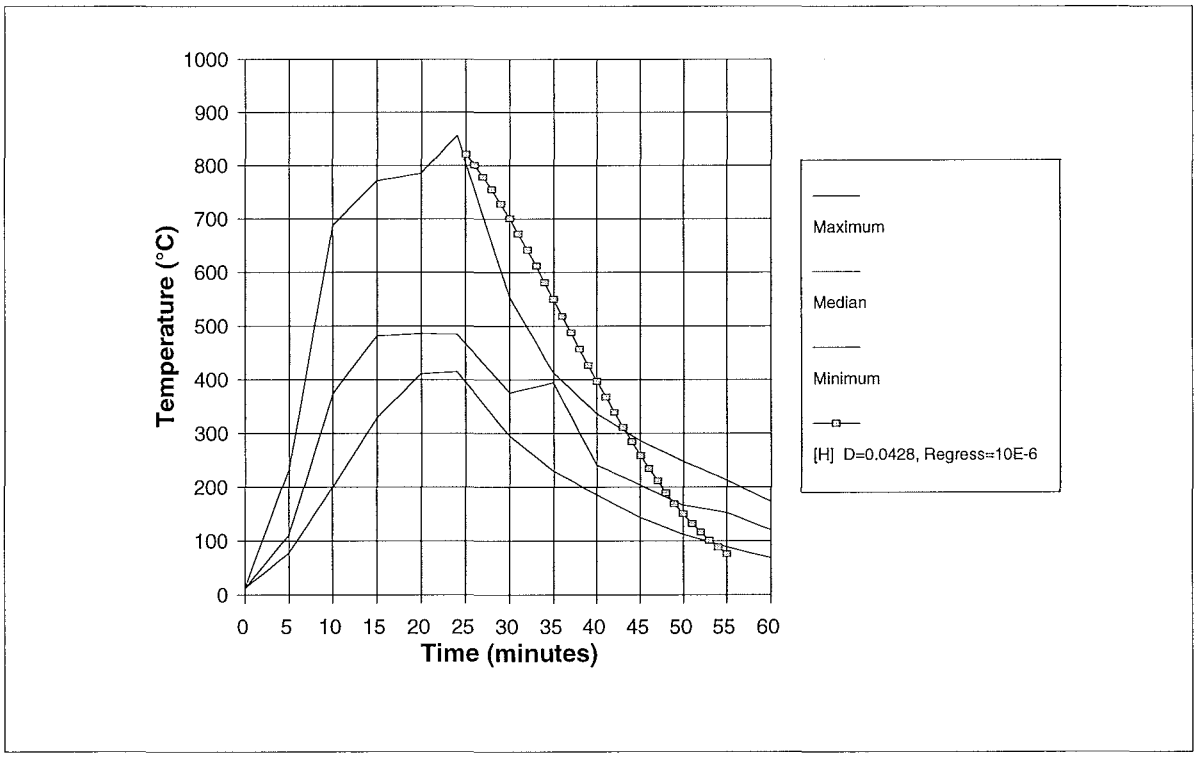

Fig B1.38 NFSC 70-24, Fire Load 30 kg/m² Floor Area, Ventilation Factor 0.157, Stick Fires, Shape = 3

B1.13 NFSC 70-21

The compartment and ventilation opening geometry, materials of construction, fuel load, and relevant parameters calculated from the specified data, are scheduled in Table B1.24.

Specified Parameters	
Compartment Length	3.68 m
Compartment Width	3.38 m
Compartment Height	3.13 m
Ventilation Height	2.18 m
Ventilation Width	1.95 m
Sill Height	0.95 m
Wall Details	3 walls of 0.115 m normal brick + 0.160 m hard brick plus 1 wall of 0.175 m lightweight concrete
Ceiling Details	0.175 m lightweight concrete
Floor Details	refractory concrete
Fuel Load	327.6 kg wood
Calculated Parameters	
Floor Area	12.44 m^2
Total Internal Surface Area	69.07 m^2
Ventilation Area	4.251 m^2
Ventilation Parameter ($A_V \sqrt{H}$)	6.277 $m^{5/2}$
Ventilation Parameter ($A_V \sqrt{H} / A_T$)	0.091 $m^{0.5}$
Fire Load Density	30 kg /m^2 of floor area
Fire Load Density	5.4 kg /m^2 of total bounding surface area

Table B1.24 NFSC 70-21 Input Data ; Fire Load 30 kg/m^2, Ventilation Factor 0.091

This fire has a moderate fire load and moderately high ventilation factor. From the initial data above, fires with the following stick size (D), regression rate (v_p), shape factor (F) and crib spacing to height ratio (S_c / H_c) were modelled, leading to the tabulated initial pyrolysis rates for stick burning, ventilation control, crib porosity control and crib fuel surface control mechanisms. The lowest non-zero rate governs the initial fire

development.

Identifier	Diam. (D) (m)	Stick Burn Regress Rate (vp) (m/s)	Shape (F)	Crib (Sc/Hc)	Pyrolysis Rate (kg/s)				
					Stick Burning	Vent. Control	Crib Porosity Control	Crib Fuel Surface (theory)	Crib Fuel Surface (progr)
A	0.041		2	0.200		0.753	0.790	0.413	0.602
B	0.050		2	0.300		0.753	0.991	0.310	0.452
C	0.064		3	0.300		0.753	0.769	0.207	0.452
D	0.033	1.0E-05	2		0.452	0.753			0.869
E	0.049	1.0E-05	3		0.452	0.753			0.681

Table B1.25 NFSC 70-21, Fire Simulation Parameters and Initial Pyrolysis Rates

NFSC 70-21, Crib Fire, Shape = 2 (Figure B1.39)

Identifier	Diam. (D) (m)	Shape (F)	Crib (Sc/Hc)	Pyrolysis Rate (kg/s)			
				Vent. Control	Crib Porosity Control	Crib Fuel Surface (theory)	Crib Fuel Surface (progr)
A	0.041	2	0.200	0.753	0.790	0.413	0.602
B	0.050	2	0.300	0.753	0.991	0.310	0.452

Simulations [A] and [B] are both crib fuel surface controlled. Simulation [A] overestimates the peak temperature by 180 °C, while simulation [B] estimates the peak temperature well, and provides a conservative estimate of the decay to about 300 °C.

NFSC 70-21, Crib Fire, Shape = 3 (Figure B1.40)

Identifier	Diam. (D) (m)	Shape (F)	Crib (Sc/Hc)	Pyrolysis Rate (kg/s)			
				Vent. Control	Crib Porosity Control	Crib Fuel Surface (theory)	Crib Fuel Surface (progr)
C	0.064	3	0.300	0.753	0.769	0.207	0.452

Simulation [C] provides a good estimate of the peak temperature, and an almost exact, approximately linear estimate of the temperature decay down to 350 °C.

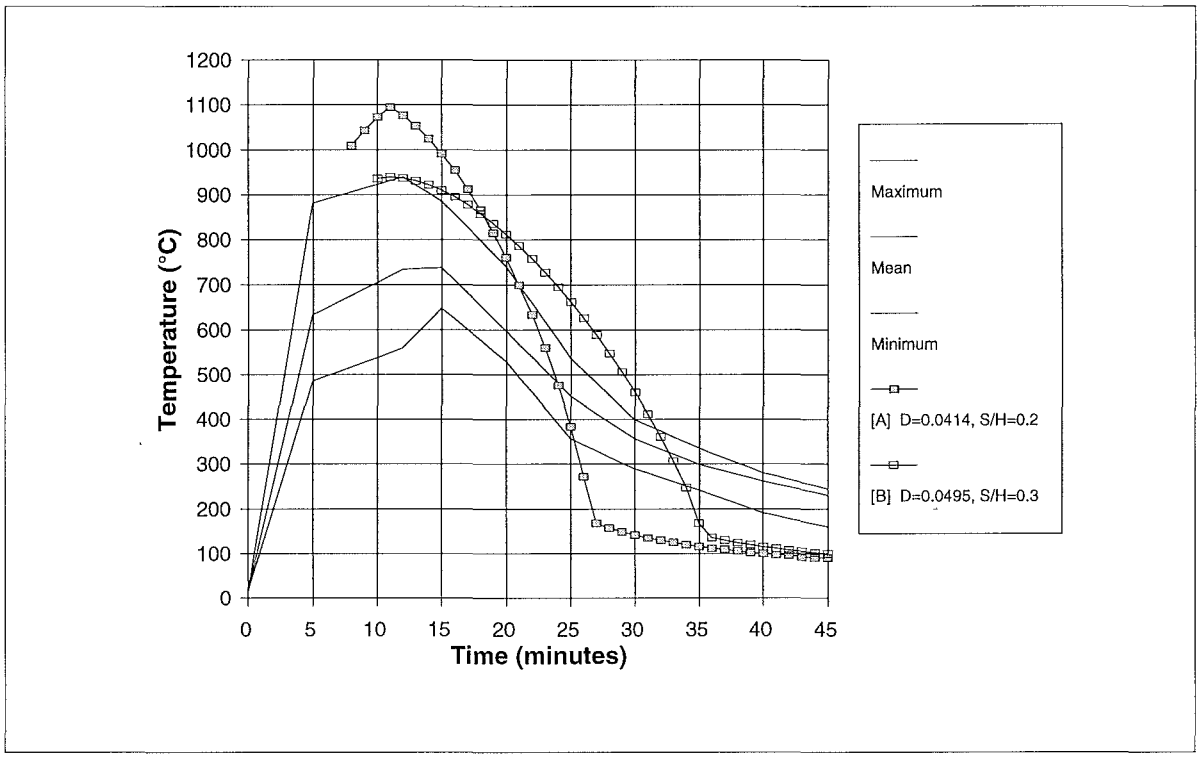

Fig B1.39 NFSC 70-21, Fire Load 30 kg/m² Floor Area, Ventilation Factor 0.091, Crib Fires, Shape = 2

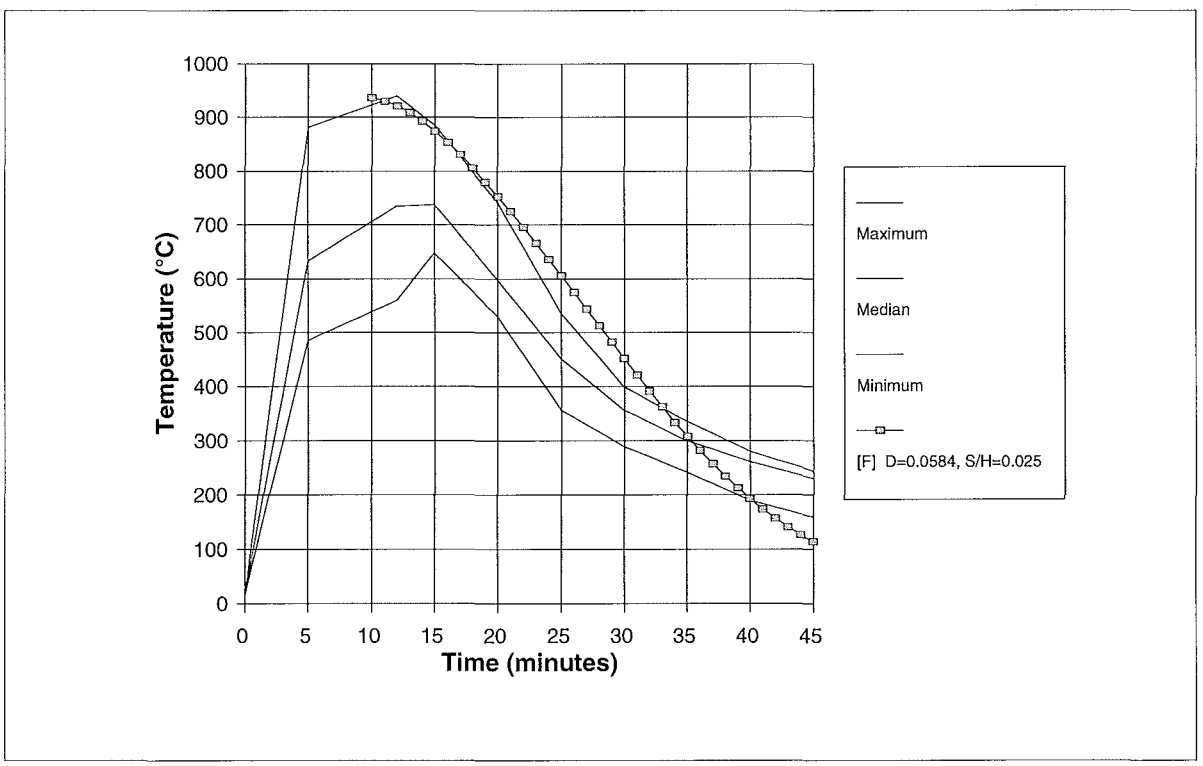

Fig B1.40 NFSC 70-21, Fire Load 30 kg/m² Floor Area, Ventilation Factor 0.091, Crib Fires, Shape = 3

NFSC 70-21, Stick Fire, Shape = 2 (Figure B1.41)

Identifier	Diam. (D) (m)	Stick Burn Regress Rate (vp) (m/s)	Shape (F)	Pyrolysis Rate (kg/s)	
				Stick Burning	Vent. Control
D	0.033	1.0E-05	2	0.452	0.753

Simulation [D] provides a good estimate of the peak temperature, and a conservative concave representation of the decay down to a temperature of about 380 °C.

NFSC 70-21, Stick Fire, Shape = 3 (Figure B1.42)

Identifier	Diam. (D) (m)	Stick Burn Regress Rate (vp) (m/s)	Shape (F)	Pyrolysis Rate (kg/s)	
				Stick Burning	Vent. Control
E	0.049	1.0E-05	3	0.452	0.753

Simulation [E] provides a good estimate of the peak temperature, and an approximately linear representation of the decay down to a temperature of about 350 °C.

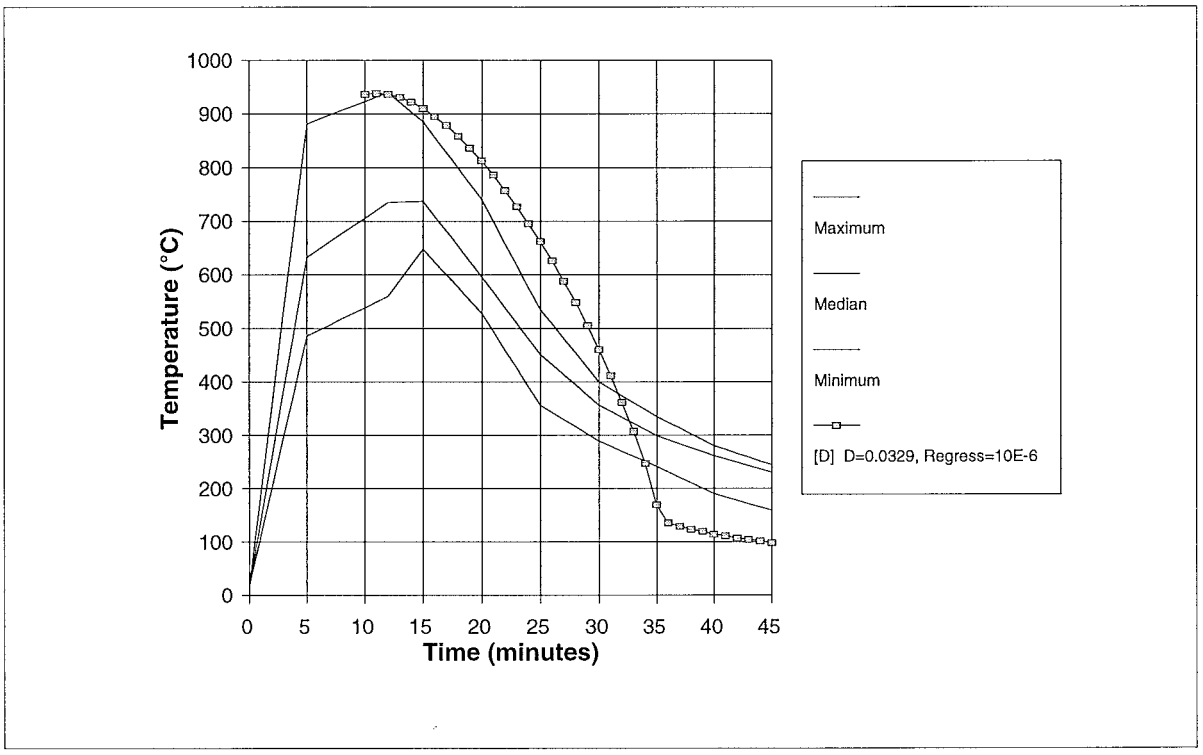

Fig B1.41 NFSC 70-21, Fire Load 30 kg/m² Floor Area, Ventilation Factor 0.091, Stick Fires, Shape = 2

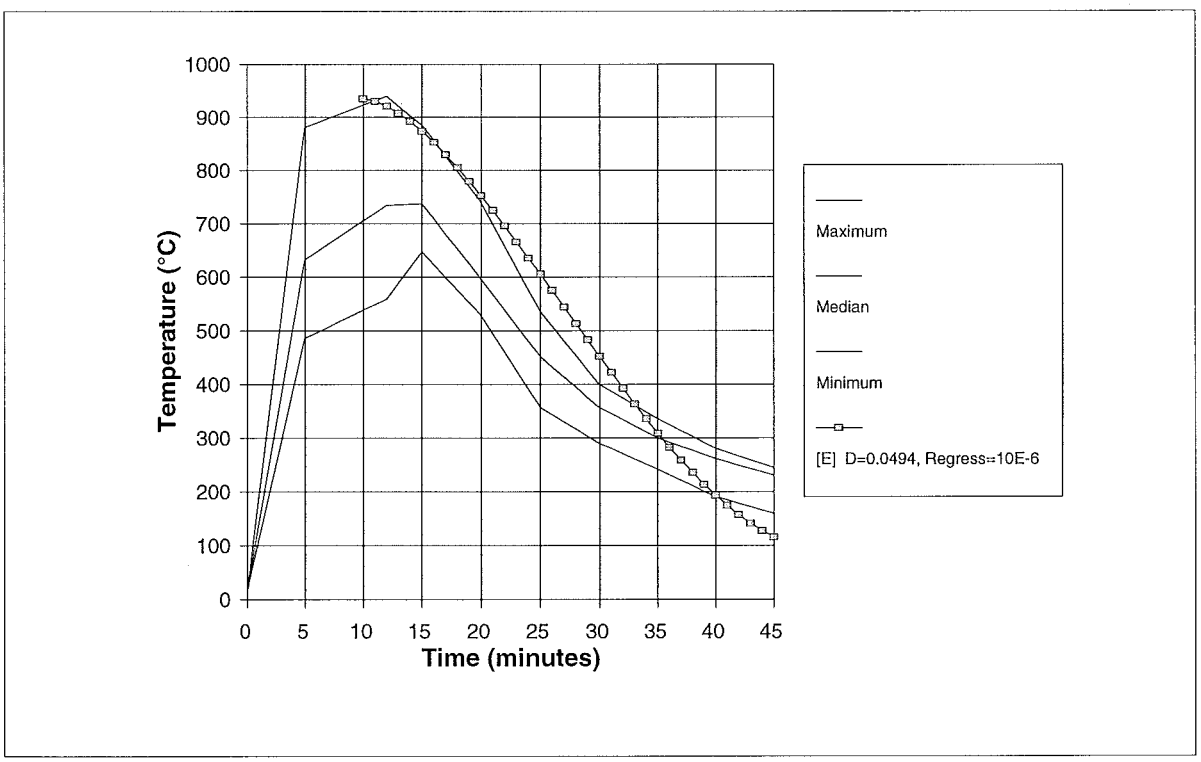

Fig B1.42 NFSC 70-21, Fire Load 30 kg/m² Floor Area, Ventilation Factor 0.091, Stick Fires, Shape = 3

B1.14 NFSC 70-22

The compartment and ventilation opening geometry, materials of construction, fuel load, and relevant parameters calculated from the specified data, are scheduled in Table B1.26.

Specified Parameters	
Compartment Length	3.68 m
Compartment Width	3.38 m
Compartment Height	3.13 m
Ventilation Height	2.18 m
Ventilation Width	1.95 m
Sill Height	0.95 m
Wall Details	3 walls of 0.115 m normal brick + 0.160 m hard brick plus 1 wall of 0.175 m lightweight concrete
Ceiling Details	0.175 m lightweight concrete
Floor Details	refractory concrete
Fuel Load	745.3 kg wood
Calculated Parameters	
Floor Area	12.44 m^2
Total Internal Surface Area	69.07 m^2
Ventilation Area	4.251 m^2
Ventilation Parameter ($A_V \sqrt{H}$)	6.277 $m^{5/2}$
Ventilation Parameter ($A_V \sqrt{H} / A_T$)	0.091 $m^{0.5}$
Fire Load Density	60 kg /m^2 of floor area
Fire Load Density	10.8 kg /m^2 of total bounding surface area

Table B1.26 NFSC 70-22 Input Data ; Fire Load 60 kg/m^2, Ventilation Factor 0.091

This fire has a high fire load and moderately high ventilation factor. From the initial data above, fires with the following stick size (D), regression rate (v_p), shape factor (F) and crib spacing to height ratio (S_c / H_c) were modelled, leading to the tabulated initial pyrolysis rates for stick burning, ventilation control, crib porosity control and crib fuel surface control mechanisms. The lowest non-zero rate governs the initial fire

development.

Identifier	Diam. (D) (m)	Stick Burn Regress Rate (vp) (m/s)	Shape (F)	Crib (Sc/Hc)	Pyrolysis Rate (kg/s)				
					Stick Burning	Vent. Control	Crib Porosity Control	Crib Fuel Surface (theory)	Crib Fuel Surface (progr)
A	0.069		2	0.300		0.753	1.416	0.361	0.527
B	0.067		2	0.300		0.753	1.479	0.387	0.565
C	0.086		3	0.300		0.753	1.148	0.258	0.565
D	0.053	1.0E-05	2		0.565	0.753			0.818
E	0.079	1.0E-05	3		0.565	0.753			0.642

Table B1.27 NFSC 70-22, Fire Simulation Parameters and Initial Pyrolysis Rates

NFSC 70-22, Crib Fire, Shape = 2 (Figure B1.43)

Identifier	Diam. (D) (m)	Shape (F)	Crib (Sc/Hc)	Pyrolysis Rate (kg/s)			
				Vent. Control	Crib Porosity Control	Crib Fuel Surface (theory)	Crib Fuel Surface (progr)
A	0.069	2	0.300	0.753	1.416	0.361	0.527
B	0.067	2	0.300	0.753	1.479	0.387	0.565

Simulations [A] and [B] are both crib fuel surface controlled. Simulation [A] slightly underestimates the peak temperature, while simulation [B] provides a very good estimate of the peak and the decay to the end of the experimental data series at about 550 °C.

NFSC 70-22, Crib Fire, Shape = 3 (Figure B1.44)

Identifier	Diam. (D) (m)	Shape (F)	Crib (Sc/Hc)	Pyrolysis Rate (kg/s)			
				Vent. Control	Crib Porosity Control	Crib Fuel Surface (theory)	Crib Fuel Surface (progr)
C	0.086	3	0.300	0.753	1.148	0.258	0.565

Simulation [C] provides a good estimate of the peak temperature, and an almost exact, approximately linear estimate of the temperature decay to the end of the experimental data series at about 550 °C.

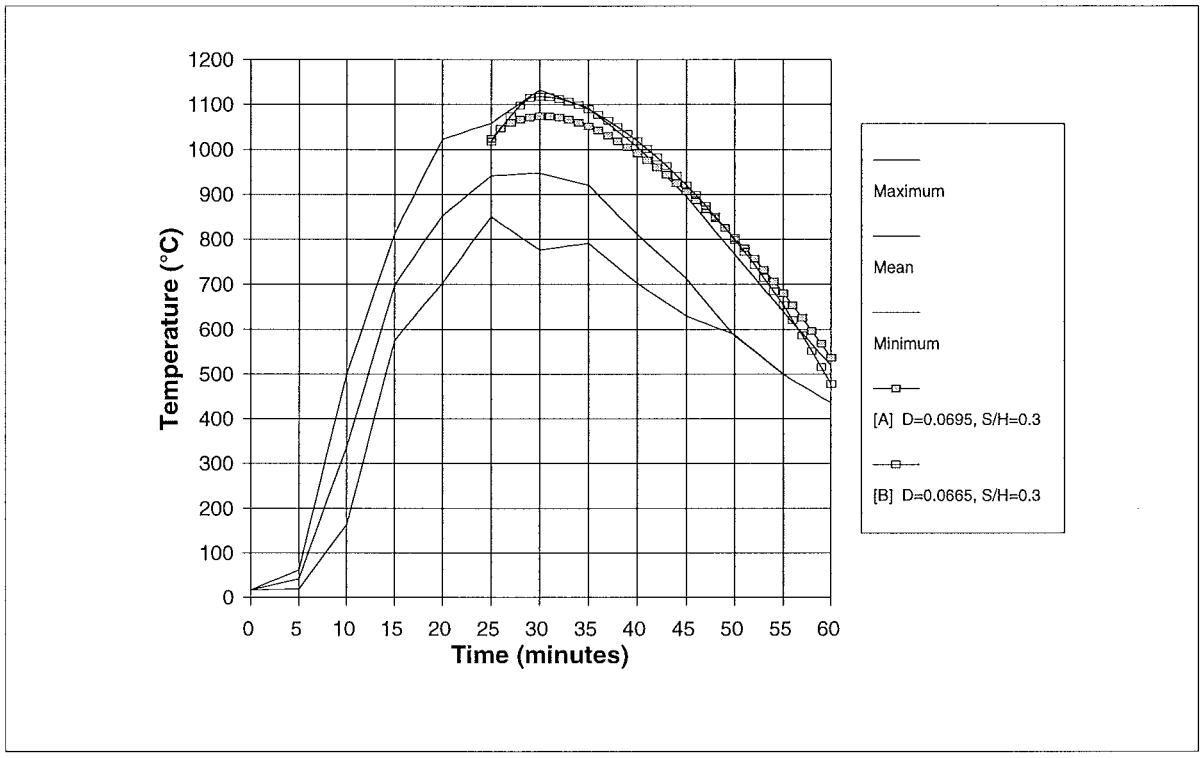

Fig B1.43 NFSC 70-22, Fire Load 60 kg/m² Floor Area, Ventilation Factor 0.091, Crib Fires, Shape = 2

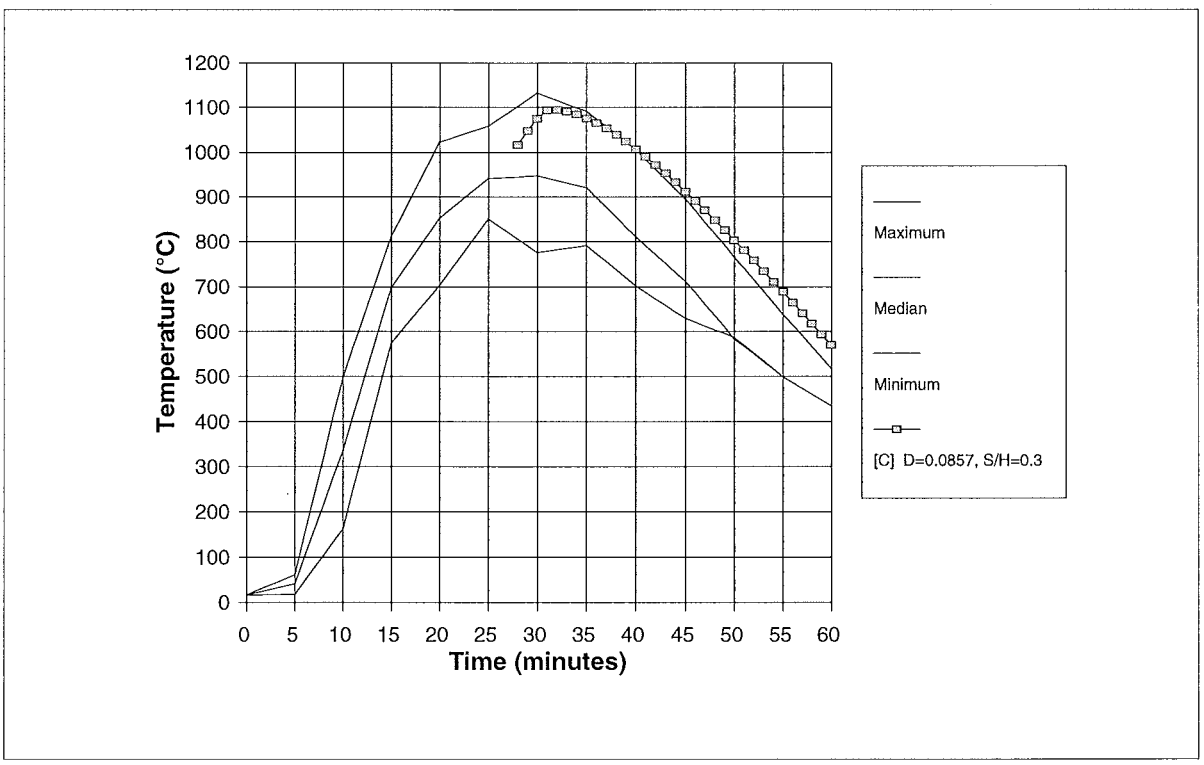

Fig B1.44 NFSC 70-22, Fire Load 60 kg/m² Floor Area, Ventilation Factor 0.091, Crib Fires, Shape = 3

NFSC 70-22, Stick Fire, Shape = 2 (Figure B1.45)

Identifier	Diam. (D) (m)	Stick Burn Regress Rate (vp) (m/s)	Shape (F)	Pyrolysis Rate (kg/s)	
				Stick Burning	Vent. Control
D	0.053	1.0E-05	2	0.565	0.753

Simulation [D] provides a good estimate of the peak temperature, and a good representation of the decay to the end of the experimental data series at about 550 °C.

NFSC 70-22, Stick Fire, Shape = 3 (Figure B1.46)

Identifier	Diam. (D) (m)	Stick Burn Regress Rate (vp) (m/s)	Shape (F)	Pyrolysis Rate (kg/s)	
				Stick Burning	Vent. Control
E	0.079	1.0E-05	3	0.565	0.753

Simulation [E] provides a good estimate of the peak temperature, and a good representation of the decay to the end of the experimental data series at about 550 °C.

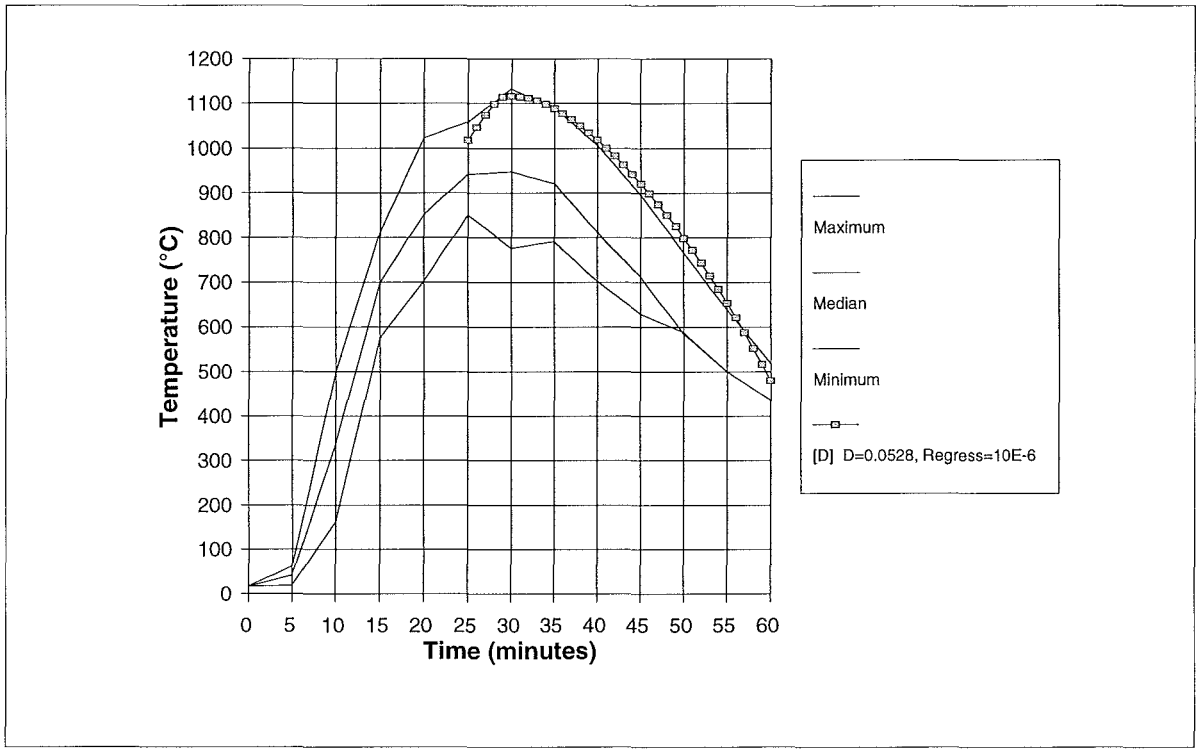

Fig B1.45 NFSC 70-22, Fire Load 60 kg/m² Floor Area, Ventilation Factor 0.091, Stick Fires, Shape = 2

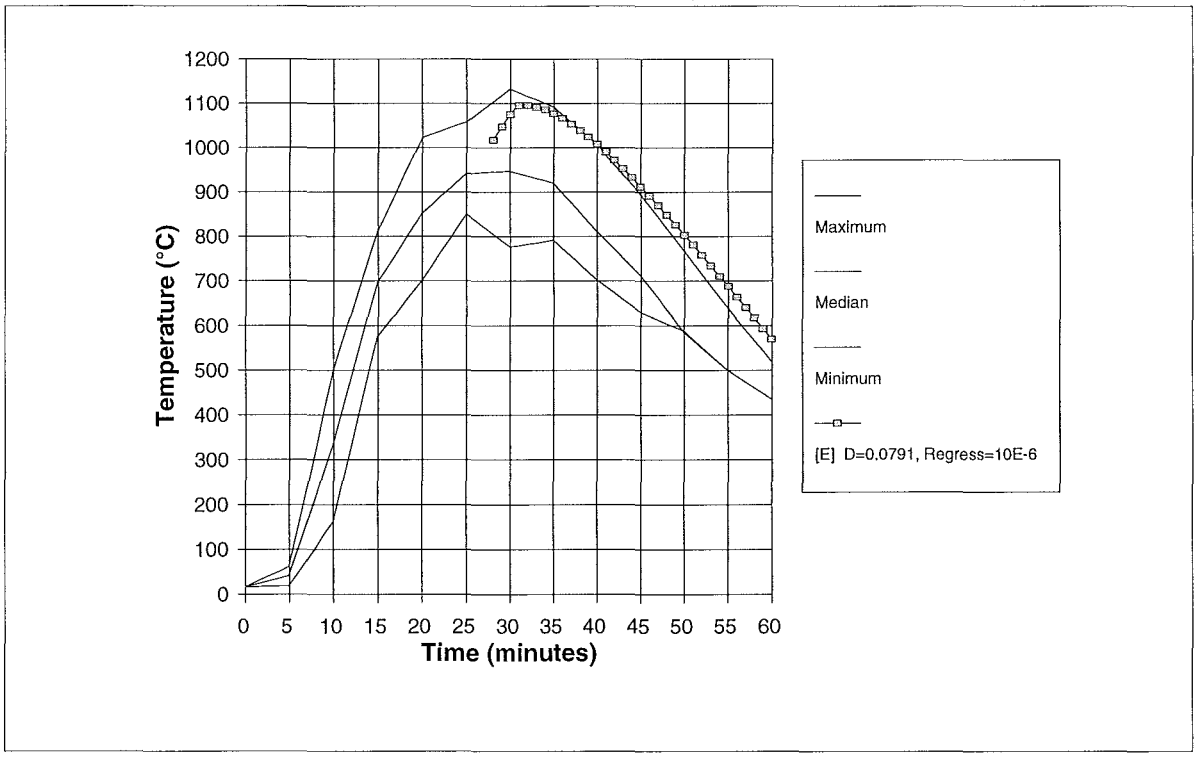

Fig B1.46 NFSC 70-22, Fire Load 60 kg/m² Floor Area, Ventilation Factor 0.091, Stick Fires, Shape = 3

B1.15 NFSC 70-17

The compartment and ventilation opening geometry, materials of construction, fuel load, and relevant parameters calculated from the specified data, are scheduled in Table B1.28.

Specified Parameters	
Compartment Length	3.68 m
Compartment Width	3.38 m
Compartment Height	3.13 m
Ventilation Height	2.18 m
Ventilation Width	1.18 m
Sill Height	0.95 m
Wall Details	3 walls of 0.115 m normal brick + 0.160 m hard brick plus 1 wall of 0.175 m lightweight concrete
Ceiling Details	0.175 m lightweight concrete
Floor Details	refractory concrete
Fuel Load	186 kg wood
Calculated Parameters	
Floor Area	12.44 m^2
Total Internal Surface Area	69.07 m^2
Ventilation Area	2.572 m^2
Ventilation Parameter ($A_V \sqrt{H}$)	3.798 $m^{5/2}$
Ventilation Parameter ($A_V \sqrt{H} / A_T$)	0.055 $m^{0.5}$
Fire Load Density	15 kg /m^2 of floor area
Fire Load Density	2.7 kg /m^2 of total bounding surface area

Table B1.28 NFSC 70-17 Input Data ; Fire Load 15 kg/m^2, Ventilation Factor 0.055

This fire has a low fire load and medium ventilation factor. From the initial data above, fires with the following stick size (D), regression rate (v_p), shape factor (F) and crib spacing to height ratio (S_c / H_c) were modelled, leading to the tabulated initial pyrolysis rates for stick burning, ventilation control, crib porosity control and crib fuel surface control mechanisms. The lowest non-zero rate governs the initial fire development.

Identifier	Diam. (D) (m)	Stick Burn Regress Rate (vp) (m/s)	Shape (F)	Crib (Sc/Hc)	Pyrolysis Rate (kg/s)				
					Stick Burning	Vent. Control	Crib Porosity Control	Crib Fuel Surface (theory)	Crib Fuel Surface (progr)
A	0.037		2	0.300		0.456	0.669	0.250	0.365
B	0.057		2	0.300		0.456	0.433	0.125	0.182
C	0.071		3	0.500		0.456	0.579	0.088	0.192
D	0.039	1.0E-05	2		0.192	0.456			0.334
E	0.058	1.0E-05	3		0.192	0.456			0.263

Table B1.29 NFSC 70-17, Fire Simulation Parameters and Initial Pyrolysis Rates

NFSC 70-17, Crib Fire, Shape = 2 (Figure B1.47)

Identifier	Diam. (D) (m)	Shape (F)	Crib (Sc/Hc)	Pyrolysis Rate (kg/s)			
				Vent. Control	Crib Porosity Control	Crib Fuel Surface (theory)	Crib Fuel Surface (progr)
A	0.037	2	0.300	0.456	0.669	0.250	0.365
B	0.057	2	0.300	0.456	0.433	0.125	0.182

Simulation [A] is crib fuel surface controlled but highly overestimates the peak temperature, and has far too fast a decay. Simulation [B] provides a very good estimate of the maximum temperature and has a conservative convex decay to the end of the experimental data series at about 250 °C.

NFSC 70-17, Crib Fire, Shape = 3 (Figure B1.48)

Identifier	Diam. (D) (m)	Shape (F)	Crib (Sc/Hc)	Pyrolysis Rate (kg/s)			
				Vent. Control	Crib Porosity Control	Crib Fuel Surface (theory)	Crib Fuel Surface (progr)
C	0.071	3	0.500	0.456	0.579	0.088	0.192

Simulation [C] provides a good estimate of the peak temperature, and a modestly conservative estimate of the decay to the end of the experimental data series at about 250 °C.

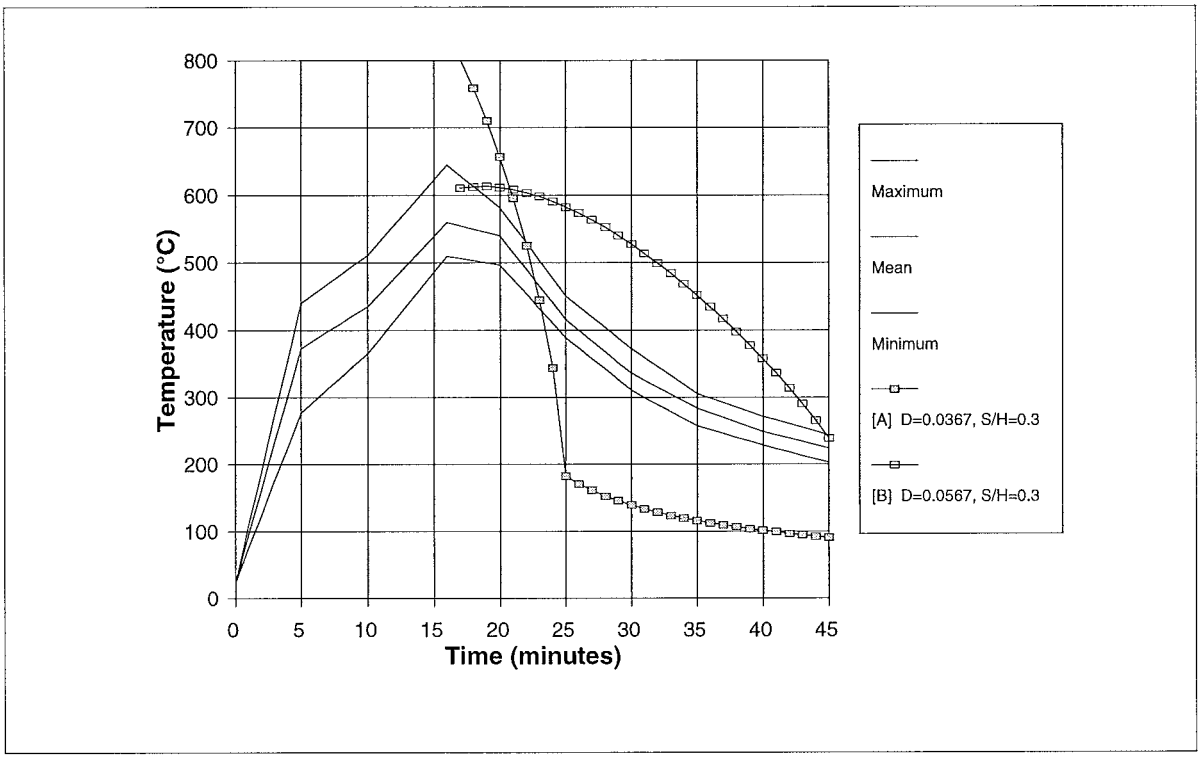

Fig B1.47 NFSC 70-17, Fire Load 15 kg/m² Floor Area, Ventilation Factor 0.055, Crib Fires, Shape = 2

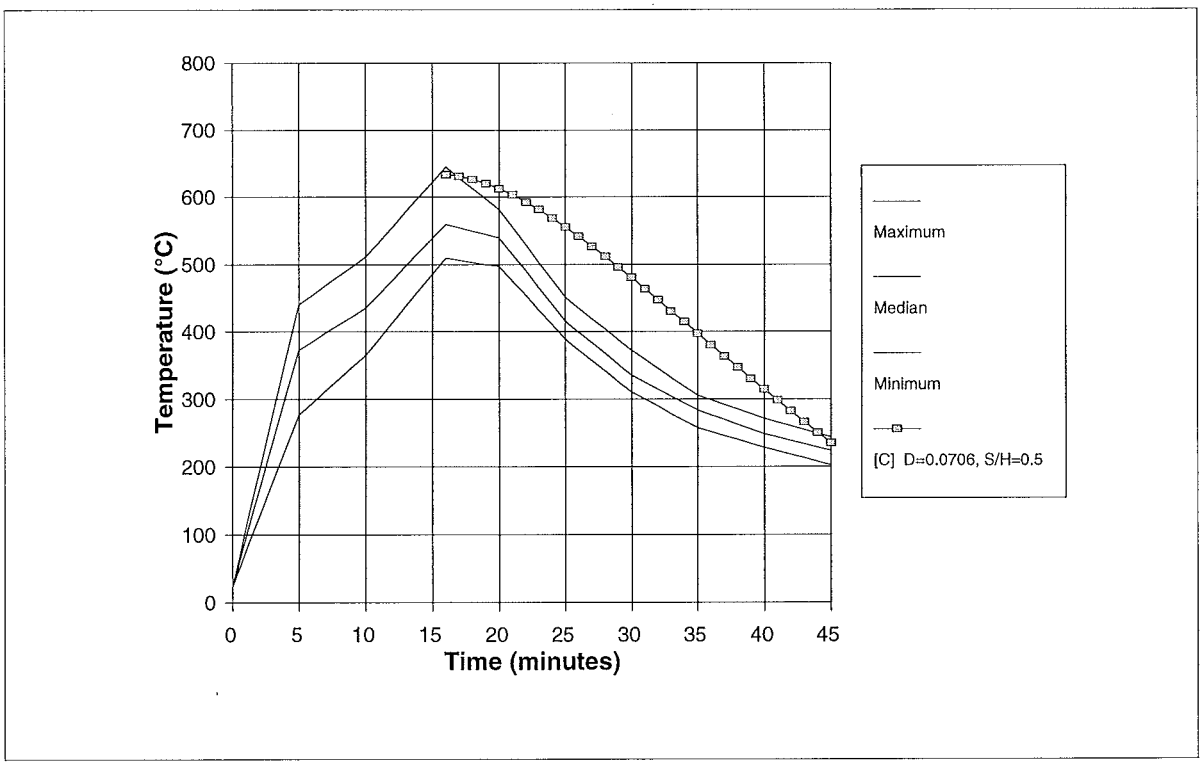

Fig B1.48 NFSC 70-17, Fire Load 15 kg/m² Floor Area, Ventilation Factor 0.055, Crib Fires, Shape = 3

NFSC 70-17, Stick Fire, Shape = 2 (Figure B1.49)

Identifier	Diam. (D) (m)	Stick Burn Regress Rate (vp) (m/s)	Shape (F)	Pyrolysis Rate (kg/s)	
				Stick Burning	Vent. Control
D	0.039	1.0E-05	2	0.192	0.456

Simulation [D] provides a good estimate of the peak temperature, and a very conservative estimate of the temperature decay to the end of the experimental data series at about 250 °C.

NFSC 70-17, Stick Fire, Shape = 3 (Figure B1.50)

Identifier	Diam. (D) (m)	Stick Burn Regress Rate (vp) (m/s)	Shape (F)	Pyrolysis Rate (kg/s)	
				Stick Burning	Vent. Control
E	0.058	1.0E-05	3	0.192	0.456

Simulation [E] provides a good estimate of the peak temperature, and a modestly conservative representation of the decay to the end of the experimental data series at about 250 °C.

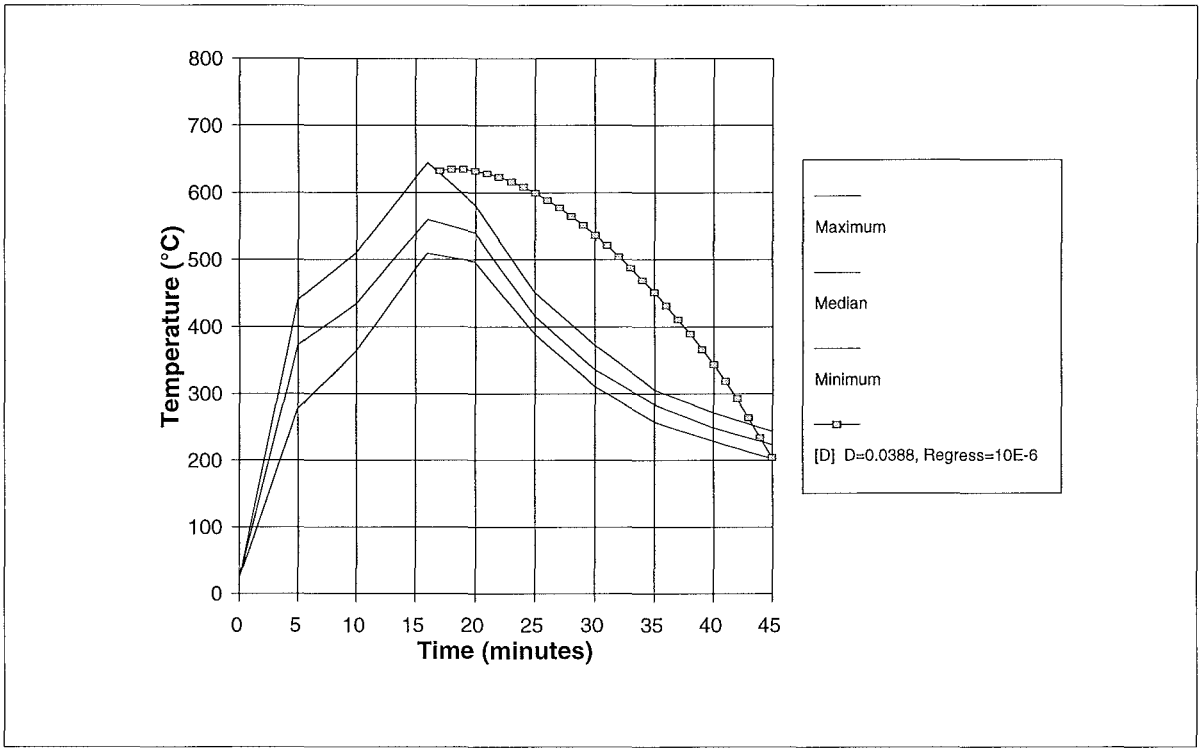

Fig B1.49 NFSC 70-17, Fire Load 15 kg/m² Floor Area, Ventilation Factor 0.055, Stick Fires, Shape = 2

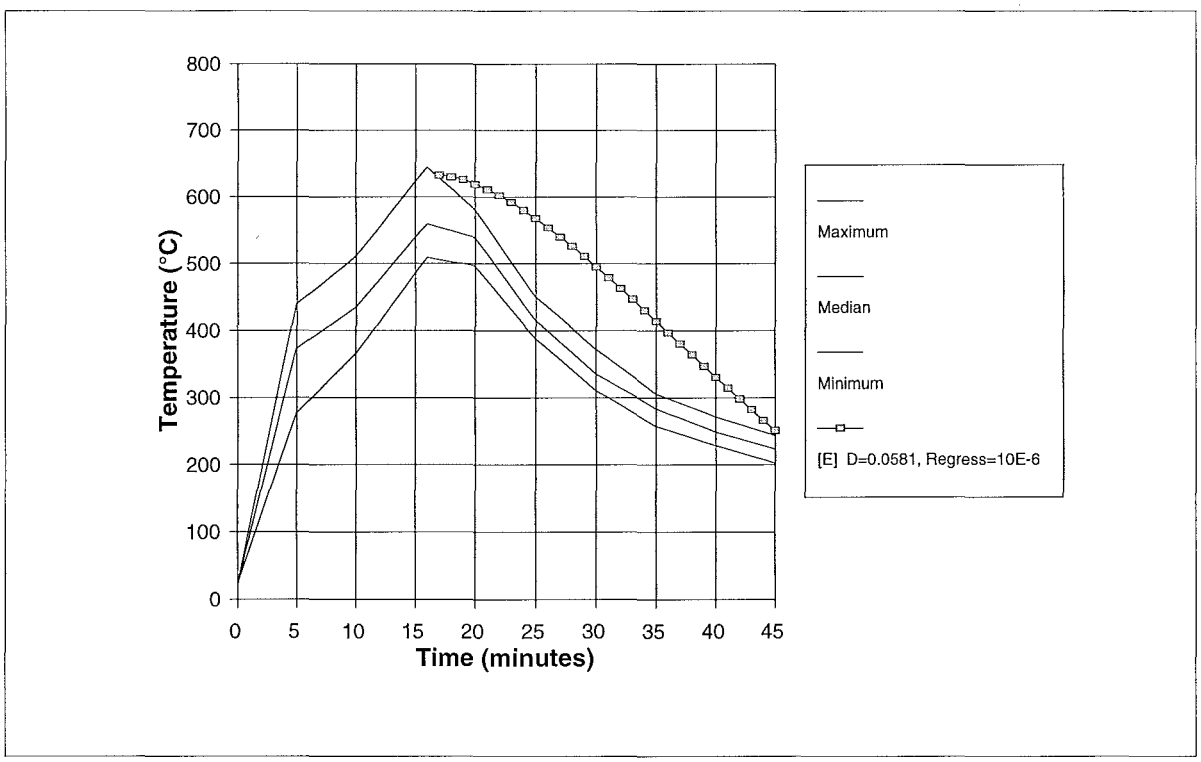

Fig B1.50 NFSC 70-17, Fire Load 15 kg/m² Floor Area, Ventilation Factor 0.055, Stick Fires, Shape = 3

B1.16 NFSC 70-23

The compartment and ventilation opening geometry, materials of construction, fuel load, and relevant parameters calculated from the specified data, are scheduled in Table B1.30.

Specified Parameters	
Compartment Length	3.68 m
Compartment Width	3.38 m
Compartment Height	3.13 m
Ventilation Height	2.92 m
Ventilation Width	2.18 m
Sill Height	0.95 m
Wall Details	3 walls of 0.115 m normal brick + 0.160 m hard brick plus 1 wall of 0.175 m lightweight concrete
Ceiling Details	0.175 m lightweight concrete
Floor Details	refractory concrete
Fuel Load	186 kg wood
Calculated Parameters	
Floor Area	12.44 m^2
Total Internal Surface Area	69.07 m^2
Ventilation Area	6.366 m^2
Ventilation Parameter ($A_V \sqrt{H}$)	10.878 $m^{5/2}$
Ventilation Parameter ($A_V \sqrt{H} / A_T$)	0.157 $m^{0.5}$
Fire Load Density	15 kg /m^2 of floor area
Fire Load Density	2.7 kg /m^2 of total bounding surface area

Table B1.30 NFSC 70-23 Input Data ; Fire Load 15 kg/m^2, Ventilation Factor 0.157

This fire has a low fire load and high ventilation factor. From the initial data above, fires with the following stick size (D), regression rate (v_p), shape factor (F) and crib spacing to height ratio (S_c / H_c) were modelled, leading to the tabulated initial pyrolysis rates for stick burning, ventilation control, crib porosity control and crib fuel surface control mechanisms. The lowest non-zero rate governs the initial fire development.

Identifier	Diam. (D) (m)	Stick Burn Regress Rate (vp) (m/s)	Shape (F)	Crib (Sc/Hc)	Pyrolysis Rate (kg/s)				
					Stick Burning	Vent. Control	Crib Porosity Control	Crib Fuel Surface (theory)	Crib Fuel Surface (progr)
A	0.054		2	0.500		1.305	0.755	0.134	0.196
B	0.067		3	0.500		1.305	0.611	0.096	0.209
C	0.036	1.0E-05	2		0.209	1.305			0.383
D	0.053	1.0E-05	3		0.209	1.305			0.301

Table B1.31 NFSC 70-23, Fire Simulation Parameters and Initial Pyrolysis Rates

NFSC 70-23, Crib Fire, Shape = 2 (Figure B1.51)

Identifier	Diam. (D) (m)	Shape (F)	Crib (Sc/Hc)	Pyrolysis Rate (kg/s)			
				Vent. Control	Crib Porosity Control	Crib Fuel Surface (theory)	Crib Fuel Surface (progr)
A	0.054	2	0.500	1.305	0.755	0.134	0.196

Simulation [A] is crib fuel surface and a good estimate of the maximum temperature and has a conservative convex decay to near the end of the experimental data series at about 150 °C.

NFSC 70-23, Crib Fire, Shape = 3 (Figure B1.52)

Identifier	Diam. (D) (m)	Shape (F)	Crib (Sc/Hc)	Pyrolysis Rate (kg/s)			
				Vent. Control	Crib Porosity Control	Crib Fuel Surface (theory)	Crib Fuel Surface (progr)
B	0.067	3	0.500	1.305	0.611	0.096	0.209

Simulation [B] provides a good estimate of the peak temperature, and a very close estimate of the temperature decay to the near end of the experimental data series at about 180 °C.

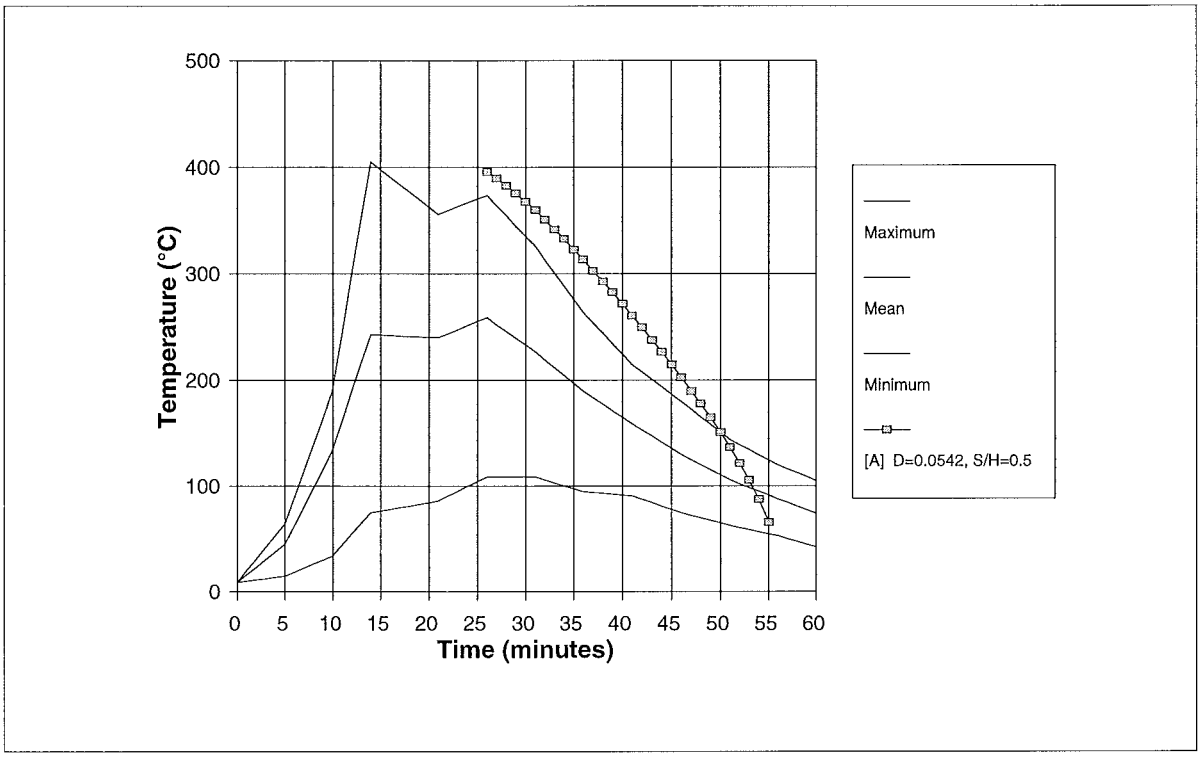

Fig B1.51 NFSC 70-23, Fire Load 15 kg/m² Floor Area, Ventilation Factor 0.157, Crib Fires, Shape = 2

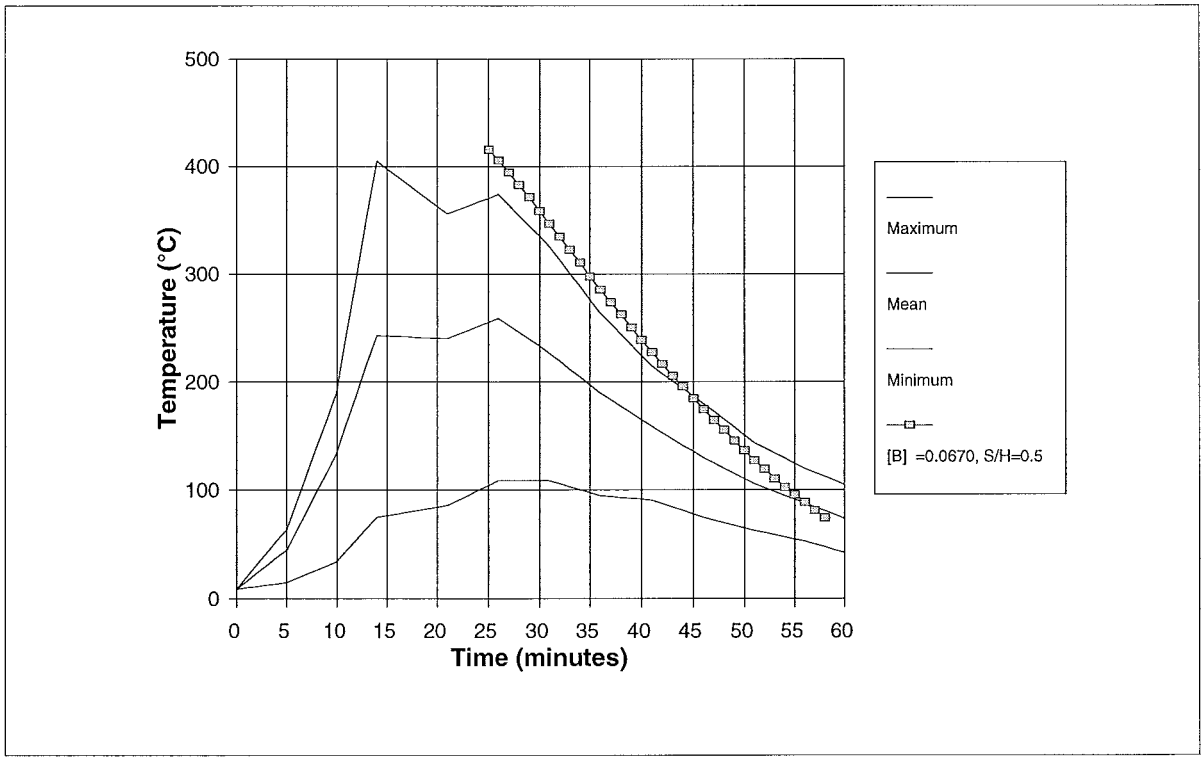

Fig B1.52 NFSC 70-23, Fire Load 15 kg/m² Floor Area, Ventilation Factor 0.157, Crib Fires, Shape = 3

NFSC 70-23, Stick Fire, Shape = 2 (Figure B1.53)

Identifier	Diam. (D) (m)	Stick Burn Regress Rate (vp) (m/s)	Shape (F)	Pyrolysis Rate (kg/s)	
				Stick Burning	Vent. Control
C	0.036	1.0E-05	2	0.209	1.305

Simulation [C] provides a good estimate of the peak temperature, and a conservative estimate of the temperature decay to about 200 °C.

NFSC 70-23, Stick Fire, Shape = 3 (Figure B1.54)

Identifier	Diam. (D) (m)	Stick Burn Regress Rate (vp) (m/s)	Shape (F)	Pyrolysis Rate (kg/s)	
				Stick Burning	Vent. Control
D	0.053	1.0E-05	3	0.209	1.305

Simulation [D] provides a good estimate of the peak temperature, and follows the experimental temperature decay curve closely to about 180 °C.

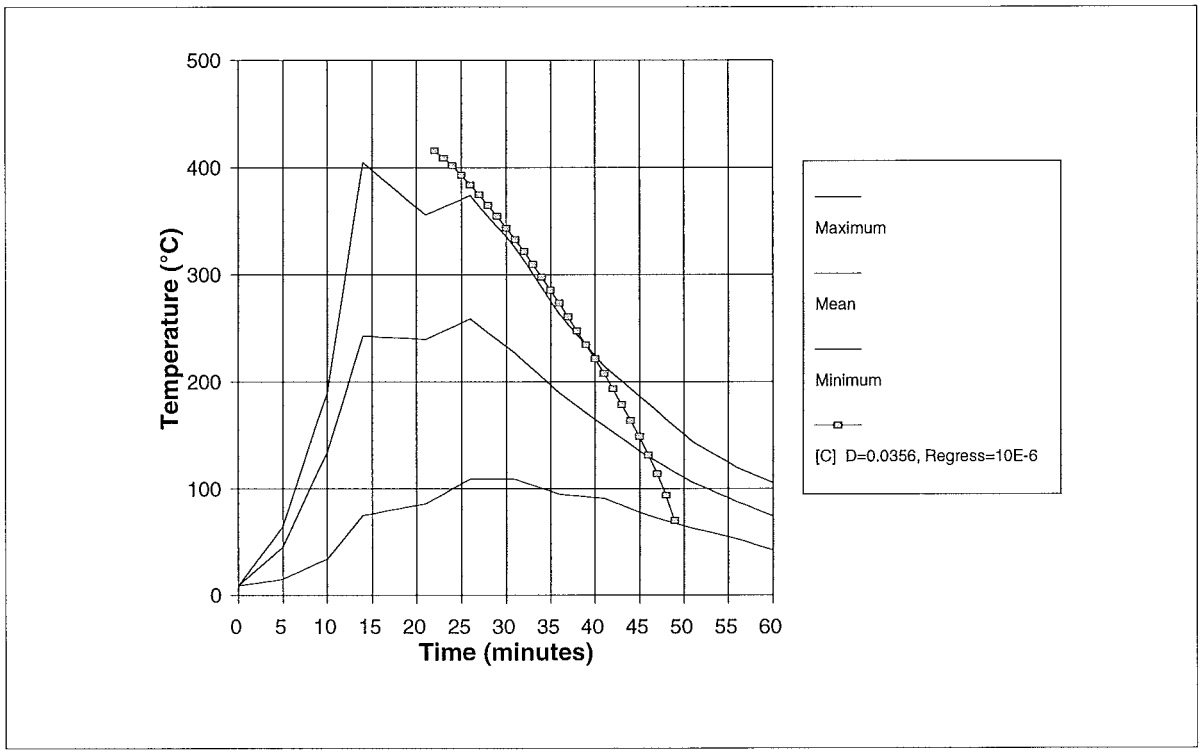

Fig B1.53 NFSC 70-23, Fire Load 15 kg/m² Floor Area, Ventilation Factor 0.157, Stick Fires, Shape = 2

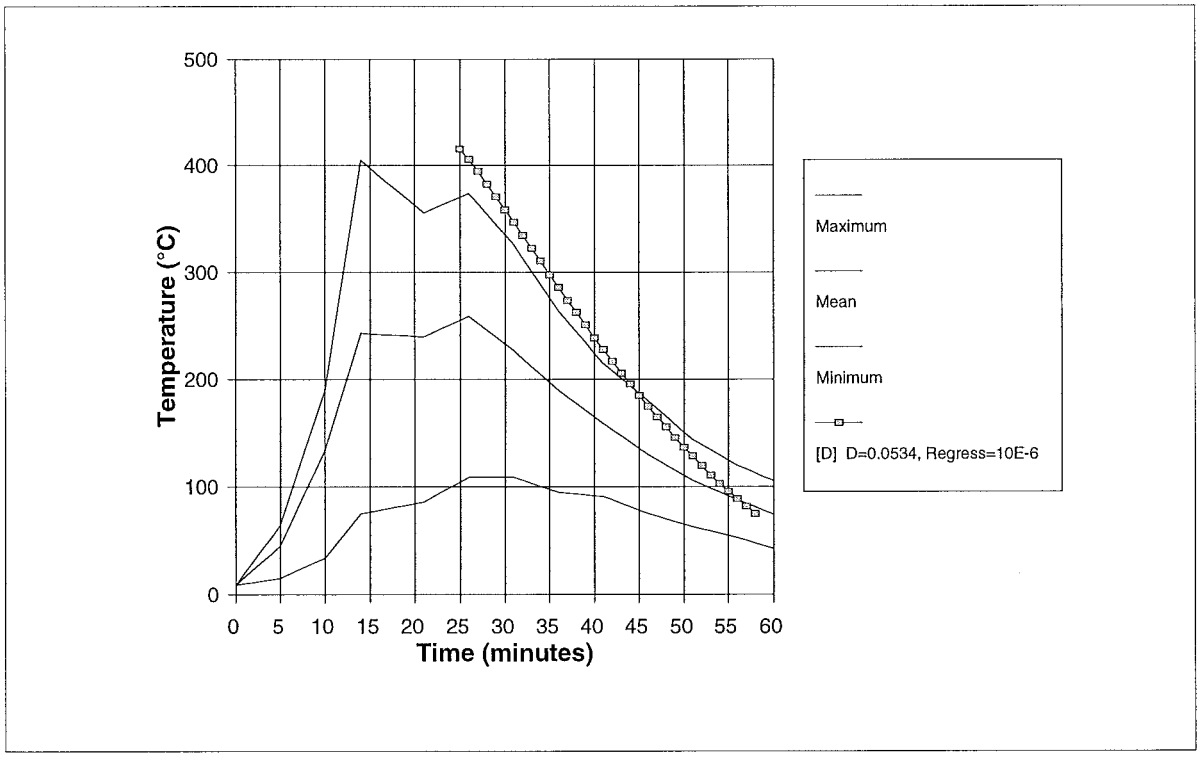

Fig B1.54 NFSC 70-23, Fire Load 15 kg/m² Floor Area, Ventilation Factor 0.157, Stick Fires, Shape = 3

Appendix B2 Fire Research Station, Cardington

B2.1 Test Fire No. 1 by Kirby, Wainman et al (1994)

Refer to Section 5.3 for a discussion of the BRE experimental programme, and the nature of the test fires. Test Fire 1 from the 1994 BRE series, has a fire load (wood cribs) of 40 kg m^{-2} of floor area, and a ventilation factor of 0.062 $m^{0.5}$. The latter ventilation factor was achieved by opening the complete end wall of the large compartment, over the full width and height.

The compartment and ventilation opening geometry, materials of construction, fuel load, and relevant parameters calculated from the specified data, are scheduled in Table B2.1.

Specified Parameters	
Compartment Length	22.855 m
Compartment Width	5.595 m
Compartment Height	2.75 m
Ventilation Height	2.75 m
Ventilation Width	5.595 m
Sill Height	0 m
Wall Details	3 walls of lightweight concrete blocks (215 mm) lined with 50 mm ceramic fibre
Ceiling Details	Aerated concrete slabs (200 mm) lined with 50 mm ceramic fibre
Floor Details	Dense concrete (75 mm) covered with fluid sand (175 mm)
Fuel Load	5115 kg wood
Calculated Parameters	
Floor Area	127.9 m^2
Total Internal Surface Area	412.2 m^2
Ventilation Area	15.39 m^2
Ventilation Parameter ($A_V \sqrt{H}$)	25.52 $m^{5/2}$
Ventilation Parameter ($A_V \sqrt{H} / A_T$)	0.062 $m^{0.5}$

Fire Load Density	40 kg /m² of floor area
Fire Load Density	12.4 kg /m² of total bounding surface area

Table B2.1 Kirby et al Test 1; Fire Load 40 kg/m², Ventilation Factor 0.062

This fire has a moderate fire load and moderate ventilation factor. Based on the analysis and simulation of the various NFSC fires in Appendix B1 above, only simulations of stick burning fires with shape factor (F) equal to 3, were carried out, since these invariably provided the most reliable simulations.

Kirby et al Test 1, Stick Fire, Shape = 3 (Figure B2.2)

Identifier	Diam. (D) (m)	Stick Burn Regress Rate (v_p) (m/s)	Shape (F)	Coeff C_d	Pyrolysis Rate (kg/s)	
					Stick Burning	Vent. Control
A	0.10	1.0E-05	3	0.68	3.069	3.062
B	0.10	8.0E-06	3	0.68	2.456	3.062
C	0.10	8.0E-06	3	0.34	2.456	3.062
D	0.10	6.0E-06	3	0.34	1.842	3.062
E	0.10	5.0E-06	3	0.34	1.535	3.062
F	0.10	5.0E-06	3	0.68	1.535	3.062

Table B2.2 Kirby et al Test 1, Fire Simulation Parameters and Initial Pyrolysis Rates

Due to the nature of this fire and the compartment geometry, the test data is quite unusual, with distinct variances between the temperature profiles at different locations in the compartment. Figure B2.1 shows 3 temperature profiles at crib lines 10, 6 and 2 (there were 11 lines of cribs in total). These were manually extracted from Figure 25 of Kirby et al (1994). Also shown is a representation of the same test fire from the NFSC data series, which is effectively a boundary curve or envelope to all fires, being exceptionally conservative for any one location within the compartment.

The COMPF2 simulations were carried out to reproduce the Crib Line 10 temperature profile. Initial simulations (Figure B2.2) all gave fires that were too hot and too short, even with a heavily reduced regression rate parameter.

As noted in Babrauskas (1979), when the ventilation aperture occupies a large fraction of the wall area, an effective discharge coefficient (C_d) of as little as half the ususal value of 0.68, best fits the data.

A series of simulations with $C_d = 0.34$ were then carried out, with very good results for Simulation [E], which accurately reproduces the temperature profile at crib line 10 in terms of maximum compartment temperature, and the decay profile.

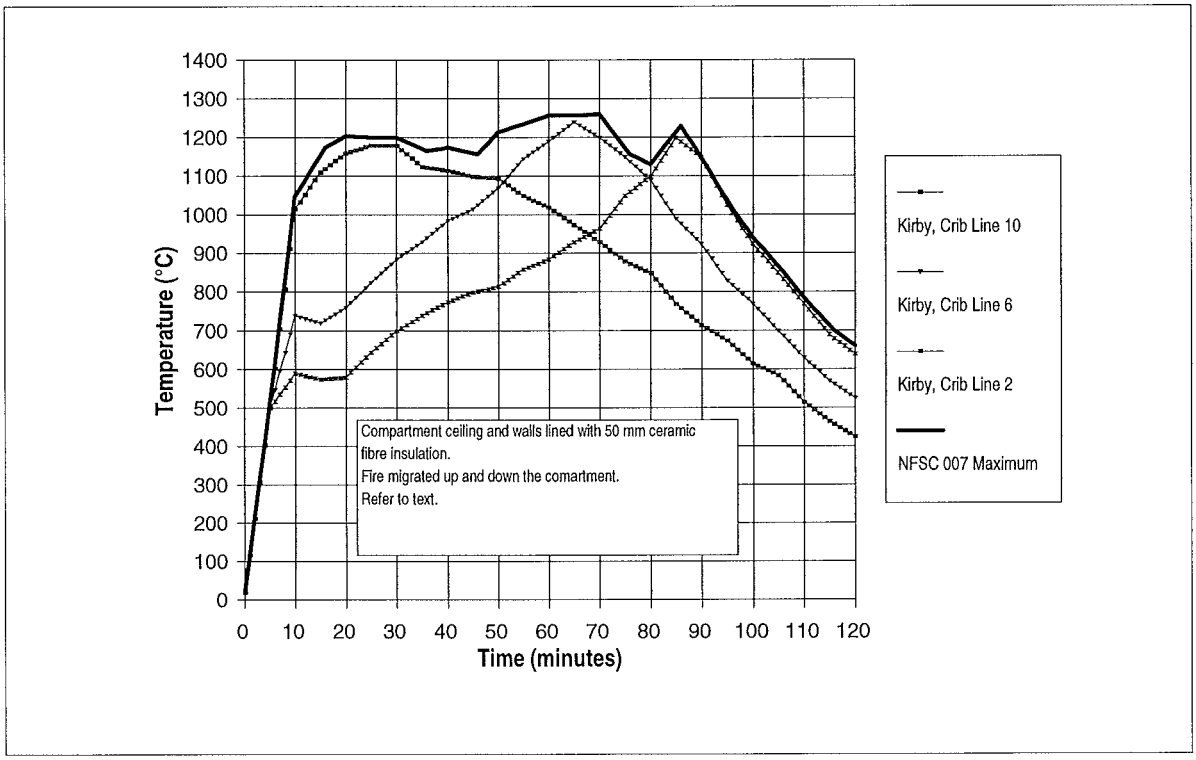

Fig. B2.1, Kirby Test 1, 40 kg/m² Floor Area, Ventilation Factor = 0.062, Temperature Data

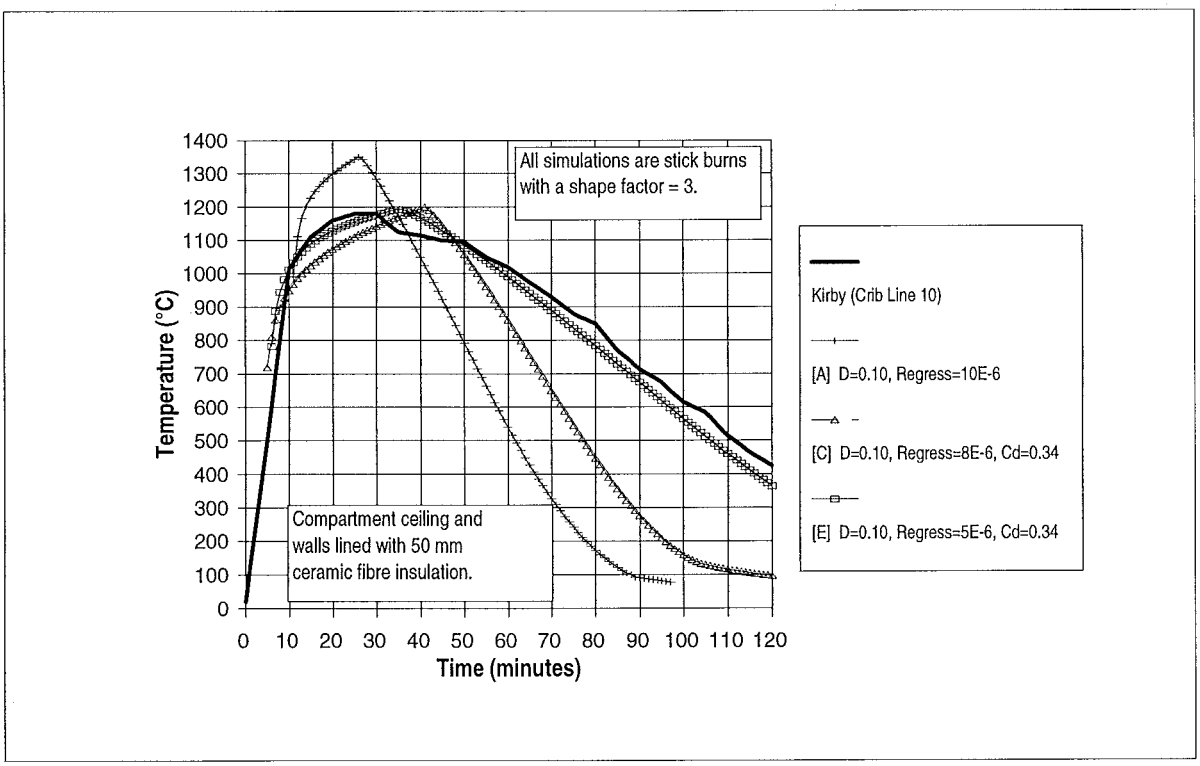

Fig. B2.2, Kirby Test 1, 40 kg/m² Floor Area, Ventilation Factor = 0.062, Stick Fires, Shape = 3

B2.2 Test Fire No. 4, Kirby, Wainman et al (1994)

Test Fire 4 from the 1994 BRE series, has a fire load (wood cribs) of 40 kg m^{-2} of floor area, and a ventilation factor of 0.022 $m^{0.5}$.

The compartment and ventilation opening geometry, materials of construction, fuel load, and relevant parameters calculated from the specified data, are scheduled in Table B2.3.

Specified Parameters	
Compartment Length	22.855 m
Compartment Width	5.595 m
Compartment Height	2.75 m
Ventilation Height	1.47 m
Ventilation Width	5.20 m
Sill Height	1.28 m
Wall Details	Walls of lightweight concrete blocks (215 mm) lined with 50 mm ceramic fibre
Ceiling Details	Aerated concrete slabs (200 mm) lined with 50 mm ceramic fibre
Floor Details	Dense concrete (75 mm) covered with fluid sand (175 mm)
Fuel Load	5115 kg wood
Calculated Parameters	
Floor Area	127.9 m^2
Total Internal Surface Area	412.2 m^2
Ventilation Area	7.64 m^2
Ventilation Parameter ($A_V \sqrt{H}$)	9.26 $m^{5/2}$
Ventilation Parameter ($A_V \sqrt{H} / A_T$)	0.022 $m^{0.5}$
Fire Load Density	40 kg /m^2 of floor area
Fire Load Density	12.4 kg /m^2 of total bounding surface area

Table B2.3 Kirby et al Test 4; Fire Load 40 kg/m^2, Ventilation Factor 0.022

This fire has a moderate fire load and low ventilation factor. Based on the analysis and simulation of the various NFSC fires in Appendix B1 above, only simulations of stick burning fires with shape factor (F) equal to 3, were carried out, since these invariably provided the most reliable simulations.

Kirby et al Test 4, Stick Fire, Shape = 3 (Figure B2.4)

Identifier	Diam. (D) (m)	Stick Burn Regress Rate (vp) (m/s)	Shape (F)	Coeff. Cd	Pyrolysis Rate (kg/s)	
					Stick Burning	Vent. Control
A	0.15	5.5E-06	3	0.68	1.125	1.111
B	0.15	5.5E-06	3	0.34	1.125	1.111
C	0.15	4.5E-06	3	0.68	0.921	1.111

Table B2.4 Kirby et al Test 4, Fire Simulation Parameters and Initial Pyrolysis Rates

Due to the nature of this fire and the compartment geometry, the test data is quite unusual, with distinct variances between the temperature profiles at different locations in the compartment. Figure B2.3 shows 3 temperature profiles at crib lines 10, 6 and 2 (there were 11 lines of cribs in total). These were manually extracted from Figure 28 of Kirby et al (1994).

The COMPF2 simulations were carried out to reproduce the Crib Line 10 temperature profile (second row back from the ventilation opening). Simulations A and B are identical except that for B, the discharge coefficient C_d was set equal to 0.34 (as above in Section B2.1). Both fires were initially ventilation limited. Simulation C was initially fuel surface controlled.

Both Simulations A and C provide good estimates of the peak temperature and decay, with [C] being marginally the better. Simulation [B] provides an under-estimate of the peak temperature by about 160 °C, and over-estimates the duration of intense combustion.

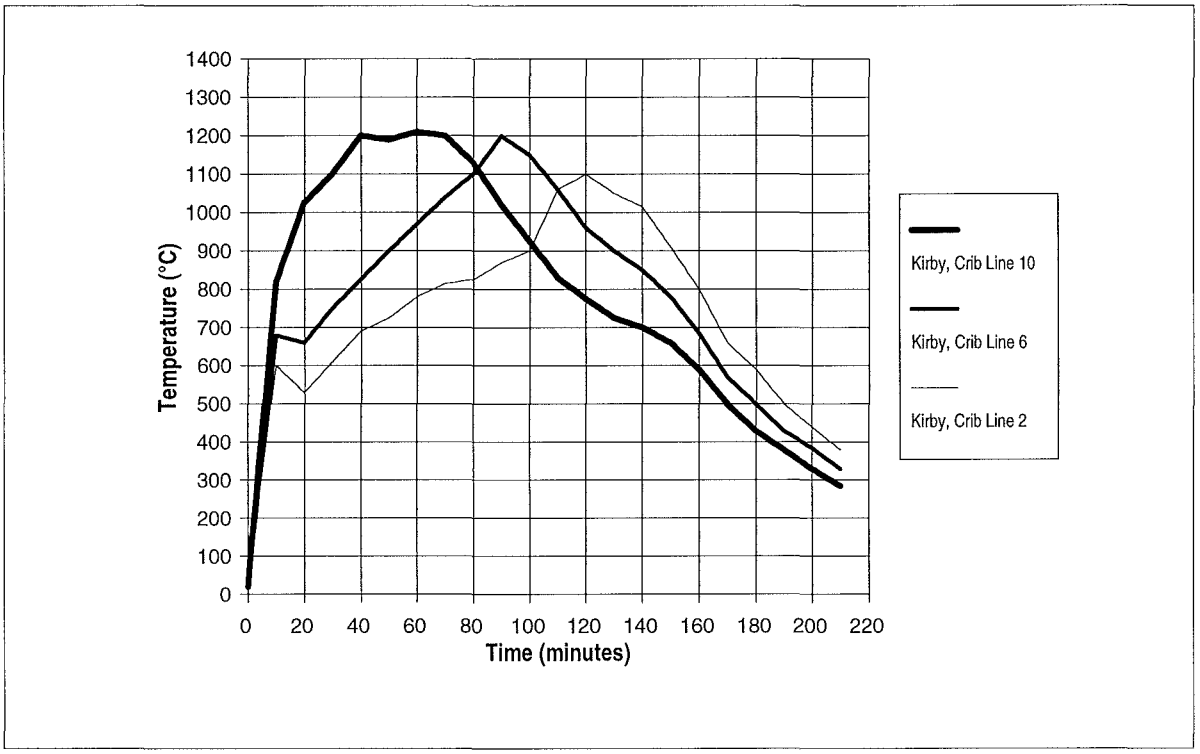

Fig. B2.3, Kirby Test 4, 40 kg/m² Floor Area, Ventilation Factor = 0.022, Temperature Data

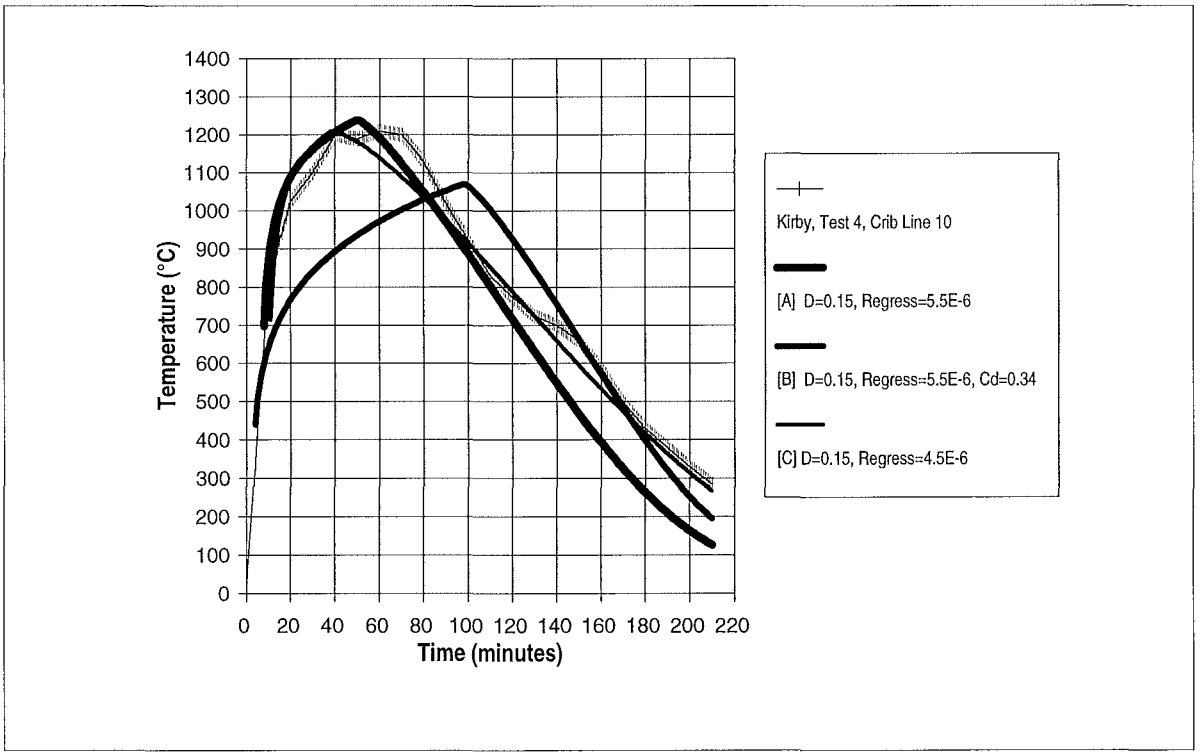

Fig. B2.4, Kirby Test 4, 40 kg/m² Floor Area, Ventilation Factor = 0.022, Stick Fires, Shape =3

Appendix B3 BHP, Melbourne

B3.1 380 Collins Street Melbourne

Refer to Section 5.3 for a discussion of the BHP experimental programme, and the nature of the test fires. The simulation of this series of fires, is complicated by the fact that structures (and their material properties) are extremely diverse, and ventilation, varied considerably with time either as glass windows broke "naturally" or doors were opened manually to accelerate the fire growth.

The 380 Collins Street fires (Proe and Bennetts, 1994), represented an office building being refurbished in Melbourne, and had an external cladding of 10 mm plate glass windows in aluminium mullions, forming a continuous curtain wall. The test compartment shape was not exactly rectangular, but averaged approximately 8.0 x 3.5 m. The slab to slab height was approximately 3.8 m with a ceiling at 2.9 m. The ceiling tile system was plaster with glass fibre insulation backing. It is evident from the photographs provided in the referenced document, that the ceiling tile system was continuous, without the normally-expected penetrations such as recessed lights, and air conditioning grilles and diffusers.

Two of the four walls were glass clad as noted, with the others being constructed of thin sheet steel to represent the thermal effects of being part of a much larger compartment, with restricted ventilation but good heat transfer properties. Ventilation of the compartment during the fire varied with time. At the completion of the test, 26 m^2 of exterior windows had fallen out below ceiling level

The compartment and ventilation opening geometry, materials of construction, fuel load, and relevant parameters calculated from the specified data, are scheduled in Table B3.1.

Specified Parameters	
Compartment Length	8.0 m
Compartment Width	3.5 m
Compartment Height	2.90 m
Ventilation Height	2.9 m
Ventilation Width	9.0 m
Sill Height	0 m
Wall Details	2 walls of sheet steel with "exterior" walls of 10 mm glass
Ceiling Details	Plaster ceiling tiles with glass fibre insulation backing.
Floor Details	Concrete overlaid with carpet
Fuel Load	1300 kg wood equivalent
Calculated Parameters	
Floor Area	28.0 m^2
Total Internal Surface Area	122.7 m^2
Ventilation Area	26.1 m^2
Ventilation Parameter ($A_V \sqrt{H}$)	44.45 $m^{5/2}$
Ventilation Parameter ($A_V \sqrt{H} / A_T$)	0.362 $m^{0.5}$
Fire Load Density	46.2 kg /m^2 of floor area
Fire Load Density	10.6 kg /m^2 of total bounding surface area

Table B3.1 380 Collins, Fire Load 46.2 kg/m^2, Ventilation Factor 0.362

This fire has a moderate fire load and extremely high ventilation factor, well beyond the range commonly reported in the literature . Based on the analysis and simulation of the various NFSC fires in Appendix B1 above, only stick burning fires with shape factor (F) equal to 3, were carried out.

Stick Fire, Shape = 3 (Figure B3.1)

Identifier	Diam. (D) (m)	Stick Burn Regress Rate (vp) (m/s)	Shape (F)	Coeff. Cd	Pyrolysis Rate (kg/s)	
					Stick Burning	Vent. Control
A	0.100	1.0E-05	3	0.68	0.780	5.334
B	0.050	1.0E-05	3	0.68	1.560	5.334
C	0.050	1.0E-05	3	0.34	1.560	5.334
D	0.025	1.0E-05	3	0.68	3.120	5.334
E	0.025	8.0E-06	3	0.68	2.184	5.334

Table B3.2 380 Collins, Fire Simulation Parameters and Initial Pyrolysis Rates

Due to the unusual nature of this fire, with both manual intervention (opening and closing the door to the outside), and window glass breaking progressively altering the ventilation to the fire, the test data is quite variable, with distinct variances between the temperature profiles at different locations in the compartment. Temperature profiles from two thermocouples at ceiling level are taken as a representation of the general characteristics.

The COMPF2 simulations were carried out to reproduce the selected temperature profile above 400 °C. Below prior to this period, the fire temperatures were affected both by the initial limited ventilation, and manual intervention. Thus during the course of the complete test burn, the fire changed from being extremely ventilation limited, to being grossly over ventilated once a significant amount of external window breakage occurred, resulting in strongly fuel surface controlled burning.

The ventilation controlled pyrolysis rate was so high, that all fires were simulated as fuel surface controlled stick burns with Shape Factor = 3.

The initial Simulation [A] (not plotted) produced a fire of far too low an intensity.

Simulation [B], although having the correct general form, underestimated the peak temperatures by about 200 °C. As noted in Babrauskas (1979), when the ventilation aperture occupies a large fraction of the wall area, an effective discharge coefficient (C_d) of as little as half the ususal value of 0.68, best fits the data. Since in this case, two

external walls were effectively fully open from near the floor to the ceiling as ventilation apertures, especially during the later stages of the fire, the same principle should be applicable. Simulation [C] was carried out identical in all respects with Simulation [B], except the discharge coefficient was set to $C_d = 0.34$. An excellent representation of the measured temperature profile resulted. The effect of the reduced discharge coefficient is to reduce the inflow of ambient air, which with the same pyrolysis and burning rate, results in higher compartment temperatures under otherwise identical conditions for this compartment with it's extremely high ventilation factor.

Of subsequent simulations with $C_d = 0.68$, Simulation [D] over-predicted the peak temperature by 200 °C and decayed too fast and Simulation [E] gave a very good estimate of peak temperature, but decayed slightly too quickly.

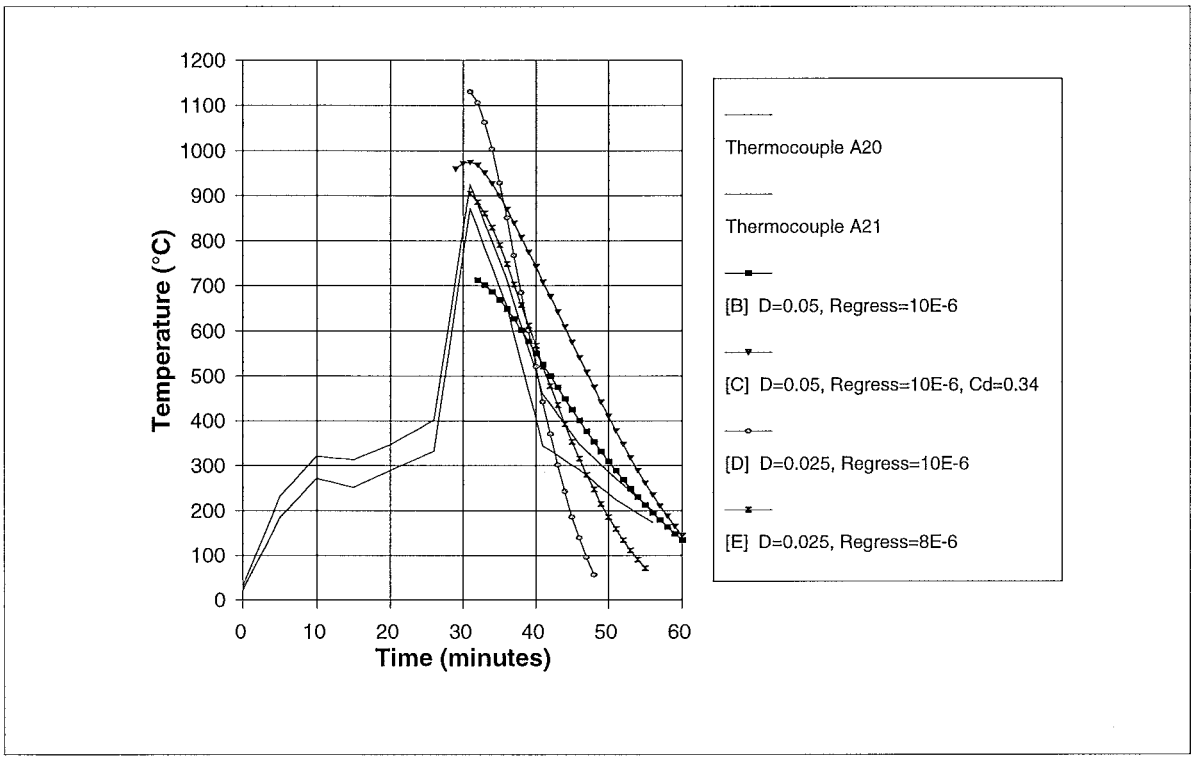

Fig B3.1 380 Collins, 46.4 kg/m² Floor Area, Ventilation Factor = 0.362, Stick Fires, Shape = 3

APPENDIX C COMPF2PC PROGRAMME STRUCTURE

Appendix C1 Programme Variables

C1.1 Programme Input Data

Programme input is via a data file with strict formatting requirements. The easiest way to create a new data file is to modify a previous data file and save it with a new name. Four output files must be defined, of which two have useful data related to an input data file summary and the calculated results of the programme. The third and fourth files are only relevant if an execution error occurs, and assist in de-bugging.

C1.2 Subroutine Details

The programme is written in Fortran 77. Each of the programme's primary modules and subroutines is described briefly.

COMPF2 — The main programme COMPF2 handles input and output duties, sets initial conditions, deals with error handling in the event of an iteration failure and calls other subroutines for calculation.

CRIB — Deals with wood crib fires. A trial gas temperature is assumed, and flow quantities and wall heat losses are calculated using DESOLV. A heat balance is determined. The new temperature is determined by the Newton method. After convergence, a new wall temperature profile is calculated by RSTA. The calculation then proceeds to the next time step. Calculation ends at the preset maximum run time MTIME, when the gas temperature drops below 353 K (70 °C) or if errors occur or convergence failure occurs.

DEQNS — Computes heat conduction through the wall using the Crank-Nicolson method. The radiation boundary condition is linearised, and updated each iteration.

ECHOID — Echoes the input data.

ICONDS Initialises starting values and makes a few simple checks on the validity of the input data.

OUTPUT Writes data to two output files at the end of each time step. One file contains temperatures in °C, burning rates etc., and the second contains heat balance values, mass fractions etc.

PFLFIX Is a pessimisation design routine. Fuel pyrolysis is calculated according to governing equations, but the ventilation is pessimised by instantaneously adjusting the window width to give the highest possible temperatures. Wood stick or wood crib fires are assumed unless PLFUEL = T, in which case a pool fire is used. The window width is not allowed to exceed a maximum as set by AWDOW / HWDOW. Calculations stop when the fuel (as specified by FLOAD) is exhausted.

POOL Pool burning pyrolysis rates are calculated according to (13), (14) and (15). Three modes of operation are possible. If STOICH=T, the steady state temperatures and pool area are determined for stoichiometric burning. IF EISCAN=T, the steady state solution is found for a given pool area greater than stoichiometric. The pool area is specified by use of the parameter EITA defined as :

$$\eta = \frac{\dfrac{A_v\sqrt{H}}{A_f}}{\left(\dfrac{A_v\sqrt{H}}{A_f}\right)_{stoich}} \qquad (20)$$

For constant window size, this becomes the ratio of pool areas. No solutions are possible for $\eta \geq 1$. The user must make sure that the pool size is sufficiently large so that $\eta \leq 1$.

PVTFIX Is a pessimisation routine, and is effectively the inverse of PFLFIX. In this routine a fixed ventilation opening is specified. The fuel release rate is instantaneously varied to always result in the highest possible burning temperature. Temperatures drop sharply after the fuel load is consumed.

RPFIX Allows comparison of measured data against predictions. Accepts tabulated combustion rates as a function of time.

STFLOW Calculates steady state wall heat conduction.

TLU Is an interpolation function.

TRIDGF A Gauss elimination procedure to solve a set of tri-diagonal matrix equations.

C1.3 Programme Operation

Data entry is relatively clumsy, and is set up as a "card deck" model.
Three modes of programme operation are possible :

	Variable Settings
Complete temperature vs time curve	STEADY=FALSE, ADIA=FALSE
Steady state temperature for a given wall	STEADY = TRUE, ADIA=FALSE
Steady state temperature for adiabatic wall	STEADY = TRUE, ADIA=TRUE
Pool Fires	PLFUEL=TRUE
Temperature vs Time for known ventilation and pool area	SIZE= STOICH=FALSE, EISCAN=FALSE
Steady state for stoichiometric pool size	EITA=1, STOICH=TRUE
Wood Crib fires (default option)	FLSPEC = PLFUEL = RPSPEC = VTSPEC = FALSE
Simple stick burning	REGRESS > 0
Nilsson's crib formulas	REGRESS = 0, Specify SH
Pessimisation over ventilation	FLSPEC=TRUE
Simple stick burning	REGRES>0, PLFUEL=FALSE
Nilsson's crib formulas	PFUEL=FALSE, REGRES=0, Specify SH

	Variable Settings
Pool burning	PLFUEL=TRUE
Pessimisation over pyrolysis rate	VTSPEC=TRUE